Master thesis

CELLULAR BEAM-COLUMNS

IN

PORTAL FRAME STRUCTURES

HOLMES
PLACE

J.G. Verweij
November 2010

Master thesis

CELLULAR BEAM-COLUMNS

IN

PORTAL FRAME STRUCTURES

Thesis committee:

Chairman
Prof. Ir. F.S.K. Bijlaard, Section Steel- and Timber Structures

Committee members
Dr. A. Romeijn, Section Steel- and Timber Structures
Ir. R. Abspoel, Section Steel- and Timber Structures
Dr. Ir. P.C.J. Hoogenboom, Section Structural Mechanics
Ir. L.J.M. Houben, Section Road and Railway Engineering

External committee member
Dr. O. Vassart, ArcelorMittal R&D

J.G. Verweij
1155482

Delft University of Technology
Civil Engineering
Section Steel and Timber Structures

November 2010

PREFACE

The present document forms the final report of my Master Thesis Project entitled *Cellular beam-columns in portal frame structures*. This Master Thesis has been carried out as being part of the Master's degree programme in Civil Engineering, Section Steel and Timber Structures, at Delft University of Technology.

Although in the past already a large deal of research was performed into the subject of the behaviour of (non-)composite cellular *beams*, almost no attention has been paid to the application of cellular members as *columns*. Especially the use in portal frame structures seems attractive for reasons of aesthetics – and therefore the investigation of it's structural behaviour is relevant. For that reason the present work is devoted to the research of the behaviour of cellular *beam-columns*.

Parts of this research have been performed while being in-company. First, at the research department of ArcelorMittal in Esch-sur-Alzette, Luxembourg, which enabled me to make use of their knowledge and software. Second, at the office of IBT – Ingenieurs in Bouwtechniek – a firm of consulting engineers in Veenendaal, The Netherlands, the last period while being on a full-time contract already.

I would like to thank respectively Dr. O. Vassart and Ir. A. van 't Land for their willingness to provide me these facilities. Moreover, I would like to express my gratitude to the other persons of the thesis committee: Prof. Ir. F.S.K. Bijlaard, Dr. A. Romeijn, Ir. R. Abspoel and Dr. Ir. P.C.J. Hoogenboom.

Finally, thanks go to all who have supported me – at any time, at any place – during my studies at Delft University of Technology.

Ede, November 2010
J.G. Verweij

TABLE OF CONTENTS

PREFACE 5

1 INTRODUCTION 15

1.1 MOTIVATION 15
1.2 OBJECTIVES 15
1.3 SCOPE 15
1.4 LIMITATIONS 16
1.5 OUTLINE 16

PART I - LITERATURE STUDY 19

2 INTRODUCTION TO CELLULAR BEAM-COLUMNS 21

2.1 OPEN-WEB SECTIONS 21
2.2 PRODUCTION METHODS 21
2.3 APPLICATION AREA 23
2.4 CURRENT RESEARCH STATUS 26
2.5 FUTURE DESIGN DEVELOPMENT 32
2.6 ADVANTAGES AND DISADVANTAGES 32

3 MECHANICAL BEHAVIOUR OF BEAMS WITH WEB OPENINGS 33

3.1 INTRODUCTION 33
3.2 GLOBAL BENDING AND SHEAR 33
3.3 LATERAL-TORSIONAL BUCKLING 34
3.4 WEB-POST FAILURE MECHANISMS 35
3.5 ADDITIONAL FAILURE MODES 36
3.6 SERVICEABILITY PERFORMANCE 36
3.7 BEHAVIOUR AT ELEVATED TEMPERATURE 37
3.8 SUMMARY OF FAILURE MECHANISMS 37

4 DESIGN METHODS FOR CELLULAR BEAMS 39

4.1 INTRODUCTION 39
4.2 LWO DESIGN METHOD 39
  4.2.1 INTRODUCTION 39
  4.2.2 SECTION CLASSIFICATION 40
  4.2.3 GLOBAL BENDING RESISTANCE 41
  4.2.4 SHEAR RESISTANCE 41
  4.2.5 SHEAR BUCKLING CAPACITY 43
  4.2.6 VIERENDEEL BENDING RESISTANCE 43
  4.2.7 BENDING RESISTANCE OF TEES 44
  4.2.8 INTERACTION WITH NORMAL FORCE 45
  4.2.9 WEB-POST HORIZONTAL SHEAR 45
  4.2.10 WEB-POST BUCKLING 45
  4.2.11 PATTERN LOADING 47
  4.2.12 SERVICEABILITY BEHAVIOUR 47
  4.2.13 STIFFENER REQUIREMENTS 48
  4.2.14 GEOMETRICAL LIMITATIONS 49
  4.2.15 GENERAL DESIGN CONSIDERATIONS 49
  4.2.16 SOFTWARE TOOL 51
4.3 BACKGROUNDS OF THE ACB PROGRAM 51

4.3.1 Introduction 51
4.3.2 Vierendeel bending 51
4.3.3 Lateral-torsional buckling 52
4.3.4 Web-post buckling 52
4.3.5 Serviceability behaviour 54
4.4 Complementary usage 55

5 PORTAL FRAME DESIGN ACCORDING TO THE EUROCODES 57

5.1 Introduction 57
5.2 Standards 57
5.2.1 Introduction 57
5.2.2 Dutch TGB1990 series 57
5.2.3 Hong Kong Steel Code 57
5.3 Global analysis 58
5.3.1 Introduction 58
5.3.2 Geometrical non-linearity 58
5.3.3 Material non-linearity 59
5.3.4 Imperfections 60
5.3.5 Structural stability 62
5.4 Design of beam-columns 64
5.4.1 Cross-sectional resistance 64
5.4.2 Buckling resistance 65
5.5 Non-uniform members 71
5.6 Conclusion 73

PART II – NUMERICAL RESEARCH 75

6 INTRODUCTION 77

7 DESCRIPTION OF THE FINITE ELEMENT SOFTWARE AND TOOLS 79

7.1 Introduction 79
7.2 Finite element software SAFIR 79
7.2.1 Capabilities and program structure 79
7.2.2 Element types 82
7.2.3 Material laws 84
7.2.4 Safir Shell 84
7.3 Pre-processors 84
7.3.1 Introduction 84
7.3.2 Crystal Pro 84
7.3.3 Mailleur Portique 86
7.4 Post-processor Diamond 86

8 GLOBAL BUCKLING OF CELLULAR MEMBERS 87

8.1 Introduction 87
8.2 Theoretical analysis 87
8.3 Finite element model 89
8.3.1 Introduction 89
8.3.2 Support conditions 89
8.3.3 Use of imperfections 91
8.3.4 Load application 94
8.4 Parameter study 94
8.4.1 Set-up 94
8.4.2 Base profile IPE140 98

8.4.3 Base profile IPE330 ... 101
8.4.4 Base profile IPE600 ... 103
8.4.5 Base profile HE200A ... 107
8.4.6 Base profile HE650M ... 107
8.5 Conclusion ... 108

9 WEB-POST BUCKLING IN COMPRESSED CELLULAR MEMBERS ... 111

9.1 Introduction ... 111
9.2 Theoretical analysis ... 111
9.2.1 LWO model ... 111
9.2.2 Arcelor's model ... 112
9.2.3 Comparison and conclusion ... 113
9.3 Finite element model ... 114
9.3.1 Introduction ... 114
9.3.2 Support conditions ... 114
9.3.3 Use of imperfections ... 115
9.3.4 Load application ... 115
9.4 Parameter study ... 115
9.4.1 Set-up ... 115
9.4.2 Base profile IPE140 ... 117
9.4.3 Base profile IPE330 ... 118
9.4.4 Base profile IPE600 ... 120
9.4.5 Base profile HE200A ... 122
9.4.6 Base profile HE650M ... 123
9.5 Conclusion ... 125

PART III – CASE STUDY ... 127

10 PORTAL FRAME STRUCTURES USING CELLULAR MEMBERS ... 129

10.1 Introduction ... 129
10.2 Design using the LWO method ... 129
10.2.1 Structure of the Excel tool ... 129
10.2.2 Analysis procedure ... 129
10.3 Design using FEA in SAFIR ... 133
10.3.1 Introduction ... 133
10.3.2 Second-order non-linear in-plane analysis with 2D beam elements ... 133
10.3.3 Second-order non-linear 3D finite element analysis with shell elements ... 134
10.4 Case study ... 135
10.4.1 Structural system ... 135
10.4.2 Load case 1: distributed vertical load ... 135
10.4.3 Load case 2: horizontal point loads ... 136
10.4.4 Load case 3: combination of both vertical and horizontal point load ... 138
10.5 Conclusion ... 139

11 CONCLUSIONS AND RECOMMENDATIONS ... 141

11.1 Introduction ... 141
11.2 Conclusions ... 141
11.3 Recommendations ... 142

REFERENCES ... 143

ANNEXES ... 151

A EUROPEAN STANDARDS ... 153

A.1 INTRODUCTION 153
A.2 EUROCODE 3: PART 1-1 154
A.3 EUROCODE 3: PART 1-5 154

B FEM RESULTS OF PARAMETER STUDY INTO GLOBAL BUCKLING........ 157

B.1 INTRODUCTION 157
B.2 BASE PROFILE IPE140........ 157
B.2.1 BUCKLING ABOUT THE WEAK AXIS 157
B.2.2 BUCKLING ABOUT THE STRONG AXIS 160
B.3 BASE PROFILE IPE330........ 164
B.3.1 BUCKLING ABOUT THE WEAK AXIS 164
B.3.2 BUCKLING ABOUT THE STRONG AXIS 168
B.4 BASE PROFILE IPE600........ 171
B.4.1 BUCKLING ABOUT THE WEAK AXIS 171
B.4.2 BUCKLING ABOUT THE STRONG AXIS 175
B.5 BASE PROFILE HE200A 178
B.5.1 BUCKLING ABOUT THE WEAK AXIS 178
B.5.2 BUCKLING ABOUT THE STRONG AXIS 181
B.6 BASE PROFILE HE650M........ 185
B.6.1 BUCKLING ABOUT THE WEAK AXIS 185
B.6.2 BUCKLING ABOUT THE STRONG AXIS 188

C FEM RESULTS OF PARAMETER STUDY INTO WEB-POST BUCKLING........ 191

C.1 INTRODUCTION 191
C.1.1 ARCELOR MODEL FOR WEB-POST BUCKLING 191
C.1.2 ARCELOR MODEL FOR VIERENDEEL BENDING 193
C.1.3 LWO MODEL FOR BOTH WEB-POST BUCKLING AND VIERENDEEL BENDING........ 196
C.2 BASE PROFILE IPE140........ 198
C.2.1 WEB-POST WIDTH S_0 = 50 MM........ 198
C.2.2 WEB-POST WIDTH S_0 = 100 MM........ 199
C.3 BASE PROFILE IPE330........ 200
C.3.1 WEB-POST WIDTH S_0 = 50 MM........ 200
C.3.2 WEB-POST WIDTH S_0 = 100 MM........ 201
C.4 BASE PROFILE IPE600........ 202
C.4.1 WEB-POST WIDTH S_0 = 62 MM........ 202
C.4.2 WEB-POST WIDTH S_0 = 124 MM........ 203
C.5 BASE PROFILE HE200A 204
C.5.1 WEB-POST WIDTH S_0 = 50 MM........ 204
C.5.2 WEB-POST WIDTH S_0 = 100 MM........ 205
C.6 BASE PROFILE HE650M........ 206
C.6.1 WEB-POST WIDTH S_0 = 70 MM........ 206
C.6.2 WEB-POST WIDTH S_0 = 140 MM........ 207

D LIST OF CONTENTS DATA-DVD 209

E ARCELOR PROFIL LUXEMBOURG........ 211

F IBT INGENIEURS IN BOUWTECHNIEK 213

G ADDRESSES 215

LIST OF SYMBOLS

The following symbols are used throughout this report. Some of these are different from that are used in the referred publications in order to prevent misunderstandings. Furthermore note that the subscript t is used throughout this report, when a formula applies to both the bottom and top tee. The subscript ϕ refers to properties or forces acting on an inclined section. Additional symbols are defined where they first occur.

a	throat thickness of the fillet weld
A_f	cross-sectional area of the flange
A_s	cross-sectional area of a horizontal stiffener
A_b	cross-sectional area of the bottom tee
A_t	cross-sectional area of the (top) tee
A_w	cross-sectional area of the web
A_v	shear area of an unperforated section
$A_{v,o}$	shear area of a perforated section
$A_{v,t}$	shear area of a tee-section
b	flange width
χ_w	shear buckling factor for contribution of the web
δ_{add}	additional deflection due to a single opening at position x
δ_b	pure bending deflection of the beam
δ_{sw}	deflection due to permanent loads
d_o	depth (or diameter) of a web opening
d_b	$= h_b - t_f$, depth of the web of the bottom tee
$d_{b,eff}$	effective depth of the web of the bottom tee (to meet classification limits)
d_t	$= h_t - t_f$, depth of the web of the (top) tee
d_w	distance of the critical section from the joint between the two half-posts
ε	$= \sqrt{235/f_y}$ with f_y in N/mm^2, coefficient for section classification
ε^1	modified coefficient for section classification (to allow for the effect of axial tension)
e^*	equivalent geometrical imperfection
e_s	offset distance of centre of stiffener from tip of the web
E	elastic modulus of steel
f	natural frequency
γ_{M0}	partial factor for resistance of cross-sections
γ_{M1}	partial factor for resistance of members to instability assisted by member checks
η	shape factor for shear area
h	height of the section
h_b	depth of the bottom tee
h_t	depth of the (top) tee
h_w	depth of the web of the section
i	radius of gyration
ϕ	angle (of inclined section to the vertical through the hole)
f_{vw}	design shear strength of a fillet weld
f_y	yield strength of steel

$f_{y,red}$	reduced yield strength to account for high shear force
f_{ys}	yield strength of stiffener
f_{yw}	design strength of the weld
$F_{s,Ed}$	design axial force in stiffener
$F_{s,Rd}$	axial resistance of stiffener
k_o	modification factor for the deflection for long openings
λ	slenderness of web-post
λ_1	slenderness value to determine the relative slenderness
$\bar{\lambda}$	non-dimensional (relative) slenderness of web-post
ℓ_e	effective length of web-post for web-post buckling
ℓ_o	actual length of opening
$\ell_{o,eff}$	effective length of opening for stability of the web (section classification)
$\ell_{v,eff}$	effective length of opening for Vierendeel bending
$\ell_{w,eff}$	effective length of web-post for web-post buckling
ℓ_w	width of the web-post at the critical section location
L	length of the beam
n	number of sides of the stiffener (single-sided stiffener: 1, double-sided stiffener: 2)
N_o	number of openings along the beam
ρ	shear utilisation factor (to determine the reduced bending moment resistance due to high shear force)
σ_c	(design) compressive stress acting on the web-post
$\sigma_{c,Rd}$	design compressive strength of the web-post
$\sigma_{w,Rd}$	principal stress resistance
$\sigma_{w,Sd}$	principal compressive stress at the critical section
s	centre-to-centre spacing of adjacent openings
s_o	edge-to-edge spacing of adjacent openings
s_e	end distance from opening to beam end
τ_{Ed}	design value of the local shear stress
t_f	flange thickness
t_s	stiffener thickness
t_w	web thickness
$t_{w,eff}$	effective web thickness, reduced
M_{Ed}	design bending moment
M_h	web-post bending moment
$M_{h,e}$	elastic bending resistance of the web-post
$M_{h,eff}$	effective web-post bending moment, acting at the critical section
$M_{pl,t}$	plastic bending moment resistance of the top tee
M_b	bending moment resistance of the bottom tee
$M_{b,red}$	reduced bending moment resistance of the bottom tee (due to axial and shear force)
M_t	bending moment resistance of the (top) tee
$M_{t,red}$	reduced bending moment resistance of the top tee (due to axial and shear force)
M_v	applied Vierendeel moment
N_{Ed}	design normal force
N_b	normal force in bottom tee
N_t	normal force in (top) tee

$N_{pl,t}$	plastic normal force resistance of a tee
$N_{pl,f}$	plastic normal force resistance of the flange
$V_{b,Rd}$	shear buckling capacity
$V_{bw,Rd}$	contribution of the web to the shear buckling capacity
$V_{bw,o,Rd}$	contribution of the web to the shear buckling capacity of a perforated web
V_{Ed}	design shear force
V_b	shear force in bottom tee
V_t	shear force in (top) tee
V_h	horizontal shear force in the web-post
$V_{h,Rd}$	shear resistance of the web-post
$V_{pl,Rd}$	plastic shear resistance of unperforated section
W_h	section modulus of the web-post at the critical section location
y_e	elastic neutral depth of tee from outer edge of flange
y_p	plastic neutral depth of tee from outer edge of flange

1 INTRODUCTION

1.1 Motivation

Cellular members – steel I-shaped structural elements with circular web openings at regular intervals – have been used as beams for more than 30 years now. However, in certain countries, like the Netherlands and Belgium, application seems to lack behind. This can probably be attributed to a combination of factors: unfamiliarity with these beams, the present concrete-minded practise for multi-storey buildings, and a lack of localised design guides.

Although cellular columns are less common, examples are available. However, in research publications no attention is paid to this topic. Structural engineers therefore have to base their designs on simplified methods of analysis and good engineering judgement. In order to exploit the full capacity of cellular columns a sound basis is needed and thus a desire exists for a more refined approach.

The subject of cellular members came to my attention mainly because of two reasons. Firstly, an open thesis subject was available for researching the possibility of using plate girders with circular openings in bridges. Secondly, at the firm of consulting engineers where I did my work placement, Ingenieursburo voor Bouwtechniek, they once applied cellular columns in a car showroom. Because of a lack of existing design guidance, they had to find their own way in making the calculations. Admittedly these were quite conservative. Knowing this, I thought it to be worthwhile to get a more refined prediction of the capacity of these members.

In my search for information on the subject of cellular members I contacted Ir. J. Naessens from the Staalinfocentrum in Belgium. He advised me to get in touch with some people within ArcelorMittal, a worldwide operating steel company. This resulted in an invitation to come to their research department in Esch-sur-Alzette, Luxembourg.

It was a consideration of particular interest that to make reliable predictions based with FEM calculations, real test data is needed for calibrating the models. Because these test results are confidential, and the calculation model to be proposed needs to be verified, it was decided that it would be best to carry out a part of the research work at ArcelorMittal's offices.

1.2 Objectives

The objectives of this research are twofold:

- to investigate the behaviour of cellular members under axial load
- to develop a suitable and easy-to-use calculation method for portal frames using cellular beams and columns

1.3 Scope

The present investigation deals with the behaviour of a single-bay pitched-roof portal frame using cellular beam-columns. Although some application examples are available where cellular members have been used as columns and in portal frame structures, no guidance exists for the design of these. Furthermore experimental and numerical test evidence lacks and the design experience is limited to the seller's technical assistance.

The use of cellular beams in portal frame structures has been recognised as a topic of interest within ArcelorMittal already, but work on a project to investigate its behaviour and application possibilities was postponed due to a shift in research priorities.

In this research a simple and straightforward calculation method for portal frames consisting of cellular beam-columns has been developed and implemented in Microsoft Excel using Visual Basic for Applications.

First the literature study discusses existing design methods for cellular beams and for portal frames. In the subsequent numerical research cellular column-behaviour has been studied in order to reveal possible differences with that of plain-webbed sections. 3D finite element portal frame analyses were carried out to verify both the proposed calculation method and its implementation. Finally the calculation method has been applied to a portal frame structure using cellular members, and the results have been compared with 3D finite element calculations.

1.4 Limitations

This study is limited to the study of the structural behaviour of cellular beams-columns in cold situation only (normal temperature range, not in fire conditions).
Furthermore the following limitations hold:

- only symmetrical sections
- no composite design
- no curved beams
- no tapered beams and columns
- only circular and elongated web-post openings are covered

The last limit is based on the most common fabrication process and the expected reason of application: aesthetics.

1.5 Outline

The present report is divided into three parts, each subdivided in a numbers of chapters.

PART I – LITERATURE STUDY

Chapter 2 gives a general introduction to cellular beam-columns with information on production methods, application area and the current state-of-the-art in research.

Chapter 3 pays attention to the various failure mechanisms that might occur for beams with web holes. The interaction between bending moment and shear force around web openings is discussed qualitatively, and the additional possible failure modes that are introduced by the presence of web holes are presented. Furthermore the serviceability behaviour is dealt with.

Chapter 4 addresses existing calculation methods for cellular beams. The additional checks required for beams with regular web openings are presented.
Thereafter the approach as developed in the ECSC project *Large web openings for service integration in composite construction* is compared with the theoretical backgrounds of the dedicated computer program ARCELOR Cellular Beams.
The treatment of these both methods has been limited to the case of non-composite simply-supported cellular beams, whereof the openings are placed at the centre-line.

Chapter 5 deals with the Eurocode regulations for the structural design of pitched-roof portal frames. It discusses how both material and geometrical non-linearity are dealt with, both on a global and a local level. Furthermore the rules that relate to non-uniform members are explained.

PART II – NUMERICAL RESEARCH

Chapter 6 introduces the second part of this report, namely the numerical investigation into the structural behaviour of cellular beam-columns.

Chapter 7 first explains the backgrounds of the specialised finite element code SAFIR that has been used throughout the research, followed by a discussion of the accompanying tools needed for pre- and post-processing the results.

Chapter 8 gives a detailed description of the study of global flexural-buckling of cellular members, made in order to confirm the theoretical results acquired in the literature study. After an elaborate explanation of the set-up of the parameter study performed, it's results are presented and discussed. From these it is concluded that the proposed simplified rule for determining the flexural buckling capacity of cellular columns can be applied safely.

Chapter 9 presents the results of another parameter study into web-post buckling of cellular beam-columns while loaded in axial compression. The implications on both the LWO model and Arcelor's own model for web-post buckling are first analysed analytically, and these theoretical results are validated against the results of the finite element parameter study.

PART III – CASE STUDY

Chapter 10 illustrates the knowledge gained in the previous parts. The LWO method is applied to the design of portal frames using cellular members. Therefore a design tool is developed in Microsoft Excel using VBA.
For different load cases, the predicted failure behaviour is compared with 2D and 3D finite element analyses, and the Excel tool developed is found to deliver safe results.

Finally chapter 11 summarizes the conclusions that can be drawn from the research performed, and gives recommendations for further research.

The report is concluded by a list of references and a number of annexes, giving some backgrounds on the European standards – as applied in this research – and more detailed results of the both parameter studies.
Furthermore a data-dvd is attached to the report which contains all analysis data and the spreadsheets and software that has been used.

PART I
-
LITERATURE STUDY

2 INTRODUCTION TO CELLULAR BEAM-COLUMNS

2.1 *Open-web sections*

Cellular beam-columns – shortly cellular beams – belong to the larger group of steel sections with web openings, thus creating a higher moment-of-inertia-to-weight ratio. When used as floor beams, open-web sections on their turn are a part of the group of floor systems which provide a means to incorporate building services within the structural depth of the floor. Basically speaking two options exist for highly serviced office buildings: either minimise the structural zone so that the building services can pass beneath, or integrate the structural members and the building services within the same horizontal zone [Chung 2002].

Integrated floor systems comprise amongst others fabricated beams with tapered webs, haunched beams, trusses, stub girders, slim floor systems and beams with single or multiple web openings. Because in these systems the available depth for construction is almost equal to the floor depth, a reduced overall height of the building can be achieved, thereby reducing cladding costs. Nowadays, in most cases the design of floor beams with web openings is carried out recognising the composite action between the steel beam and the concrete slab on top of it.

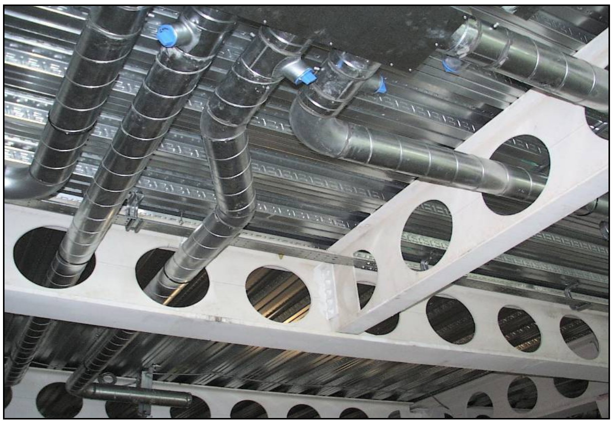

Figure 2.1 Service integration through web openings in cellular floor beams

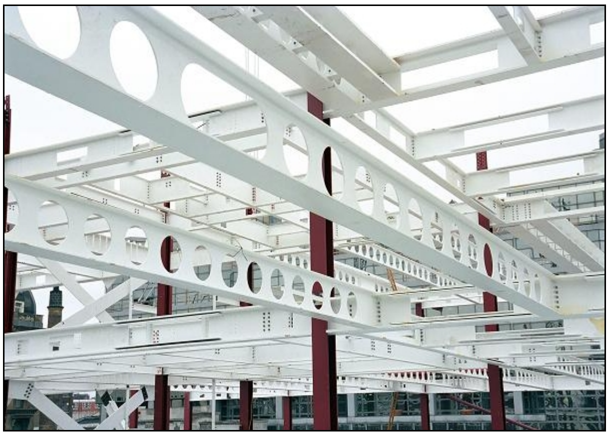

Figure 2.2 Various opening shapes in cellular floor beams

Steel members can be equipped with single of multiple web openings, which can take different shapes. When these openings are circular and regularly spaced, the members are designated cellular. Depending on the fabrication process other opening shapes are possible, including square, rectangular, hexagonal (standard castellated section) and octagonal shapes.

2.2 *Production methods*

Cellular beams are produced by a range of steel manufacturers, using their own patented processes. The process applied by Fabsec (UK) is to fabricate the whole girder by welding profiled steel plates to form the flanges and the web of the section. Prior to the welding process, openings are cut in the web plate. All dimensions can be adjusted, but no beneficial fillet weld effect is present.

More commonly applied is another process, that consists of flame cutting the web of an existing H or I-shaped hot-rolled section, and then welding the separated sections tip-to-tip together. The material that gets cut out by the two-way flame cutting process is reused in the steel mills. Amongst others ArcelorMittal (Luxembourg) and Westok (UK) use this method to produce their cellular beams.

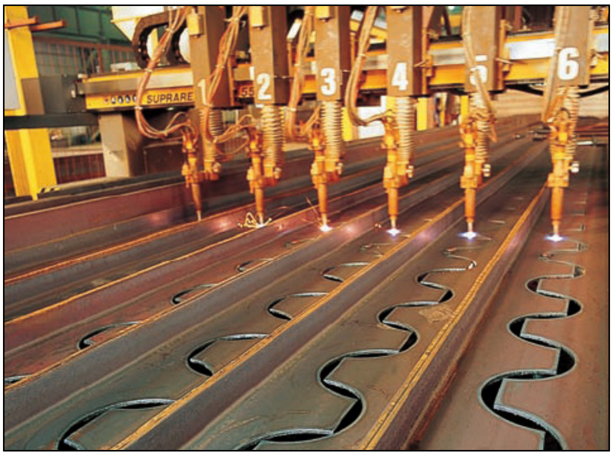

Figure 2.3 Fabrication process: flame cutting of hot-rolled profiles

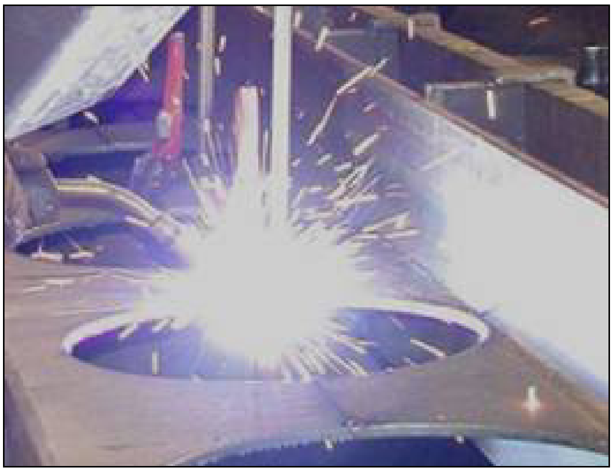

Figure 2.4 Fabrication process: welding the separated tee-sections together

Manufacturers of cellular beams in other countries are CMC Steel Products (USA), Macsteel Trading (South Africa), Peiner Träger GmbH(Germany) and Grünbauer BV (The Netherlands). Some manufacturers (e.g. Westok, Macsteel Trading) produce exclusively cellular beams, while for others (e.g. ArcelorMittal, Peiner Träger GmbH) they only form a part of their whole product range.

When producing cellular beams by flame cutting and welding, the top and bottom sections do not have to be the same: by using different base sections it is possible to produce an asymmetric cellular section.

Both production processes allow the height of the resulting section to be adjusted to a great extend. All beams are made according to the specifications of the designer. They can easily be precambered such that the death load deflections will not govern the design.

Producing curved or tapered sections is also provided in the same process flow. Tapered cellular beams are produced by cutting the web at an angle to the centroidal line. Curved beams are produced by adjusting the cutting pattern to create different bottom and top tees. Then these tees are bent to the required radii and welded together.

Curving in plan is also possible, but care must be taken of the fact that the torsional stiffness is relatively low.

When the chosen section fails to perform satisfactory, the beam can be reinforced locally. In high shear areas near the supports it may be necessary to fill or reinforce one or more openings. Buckling of a web-post can be avoided by adding two-part hoops, or a simple (vertical) flat. Where concentrated loads are introduced simple plates can be welded above the openings to avoid local plastic deformation (ovalisation).

It is preferable though, to avoid infills and stiffeners as much as possible by adjusting the cell configuration, to reduce costs.

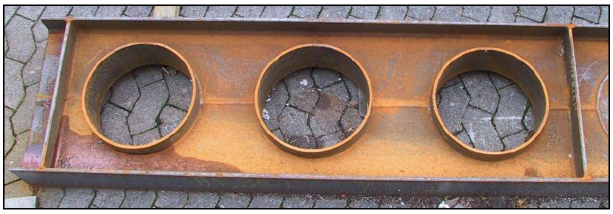

Figure 2.5 Circular reinforced openings

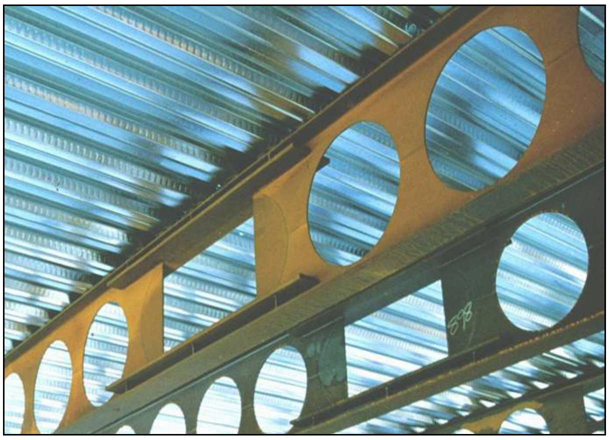

Figure 2.6 Arrangement of simple plates to avoid local plastic deformation

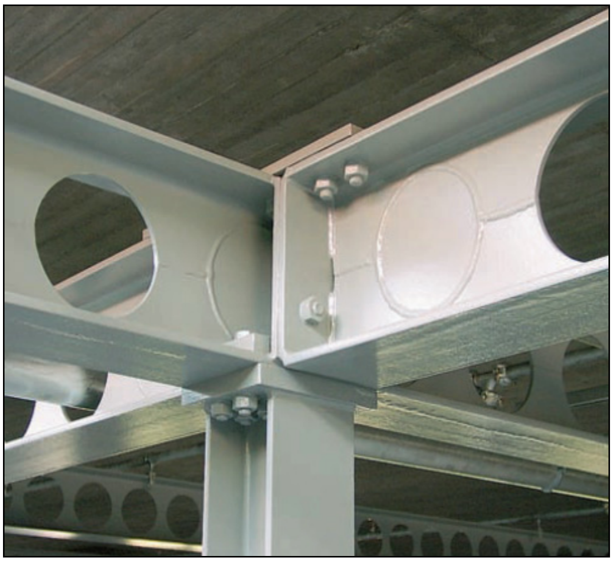

Figure 2.7 Filled web openings at support for increased shear resistance

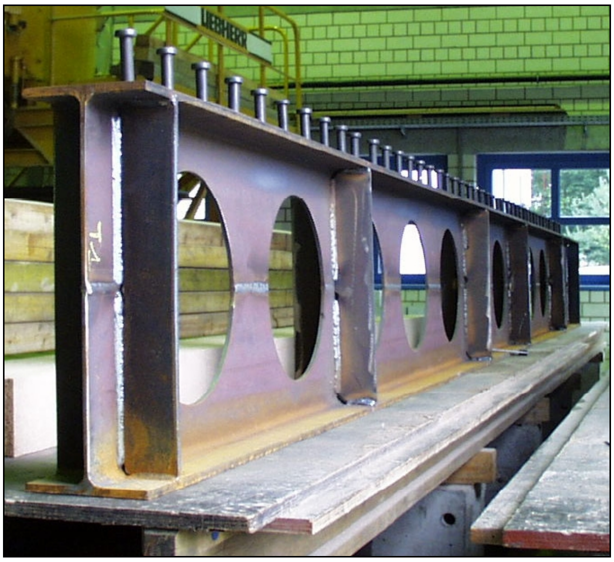

Figure 2.8 Web-post stiffeners and headed studs for composite application

Compared to castellated beams – with hexagonal opening shapes, and thus no material loss – the flexibility instead of standard dimensions, is a major advantage. Therefore the use of optimised cellular sections will result in lighter beams than when use would be made of the most efficient castellated sections.

Cellular beams are available in different steel grades. Usually floor beams require higher steel grades like S355 and S460, where the standard grade S235 suffices for roof beams.

2.3 Application area

Cellular beams are widely used nowadays. However, in certain countries, like the Netherlands (and Belgium), application seems to lack behind. It seems that there is a lot of unfamiliarity and a lack of localised design guides for practice with these beams.

But there are more fundamental causes to point out. First, in the Netherlands multistorey buildings with more than four floors are traditionally the domain of concrete [BmS 2002]. Second, the price of individual cellular beams is indeed higher than that of standard rolled profiles.

It has however been shown by many successful designs (especially in the UK, but among others also in Germany and France) that steel is really a viable alternative, moreover, that integrated design may lead to a lower price of the total building, notwithstanding the higher price of the individual cellular beams.

The use of cellular beams for floor structures is well developed. Composite construction makes shallower and lighter construction possible. Both the load bearing capacity and the stiffness of the beam are enhanced greatly by composite action. Cellular floor beams may be used as long span secondary beams, or heavily loaded primary beams.

Flexibility in the use of the floor area and reduction of the storey height and thus of the cost for the façade are the main reasons why cellular beams contribute to a sound and economical design.

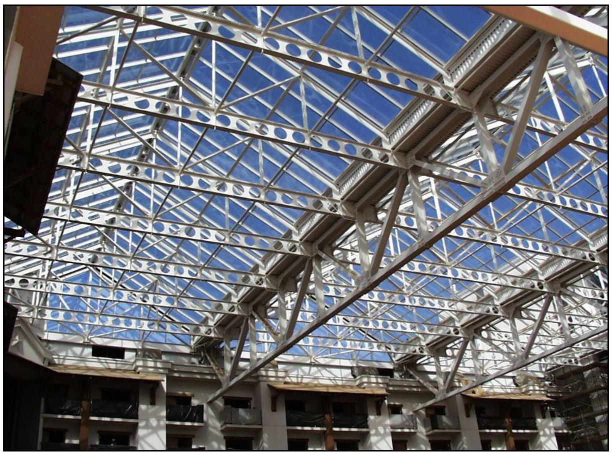

Figure 2.9 Hotel atrium

Design procedures and programs are available nowadays, which enable easy calculation for a wide range of possibilities. Composite and non-composite designs, symmetric and asymmetric designs, stiffened and unstiffened openings, regular and irregular web openings are all covered. Calculation procedures for determining the fire resistance of these sections have been developed too. In general a fire engineering calculation using finite element methods will be necessary. Although methods for a more straightforward assessment of the required thicknesses of intumescent coatings are available, usually they rely on confidential test results and therefore have a limited range of application. Furthermore public test results on the behaviour of cellular beams protected with intumescent coatings suggest that it will be difficult to specify simple generic rules to allow for the increased web-post temperature.
In roof structures cellular beams are also frequently applied, either curved or flat.
For curved roofs cellular beams are the ideal solution, because curving of the beams is already part of the production process and as such available at no extra cost.
Moreover, economies are achieved in comparison with plain curved beams due to weight savings. The radius of the arch is not limited by the full span length, but by the parts whereof de total arch consists.
Another well appreciated facet of curved cellular beams is their inherent aesthetical value and their light impression.
In the range of roof spans of over 30m, cellular beams are able to serve as an alternative to lattice girders, having the advantage of lower cost of labour. Long spans of over 50m have been realised already.

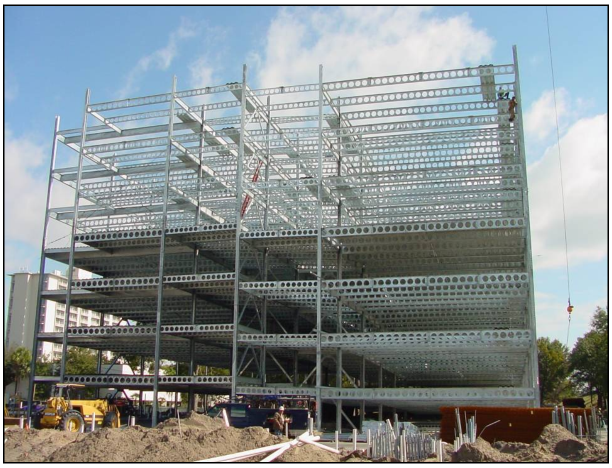

Figure 2.10 Apartment building

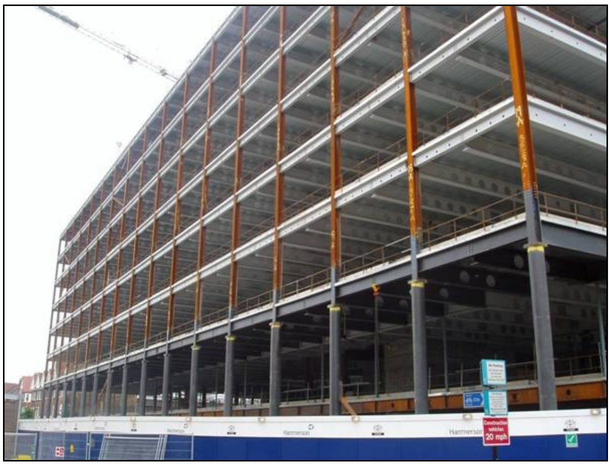

Figure 2.11 Office building

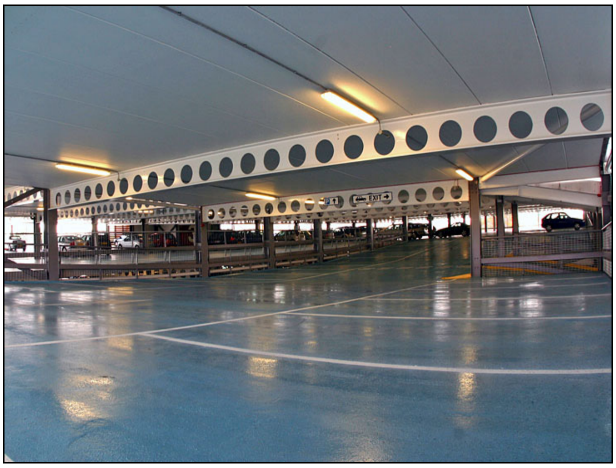

Figure 2.12 Parking garage

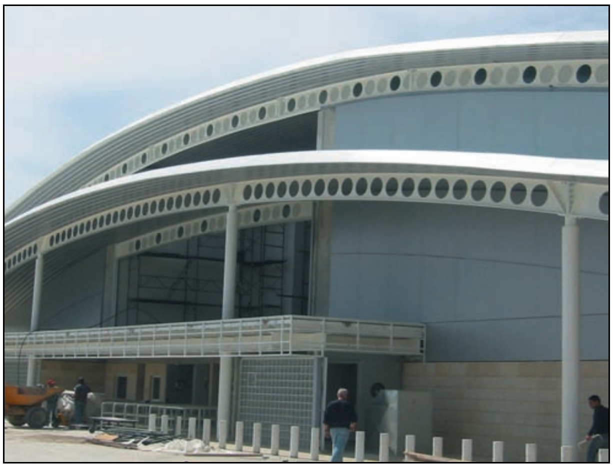

Figure 2.13 Curved roof beams

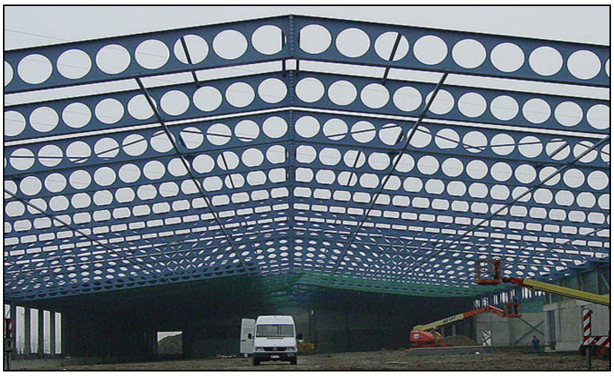

Figure 2.14 Industrial hall

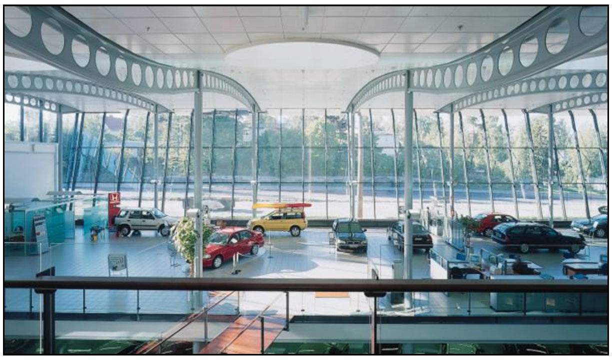

Figure 2.16 Roof structure with curved cellular beams

Contrary to the considerable amount of research devoted to the behaviour of cellular beams, resulting in design guides for practice, no published design guide exists for the application of cellular members as columns. Despite the lack of sound laboratory test evidence and the absence of practical design methods, still project are realised in which cellular members are applied vertically.

There seem to be two primary reasons to use cellular columns: economics and aesthetics. In tall single structures, such as high-bay warehouses and so-called 'super sheds', the choice is mainly driven by economics. The increased inertia of cellular columns is required to minimise the horizontal deflections induced by wind loads. In lower height columns the decision to use cellular columns is more likely to be driven by aesthetics.

Obviously the axial capacity of cellular columns is less than that of sections with a full cross-sectional area. At first sight the impact of creating web holes seems much greater for columns than for (long span) beams.

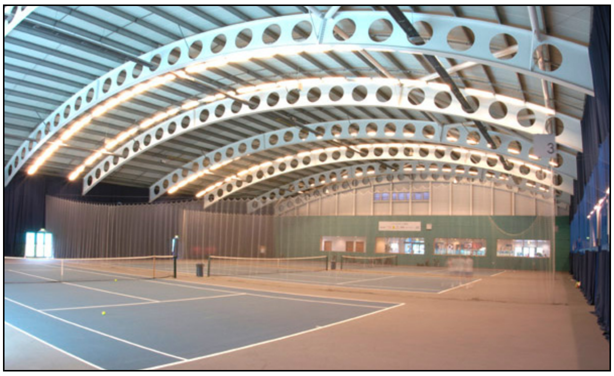

Figure 2.15 Sports hall

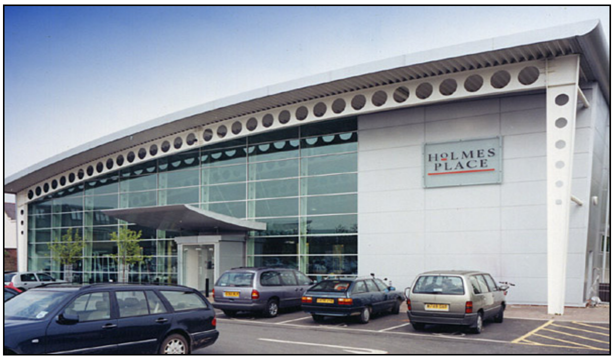

Figure 2.17 Cellular portal frame structure with tapered perforated columns

In beams the loading is mostly resisted by bending action, while in columns normally axial forces dominate. Because the web contributes more to the (pure) axial capacity than to the bending moment resistance (in the strong direction), the influence of web perforations on the pure axial capacity is more severe.

However, for slender columns it is not the pure axial capacity but the buckling resistance (in the weak direction) that governs column design. This buckling capacity depends, amongst others, on the radius of gyration being the square root of the second moment of inertia divided by the area. By the presence of a web opening this radius increases, and so does the buckling factor (ratio between the buckling capacity and the pure axial load capacity). For slender columns this increase almost outweighs the reduction in pure axial load capacity, so that the buckling load of a cellular column is nearly equal to that of the same member without perforations, but with reduced horizontal displacements.

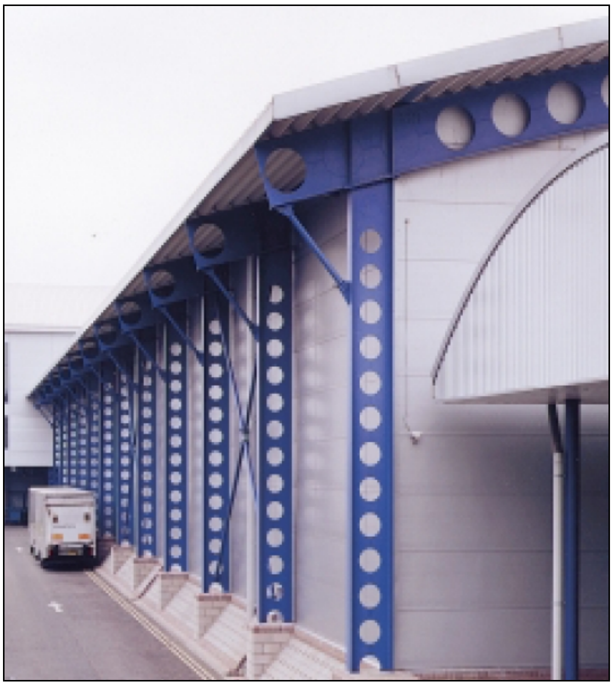

Figure 2.18 High-bay portal frame structure using cellular members

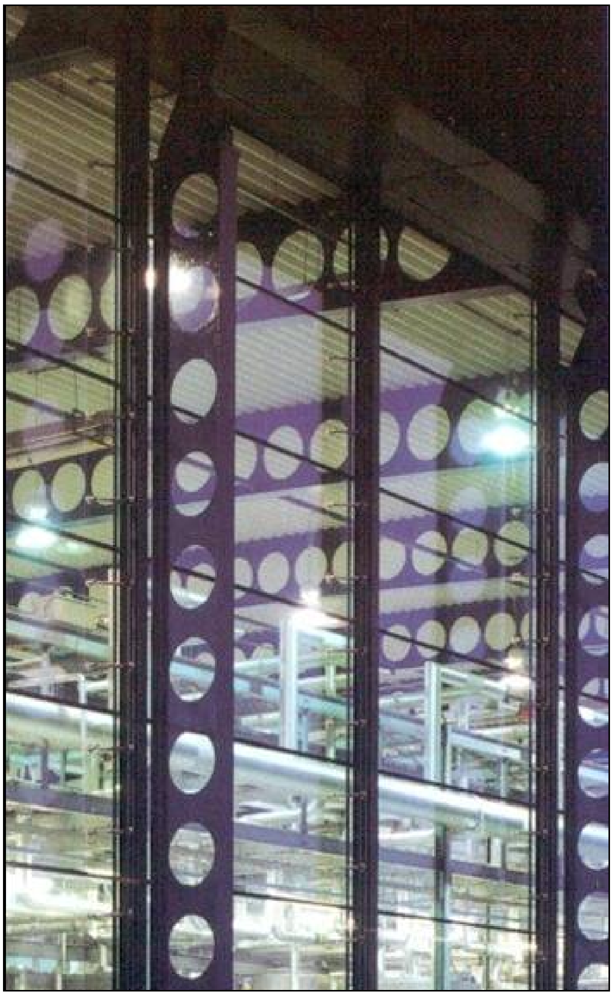

Figure 2.19 Cellular wind columns to support a glass façade

Lower height columns usually have a higher degree of axial load capacity utilisation and suffer less from buckling instability, and thus the application of cellular columns is not likely to prove economical.
But although the structural performance may be not optimal – as is the case for many solutions – the visual attractive appearance of cellular columns may very well give reason to use them anyway.
Structural efficiency is just one of all possible design criteria. For example, it is very well possible that for reasons of aesthetics it is decided that tapered columns are appropriate. But in that case a cellular taper will be the most economical solution, because no extra treatment is required.

2.4 Current research status

Beams with web openings have been a popular research theme over the past few decades. The many research projects, comprising both theoretical and experimental investigations, can be subdivided into two main categories: beams with either individual or with multiple (regularly spaced) web openings. These openings may be treated as individual when the spacing between the openings is sufficiently large to ensure that adjacent openings do not interact. Furthermore it is possible to distinguish between taking into account the composite action with the concrete floor slab or not, and whether opening reinforcement is dealt with. In the past all these categories were approached as separate design problems [Darwin 2000].
For over 100 years the influence of creating openings on the elastic stress distribution has been studied, e.g. by Chan & Redwood [1974]. However, for a number of reasons the acquired solutions are not very useful for estimating the resistance of a perforated beam. Suggested design methods most often have a very limited scope of applicability, and give only a coarse approximation of the beams's resistance by today's standards. Elastic design also ignores load capacity after first yield,

and is therefore especially inappropriate for beams with rectangular web openings, where large peak stresses will occur due to local bending. Therefore quite a lot of research has been carried out to develop more convenient design methods, and to point out which limits are applicable.

Because of the high specifications in building services in modern building construction, large individual openings are often formed in the webs of steel beams to provide passage at specific locations. These openings may have a severe penalty on the load carrying capacities of floor beams, the influence depending on the shape, size and location of the web opening.

In the 1980s and 1990s a large number of tests on steel and composite beams with discrete rectangular openings were conducted at different universities. As a result, practical design recommendations were developed and published either as separate publications:

- CIRIA/SCI P068
- Darwin 1990

or as articles in the technical journals:

- Redwood & Cho 1993
- ASCE 1992
- Chung & Lawson 2001

These design methods provide additional rules and criteria to which the design in the openings regions has to be tested. Procedures for determining the increase in deflection were developed too, most times based on elementary bending theory, but with suitable modification to account for the reduction in shear stiffness.

While these methods are geared to the design of beams with rectangular openings, beams with circular web openings may be designed by exploiting similarities in the behaviour of rectangular and circular openings.

A commonly used rule is to multiply the diameter of a circular web opening by a favourable factor of 0.45-0.50 to determine the length of an ‘equivalent rectangular opening’. This rule was first proposed by Redwood [1973], and it provides a safe though conservative approximation [Ko & Chung 2002].

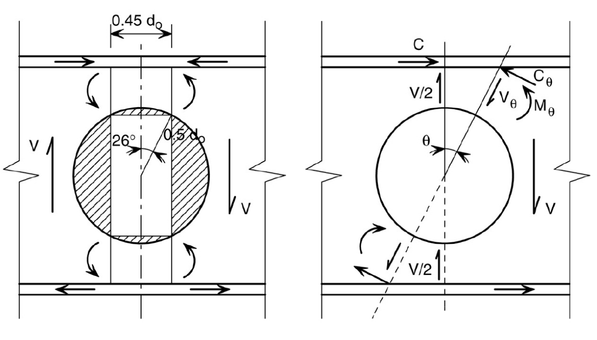

Figure 2.20 Dealing with Vierendeel bending either by an ‘equivalent rectangular opening’ or by inclined section verifications

For other opening shapes, such a modification is possible too. In a comprehensive parametric study using the finite element method, it was shown that steel beams with web openings of various shapes and sizes behave similarly amongst each other under a wide range of applied moments and shear forces, the key dimensional parameter of influence being the critical opening length. This holds for the failure modes, the load-deflection behaviour, the yield patterns as well as for the shape of the moment-shear interaction curves [Liu & Chung 2003, Chung *et al* 2003].

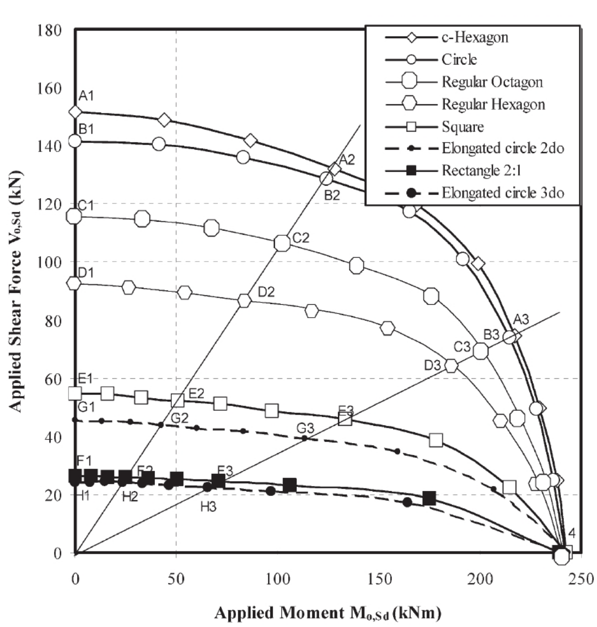

Figure 2.21 Similar moment-shear interaction curves for various opening shapes

Castellated beams were used in the 1930s already. Especially in the time when material costs were high and labour costs low, it was attractive to devise methods which increase the stiffness of steel members, without increasing the weight of steel required.

Early studies concentrated on in-plane response in both the elastic and plastic ranges. Theoretical solutions were derived, and extensive measurements were made of the stress distributions across the cross-section. Among the various methods used are photo-elastic investigations, elementary beam theory, curved beam analysis, Vierendeel analogy, finite difference techniques, various finite element schemes, etc. [Gibson & Jenkins 1957, Kolosowski 1964, Nethercot & Kerdal 1982, Nadjai *et al* 2007].

While elementary beam theory (with a reduced web-section) is the simplest method of analysis of a castellated beam, the results calculated by this method deviate appreciably from the actual values for stresses and deflections. This is because local bending is neglected in this approach [Handbook castellated beams].

The application of the theory for Vierendeel beams to the opening regions proved more successful and is still being used. At an opening location the cross-section consists of two T-sections. They carry the global bending moment as axial force and the shear causes additional local bending moments.

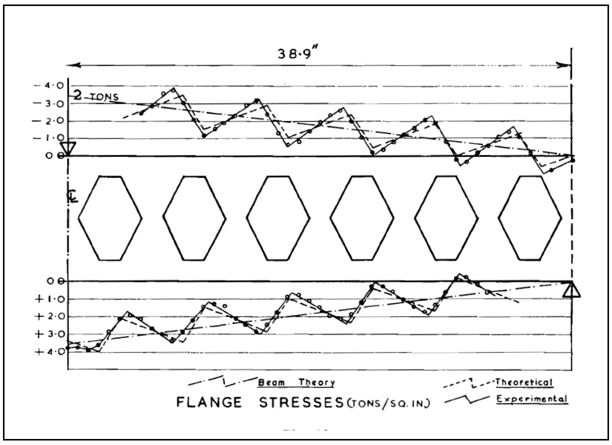

Figure 2.22 Comparison of experimental and predicted flange stresses

Usually the point of contra-flexure is assumed at mid-length of the T-sections, together with a linear variation over de opening.

Because web holes in castellated and cellular beams are closely spaced, they can interact with each other, which may lead to buckling or crippling of the posts. These interaction effects require due attention, as for slender webs they can govern the ultimate load capacity [Uenoyo & Redwood 1978].

Effectively a beam containing web holes behaves like an assembly of individual structural components, and thus it should be checked against different possible failure modes. These were summarised by Kerdal in a review of earlier carried-out experimental programmes [Kerdal & Nethercot 1984].

Compared to plain-webbed beams, the presence of web holes means that additional failure mechanisms are introduced like formation of a Vierendeel mechanism, buckling of the web-posts, weld rupture and horizontal shear failure of the web-post.

Quantitative data on the lateral-buckling behaviour of castellated beams was provided by Kerdal, who showed that this behaviour is similar to that of plain-webbed beams [PhD Kerdal, Nethercot & Kerdal 1982].

With the increase of calculation possibilities and to be in line with new building codes, design methods were updated and refined to allow a more accurate, and thus more competitive prediction of the ultimate load capacity. Attention was paid to an improved assessment of the web buckling phenomena [Zaarour & Redwood 1996, Redwood & Demirdjian 1998] and to the effect of composite action on castellated beams [Redwood & Cho 1993, Redwood 2000].

Cellular beams were first used in Switzerland in the 1970s [Stahlbau 1970s], but application became common not before the 1990s. Their introduction, together with modern building practises, like the use of long-span floors in offices and the tendency to design more slender structures, caused a revival in the research to beams with web openings.

Of course a lot of research, both theoretical and numerical, was carried out by the manufacturers of cellular beams themselves.
In 1990 the Steel Construction Institute (SCI) in the UK published a guide specifically directed towards the calculation of cellular beams [SCI P100]. The calculation method in this guide, entitled *Design of composite and non-composite cellular beams*, consists in comparing the applied actions on an inclined section with the resistance of that section, whereby the inclination angle is varied so that iterations are required to locate the critical cross-section. A linear interaction formula is used to allow for coexistence of shear forces and bending moments.
This method was later incorporated into the draft annex pre-standard Eurocode 3-1-1 Amendment A2: Annex N – *Openings in webs* [ENV1993-1-1, Annex N]. When it came to converting the ENVs to ENs, it was decided not to convert Annex N, because no consensus could be reached between the participating countries on the level of detail to be included, and also to limit the volume of EC3.
It has become common practise to distinguish between the Low Moment Side (LMS), where the local bending moment counteracts the global bending moment, and the High Moment Side (HMS), where the local and global moment act in the same direction.
In the approach of SCI P100 the ultimate capacity is limited by the formation of one plastic hinge at the Low Moment Side.
Because it was expected that for true failure by a Vierendeel mechanism four plastic hinges are required, this mechanism was investigated in more detail by Chung *et al* [2001] and a simple empirical moment-shear interaction curve was proposed.
It appears that shear yielding is very important as it promotes the formation of plastic hinges at the High Moment Side. In the paper a design method is proposed in which load distribution across the web opening that results from the formation of plastic hinges at both the LMS and HMS is incorporated.

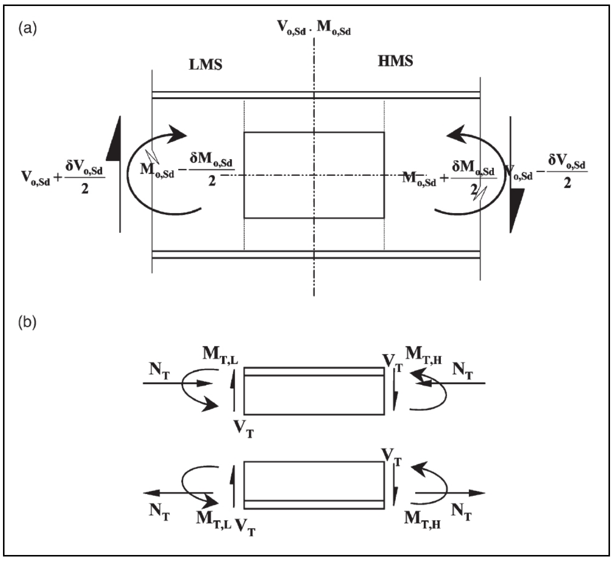
(a)
$V_{o,Sd}\cdot M_{o,Sd}$
LMS
HMS
$V_{o,Sd}+\frac{\delta V_{o,Sd}}{2}$
$M_{o,Sd}-\frac{\delta M_{o,Sd}}{2}$
$M_{o,Sd}+\frac{\delta M_{o,Sd}}{2}$
$V_{o,Sd}-\frac{\delta V_{o,Sd}}{2}$
(b)
N_T
$M_{T,L}$
V_T
$M_{T,H}$
N_T
V_T
N_T
$M_{T,L}$
V_T
V_T
$M_{T,H}$
N_T

Figure 2.23 Low Moment Side (LMS) and High Moment Side (HMS)

The method is valid for class 1/2 (plastic/-compact) sections on the assumption that instability is prohibited.
Chung recognises two design approaches to assess the structural behaviour of beams with web openings [Chung *et al* 2001]:

- T-section approach
- perforated section approach

In the T-section approach all global actions are represented as local forces and moments and these are checked against the section capacities of the T-sections, taking into account the combined effect of axial and shear force on the bending moment capacity.
The perforated section approach aims at comparing the global actions directly with the capacity of the perforated section under coexisting shear force and bending moment, e.g. in ASCE [1992] and Chung *et al* [2001].
The design procedure in the first method is rather complicated. Due to the complexity of the interaction, usually simplifications are made in order to limit the calculation effort, leading to conservative results.
In the second method simple, empirical moment-shear interaction curves are often used. Although the design rules are relatively simple, the empirical nature of the implicit allowance for the Vierendeel moment limits its scope of applicability.

The method used in the design software provided by ArcelorMittal takes its starting point in the method as described in SCI P100 and Annex N (inclined T-sections). Its scope however has been extended to cover asymmetric and composite beams as well. Furthermore the method to verify the web-post buckling phenomena has been greatly improved, and also the method to calculate deflections.

So far almost all research described took place either in the USA or Canada or in the United Kingdom (by SCI). Guidance intended for use in mainland Europe has been rather limited. For example, in Dutch only information on the analysis of castellated beams is available, which is entirely based on a smart application of the current building codes [BmS Constr A]. No reference is made to more advanced methods of calculation, and application is limited to standard castellated beam ranges.

When it became clear that Annex N would not be included in the final Eurocode, work was undertaken with the objective to update and improve the rules of the Annex, to widen its scope to composite girders and to come to design recommendations at an European level. In 2001 the ECSC project *Large web openings for service integration in composite floors* [LWO] started and was finished in 2003.

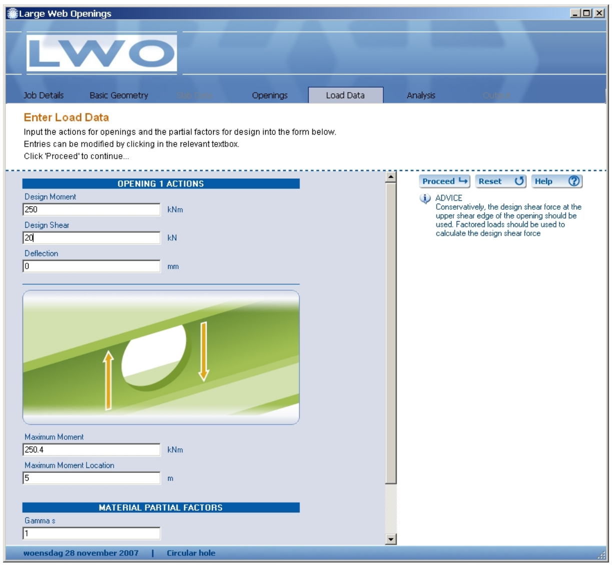

Enter Load Data

Input the actions for openings and the partial factors for design into the form below.
Entries can be modified by clicking in the relevant textbox.
Click 'Proceed' to continue...

Design Moment: 250 kNm
Design Shear: 20 kN
Deflection: 0 mm

ADVICE
Conservatively, the design shear force at the upper shear edge of the opening should be used. Factored loads should be used to calculate the design shear force

Maximum Moment: 250.4 kNm
Maximum Moment Location: 5 m

Gamma s: 1

woensdag 28 november 2007 | Circular hole

Figure 2.24 One of the outcomes of the LWO+ project: design software

The aim of the project was to experimentally and theoretically investigate the behaviour of steel and composite beams with web openings. All test results could be verified by adequate finite element simulations. For web-post buckling, a new model was proposed which is able to deal with rectangular, circular and elongated openings in a consistent manner using a 'strut analogy'.

LWO not only covers design under normal (cold) conditions, but also under fire conditions. Furthermore work was performed to contribute to improved manufacture of cellular beams.

The outcomes of the project are an extensive design guide, together with a condensed version in Eurocode-style format (proposed as a new Annex N), simplified design aids to quickly estimate a section size in predesign stage and a software for the calculation of composite beams containing web openings.

Regarding the behaviour in fire conditions, it was concluded that in general the inner edge of openings should be protected in order to avoid a specific assessment of the temperature field. Because only one loaded test was conducted, no definite guidance on the use of sprayed protection could be formulated.

In 2005 the LWO project was followed by a RFCS valorisation project [LWO+] to promote the knowledge gained (finished in 2006).

The results of the ECSC project were updated and disseminated to practitioners, and a new software was developed for design in cold condition, together with the preparation of State-of- the-Art reports in different languages.

The background theory to the design method developed in the LWO project was also presented in a number of journal papers:

- Lawson & Hicks 2005
- Lawson *et al* 2006

These also compare the outcomes of the design model to FEM analyses and real test results. However, specific topics like the fire resistance and the vibrational behaviour of those beams are not considered herein.

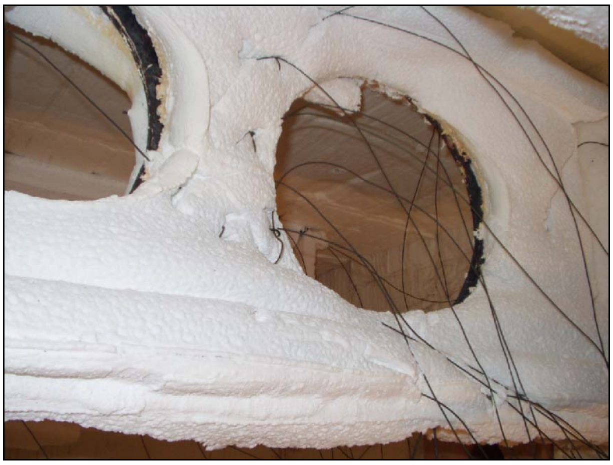

Figure 2.25 Swelling of intumescent coating due to fire

Furthermore an Access Steel resource [SN019] was prepared. This document, which is primarily aimed at practising engineers, provides the approach that was developed in the scope of the LWO project, and also gives simple design rules for openings of limited size placed at specific locations.

As a result an unified analytical design method for analysis at ambient temperature was made available to the European market.

In 2004 the *International Institute of Cellular Beam Manufactures* (IICBM) was formed, with the aim to help develop standards for the design and manufacture of cellular beams.

While the assessment of vibrational behaviour of floors using cellular beams is analogous to that of floors with plain-webbed beam, see Vibration Guide [2007], the behaviour in fire conditions is far more complex.

Until recently almost all research was concerned with design in cold situation. In more recent research attention was paid to the behaviour in fire conditions too.

From a first investigation it became clear that the openings give rise to increased web-post temperatures. Thereby the strength of the web-post may very well be critical [TN 2002].

The increased web-post temperatures were validated and confirmed for protected beams by Bailey [2004, UMIST]. For unprotected steel cellular beams no increase in web-post temperature was observed.

In the United Kingdom passive fire protection (sprayed, board) for castellated beams was usually based on a rule which says to determine the required thickness of fire protection material for the original section (from which the castellated section was cut), and then increase the thickness by 20%.

In absence of other information, this rule was often applied to cellular beams protected with intumescent coatings (active) also.

However, from the aforementioned test results it became clear that this 20% rule cannot be safely applied to cellular beams. Web-post failure (buckling, horizontal shear) often controls the design of cellular beams, and thus the increased temperatures in this zone require thorough attention. Therefore further research was conducted to understand the mechanics of the structural behaviour of cellular beams in fire, and to provide more realistic rules to determine the required thickness of intumescent coatings.

The SCI prepared a number of reports which deal with the fire design of cellular beams. Generic design guidance exists in the form of SCI RT1085. Product specific versions have been issued to intumescent manufactures, which allow more favourable limiting temperatures based on the actual performance of their particular product.

It has become apparent that failure modes are not necessarily the same for design at ambient temperature and in fire conditions. Therefore it is not adequate to base the fire protection requirements on room temperature structural analysis, as is possible for plain beams, but a separate analysis at elevated temperatures must be conducted [Simms 2007].

Now research is carried out on the fire behaviour of composite cellular beams. It has been pointed out that some axial restraint will enhance the ultimate load capacity of composite cellular beams in fire conditions greatly [Thesis Rini]. Furthermore work is going on to provide quantitative data on the structural web-post failure temperature of composite cellular beams [Nadjai *et al* 2007].

2.5 Future design development

In view of the research work already done, some areas of interest to be covered in future developments are:

- catenary effect in fire conditions for composite floors
- fire behaviour of beams with rectangular web openings
- incorporation of axial loading and different types of support conditions
- behaviour and design of tapered cellular members

It is noted here that no activities from the IICBM have been seen since 2005. Two main partners however, ArcelorMittal and Westok, have agreed to cooperate in research activities and to develop a new software for the design of cellular beams jointly. This software will also cover the design of tapered beams, elongated openings, etc. When the final versions of the Eurocodes will come into force, designers from the United Kingdom as well as those from mainland Europe will be able to use the same tool.

2.6 Advantages and disadvantages

This section summarizes the main advantages and disadvantages of cellular members.

Advantages

- increased spans possible (flexibility)
- passage of services through web openings feasible (functionality)
- specifications are easy to adjust towards specific needs (adaptability)
- the offer of a new means of architectural expression (appearance)
- availability of high-performance design tools (support)
- material savings and reduction of the number of foundations (sustainability & economics)

Disadvantages

- less suitable for concentrated loads
- more calculation effort required
- severe reduction in pure axial capacity
- increased production costs

3 MECHANICAL BEHAVIOUR OF BEAMS WITH WEB OPENINGS

3.1 Introduction

The presence of the holes in the web means that the beam's structural behaviour will be different in a number of respects from that of plain, uniform members. Not only the relative importance of the usual modes of failure is altered, but also new possible failure mechanisms are introduced. In this chapter the mechanical behaviour of beams with web openings is discussed, together with a description of the various possible failure mechanisms. Criteria to check against these failure modes are provides in the next chapter. Most attention is given in this chapter to the behaviour and failure mechanisms that differ from that of plain-webbed beams. Failure modes that are largely similar to these of standard sections are only briefly touched.
As no public test data is available regarding the behaviour of columns with web openings, only beams are dealt within this chapter.

3.2 Global bending and shear

One of the most obvious observations from tests is the large dependence of the behaviour of beams with web openings on the ratio of moment to shear, the M/V-ratio.
For simply supported beams carrying a uniform distributed load, the location of maximum applied moment (mid-span) differs from the maximum shear position (at the supports). Therefore first separate attention is given to the bending moment capacity and the vertical shear capacity.
As the global bending moment capacity is to a large extend determined by the flanges, the influence of the web perforation is rather small. Global bending of the beam will be resisted predominantly by tension in the bottom tee and compression in the upper tee.
It was already described by Toprac & Cooke [1959] that in a span, subjected to a pure bending moment, the T-sections above and below the holes yield in a manner similar to that of a plain-webbed beam. The spread of yield towards the central axis was stopped by the presence of the holes by which time the two throat sections had become completely plastic in compression and in tension. Halleux [1967] was the first to introduce plastic theory for the analysis of the behaviour of castellated beams. For fully braced specimens under pure bending, the occurrence of a pure flexural mechanism was observed indeed. Thus the behaviour is just like a plain-webbed beam.
It is obvious that the influence of web holes on the shear capacity is more pronounced. Generally it is the web that transmits the vertical shear force. The shear capacity at an opening location may be calculated by addition of the respective shear capacities of the top and bottom tee.
When the bending and the shear mechanisms are considered separately, they are rarely the critical modes of failure in cellular beams. However, for openings in the region where both shear force and bending moment are present, additional bending is created due to the transfer of the shear force across the opening.
For low M/V-ratios the effects of secondary bending may even dominate to the extend that the sign of stresses at the Low Moment Side is reversed.

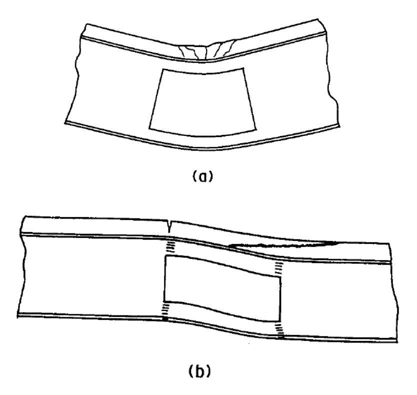

Figure 3.1 Failure of a composite beam:
a) pure bending
b) low moment-to-shear ratio

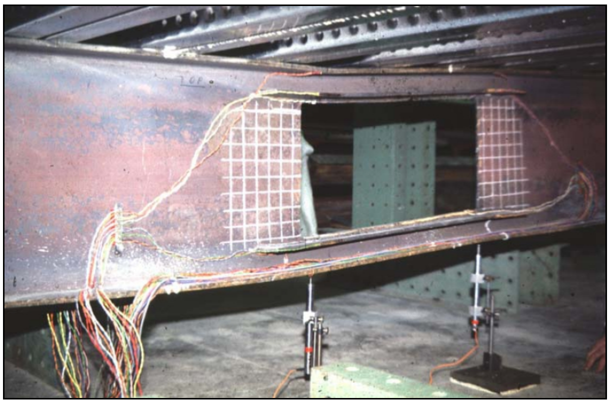

Figure 3.2 Vierendeel bending over a rectangular opening

This mechanism was first reported by Alffillisch *et al* [1957] (and also discussed by Toprac & Cooke and Halleux). In fact it is an extension of the flexure mechanism, but now with V≠0. It shows a very pronounced distortion in the manner of a parallelogram. Because of the analogy with the structural response of a Vierendeel girder, the occurrence of these secondary effects is often labelled Vierendeel behaviour.

Generally four plastic hinges at the 'corners' of a hole are required for the mechanism to develop. Failure due to this so-called Vierendeel mechanism, or a shear force mechanism, is always accompanied by excessive plastification at the plastic hinge locations. For large single web openings this mechanism is likely be decisive.

The Vierendeel moment has to be resisted by T-sections, whose capacity is reduced by the presence of axial and shear forces.

From the study of the geometrical properties of castellated beams which failed due to the formation of a Vierendeel mechanism, it is clear that this type of mechanism is more likely to develop in beams with some combination of a short span, a wide web-post and shallow tee-sections [Kerdal & Nethercot 1984]. This is because an increased size of the web-post will produce a larger secondary moment and thus stresses which are more close to those produced in a full bending situation, and also because short spans usually carry higher loads so shear force become dominant compared to the (global) bending moment. With increasing opening length the Vierendeel moment will further increase, reducing the ultimate load capacity. Enlarged openings are therefore best placed in areas where shear forces are relatively low and the full bending resistance is not yet utilised, i.e. in the area between the support and mid-span (for simply supported beams).

3.3 Lateral-torsional buckling

For beams that are not axially loaded, the only global buckling mode is lateral-torsional buckling. If no adequate lateral support is provided, this mode will almost always be dominant over the flexure mechanism. Although it has been shown that the lateral-torsional buckling capacity is indeed influenced by the presence of web openings [Thevendran & Shanmugam 1990], tests revealed no fundamental differences in behaviour: both plain-webbed and castellated beams exhibited the same laterally buckled configuration consisting of a smooth continuous profile and no distortion of the web-posts was observed [Kerdal & Nethercot 1984]. Therefore it was concluded that the provisions in the codes for the determination of the lateral buckling strength of plain-webbed beams could also be used for castellated beams, making use of the cross-sectional properties at the opening location. The alternative approach of calculating the resistance against lateral buckling of the tee-section in compression, with the effective length taken between two points of adequate lateral support, is known to be conservative.

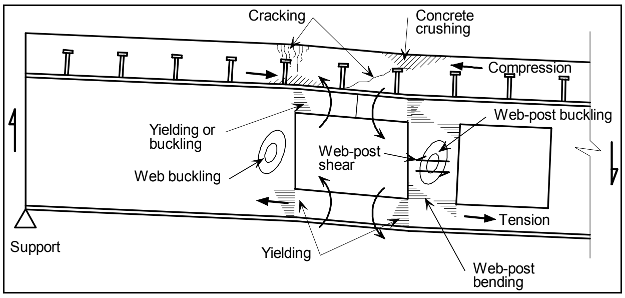

Figure 3.3 Modes of failure at closely spaced openings (composite)

3.4 Web-post failure mechanisms

Large single web openings are usually spaced at sufficient distance to avoid interaction. However, for closely spaced openings this interaction is inevitable and some new failure modes are introduced.

It follows from horizontal equilibrium that the web-post has to transmit a horizontal shearing force, being equal to the difference in tensions in the bottom chords (positive bending). In addition the web-posts in asymmetric and composite beams will also be subject to in-plane bending moments in order to maintain equilibrium between the top and bottom tees.

For narrow posts, the horizontal shear capacity, and for asymmetric openings the pure bending resistance might be decisive. For slender posts however, failure is more likely to occur by web-post instability.

In general two kinds of web-post buckling exist: lateral-torsional buckling due the horizontal shear and web crippling under concentrated loads.

The latter mode is best avoided by not placing any concentrated load above an opening region. Otherwise the beam should be reinforced locally.

Web-post buckling due to shear transfer is in many cases the controlling mechanism. From the horizontal shearing force, combined with the vertical shear forces that act on the tees, diagonal tensile and compressive action is developed in the web-post, which may cause (local) lateral-torsional buckling.

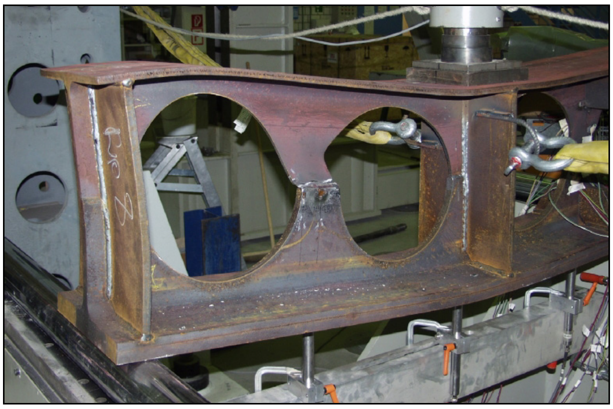

Figure 3.4 Web-post yielding due to horizontal shear

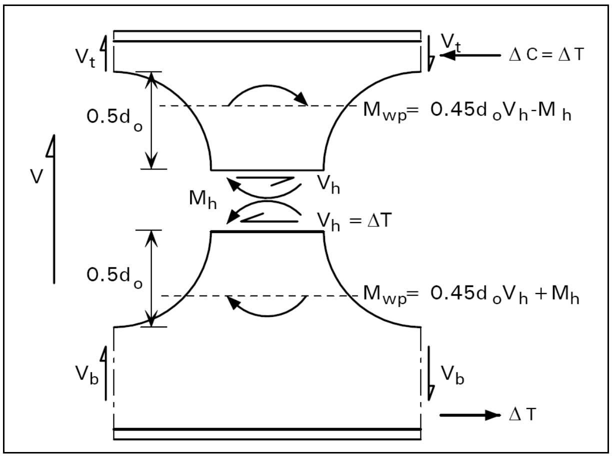

Figure 3.5 Forces in a web-post with an asymmetrically placed opening

The tendency to buckle depends on the width and height of the web-post and the d/t-ratio of the web. Due to the complexity of the problem, several design methods have been proposed. The method in SCI P100 was of empirical nature, with a limited scope of applicability. The present design method, resulting from the LWO-projects, is based on a simple but more general strut model, that also covers rectangular and asymmetric openings.

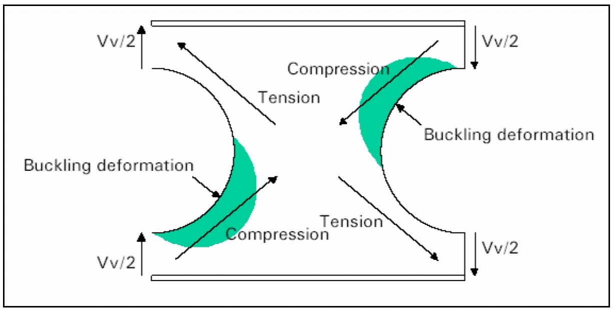

Figure 3.6 Web-post buckling behaviour

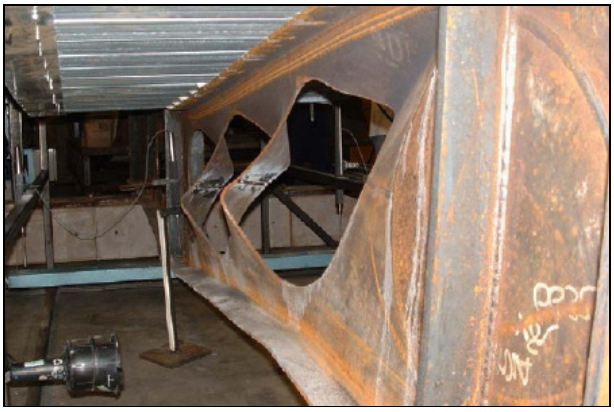

Figure 3.7 Web-post lateral-torsional buckling due to (vertical) shear

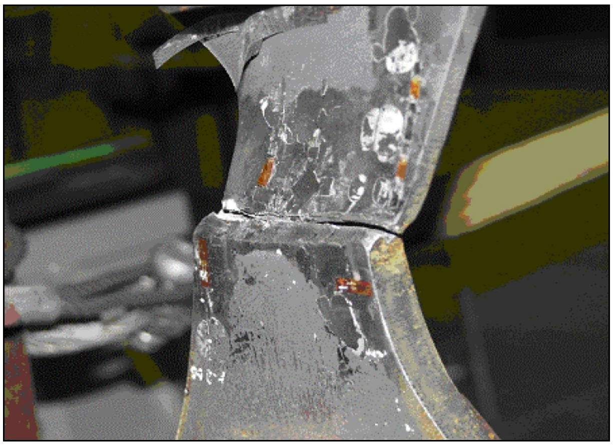

Figure 3.8 Horizontal weld rupture

In the ACB program another model for web-post buckling is used, that was developed as a part of an optimisation study to cellular beams carried out by CTICM on behalf of Arcelor. Generally said it is a more advanced model, which also covers asymmetric sections and takes into account the post-critical reserve strength. However, the coefficients to calculate the critical forces in the web-post and in the T-sections are not available in public, as they were derived from a large measurement programme of web-post imperfections in ARCELOR Cellular Beams, whereof the results are proprietary.

3.5 Additional failure modes

Apart from the above mentioned failure mechanisms, there are some additional possible failure modes. In many cases however they will not govern the design.
The weld between the two halves of a cellular beam that is produced from hot-rolled sections is always assumed not to influence the global and local structural behaviour. The required thickness is determined such that the horizontal shear force can be transmitted.
It has been shown that it is not necessary to make full butt welds. Two-sided fillet weld without chamfering have proved to be the most efficient and economical solution.
Local flange buckling is prevented by using class 3 plate parts or lower. Cellular beams made out of hot-rolled sections most often have flanges that are at least class 2 (compact), so that the full plastic capacity can be utilised. The web class may be higher, but local web buckling is prevented by using the limiting values for a class 3 web when the outstand of the web of a compressed tee is classified class 4, so that the elastic properties are used.
Shear buckling can occur in high shear areas (e.g. near supports) and is also influenced by the presence of web openings. It may govern the design of a beam with single openings, but for cellular beams usually other failure modes are dominant.
For rectangular web openings, buckling of the compressed tee should be checked. In cellular beams this failure mechanism has not been observed before reaching the cross-sectional capacity of the tee. Elongated openings were shown to behave like rectangular openings, and thus are susceptible to tee buckling too.

3.6 Serviceability performance

There are two effects due to web perforations which cause an increase in deflections. First, the second moment of area is reduced which adds to the pure bending deflection. Second, at an opening position vertical load has to be transferred by local bending instead of by shear. This term is usually called additional shear deflection and can be significant for long openings.
For cellular beams the total additional deflections usually does not exceed 20%.
Regarding vibrations, the same behaviour as for unperforated beams is observed, so that the natural frequency may be estimated by the same approximation methods (allowing for the effect of the openings).

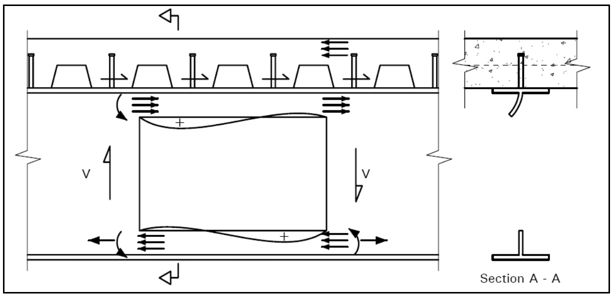

Figure 3.9 Tee buckling above a rectangular opening

3.7 Behaviour at elevated temperature

As already noted in chapter 2, on beforehand it cannot be said whether the failure mode at increased temperature will be the same as at room temperature. The web openings cause increased temperatures in the web-posts. Therefore a separate analysis in fire conditions will be necessary, accounting for the different modes of failure.

3.8 Summary of failure mechanisms

In conclusions there exist a number of failure mechanisms for beams with web openings. For non-composite cellular beams they can be summarised as follows:

Global failure modes

- pure bending
- pure shear
- interaction
- lateral-torsional buckling

Local instability modes

- shear buckling
- local flange buckling
- local web buckling

Failure at opening locations

- Vierendeel bending
- tee buckling (not for circular openings)

Web-post failure modes

- horizontal shear
- web-post moment
- interaction
- lateral-torsional buckling
- web crippling
- weld rupture

In design it is necessary to ensure that all relevant failure mechanisms are addressed. However, this may often be done in an implicit way. Furthermore, it is noted that not all modes of failure are as important. While the Vierendeel mechanism has been researched extensively (e.g. by Chung), for beams with multiple openings usually other failure modes dominate. Cellular beams are likely to fail by web-post buckling and when this is prevented, by lateral-torsional buckling. Optimisation is only to be gained when calculation methods for governing failure mechanisms are refined.

4 DESIGN METHODS FOR CELLULAR BEAMS

4.1 Introduction

In the past a number of methods have been developed to deal with web openings in beams. Most of these methods suffer from inaccuracy and/or being very tedious and time consuming. Furthermore the underlying theory often does not cover all possible failure mechanisms. In a way they are also old-fashioned. With increasing computation capabilities, far more detailed analyses are possible, taking into account initial deformations, material non-linearity etc.

Still these analyses take a lot of time and they are not pointed to every day's design practice. In addition, many medium-sized firms of consulting engineers do not have advanced finite element modelling tools available. Therefore design approaches which are formulated in analytical terms still prove their value. Even when performing an advanced analysis the use of simplified methods of calculation is essential to check the outcomes.

Because of the interaction between bending and shear –the behaviour of cellular beams depending on a large number of parameters – it is not possible to predict in advance which cross-section will be subjected to the least favourable combination of internal forces. The capacity has therefore to be verified at a large number of locations (openings, web-posts).

Because these calculations are quite tedious to perform all by hand, several manufacturers of cellular beams provide a computer program to ease the calculation. Most times these programs are also equipped with confidential results from tests (fire protection, web-post buckling model, etc), such that an enhanced capacity can be predicted.

Thus for the more general cases two options exist nowadays for the calculation of cellular beams for mainland Europe: either use the software from the manufacturer, or apply the method as developed in the LWO-projects. For designs that are outside the scope of these methods, a more advanced calculation has to be carried out (e.g. finite element analysis).

In the present chapter the LWO design method is addressed. Furthermore attention is given to some backgrounds of the ACB program for comparison.

4.2 LWO design method

4.2.1 Introduction

The ECSC project *Large web openings for service integration in composite floors* (LWO) aimed to investigate experimentally and theoretically the behaviour of steel and composite beams with web openings. One of the outcomes has been a detailed design procedure that is consistent with the Eurocodes. The method extends the guidance offered in earlier publications (SCI P068 and P100) and is applicable to hot-rolled and fabricated sections with discrete or regular spaced openings.

It covers the design of simply supported beams for the followings cases:

- highly asymmetric composite sections
- large individual openings or multiple regular spaced openings
- rectangular or circular opening shapes
- openings placed (non-)centrally in the depth of the section
- slender webs
- narrow web posts
- elongated circular openings
- fabricated sections
- notched beams
- adjacent openings

Not covered are:

- continuous beams
- tapered fabricated sections
- fire engineering design

Before, no design recommendation existed at an European level to permit design of beams with large web openings without carrying out particular tests for the individual purpose.

Here, the parts of the design method are treated that apply to *non-composite cellular beams whereof the openings are placed at the centre-line.* Eccentricities have been left out. Elongated and stiffened openings are also covered. The discussion is limited to cellular beams made out of one hot-rolled section. For fabricated beams usually some stiffening is necessary to control local buckling effects.
It is noted that, as the design method applies to *simply supported beams in bending*, usually the top tee will be in compression and the method is formulated accordingly.

4.2.2 Section classification

The role of cross-section classification is to identify the extent to which the resistance and rotation capacity of cross-sections is limited by its local buckling resistance. For each part subject to compression the class is determined depending on the width-to-thickness ratio.
The classification of the flanges may be taken as in Eurocode 3-1-1. For cellular beams made from hot-rolled sections the flange may usually be treated as class 2 or better.
Likewise the class of the unperforated web can be determined. At an opening location additional classification rules are applicable, which were taken from Annex N.
The outstand of the web of the tee is classified depending on the ratio of the effective length of the opening for stability of the web, $\ell_{o,eff}$, to the outstand depth $d_t = h_t - t_f$.
Two criteria exist, whereof *one* has to be met. Note that webs with an opening that satisfies the lower limit on $\ell_{o,eff}$ (so for small openings) are classified independently of d_t.

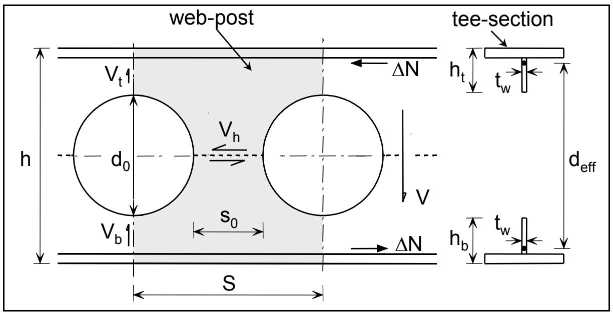

Figure 4.1 Dimensions of a web-post

Class 2 web

- if $\ell_{o,eff} \le 32 t_w \varepsilon$ or
- if $d_t \le \dfrac{10 t_w \varepsilon}{\sqrt{1 - \left(\dfrac{32 t_w \varepsilon}{\ell_{o,eff}}\right)^2}}$

For a class 2 section, the plastic properties of the tee may be used.

Class 3 web

- if $\ell_{o,eff} \le 36 t_w \varepsilon$ or
- if $d_t \le \dfrac{14 t_w \varepsilon}{\sqrt{1 - \left(\dfrac{36 t_w \varepsilon}{\ell_{o,eff}}\right)^2}}$

For a class 3 section, the elastic properties of the tee should be used. Alternatively, effective plastic properties may be determined using the limiting value of d_t for a class 2 web.
Webs that fail to satisfy the class 3 limits, are classified as class 4. However, their effective sections properties may be calculated using the limiting value of d_t for a class 3 web.

The effective length *for stability of the web* $\ell_{o,eff}$ depends on the shape of the opening:

- for rectangular openings:
  $\ell_{o,eff} = \ell_o$ (not treated here)
- for circular openings:
  $\ell_{o,eff} = 0.7 d_o$
- for elongated openings:
  $\ell_{o,eff} = \ell_o - 0.3 d_o = s + 0.7 d_o$

The above limits for d_t are in fact equal to the limits for outstand flanges in compression according to EN1993-1-1 ($10 t_w \varepsilon$ resp. $14 t_w \varepsilon$), but modified to take into account the stabilising effect that occurs due to the finite length of the opening (unless the other limit is met).

Here these limits are formulated for d_t so the radius of the root fillet is not taken into account. In Eurocode 3 the limits apply to the flat portions in compression so equal limiting values are applicable to both fabricated and hot-rolled sections. It thus seems reasonable to apply these limits to $c = h_t - t_f - r$ instead.

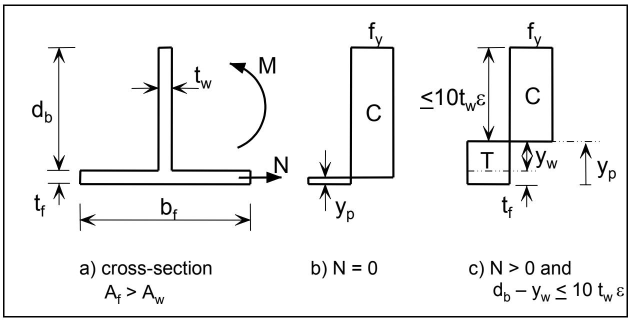

Figure 4.2 Stress blocks for T-section in local bending: effect of tension force

However, in publications dealing with the LWO method this radius is generally ignored. For positive global bending, the *bottom tee* will be (partly) tensioned in addition to the Vierendeel bending that occurs in the Tee-sections (whereof the sign can both positive/negative). Therefore a smaller part of this web will be in compression. Allowance may be made for the favourable effect of this on the stability of the web of an unstiffened tee, as follows.

Class 3 webs may be treated as class 2 if:

$$\frac{N_b}{N_{pl,b}} \geq 1 - \frac{20t_w^2 \varepsilon f_y}{N_{pl,b}}$$

The limiting case is illustrated in Figure 4.2c, where the depth of the web in compression equals exactly $10t_w\varepsilon$. For the bending moment two equal areas of $10t_w^2\varepsilon$ are available (in the web and flange) and the part in between is reserved for tension.

When the condition is not met, the effective (plastic) depth can be calculated accurately by:

$$d_{b,eff} = \frac{N_b - N_{pl,f} + 20t_w^2 \varepsilon f_y}{t_w f_y}$$

where $N_{pl,f}$ is the tensile resistance of the flange of the bottom tee.
As this expression requires the input of N_b, for simplicity the plastic properties may be determined using $d_{b,eff} = 10t_w\varepsilon$.

Herein no stabilising effect of the finite length of the opening is taken into account, but the mere limit of $10t_w\varepsilon$ is kept. It seems to make sense to include this effect in a similar way as done for the classification limits for d_t (i.e. relaxation of the $10t_w\varepsilon$ limit).

Class 4 webs may be treated as class 3 subject to one of the following conditions:

- if $\ell_{o,eff} \leq 36t_w\varepsilon^1$ or
- if $d_b \leq \dfrac{14t_w\varepsilon^1}{\sqrt{1-\left(\dfrac{36t_w\varepsilon^1}{\ell_{o,eff}}\right)^2}}$

where:

$$\varepsilon^1 = \frac{\varepsilon}{\sqrt{1 - N_b / N_{pl,b}}}$$

Double-sided stiffened webs can be treated as internal compression elements to EC3.

4.2.3 Global bending resistance

At an (symmetrical placed) opening position the applied global bending moment has to be resisted by compression and tensile forces in the top and bottom tees:

$$N_t = \frac{M_{Ed}}{h - 2y_e} \leq A_t f_y$$

The elastic neutral axis depth of a tee reads:

$$y_e = \frac{A_w\left(t_f + d_t/2\right) + A_f t_f/2 + A_s\left(t_f + d_t - e_s\right)}{A_w + A_f + A_s}$$

where A_s is the cross-sectional area of the horizontal stiffeners, which centres are placed at a distance e_s from the tip of the outstand web (so symmetrically placed with respect to the opening).

4.2.4 Shear resistance

The effect of web openings on the shear resistance is severe. However, for most long spans the utilisation of the unperforated web in shear is relatively low and thus a considerable reserve of shear resistance exists.

The pure shear check of a perforated section is an upper-bound to the capacity. Due to the nature of shear transfer across the openings (Vierendeel bending), the full shear resistance is not mobilised.

For *plastic design* (class 1 or 2 sections) the shear capacity is defined as:

$$V_{pl,Rd} = \frac{A_v\left(f_y/\sqrt{3}\right)}{\gamma_{M0}}$$

where A_v is the shear area. For a perforated section a reduced shear area $A_{v,o}$ applies.

This shear area is defined different in the various publications that deal with the LWO design method. As for symmetrical sections with centrally placed web openings the tees are equal, the total shear area can also be determined from:

$$A_{v,o} = 2A_{v,t}$$

LWO design guide Section 2.5

The shear area for pure vertical shear, established from the web area of the perforated hot-rolled section, is given by:

$$A_{v,o} = \left(h - d_o\right)t_w$$

where h is the beam depth.

This expression includes a small part of the flange, $t_f t_w$.

It is noted furthermore that the use of only the web area is very conservative for rolled sections with large flanges. For tee-sections, according to EN1933-1-1 even a lower shear area should be used:

$$A_{v,t} = 0.9\left(A_t - b\,t_f\right)$$

So the root radii are considered, but a shape factor of 0.9 is applied to account for the non-uniform stress state in a tee.

LWO design guide Section 8.5

In this chapter of the (same) design guide, the application rules for design of beams with web openings are given in a condensed format. It defines the shear area of a tee (implicitly) as:

$$A_{v,t} = 0.9\left[\left(2r + t_w\right)t_f/2 + d_t t_w\right]$$

The shape factor for a tee is kept here, but a part of the flange is taken into account also, analogous to the expression in the Eurocode for rolled I and H sections. However, the radii of the root fillets itself are not considered.

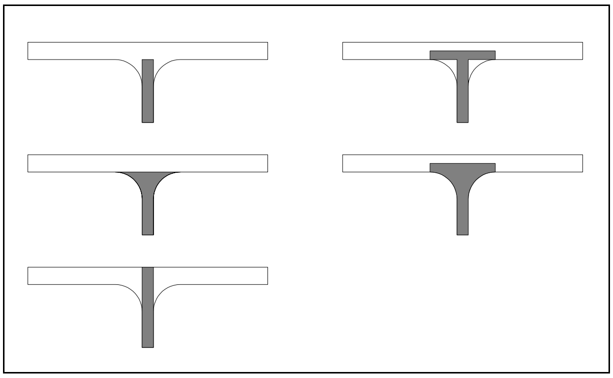

Figure 4.3 Various shear areas for a tee

Eurocode design method

Together with the full LWO design guide, a shorthand version was produced separately. It resembles the aforementioned chapter 8 of the LWO design guide. It presents the shear force capacity as the plastic shear resistance of the unperforated cross-section, decreased with the shear capacity due to the web opening. Thus the shear area effectively becomes (for cellular beams made from hot-rolled sections):

$$A_{v,o} = A - 2b\,t_f - d_o t_w + \left(t_w + 2r\right)t_f$$

which in fact removes the 0.9 shape factor, utilises a part of the flange and takes into account the root radii itself also.

So different expressions for the shear area are given, all in publications which result from the same LWO project. The results will not differ much from each other however.

For horizontally stiffened tees the stress state will be similar to that observed in I or H sections, so the shape factor may be set to 1.0.

For *elastic design* (class 3 or 4 sections) the maximum occurring shear stress is limited to:

$$\frac{\tau_{Ed}}{f_y/\left(\sqrt{3}\gamma_{M0}\right)} \leq 1.0$$

This verification is conservative because it excludes partial plastic shear distribution, which is permitted in elastic design.

For I or H sections the shear stress in the web may be taken as:

$$\tau_{Ed} = \frac{V_{Ed}}{A_w} \text{ if } A_f/A_w \geq 0.6$$

In the LWO publications no remarks are made regarding the elastic shear capacity, but the plastic shear capacity is used always.

When the applied shear force is greater than half the plastic shear resistance of the cross-section, allowance should be made for its effect on the bending moment resistance. For $V_{Ed} / V_{Rd} > 0.5$ the bending moment resistance may be calculated by using either a reduced yield stress for the shear area:

$$f_{y,red} = (1-\rho) f_y$$

or an effective thickness for the web:

$$t_{w,eff} = (1-\rho) t_w$$

where:

$$\rho = \left(\frac{2V_{Ed}}{V_{pl,Rd}} - 1 \right)^2$$

In elastic design, each stress situation should satisfy the Von Mises yield criterion.

4.2.5 Shear buckling capacity

Standard hot-rolled sections are not susceptible to shear buckling. As the height of beams with web openings is increased, the h_w / t_w-ratio also increases. For an unperforated section shear buckling should be checked if:

$$\frac{h_w}{t_w} > 72 \frac{\varepsilon}{\eta}$$

where $h_w = h - 2t_f$ and for the shear area factor may be taken $\eta = 1.20$ for steel grades up to and including S460 (recommended value, also adopted in the Dutch annex). When only the contribution on the web is taken into account (as the flanges will be utilised by the bending moment), the shear buckling resistance according to EN1993-1-5 reads:

$$V_{b,Rd} = V_{bw,Rd} = \frac{\chi_w f_y h_w t_w}{\sqrt{3}\gamma_{M1}}$$

The shear buckling capacity of a web with an isolated opening is calculated by a reduction to the capacity of a unperforated web:

$$V_{b,o,Rd} = 0.9 V_{b,Rd} \left(1 - \frac{\sqrt{d_o \ell_o}}{h_w} \right)$$

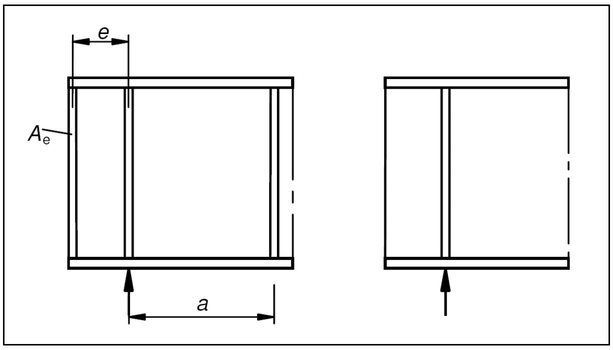

Figure 4.4 End post conditions: rigid (left) and non-rigid (right)

When the openings is at least $0.8h_w$ from the end of the beam, $V_{b,Rd}$ may be taken as that for a rigid end post as defined in EN1993-1-5, irrespective of the actual end post. For circular openings ℓ_o equals d_o so the reduction factor becomes:

$$0.9\left(1 - \frac{d_o}{h_w}\right)$$

This reduction factor has been found by trial-and-error from a parameter study and is only applicable to openings which satisfy certain geometrical limits (given further on). The factor of 0.9 only appears in the design guide, but not in the research report itself. It has also been left out in the most recent publication, the Access Steel resource *NCCI: Design rules for web openings in beams* [SN019].

The model for shear buckling is based on tension field action and is therefore only applicable to isolated openings. It requires compression to be developed in the web. For regular spaced openings this cannot occur. However, in that case web-post buckling will be more critical, while for large openings Vierendeel bending will dominate.

4.2.6 Vierendeel bending resistance

Vierendeel bending occurs at the four 'corners' of an opening and is required to maintain equilibrium across the opening. As a part of the web is removed, the shear force has to be transferred by bending of the tees.

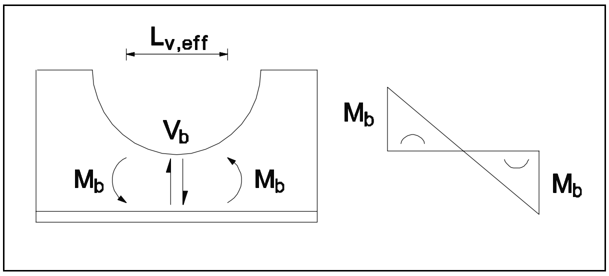

Figure 4.5 Shear force limitation due to Vierendeel bending

The total applied Vierendeel moment is calculated by:

$$M_v = V_{Ed}\ell_{v,eff}$$

where $\ell_{v,eff}$ is the effective opening length *for Vierendeel bending*.

According to the *LWO design guide*:

- for rectangular openings:
  $\ell_{v,eff} = \ell_o$ (not treated here)
- for circular openings:
  $\ell_{v,eff} = 0.45d_o$
- for elongated openings:
  $\ell_{v,eff} = \ell_o - 0.5d_o = s + 0.5d_o$

For sake of consistency, the effective opening length for Vierendeel bending of an elongated opening should be taken as:

$$\ell_{v,eff} = \ell_o - 0.55d_o = s + 0.45d_o$$

as is done in the *Eurocode design method* that was published separately (the proposed new Annex N).

The shear force that can be transferred across an opening is limited due to Vierendeel bending (see Figure 4.5):

$$V_b \le 2M_{b,red}/\ell_{v,eff}$$

The global shear force therefore is limited by:

$$V_{Ed} \le \left(2M_{b,red} + 2M_{t,red}\right)/\ell_{v,eff}$$

or formulated in terms of the total Vierendeel bending moment:

$$M_v \le 2M_{b,red} + 2M_{t,red}$$

In these formulas $M_{t,red}$ and $M_{b,red}$ are the bending moment resistances of the top and bottom tee respectively, reduced for axial tension and shear.

For symmetrical cellular beams $V_b = V_t = \frac{1}{2}V_{Ed}$ Furthermore M_t and M_b are equal. When the beam is loaded only perpendicular to its axis, and *no global axial force* N_{Ed} is applied, the same holds for $M_{b,red}$ and $M_{t,red}$ and thus the verification can be performed by:

$$M_v \le 4M_{t,red}$$

For circular openings this criterion generally will not be decisive, as the tee-section height increases towards the web-post. Therefore the shear force will not be further limited by the Vierendeel bending moment capacity.
It is important however for rectangular openings.

4.2.7 Bending resistance of tees

For $A_s \le A_f - A_w$ (which will most likely be the case) the plastic neutral axis is located in the flange:

$$y_p = \frac{A_w + A_f + A_s}{2b}$$

and the corresponding plastic bending moment resistance reads:

$$\begin{aligned} M_{pl,t} = {} & A_w f_y \left(d_t/2 + t_f - y_p\right) + \\ & A_f f_y \left(t_f/2 + y_p^2/t_f - y_p\right) + \\ & A_s f_y \left(t_f + d_t - e_s - y_p\right) \end{aligned}$$

Otherwise the plastic neutral axis is located in the web of the tee:

$$y_p = \frac{A_w + A_f + A_s}{2t_w}$$

and the corresponding plastic bending moment resistance is given by:

$$\begin{aligned} M_{pl,t} = {} & A_w f_y \left(\left[y_p - t_f\right]^2/d_t + d_t - 2y_p\right) + \\ & A_f f_y \left(y_p - t_f/2\right) + A_s f_y \left(t_f + d_t - e_s - y_p\right) \end{aligned}$$

For class 3 flanges or class 4 webs that are reduced to class 3 limits, the elastic resistance has to be used.

The elastic bending moment is calculated by:

$$M_{el,t} = \frac{1}{\max\left(d_t + t_f - y_e, y_e\right)} \cdot \Big(A_w f_y d_t^2/12 + A_w f_y \left[t_f + d_t/2 - y_e\right]^2 + \cancel{A_f f_y t_f^2/12} + A_f f_y \left[y_e - t_f/2\right]^2 + \cancel{A_s f_y t_s^2/12} + A_s f_y \left[t_f + d_t - e_s - y_e\right]^2 \Big)$$

The terms that are struck-through may be neglected for simplicity.

4.2.8 Interaction with normal force

The bending resistances of the tees are reduced when subjected to axial load.
For unstiffened tees in all cases a quadratic interaction formula may be used.

$$M_{pl,t,red} = M_{pl,t}\left(1 - \left[N_t / N_{pl,t}\right]^2\right)$$
$$M_{el,t,red} = M_{el,t}\left(1 - \left[N_t / N_{el,t}\right]^2\right)$$

For stiffened tees a linear reduction applies conservatively to the plastic bending moment resistance:

$$M_{pl,t,red} = M_{pl,t}\left(1 - \left[N_t / N_{pl,t}\right]\right)$$
$$M_{el,t,red} = M_{el,t}\left(1 - \left[N_t / N_{el,t}\right]^2\right)$$

The interaction of bending with normal force may be ignored for $N_t \le 0.25 N_{pl,t}$.

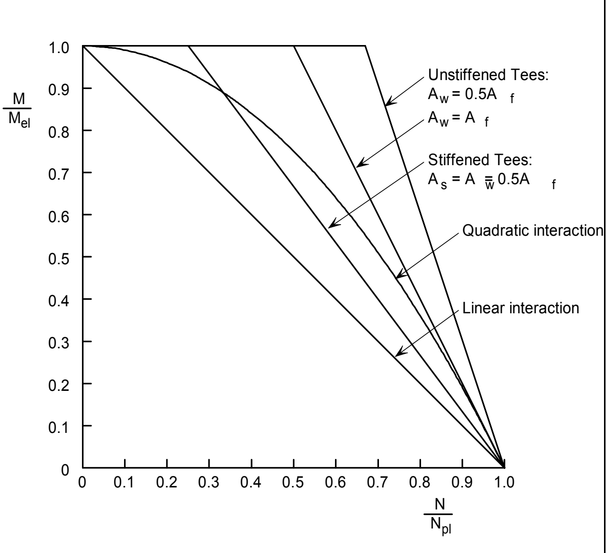

Figure 4.6 Interaction curves for tees under bending moment and axial force

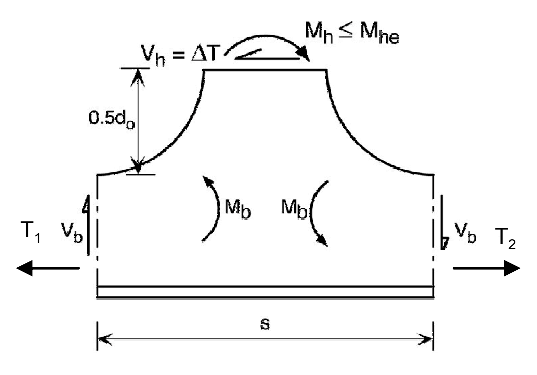

Figure 4.7 Equilibrium of the bottom web-post

4.2.9 Web-post horizontal shear

Web-post shear occurs due to the development of longitudinal forces in the tee-sections, necessary to resist global bending.
The horizontal shear force at the centre-line of the opening is given by:

$$V_h = \Delta T = T_2 - T_1 = \frac{M_2 - M_1}{h - 2y_e} = \frac{V_{Ed}\, s}{h - 2y_e}$$

For symmetrical (non-composite) cellular beams, where $V_b = V_t = V_{Ed}/2$, it then follows from moment equilibrium that the web-post moment $M_h = 0$ (for constant vertical shear).
The horizontal shear resistance of the web-post is given by:

$$V_{h,Rd} = s_o t_w f_y / \sqrt{3}$$

where s_o denotes the centre-to-centre spacing of the openings. Tests have shown that the pure shear strength may be developed in the web-post, despite the complex stress state that exists in the web.
The above formulas are also applicable to the analysis of adjacent circular and/or elongated openings in cellular beams, wherefore the appropriate centre-to-centre spacing has to be taken: $s = \frac{3}{2}\left(s_o + d_o\right)$ resp. $s = 2\left(s_o + d_o\right)$.

4.2.10 Web-post buckling

An upper bound to the web-post buckling resistance may be formulated by the bending moment resistance at a distance of $0.5d_o$ from the centre-line of the opening. The moment acting on the top or bottom of the web-post is then given by $0.5V_h d_o \pm M_h$, but because of

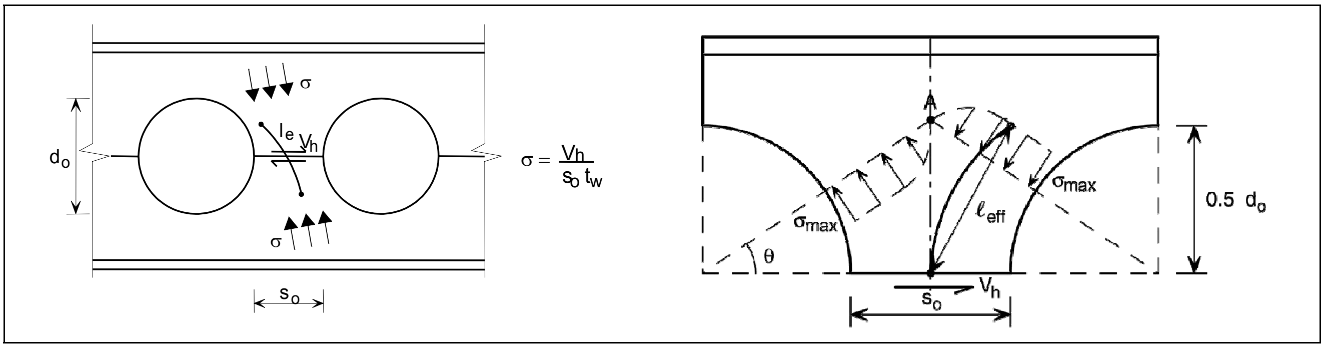

Figure 4.8 Strut model for web-post buckling

the increased width of the web-post that resists this moment, this criterion generally will not be important for circular openings. For rectangular openings (not treated here) however, web-post bending (i.e. Vierendeel bending) is likely to control design.

The buckling phenomenon is assessed by a simple compression field model. It covers cellular, rectangular and elongated openings, which may be asymmetrically placed, and can be closely or widely spaced.
The transition from widely spaced to closely spaced openings is taken to occur at an edge-to-edge spacing equal to the opening depth, i.e. for $s_o = \ell_o$.
It is noted that in the model the critical sections is assumed to be located at $0.5d_o$ from the centre-line of the web-post although for circular openings the critical height is closer to $0.45d_o$. However, for simplicity the same value is taken as for rectangular openings.

The basic verification reads:

$$\sigma_c \le \sigma_{c,Rd}$$

The compressive strength is established from buckling curve c in EN1993-1-1, with an effective slenderness:

$$\bar{\lambda} = \frac{\lambda}{\lambda_1} = \frac{1}{\lambda_1} \cdot \frac{\ell_e}{i} = \frac{1}{\lambda_1} \cdot \frac{\ell_e}{t_w / \sqrt{12}}$$

where ℓ_e is the effective length of the web-post and $\lambda_1 = \pi\sqrt{E/f_y} = 93.9\varepsilon$.

Closely spaced openings: $s_o \le d_o$
For simplicity the horizontal shear stress acting on the narrowest part of the web-post is used in the design model to represent the compressive stress:

$$\sigma_c = \frac{V_{h,eff}}{s_o t_w}$$

where the effective horizontal force in the web-post takes into account the web-post moment:

$$V_{h,eff} = V_h \pm 2M_h / d_o$$

which for centrally placed openings thus reduces to V_h.
The effective length of the web-post for circular openings is given by:

$$\ell_e = 0.5\sqrt{s_o^2 + d_o^2} \le 0.7d_o$$

Widely spaced openings: $s_o > d_o$
When some openings in a cellular beams are filled, the web-post buckling check may be performed based on a model with widely spaced openings, where the interaction between the openings can be neglected.
The design compressive stress in the web-post is taken as vertical shear force in the tee acting over an effective web-post width of $0.5d_o$:

$$\sigma_c = \frac{V_t}{0.5d_o t_w}$$

The effective length is taken as the limiting value, $\ell_e = 0.7d_o$.

The web-post buckling criterion can be re-arranged in terms of the global shear force:

$$V_{Ed} \le \frac{4M_b / \ell_{v,eff} + \sigma_{c,Rd} t_w s_o (d_0 / s)}{1 + d_0 / (h - 2\,y_e)}$$

Web-post buckling in cellular beams does not need to be checked if $d_o \le 20 t_w \varepsilon$.

When ring stiffeners are applied to both openings near the web-post, the effective length may be further reduced by a factor of 0.7 as buckling along the edge of the opening is prevented. Ring stiffened openings with a diameter less than $40 t_w \varepsilon$ may be considered as fully restrained against web-post buckling.

The restraining effect is less when ring stiffeners are present at one side of the web-post only. In that case the reduction factor to the effective length of the strut becomes 0.85. For wider web-posts with $s/d_o \ge 1.5$ no effect of the adjacent ring stiffener is to be taken into account.

4.2.11 Pattern loading

It's important to realise all possible load combinations. While for plain-webbed beams it is usually sufficient to check the capacity for a fully loaded span, for beams with web openings it is necessary to consider the load really as free to account for the effects of pattern loading. A minimum shear force of 15% of the maximum shear force at the supports is recommended to replicate these effects. The value of the horizontal shear force must be compatible with this minimum vertical shear force.

In construction condition the mid-span section may be loaded by co-existent bending moment and shear while under service loading only bending occurs. Then the minimum shear force is taken as 25% of the maximum shear force, which represents the worst case of loading acting on half of the span.

Because pattern loading also reduces the bending moment, this coincident moment may be taken as 85% respectively 75% of the maximum moment in the span for the relevant design case.

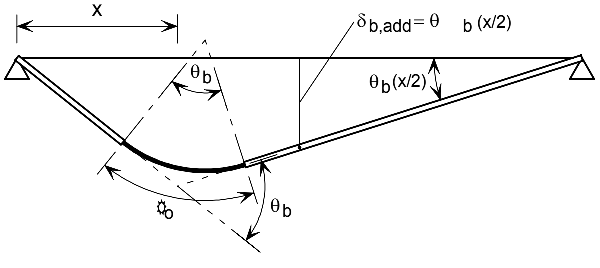

(a) Additional bending deflection due to opening

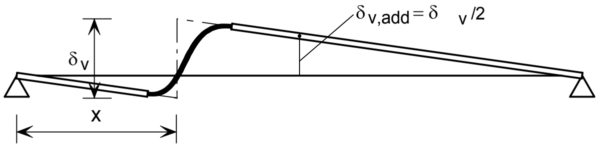

(b) Additional shear deflection due to opening

Figure 4.9 Components of deflections due to web openings

Of course it is also possible to allow for these effects by considering all the relevant loading combinations.

4.2.12 Serviceability behaviour

Serviceability performance is established using elastic properties. From tests it has been observed that the load-deflection response is quite similar to that of plain-webbed beams. Therefore simplifications are possible when assessing the additional deflections due to the presence of large web openings. The increased deflections are caused by two of effects:

- additional deflection due to loss of flexural stiffness due to openings
- additional shear deflection due to Vierendeel bending effects at large web openings

The following approximate empirical formula gives the additional deflection for a single openings, as relative to the pure bending deflection δ_b without openings:

$$\frac{\delta_{add}}{\delta_b} = k_o \left(\frac{\ell_o}{L}\right)\left(\frac{d_o}{L}\right)\left(1-\frac{x}{L}\right) \quad \text{for } x \le 0.5L$$

This formula is based on the pure bending deflection due to the loss of stiffness at the opening, but is extended to include the influence of the deflection in the high shear regions by the term $(1 - x/L)$.

The modification factor k_o is given by:

$k_o = 1.5$ for stiffened openings

$k_o = 2.0$ for unstiffened openings

For circular openings a reduction factor of 0.5 applies, so that the opening length may be taken as $0.5d_o$. The formula becomes more conservative for shorter openings where Vierendeel deflections are less.

For multiple similar sized openings, the additional deflection is given by:

$$\frac{\delta_{add}}{\delta_b} = 0.5N_o k_o \left(\frac{\ell_o}{L}\right)\left(\frac{d_o}{L}\right)$$

The factor of 0.5 represents the combined effect of the distribution of moment and shear along the beam.
Generally the total deflection of a cellular beams is $10-15\%$ more than that of the equivalent unperforated beam.

The same calculations may be used for assessment of the natural frequency. calculations. Similar to plain-webbed beams, as a good approximation the natural frequency is given by:

$$f = 18/\sqrt{\delta_{sw}}$$

where δ_{sw} is the maximum deflection in mm due to permanent loads (selfweight plus finishes plus 10% of the imposed loading).

4.2.13 Stiffener requirements

The effect of *ring stiffeners* is to reduce the tendency of the web to buckle. In the LWO web-post buckling model the presence of ring stiffeners is taken into account.
However, in the publications dealing with the LWO method no rules have been given to determine the increase in strength due to the presence of the ring stiffeners.

On the contrary, rules are provided to deal with the effect of *horizontal stiffeners* on the local bending resistance of the tees (see 4.2.7), but no account is taken of it's influence on the web-post buckling behaviour. In addition the rules seems applicable directly to stiffened rectangular openings only.

The stiffeners itself have to be classified (just as the tee-sections, wherefore see 4.2.2), and should not exceed the limits for a class 3 (semi-compact) section. For plastic design, the width outside the class 2 limit is considered as ineffective.

The maximum size of the stiffener is generally controlled by the ability of the web to resist the local anchorage forces, which are transferred by the weld between the stiffener and the web. The anchorage length ℓ_a beyond the opening therefore at both sides should satisfy the following criteria:

- a quarter of the opening length: $\ell_a \geq 0.25\ell_o$
- shear resistance of the fillet welds: $\ell_a \geq \dfrac{F_{s,Ed}}{2naf_{vw}}$ (2 welds for each side)
- shear resistance of the stiffeners: $\ell_a \geq \dfrac{F_{s,Ed}}{nt_s f_{ys}/\sqrt{3}}$ (one side or both)
- shear resistance of the web: $\ell_a \geq \dfrac{F_{s,Ed}}{2t_w f_y/\sqrt{3}}$ (above/below stiffener)

where:

$F_{s,Ed}$	is the design axial force in the stiffener (may be taken equal to the design resistance $F_{s,Rd}$)
n	denotes the number of sides of the stiffener: 1 for a single-sided stiffener 2 for double-sided stiffeners
a	is the throat thickness of the fillet weld
f_{vw}	is the design shear strength of a fillet weld (see EN1993-1-8)
f_{ys}	is the yield strength of the stiffener

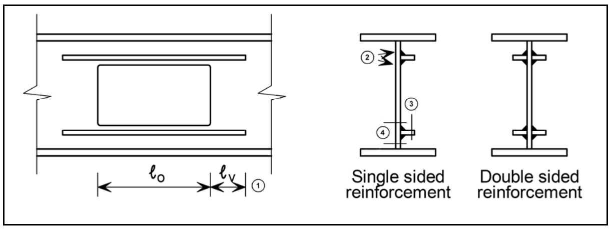

Figure 4.10 Single-sided and double-sided horizontal stiffeners

These are the (corrected) limits as defined in the proposed new Annex N (Eurocode design method). In the full design guide some more simple expressions are given, not checking for all possible shear force failures. These rules do limit the maximum anchorage length to twice the width of the stiffener $(2d_s)$, which accounts for the fact that the shear load transfer will occur mainly over the first part of the stiffener beyond the opening.
Furthermore it prescribes an maximum ratio between the web and the stiffener thickness, $t_w / t_s \le 1.2$ in the limit when $\ell_a = 2d_s$ or linearly reduced for smaller anchorage lengths. For single-sided stiffeners a further reduction factor of 0.8 applies in order to account for transverse bending of the stiffener.

While these limits seem reasonable to a certain extend, the Eurocode itself does not provide such severe limits. Furthermore for cellular beams the actual anchorage length is not really limited by the presence of the holes, as the circular shape of the holes ensure that a proper part of the web is connected to the stiffener. After all, for portal frames it is expected that stiffeners will be used only when point loads cannot be avoided above a opening (e.g. for rafters in roofs) and not for creating elongated or even rectangular openings.
Therefore, and for clarity, it makes sense to just use the four criteria on the anchorage length as given in the *Eurocode design method*.

Further the cross-sectional area of the stiffeners should not exceed half the area of the cut-out by the hole, in order to ensure that the adjacent web is strong enough to resist the forces transferred from the stiffeners:

$$A_s \le 0.5 d_o t_w$$

The practicality of connecting the stiffeners to the web should be given due attention. For welding the offset of the stiffener should be sufficient.
The weld size may be determined from:

$$a = \frac{F_{s,Rd}}{2\ell_a f_{vw}}$$

where $F_{s,Ed}$ again may be taken equal to $F_{s,Rd}$.

Vertical stiffeners may be required at secondary beam locations or in case of heavy point loads. When provided they should be full-depth.

4.2.14 Geometrical limitations

Geometric limits on the positions and sizes of web openings are appropriate in order to ensure adequate design. Such limits are given in Table 4.1. These are not 'hard' limits, but may be relaxed if justified by sufficient test data or more advanced calculation methods. The limits are based on background research for design cases where beams are subject to uniformly distributed load or multiple point loads.

4.2.15 General design considerations

Elongated openings are best placed in areas where shear forces are low, i.e. around mid-span of a simply supported beam. A further general advice is to avoid stiffeners as much as possible, as they contribute substantially to the total costs.

Floor beams are designed for maximum load capacity. Therefore often steel grades of S355 and up are used.

Roof beams are designed for maximum stiffness, and thus the height is maximised. Only when strength capacity becomes important higher steel grades are used.

Table 4.1 Geometrical limits for symmetrical cellular beams (with elongated openings)

Parameter	**Limit**		**Comment**
	circular	elongated	
opening diameter	$d_o \leq 0.8h$	$d_o \leq 0.7h$	sensible limit which satisfies the limits below
spacing	$s_o \geq 0.2d_o$	$s_o \geq 0.5d_o$ $\geq 0.5\ell_{v,eff}$	if elongated opening is placed next to the support
end distance	$s_e \geq 0.5d_o$ $\geq 0.5h$	$s_e \geq h$ $\geq \ell_{v,eff}$	governed by horizontal shear stresses and web buckling at the first opening
depth of tees	$h_t \geq t_f + 30\,mm$	$h_t \geq 0.1h$	
opening length	–	unstiffened: $\ell_{v,eff} \leq 2d_o$ stiffened : $\ell_{v,eff} \leq 2d_o$	
minimum distance to point load	$0.5h$ $0.25d_o$	h $0.5d_o$	separate buckling check needed at point load position

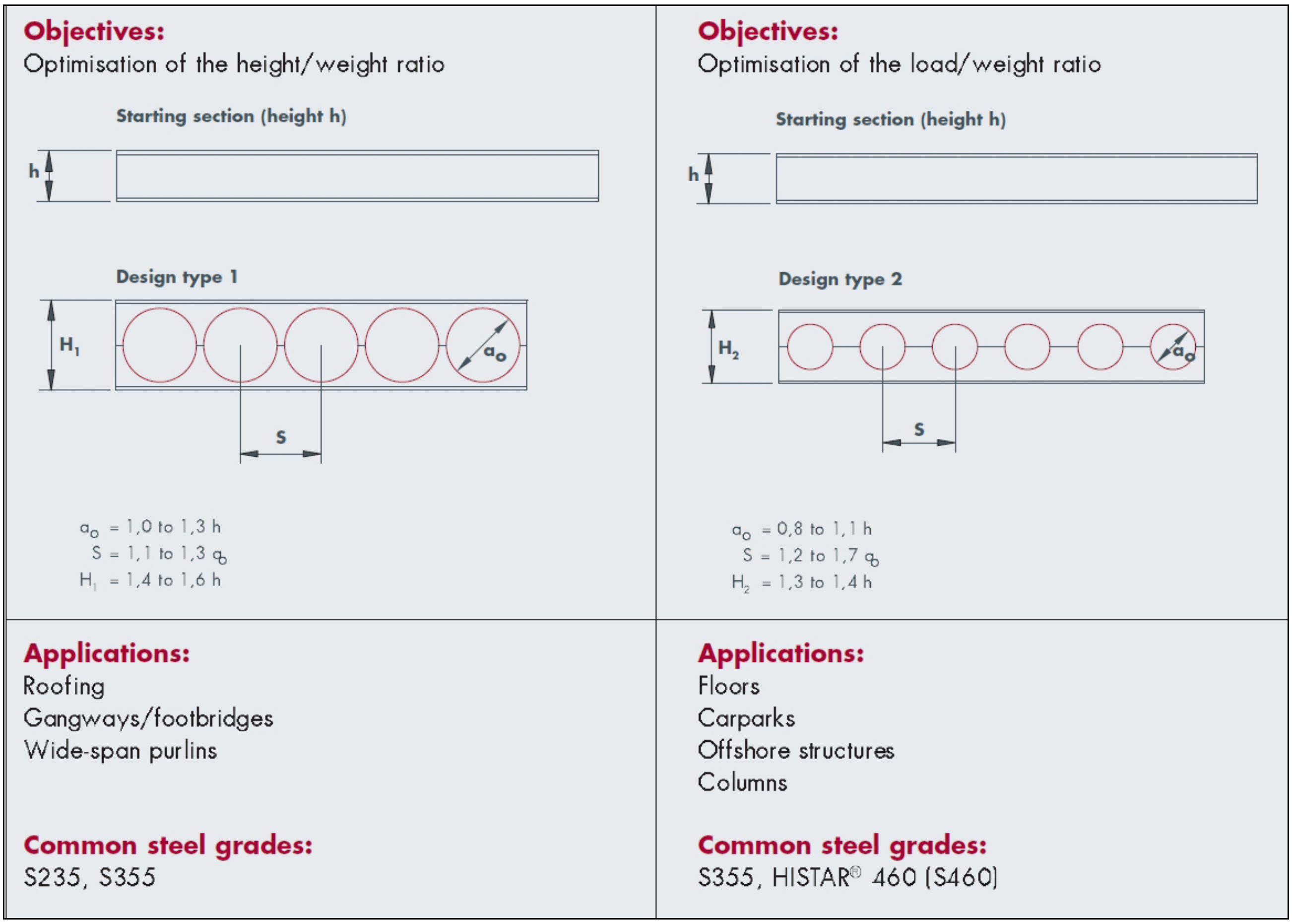
Starting section (height h)
h
Design type 1
H_1
a_o
s
a_o = 1,0 to 1,3 h
S = 1,1 to 1,3 a_o
H_1 = 1,4 to 1,6 h
Starting section (height h)
h
Design type 2
H_2
a_o
s
a_o = 0,8 to 1,1 h
S = 1,2 to 1,7 a_o
H_2 = 1,3 to 1,4 h

Objectives:
Optimisation of the height/weight ratio

Applications:
Roofing
Gangways/footbridges
Wide-span purlins

Common steel grades:
S235, S355

Objectives:
Optimisation of the load/weight ratio

Applications:
Floors
Carparks
Offshore structures
Columns

Common steel grades:
S355, HISTAR® 460 (S460)

Figure 4.11 Different objectives for cellular beam design, depending on application

4.2.16 Software tool

As a part of the LWO+ project, a software tool was developed and published on the project site http://lwo.steel-sci.org. The tool is intended to be used for preliminary design of beams with one or two (single) web openings, and implements the design guidance as developed in the LWO projects and described here. It primarily focussed on composite beams. However, there were a number of errors discovered when giving it a try:

- for circular openings the opening diameter d_o is not read, but that of rectangular/elongated openings is used
- the area of the steel beam is not properly given in the output
- the position of the elastic neutral axis is calculated inconsequently, by
  $$y_e = \frac{1}{A_f + A_w \cancel{+ A_r r^2}} \cdot \left[A_f\left(t_f/2\right) + A_w\left(t_f + d_t/2\right) + A_r r^2\left(t_f + k_c r\right)\right]$$
  where the struck-through term (area of the root fillets) is omitted
- the parameter $\varepsilon = \sqrt{235/f_y}$ is equal to 1.0 for steel grade S460

Because of these errors, this program is not yet considered ready-for-use.
Furthermore, as the tool does not cover cellular beams and no additional axial forces, a more enhanced implementation would still be useful.

4.3 Backgrounds of the ACB program

4.3.1 Introduction

It has already been mentioned that the manufacturers of cellular beams themselves have played an active role also in the development of design procedures. Design tools have been made available to customers (aiming at engineering offices) which allow a full design of cellular beams. These programs most time only cover the design of simply supported beams. Within this scope, they are rather sophisticated as they are often product-specific, and therefore advanced proprietary calculation models can be included.

The current section deals with the calculation method implemented in the ACB program from ArcelorMittal. As this method is based on the ENV1993-1-1, the classification limits are slightly different. Furthermore the scope is explicitly limited to cellular beams. No rules are included to account for elongated or rectangular openings. However, filled openings and ring stiffeners can be dealt with. In addition the geometrical limitation on the spacing of adjacent openings is somewhat relaxed:

$$s_o \geq \max\left(50\text{mm}; 0.08d_o\right) \qquad \text{(ACB)}$$
$$s_o \geq 0.2d_o \qquad \text{(LWO)}$$

It may be noted furthermore that the root fillets are consequently accounted for in the ACB program (while left out in the LWO method).

In the next subsections attention will be given to a number of design aspects which are approached notably different from the method as devised in the LWO projects.

4.3.2 Vierendeel bending

The resistance of a section at the location of an opening allowing for Vierendeel action is checked for each section inclined at angle ϕ to the vertical from $-\phi_{max}$ to $+\phi_{max}$ by increments of $1°$, where:

$$\phi_{max} = \arctan\left(\frac{d_o + s_o}{2h_t}\right)$$

For each inclined section the section properties are calculated, and the forces acting on the inclined section are determined from equilibrium (see Figure 4.12):

$$N_{\phi,Sd} = N_{m,Sd}\cos\phi - V_{m,Sd}\sin\phi$$
$$V_{\phi,Sd} = N_{m,Sd}\sin\phi\left(A_{v,\phi}/A_v\right) - V_{m,Sd}\cos\phi$$
$$M_{\phi,Sd} = N_{m,Sd}\left(y_e - y_{e,\phi}\right) + V_{m,Sd}\left(h/2 - y_{e,\phi}\right)\tan\phi$$

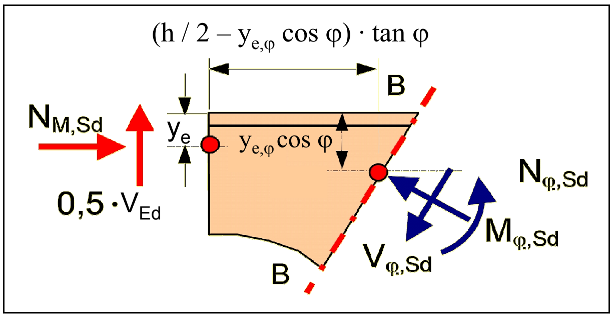

Figure 4.12 Forces acting on an inclined section

The equivalents of symbols that are defined different from the LWO usage, are given by:

$$N_{m,Sd} = N_t$$

$$V_{m,Sd} = V_t = 0.5V_{Ed}$$

This approach was given also in Annex N to ENV1993-1-1, but was not included in the final Eurocode-package.

4.3.3 Lateral-torsional buckling

In the LWO method lateral-torsional buckling of non-composite beams was not specifically discussed. For composite beams, modifications were proposed to the model in Eurocode 4 (EN1994-1-1) to take into account the effect of the web openings. This model is based on the beam's behaviour as a whole.

The ACB program however checks for lateral-torsional buckling by means of a criterion for resistance to lateral flexural buckling of the compression flange between supports:

$$\Gamma_{LT} = \frac{N_{m,Sd}}{N_{f,b,Rd}}$$

where:

$N_{m,Sd}$ is the maximum compressive axial force in the member

$N_{f,b,Rd}$ is the resistance to flexural buckling in the plane of the flange (using curve 'c')

This approach does not take into account the contribution of the web and the lower flange. However, since web-post buckling will normally govern over lateral-torsional buckling, there is no immediate need to improve the method.

4.3.4 Web-post buckling

One of the advantages of a product-specific software tool was mentioned to be the possibility to include advanced proprietary calculation models. As the scope of the ACB program is limited to cellular beams, the web-post buckling model only needs to cover circular web openings. It is therefore worthwhile to pursue the closest match of the model with reality as possible. So quite some research effort to the web-post buckling phenomenon has been made by and on behalf of ArcelorMittal. The current web-post buckling model has been developed by CTICM, as part of an optimisation study.

The criterion for resistance to buckling of an intermediate web-post is formulated as:

$$\Gamma_b = \frac{\left|\sigma_{w,Sd}\right|}{\kappa\,\sigma_{w,Rd}}$$

where:

$\sigma_{w,Sd}$ is the principal compressive stress in the half-post being studied, calculated for the critical section

$\sigma_{w,Rd}$ is the principal stress resistance for the half-post being studied

κ is a factor for post-critical reserve strength

The critical section of a half-post is the section where the horizontal shear V_h results in the maximum bending stress in the plane of the web, without taking account of an possibly present web-post bending moment

This critical section is located at an distance:

$$d_w = \frac{d_o}{2}\sqrt{\frac{\sqrt{\alpha^4 + 8\alpha^2} - 2 - \alpha^2}{2}}$$

from the joint between the two half-posts, where $\alpha = (d_o + s_o)/d_o = 1 + s_o/d_o$.

The width of the web-post at the critical section location is obtained by:

$$\ell_w = d_o\left(\alpha - \sqrt{1-\left(\frac{2d_w}{d_o}\right)^2}\right)$$

Due to global shear transfer, stress diagrams show a tension and compression diagonal in the web-post. At the location of the critical section an uniaxial tensile stress situation exists near the edge.

The value of the principal compressive stress acting along the edge of the opening at the critical section reads:

$$\sigma_{w,Sd} = \frac{6M_{c,Sd}}{\ell_w^2 t_w\left(1-4\left[d_w/d_o\right]^2\right)}$$

For a symmetrical cellular beams the bending moment at the critical section reads:

$$M_{c,Sd} = V_{h,Sd} d_w \pm M_{h,Sd}$$

The principal stress resistance is calculated by:

$$\sigma_{w,Rd} = \chi\,\xi\,f_y / \gamma_{M1}$$

where:

χ	is the reduction factor for out-of-plane buckling of the web-post (using curve 'a')
ξ	is the shape factor for the critical section, given by $\xi = 1.5 + \frac{2\cdot 10^{-5}}{(1-\alpha)^4}$

The buckling factor is calculated by:

$$\chi = \frac{1}{\phi + \sqrt{\phi^2 - \bar{\lambda}^2}}$$

where:

$$\phi = 0.5\left[1 + 0.21\left(\bar{\lambda} - 0.2\right) + \bar{\lambda}^2\right]$$

$$\bar{\lambda} = \sqrt{\frac{\xi f_y}{\sigma_{w,Cr}}}$$

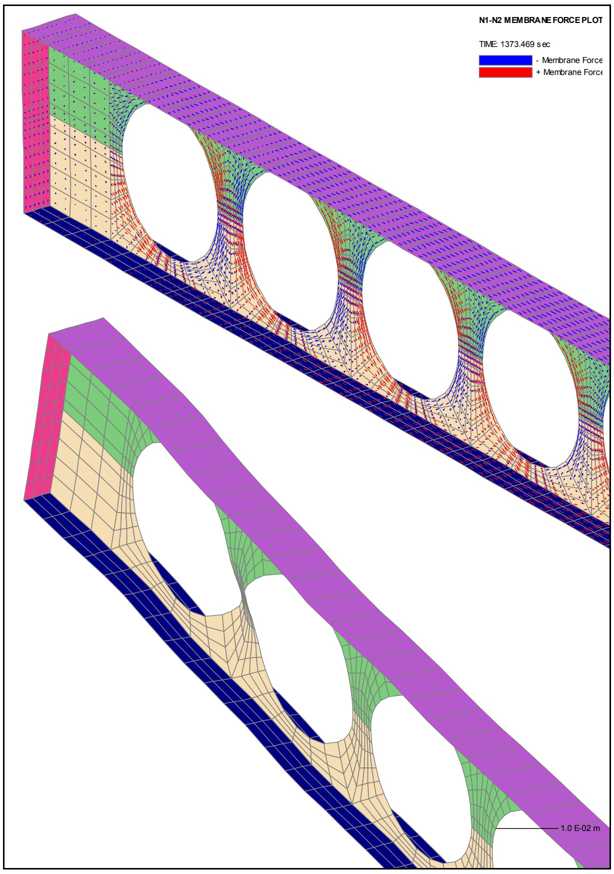

Figure 4.13 Web-post buckling: stress trajectories and deformation

The reduced slenderness $\bar{\lambda}$ of the web-post depends on the critical principal stress for instability:

$$\sigma_{w,Cr} = \alpha_{Cr} \cdot \sigma_{w,Sd}$$

which is either calculated for the upper or the lower half-post. It is noted that the critical principal stress thus depends on the loading, as the stress $\sigma_{w,Sd}$ occurs in the formula.

The critical coefficients α_{Cr} for the upper and lower half-posts take into account the interaction between the two members, and are given by:

$$\alpha_{Cr,up} = \max\left(\beta_{Cr,up};\frac{2\beta_{Cr,up}\beta_{Cr,low}}{\beta_{Cr,up}+\beta_{Cr,low}}\right)$$

$$\alpha_{Cr,low} = \max\left(\beta_{Cr,low};\frac{2\beta_{Cr,up}\beta_{Cr,low}}{\beta_{Cr,up}+\beta_{Cr,low}}\right)$$

These expressions for α_{Cr} depend in turn on the critical coefficients β_{Cr} for the upper and lower half-posts, only taking into account compression in the members and shear in the web-post, which are given by:

$$\beta_{Cr,up} = \frac{1}{\dfrac{V_h}{V_{h,Cr,up}} + \dfrac{N_{m,up}}{N_{m,up,Cr}}}$$

$$\beta_{Cr,low} = \frac{1}{\dfrac{V_h}{V_{h,Cr,low}} - \dfrac{1}{2}\dfrac{N_{m,low}}{N_{m,low,Cr}}}$$

Note that these coefficients are calculated assuming a beam subjected to a positive bending moment, thus with the *lower member in tension* and the *upper member in compression.*

The axial forces in the webs of the upper and lower members are calculated by:

$$N_{m,up} = \frac{A_{w,up}}{A_t} \min\left(N_{m,up(i)} ; N_{m,up(i+1)}\right)$$

$$N_{m,low} = \frac{A_{w,low}}{A_b} \min\left(N_{m,low(i)} ; N_{m,low(i+1)}\right)$$

For symmetric cellular beams the web areas $A_{w,up}$ and $A_{w,low}$ are equal for the upper and the lower member.

The indices i and $i+1$ refer to the low moment side (LMS) and the high moment side (HMS) respectively and denote the forces acting on the left and right tee-sections at the location of an opening, see Figure 4.14.

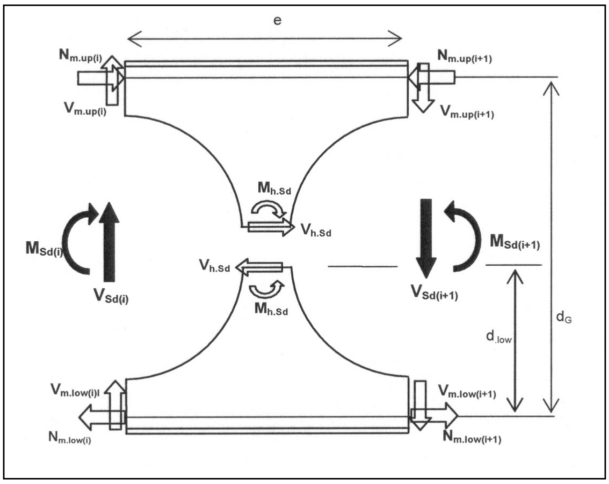

Figure 4.14 Member forces acting on the left and right tee-sections

The critical forces $V_{h,Cr}$ for shear in the web-post and $N_{m,Cr}$ for compression in a member are given by:

$$V_{h,Cr} = P_E\left(C_0 + C_1 t_w\right)$$

$$N_{m,Cr} = P_E\left(D_0 + D_1 t_w\right)$$

where P_E is the reference Euler buckling load:

$$P_E = \frac{\pi^2 E}{d_o^2} s_o t_w^3$$

The coefficients $C_0, C_1, D_0,$ en D_1 are proprietary and depend on the geometric properties of the web containing an circular openings. Expressions for these were derived from a large measurement programme of web-post imperfections in ARCELOR Cellular Beams, accompanied by experimental data.

Finally, the value of the factor for post-critical reserve strength κ in the expression for the web-post buckling criterion Γ_b is obtained by:

$$\kappa = 1 + 0.625(\psi - 0.3)$$

where the non-dimensional factor ψ for the appropriate tee-section (up/low) is given by:

$$\psi = \frac{M_{pl,t}}{\left(d_o + s_o\right) V_t}$$

4.3.5 Serviceability behaviour

The LWO method for calculating deflections of a beam with web openings consists of determining the additional effect that the opening will have relative to the pure bending deflection.

The ACB method of calculating deflections for a cellular beam follows another approach, wherein the cellular beams is broken into three different panel types (Figure 4.15):

- panel type 'X'
- panel type 'C'
- panel type 'P' (French: pleins = filled)

For any point along the beams the deflection is calculated as a sum of the contributions of each panel to that at the considered position.

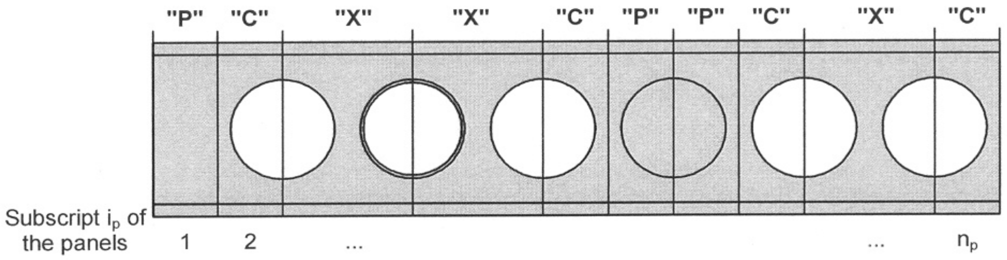

Figure 4.15 Subdivision of a cellular beam into panels for deflection calculation

The expressions for these contributions are formulated using the reciprocal theorem of Maxwell-Betti.

The method accounts for both local and global bending as well as for shear deflections in the members and the web-posts. Still it is based on first-order theory, so the influence of an applied axial force on the deflection is not taken into account.

4.4 Complementary usage

From the present chapter is follows that the design of simply supported cellular beams is developed rather well. Only the part of both discussed methods that apply to steel cellular beams was treated here, although the design of composite cellular beams is covered by both methods as well.

It is important to realise here that the LWO method primarily deals with single openings, though it has been extended to cover beams with multiple openings as well.
The ACB method totally focuses on cellular beams. Therefore it does not cover the design beams with rectangular openings. Furthermore, the scope of the method is limited by the production process. Constraints are put on the maximum web-post width by the process of flame cutting and welding. Therefore the ACB method is neither a method of choice for the design of beams with only a few web openings. Beams with a single web opening are not likely to be produced from cellular beams either.

For a single opening the LWO method is more appropriate and also most straightaway to apply. However, for the calculation of beams with multiple circular openings the procedure is still quite laborious.
While the ACB method would be rather labour intensive to perform by hand, the availability of the software tool solves this problem. Its web-post buckling method also is much more developed thus a higher accuracy can be obtained.

At he same time, the LWO method is easy to extend (and has been extended indeed) to cover other designs, like tapered beams, irregular openings, etc. Especially it seems hard to extend the web-post buckling of the ACB program to other opening shapes.

Concluding it can be said that depending on the problem at hand, the presence of more design methods and the availability of sophisticated tools allow a choice for the most appropriate method for the specific case.

The chosen method does not have to be necessarily one of the above, as it may be advantageous to consider more advanced finite element models. Still methods are required then which enable the designer of getting insight to the problem and provide a means of pre-designing and checking the calculation results. For day-to-day practise such methods remain a must, and actually will suffice in many cases.

5 PORTAL FRAME DESIGN ACCORDING TO THE EUROCODES

5.1 Introduction

The present chapter treats the design of portal frames using cellular members. The main focus is on design according to the provisions given in Eurocode 3. Reasons wherefore are provided in the next section.

The subject of the design of portal frames using cellular members is subdivided into the following different topics:

- global analysis to determine the internal forces and moments
- structural stability of portal frames
- beam-column design
- design of non-uniform members

The following sections do not give an exhaustive treatment of portal frame design in general. Cellular columns in portal frames are likely to be applied for reasons of aesthetics. In such a case haunches may very well need to be avoided. They also do not change the global behaviour (in qualitative terms), and are therefore not discussed furthermore.

5.2 Standards

5.2.1 Introduction

For the European market, the most important set of standards is formed by the upcoming Eurocodes. Because of this, and because they are relatively new and therefore contain to a certain extent the most recent developments and insights, the European standards were taken as the primary source when referring to standards. In Annex A an overview is given of the scope and contents of the Eurocodes. Furthermore the LWO method has been formulated in terms and style of the Eurocodes already.

With regard to other standards, it is to be noted that even that if the underlying philosophy of a standard allows it to provide detailed receipts for structural analysis of various structural concepts, the developments in cellular members are relatively new and therefore most guidance is still to be found in additional publications. Two standards are briefly touched in the following subsections:

- Dutch TGB1990 series
- Hong Kong Steel Code

The last one is relatively new, and as it is aimed at practising engineers (it adopts a similar style as found in the British Code), some design guidance on web openings – which are often applied in multi-storey buildings – may be expected.

5.2.2 Dutch TGB1990 series

The Dutch standards for steel structures (TGB1990 series) do not cover beams with web openings [NEN6770 and up]. Besides a remark that says that when checking the resistance against lateral-torsional buckling, for castellated beams an effective web thickness may be used, no verification rules are given for the design of members with web openings (apart from bolt holes).

Still it is possible to design structures in accordance with the functional requirements laid down in the *Dutch Building Decree* [Building Decree 2003] by application of the so-called equivalence principle, but the designer then has to resort to other sources of information or more rigorous calculation methods like finite element modelling.

No further guidance is given for the application of such methods. Therefore the Dutch standards are not treated here.

5.2.3 Hong Kong Steel Code

Some general guidance to the design of beams containing web openings is given by the *Hong Kong Code of Practise for the Structural Use of Steel 2005* [Hong Kong Steel Code].

Most of the clauses are functional however, and the code does not provide means of analyzing the behaviour of cellular beams. Furthermore it is explicitly stated that the designer should refer to specialist literature

or carry out an detailed analysis, e.g. by finite element modelling, to check for web-post buckling or to allow for point loads close to an opening.
The provisions in this code of practice that deal with web openings resemble strongly those given in the simplified approach described in Access Steel resource *NCCI: Design rules for web openings in beams* [SN019]. As this document was prepared based on the recommendations given in the LWO publications (which are discussed in the previous chapter), the Hong Kong Steel Code is also not dealt with separately here.

5.3 Global analysis

5.3.1 Introduction

The design of steel structures using EN1993 should be in accordance with the general rules given in EN1990. These requirements are deemed to be satisfied when limit state design is used in conjunction with the partial factor method, the load combinations given in EN1990, and the actions given in EN1991. Further, the analysis should be appropriate for the limit state under consideration.
Prior to any check on the capacity of the members (per limit state), the internal forces and moments due to the applied actions have to be determined. This is the main objective of the so-called global analysis.

5.3.2 Geometrical non-linearity

Unlike some other (older) standards, Eurocode 3 as a rule requires explicit consideration of the effects of the deformed geometry (so-called second-order effects), though first-order analysis using the initial geometry of the structure is still allowed under certain limits.

For structures whereof the increase of the relevant internal forces or moments or any other change of structural behaviour caused by deformations can be neglected, clause 5.2.1(3) permits first-order analysis, if the following criterion is satisfied:

$$\alpha_{cr} = \frac{F_{cr}}{F_{Ed}} \geq 10 \quad \text{for elastic analysis}$$

$$\alpha_{cr} = \frac{F_{cr}}{F_{Ed}} \geq 15 \quad \text{for plastic analysis}$$

In the above formulae, F_{cr} is 'the elastic critical buckling load for global instability mode based on initial elastic stiffnesses' and F_{Ed} is 'the design loading on the structure'.
The distinction in the limits for elastic and plastic analysis is because the structural behaviour may be significantly influenced by non-linear material properties in the ultimate limit state (e.g. when the frame forms plastic hinges).

The calculation of the *(elastic) critical load multiplier* α_{cr} requires the elastic critical buckling load F_{cr} of the portal frame to be determined, thus an eigenvalue analysis. The tools to carry out such an analysis are not commonly in use by engineering offices yet. In order to avoid these more advanced calculation, approximations to α_{cr} have been developed (especially to check for the predominant global sway instability mode in common buildings like portal frames).

In clause 5.2.1(4)B the following approximative formula is given which also applies to portal frames, provided the roof slope may be considered as shallow and the axial compression in the beams (rafters) is not significant:

$$\alpha_{cr} = \left(\frac{H_{Ed}}{V_{Ed}}\right)\left(\frac{h}{\delta_{H,Ed}}\right)$$

where, applied to pitched roof portal frames:

H_{Ed} = the design value of the total horizontal reaction
V_{Ed} = the total design vertical load
$\delta_{H,Ed}$ = the horizontal displacement at the eave due to all horizontal loads
h = the storey height

In calculating the response $\delta_{H,Ed}$ all horizontal loads like wind and fictitious horizontal loads resulting from a lack of verticality, lack of straightness etc. have to be taken into account. It might be more convenient though, to determine $\delta_{H,Ed}$ as resulting from fictitious horizontal forces alone, due to initial sway imperfections (i.e. exclude the effects of any other horizontal loads, such as wind loads). This approach is justified as calculating $H_{Ed} / \delta_{H,Ed}$ is equal to determine the sway stiffness of the frame.

The notes to this clause provide some more quantitative information to the qualitative requirements for application mentioned. First, it is stated that in the absence of more detailed information a roof slope may be taken to be shallow if it is not steeper than 1:2 (approximately 26°). Second, again in the absence of more detailed information, it is stated that the axial compression in the beams or rafters may be assumed to be significant if:

$$\bar{\lambda} \geq 0.3\sqrt{\frac{A f_y}{N_{Ed}}}$$

In calculating the non-dimensional slenderness, the beams or rafters should be considered as hinged at its ends with the length equal to the system length measured along the beams or rafters.

The formula for α_{cr} given in clause 5.2.1(4)B was originally developed by Horne [1975] (although admittedly for multi-storey frames). As the wording in the clause already indicates ('may be calculated using the following approximative formula'), the critical load multiplier may – and sometimes *must*, e.g. when the requirements to apply this formula are not met – still be obtained by other means like a more accurate approximation or even by an advanced eigenvalue analysis.

Such an improved approximation was given by King [2003] and cited in Lim *et al* [2005]. In the paper it is stated that Horne's method for estimating α_{cr} (and so that of Eurocode 3) is unconservative when applied to portal frames, because it does not take into account the axial force in the rafters. (This has been partially overcome by the second limiting condition.) Furthermore Horne's formula may underestimate second-order effects in the columns. Therefore the next modification was proposed to account for these deficiencies (with adapted notation):

$$\alpha_{cr,King} = 0.8\left\{1 - \left(\frac{N_{Ed}}{N_{cr}}\right)_{max}\right\} \cdot \alpha_{cr,Horne}$$

where $\alpha_{cr,Horne} = \alpha_{cr}$ as given in Eurocode 3 and N_{Ed} and $N_{cr} = \pi^2 EI/L^2$ refer to the axial force in the rafters. This formula is stated to provide a conservative though reasonable estimate of the elastic critical buckling load factor, which avoids the need to use specialized software.

5.3.3 Material non-linearity

Material non-linearity (i.e. plastification) can be allowed for in the global analysis itself already and/or when checking for the cross-sectional resistance. The following global analysis methods for dealing with plastification are allowed:

- elastic-plastic analysis with plastified sections and/or joints as hinges
- non-linear plastic analyses considering the partial plastification of members in plastic zones
- (first-order) rigid-plastic analysis neglecting the elastic behaviour between hinges

Global plastic analysis is allowed only where the structure has sufficient rotation capacity at the actual locations of the plastic hinges (whether this is in the members or the joints).

Table 5.1 Classification of the analysis on the basis of the class of cross-section

Class	Criterion	Structural analysis
1	Cross-sections with rotation capacity to form plastic hinges and zones without reduction of the resistance	plastic-plastic
2	Cross-sections which are able to develop plastic moment resistance but with limited rotation capacity	elastic-plastic
3	Cross-sections which can achieve the yield strength in the outer compression fibre, but where the plastic moment resistance cannot be developed	elastic-elastic
4	Cross-sections which fail of local buckling before attainment of the yield stress, so local buckling has to be taken into account according to EN1993-1-5	elastic-elastic

By means of cross-section classification it can be verified whether or not a cross-section is able to develop its full plastic resistance.

The precise role of cross-section classification is to identify the extent to which the resistance and rotation capacity of cross sections is limited by its local buckling resistance. Criteria on the width-to-thickness ratio of the parts of the section subjected to compression, (either totally or partially) under the load combination considered are given in Section 5.6 of Eurocode 3. Sections that fall out of these limits are class 4 and should be designed using EN1993-1-5.

Common practice has become to conduct a global analysis first, followed by member checks for cross-section resistance and member stability. Table 5.1 above gives the different possible combinations of global analysis and check for member resistance.

Although global plastic analysis is allowed for class 1 sections (at least at the parts where plastic hinges rotate), on mainland Europe single-storey portal frames are usually designed using elastic global analysis to determine the structure's response (internal forces and moments) to the applied actions – which is always allowed.

Mostly hot-rolled profiles are applied which can usually classified as class 1 or 2, thus being able to develop their full plastic resistance.

Although the above presented approach may be most straightforward and efficient when designing well-known 'standard' structures like portal frames, Finite Element methods of analysis may also be applied. In EN1993-1-1 reference is made to EN1993-1-5 (especially Annex C) for guidance on the use of FEA methods.

5.3.4 Imperfections

Apart from geometrical and material non-linearity, allowance should also be made for all kinds of imperfections which may have an destabilising effect on the structure or in any other respect modify the structural behaviour. Equivalent geometric imperfections should be used, which cover the possible effects of all (types of) imperfections *unless* these effects are included already in the resistance formulae for member design.
These imperfections include:

- residual stresses
- lack of verticality
- lack of straightness
- lack of fit
- minor eccentricities

Both imperfections on a global and a local level should be taken into account, in and out of plane, and should be chosen in the most unfavourable direction and form.
Generally global sway imperfections of frames are denoted as $P-\Delta$ (P – big delta), while local bow imperfections are denoted as $P-\delta$ (P – small delta) imperfections, see Figure 5.1. This notation uses P for the compressive axial force and Δ or δ for the displacement.

For frames sensitive to buckling in a sway mode, the effect of imperfections should be allowed for in the frame analysis by means of an initial sway imperfection, possibly together with individual bow imperfections of the members.
The global initial sway imperfection angle may be determined from $\phi = \phi_0 \alpha_h \alpha_m$ where:

ϕ_0 = the basic value: $\phi_0 = 1/200$

α_h = the reduction factor for height h applicable to columns:

$$\alpha_h = \frac{2}{\sqrt{h}} \text{ but } \frac{2}{3} \le \alpha_h \le 1.0$$

h = the height of the structure in meters

α_m = the reduction factor for the number of columns in a row:

$$\alpha_m = \sqrt{0.5\left(1+\frac{1}{m}\right)}$$

m = the number of columns in a row including only those columns which carry a vertical load N_{Ed} not less than 50% of the average value of the column in the vertical plane considered

When $H_{Ed} \ge 0.15\, V_{Ed}$ the sway imperfections may be disregarded for building frames.

When needed relative local bow imperfections of members for flexural buckling may be obtained from Table 5.2 depending on the buckling curve, where e_0 denotes the amplitude and L is the member length.

Table 5.2 Design value of initial local bow imperfection

buckling curve	elastic analysis	plastic analysis
	e_0/L	
a_o	1/350	1/350
a	1/350	1/350
b	1/350	1/350
c	1/350	1/350
d	1/350	1/350

From the sway imperfection angle the initial sway displacements can be determined. However, for convenience the effects of initial sway imperfection and possibly also local bow imperfections may be replaced by systems of equivalent horizontal forces, introduced for each compressed column, see Figure 5.2.

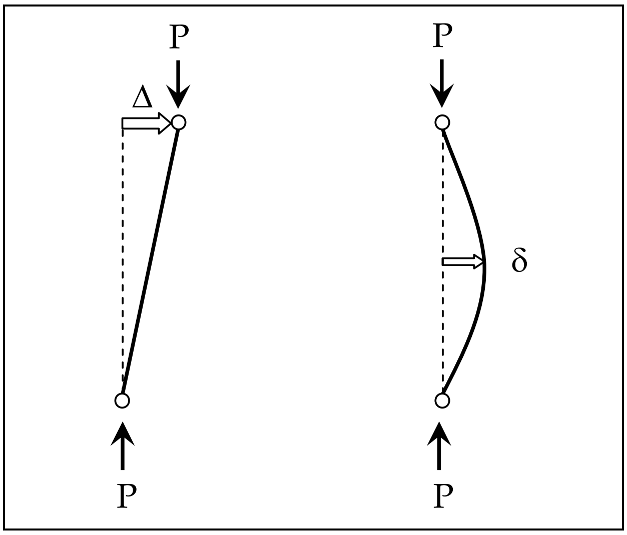

Figure 5.1 $P-\Delta$: sway displacement
$P-\delta$: initial bow displacement

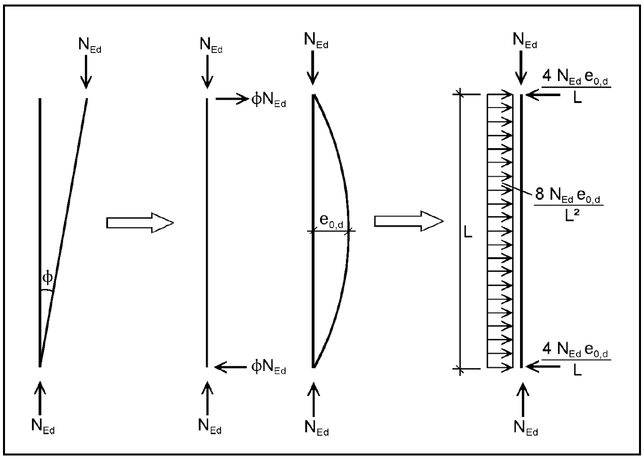

Figure 5.2 Equivalent horizontal forces

Alternatively to modelling global sway and possibly also (see next subsection) initial bow imperfection as described above, the shape of the elastic critical buckling mode of the structure may be applied as a unique global and local imperfection. This is however only suitable for computer implementation, as it requires to model an continuous initial deformed geometry of the whole structure.

5.3.5 Structural stability

When the criterion on α_{cr} has not been met, second-order effects have to be taken into account in the analysis. Eurocode 3 allows different strategies for treating stability. Depending on the type of frame and the global analysis, second-order effects and imperfections may be accounted for:

- both totally by the global analysis
- partially by the global analysis and partially through individual stability checks of the members
- by individual stability checks of the equivalent members

The choice for one of these strategies determines which formulae are applicable or not for checking the cross-sectional resistance and member stability.

Full global second-order analysis taking into consideration all kinds of imperfections

When all imperfections – both global sway and local bow imperfections – are allowed for in global second-order analysis, no individual stability check for the members according to Section 6.3 of EN1993-1-1 is necessary.
Only the cross-sectional resistance should be verified afterwards, unless it is already included in the analysis by an advanced elastic-plastic analysis routine which is able to take into account (partial) plastification together with an appropriate yield criterion (e.g. the Von Mises criterion).

Global second-order analysis without taking into consideration the member imperfections

It is also allowed to perform an global frame analysis in which only frame imperfections are included in the global analysis, while leaving second-order effects in individual members or certain individual member imperfections (e.g. for lateral-torsional buckling) out. In that case the individual stability of members should be checked according to the relevant criteria given in Section 6.3 for the effects not included in the global analysis.

For each member the end moments and forces should be taken from the global analysis, and as the frame sway mode is already included in the global analysis, the buckling length of the individual members may (conservatively) be taken equal to the system length:

$$L_{cr} = L_{sys}$$

Normally the action effects at the members' end (especially the bending moments) are affected by global sway imperfections but not significantly by local bow imperfections, and thus the last may be neglected in the global analysis.
However for frames with very slender members neglecting the local bow imperfections in the global analysis is not allowed for each compressed member where both of the following conditions are met:

- at least one moment resistant joint at one member end, and
- $\bar{\lambda} \geq 0.5\sqrt{\dfrac{A\,f_y}{N_{Ed}}}$

where N_{Ed} is the design value of the compression force and $\bar{\lambda}$ is the in-plane non-dimensional slenderness calculated for the member considered as hinged at its ends.

As the non-dimensional slenderness $\bar{\lambda}$ reads:

$$\bar{\lambda} = \sqrt{\frac{A f_y}{N_{cr}}}$$

this means that when $N_{Ed} \geq 0.25 N_{cr}$ the initial bow imperfection has to be considered explicitly in the global analysis (for that particular member).

First-order global analysis considering no global or local imperfections: the equivalent column method
For basic cases EN1993-1-1 allows the stability of the whole frame to be assessed by checks on individual equivalent members only.
The buckling lengths values used in stability checks according to Section 6.3 should allow then for the stiffness behaviour of members and joints, the presence of plastic hinges and de distribution of compressive forces under the design loads. No imperfections or second-order effects have to be regarded in the global analysis at all when determining the internal forces and moment to be used in resistance checks according to Section 6.2..

For frames whereof the joints may be classified as continuous and whereof the sections are at least class 2, this implies that the buckling lengths of the individual columns may be determined from the global elastic critical load (for the load combination in consideration).
From a global buckling analysis the elastic critical buckling factor α_{cr} (also commonly denoted $\lambda_{(cr)}$) may be obtained, and the axial forces N in the columns may be calculated by a first-order elastic analysis.

Given that the loading on the frame has to be multiplied by α_{cr} to cause elastic buckling, the buckling load each single column may be expressed as:

$$F_{cr} = \alpha_{cr} N$$

Then together with the classical expression for the critical buckling load of a single column in terms of the buckling length:

$$F_{cr} = \frac{\pi^2 EI}{L_{cr}{}^2}$$

it follows that the buckling length to use for the equivalent member reads:

$$L_{cr} = \sqrt{\frac{\pi^2 EI}{\alpha_{cr} N}}$$

The scope of this method for verifying the stability of a frame may be limited however by the National Annex. Indeed the Dutch annex sets limits on the use of this method. Rules are provided which forbid especially to neglect the increase in the end moments in the beams. The UK National Annex prohibits the use of the clause in question – 5.2.2(8) – at all. Care should be taken in verifying whether the obtained frame buckling load is really a *global* mode, especially in more complex structures.

Methods to include second-order effects
When second-order effects are to be allowed for in the global analysis, they may be calculated by using an analysis appropriate to the structure. These methods may include step-by-step or other iterative procedures.

For single-storey frames designed on the basis of elastic global analysis the second-order sway effects due to vertical loads may be calculated by increasing the horizontal loads H_{Ed} (e.g. wind) and equivalent loads $V_{Ed}\,\phi$ due to (global sway) imperfections according to first-order theory by the factor:

$$\frac{1}{1 - 1/\alpha_{cr}} = \frac{\alpha_{cr}}{\alpha_{cr} - 1}$$

provided that $\alpha_{cr} \geq 3.0$. If this limit is not satisfied (i.e. $\alpha_{cr} < 3.0$) a more accurate second-order analysis has to be performed.

Again the roof slope shall be shallow and the axial compression in the beams or rafter shall be not significant, just like the conditions for application of Horne's approximation of α_{cr} given in section 5.3.2 already.

This method is usually termed the *amplified sway method* and has become the most familiar method to design portal frames.

Summarizing: the effects of the deformed geometry have to be accounted for in the analysis when relevant. The susceptibility to second-order effects can be established by (an approximation of) the critical buckling factor α_{cr}. When a linear elastic global analysis is carried out with inclusion of global sway imperfections (and initial bow imperfections if needed) the second-order effects may be:

- neglected if $\alpha_{cr} > 10$
- determined by the amplified sway method if $3.0 \leq \alpha_{cr} \leq 10$

Otherwise the second-order effects and member imperfections have to be accounted for in the global analysis itself.

The stability of the members may be verified according to Section 6.3 using the – appropriately amplified – forces and moments obtained from the global analysis with buckling lengths taken equal to the system lengths, in consideration of the member imperfections.
For sections which are class 2 or higher, the plastic resistance may be utilised.

5.4 Design of beam-columns

5.4.1 Cross-sectional resistance

As a general statement clause 6.2.1(1) requires that in each cross-section the design value of an action effect should not exceed the corresponding design resistance. The clause is further widened by the requirements that if several action effects act simultaneously neither the combined effect should exceed the resistance for that combination.
Rules are provided in Section 6.2 for the verification of the separate resistances, together with interaction formulae.
Unless other interaction criteria apply, the Von Mises criterion may be applied for elastic verification of any critical point of a cross-section. This formula is conservative however, as it excludes partial plastic stress distribution, which is permitted in elastic design.

Plastic resistances may be used as well (where applicable), whereof the stress distribution should be in equilibrium with the internal forces and moments without exceeding the yield strength, and which distribution should be compatible with the associated plastic deformations.

As a conservative approximation it is always allowed to apply a linear summation of the utilisation ratios for each stress resultant:

$$\frac{N_{Ed}}{N_{Rd}} + \frac{M_{y,Ed}}{M_{y,Rd}} + \frac{M_{z,Ed}}{M_{z,Rd}} \leq 1$$

Allowance should be made for the possible reduction of the design resistances caused by shear (buckling) effects.

In the remainder of Section 6.2 expressions are given to calculate these design resistances (either elastic or plastic), together with more efficient rules to take interaction into account or even leave it out for limited cases.
Explicit formulae are given to assess the influence of the axial force on the moment capacities, depending on the ratio:

$$n = \frac{N_{Ed}}{N_{pl,Rd}}$$

Furthermore, when the utilisation ratio of the shear force exceeds 0.50 a reduced yield strength should be used when calculating the moment and/or axial force resistance.

5.4.2 Buckling resistance

Basically the cross-sectional resistance serves as an upper-bound to the ultimate capacity. For slender members which are not (sufficiently) restrained against buckling the member resistance will be decisive rather than the cross-sectional resistance.

In accordance with existing design practise, EN1993-1-1 aims primarily at providing rules for the design of uniform members:

- … in compression (6.3.1)
- … in bending (6.3.2)
- … in bending and compression (6.3.3)

Compression: (torsional)-flexural buckling
Uniform members in compression should be verified against buckling by means of:

$$\frac{N_{Ed}}{N_{b,Rd}} \leq 1$$

The design buckling resistance $N_{b,Rd}$ of the compression member should be taken as:

$$N_{b,Rd} = \chi \frac{A f_y}{\gamma_{M1}} \qquad \text{(class 1, 2, 3)}$$

where χ is the reduction factor for the *relevant buckling mode*. It depends on the appropriate non-dimensional relative slenderness:

$$\bar{\lambda} = \sqrt{\frac{A f_y}{N_{cr}}} \qquad \text{(class 1, 2, 3)}$$

to deliver:

$$\chi = \frac{1}{\phi + \sqrt{\phi^2 - \bar{\lambda}^2}} \quad \text{but} \quad \chi \leq 1$$

where $\phi = 0.5\left[1 + \alpha\left(\bar{\lambda} - 0.2\right) + \bar{\lambda}^2\right]$.

The imperfection factor α corresponds with the applicable buckling curve as given in Table 5.3.

Table 5.3 Imperfection factors for buckling curves [EN1993-1-1 Table 6.3]

curve	**a_0**	**a**	**b**	**c**	**d**
factor α	0.13	0.21	0.34	0.49	0.76

For slenderness $\bar{\lambda} \leq 0.2$ the buckling effects may be ignored and only cross-sectional checks apply.
The buckling curve to use should be selected from EN1993-1-1 Table 6.2. It depends on the cross-section type, h/b-ratio, axis of bending, flange thickness, steel grade, etc.

For *flexural buckling* $\bar{\lambda}$ is given by:

$$\bar{\lambda} = \sqrt{\frac{A f_y}{N_{cr}}} = \frac{L_{cr}}{i} \cdot \frac{1}{\lambda_1} \qquad \text{(class 1, 2, 3)}$$

where:

$$i = \sqrt{\frac{I}{A}} \quad \text{about the relevant axis}$$

$$\lambda_1 = \pi\sqrt{\frac{E}{f_y}} = 93.9\varepsilon \quad \text{with} \quad \varepsilon = \sqrt{\frac{235}{f_y}}$$

L_{cr} is the buckling length *in the buckling plane considered*

As explained in the previous section, the buckling length has to be determined taking second order sway effects into account, either by either by the end moments of the member (with $L_{cr} = L_{sys}$) or by means of an appropriate buckling length respectively.

For *torsional or torsional-flexural buckling* the non-dimensional slenderness $\bar{\lambda}_T$ reads:

$$\bar{\lambda}_T = \sqrt{\frac{A f_y}{N_{cr}}}$$

where $N_{cr} = N_{cr,TF}$ but $N_{cr} \leq N_{cr,T}$ in which:

$N_{cr,TF}$ is the elastic torsional-flexural buckling force
$N_{cr,T}$ is the elastic torsional buckling force

For torsional or torsional-flexural buckling the appropriate buckling curve may be determined from EN1993-1-1 Table 6.2 considering the one related to the z-axis.

No further information is given in EN1993-1-1 on the determination of the buckling length or the elastic critical force for torsional buckling. However, for doubly-symmetric I and H sections torsional and torsional-flexural buckling will not give a lower mode than flexural buckling (provided that both flanges are restrained at positions of lateral restraint).

Bending: lateral-torsional buckling

Likewise for buckling of axially compressed members, the verification against lateral-torsional buckling of a laterally unrestrained uniform member proceeds as follows:

$$\frac{M_{Ed}}{M_{b,Rd}} \leq 1$$

The design buckling resistance moment $M_{b,Rd}$ for uniform members should be taken from:

$$M_{b,Rd} = \chi_{LT} \frac{W_y f_y}{\gamma_{M1}}$$

where W_y should be taken according to the class of the cross-section considered.

Likewise for flexural buckling, the reduction factor χ_{LT} should be based on an appropriate non-dimensional slenderness:

$$\bar{\lambda}_{LT} = \sqrt{\frac{W_y f_y}{M_{cr}}}$$

So the structure of the verification format is analogous to that of (torsional)-flexural buckling. However, for rolled sections of equivalent welded sections a different alternative approach is allowed to determine the non-dimensional slenderness.

While in general for uniform bending members χ_{LT} should be determined from:

$$\chi_{LT} = \frac{1}{\phi_{LT} + \sqrt{\phi_{LT}^2 - \bar{\lambda}_{LT}^2}} \quad \text{but} \quad \chi_{LT} \leq 1$$

where

$$\phi_{LT} = 0.5\left[1 + \alpha_{LT}\left(\bar{\lambda}_{LT} - 0.2\right) + \bar{\lambda}_{LT}^2\right]$$

as an alternative it is allowed for rolled or equivalent welded sections to obtain χ_{LT} from a modified expression:

$$\chi_{LT} = \frac{1}{\phi_{LT} + \sqrt{\phi_{LT}^2 - \beta\bar{\lambda}_{LT}^2}} \quad \text{but} \quad \begin{cases} \chi_{LT} \leq 1 \\ \chi_{LT} \leq \dfrac{1}{\bar{\lambda}_{LT}^2} \end{cases}$$

where

$$\phi_{LT} = 0.5\left[1 + \alpha_{LT}\left(\bar{\lambda}_{LT} - \bar{\lambda}_{LT,0}\right) + \beta\bar{\lambda}_{LT}^2\right]$$

with $\bar{\lambda}_{LT,0} = 0.4$ and $\beta = 0.75$

For this more efficient alternative formulation – which will apply to the majority of steel portal frame structures – the buckling curve should be obtained from EN1993-1-1 Table 6.5 which is reproduced in Table 5.4.

Moreover, in order to better take into account the moment distribution between the lateral restraints of members the reduction factor may be modified as follows:

$$\chi_{LT,mod} = \frac{\chi_{LT}}{f} \text{ but } \chi_{LT,mod} \leq 1$$

with: $f = 1 - 0.5\left(1 - k_c\right)\left[1 - 2.0\left(\bar{\lambda}_{LT} - 0.8\right)^2\right]$

but $f \leq 1.0$

The correction factor k_c may be obtained from Table 6.6 of EN1993-1-1, partly reproduced in Table 5.4 on the right.

Table 5.4 Lateral-torsional buckling curves for rolled or equivalent welded sections [EN1993-1-1 Table 6.5]

cross-section	**limits**	**buckling curve**
rolled I-sections	$h/b \leq 2$	b
	$h/b > 2$	c
welded I-sections	$h/b \leq 2$	c
	$h/b > 2$	d

The buckling curves for lateral-torsional buckling are based on bending moments constant along the member. For moment diagrams other than constant (worst case) higher values of χ_{LT} will be obtained.

This is included to a certain extent already by a reduced value of $\bar{\lambda}_{LT}$ due to the increased elastic critical moment M_{cr} for non-uniform moment distributions.

However, no effects of plastification are accounted for in the calculation of this *elastic* critical moment. Beams with variable bending along the member experience differently distributed (reduced) plastic zones, which do not so badly affect the deformed shape of the member as in the case of plastic weakening at mid-span under constant bending moment.

In order to exploit the additional beneficial effect of the shape of the moment diagram being other than constant the factor f may be used to calculate a improved $\bar{\lambda}_{LT}$ value, called $\chi_{LT,mod}$. Both values of $\chi_{LT,mod}$ and f are thus calculated based on the non-dimensional slenderness $\bar{\lambda}_{LT}$ which includes already the shape of the moment diagram (by M_{cr}).

It may be noticed that a plateau is defined by:

$$\bar{\lambda}_{LT} \leq \bar{\lambda}_{LT,0} = 0.4$$

for which lateral-torsional effects may be ignored so that only cross-sectional checks apply. This plateau is *not* observed in numerical simulations – even not when strain hardening is included – but was obtained from experimental results on I-shaped beams in this slenderness range.

It is justified however by the fact that the plastic moment resistance $M_{pl,Rd}$ *on average* underestimates the moment capacity by 14% – the real behaviour of plastic bending turns out to be more complex than calculations based on the strength of simple tensile coupon tests.

So far no attention was paid to the calculation of the key parameter of the elastic critical moment M_{cr} itself. As lateral-torsional buckling consists in a spatial buckling mode where both bending about the minor axis of the cross-section and torsion about the longitudinal axis of the member are involved, the mathematical formulation of the problem is rather complex.

The elastic critical moment M_{cr} in itself is not a realistic presentation of the beam's bending resistance, but its determination allows for taking into account a number of properties:

- the mechanical and geometric section properties (flexural rigidity about minor axis, torque rigidity, warping rigidity, dissymmetry parameter)
- the loading characteristics (moment distribution, level of transverse load application)

Table 5.5 Examples of correction factor k_c [taken from EN1993-1-1 Table 6.6]

moment distribution	**correction factor**
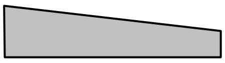 $\lvert\psi\rvert \leq 1$	$\dfrac{1}{1.33 - 0.33\psi}$
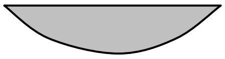	0.94
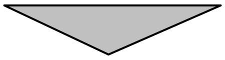	0.86

- the support conditions (for bending in the primary bending plane, lateral bending, torsion, warping)
- the restraint properties (lateral or torsional restraints, location of these restraints along the beam span and over the section depth)

In Annex F to the pre-standard ENV1993-1-1 a so-called *3-factor formula* was given to evaluate M_{cr} for a beam with uniform cross-section being symmetrical about the minor axis loaded in bending about the major axis. For uniform beams with doubly symmetric cross-section this formula reads simplified:

$$M_{cr} = C_1 \cdot \frac{\pi^2 EI_z}{(k_z L)^2} \left\{ \sqrt{\left(\frac{k_z}{k_w}\right)^2 \frac{I_w}{I_z} + \frac{(k_z L)^2 GI_t}{\pi^2 EI_z} + \left(C_2 z_g\right)^2} - C_2 z_g \right\}$$

where the $C_i - \text{factors}$ depend on both the bending moment distribution and the end restraint conditions:

- C_1 is the major factor introducing the bending conditions
- C_2 is linked to the coordinate z_g of load application point from the shear centre
- C_3 (omitted here) allows for the effect of cross-sectional mono-symmetry about the minor axis of the section

The factors k_z and k_w are effective length factors depending on the end restraint conditions:

- k_z refers to the end rotation constraint
- k_w refers to the end warping constraint

These $k_i - \text{values}$ vary from 0.5 for full restraint to 1.0 for no restraint. Fork end restraints have $k_w = k_z = 1.0$.

Values for the $C_i - \text{factors}$ have been tabulated, e.g. in ENV1993-1-1 itself, in the ECSC-report to *Lateral torsional buckling in steel and composite beams* [LTB] or in Access Steel resource SN003.

As an alternative approach a *single-factor formula* has been suggested:

$$M_{cr} = C \cdot M_{cr}^0$$

where:

$$M_{cr}^0 = \frac{\pi}{L} \cdot \sqrt{EI_z GI_t}$$

The C-factor includes all influences of moment distribution, restraint conditions, introduction of loads out of the shear centre, warping rigidity, and cross-sectional mono-symmetry. *For given restraint conditions and a given type of loading* the C-factor is a function of the following three parameters:

- influence of warping rigidity:
  $$\kappa_{wt} = \frac{1}{L}\sqrt{\frac{EI_w}{GI_t}}$$
- influence of mono-symmetry:
  $$\gamma_{zt} = \frac{z_g}{L}\sqrt{\frac{EI_z}{GI_t}}$$
- influence of application of load above or beneath the shear centre:
  $$\zeta_{zt} = \frac{z_j}{L}\sqrt{\frac{EI_z}{GI_t}}$$

Tables have been set up for doubly-symmetric hot-rolled sections basic cases to determine the C-factor for basic cases of beam and load configuration, e.g. in reference [LTB].

However it is also possible to obtain the elastic critical moment by means of numerical (FEM-)simulations or by using a dedicated software like LTBEAM which calculates a *critical load multiplier* to the actual beam and load characteristics, taking into account possible restraints etc. For comparison purposes, the C-factor can be back-calculated.

In Section 6.3.2.4 of EN1993-1-1 a simplified assessment method given which verifies whether the length L_c between restraints or the resulting slenderness of the equivalent compression flange $\bar{\lambda}_f$ satisfies the equation:

$$\bar{\lambda}_f = \frac{k_c L_c}{i_{f,z}\lambda_1} \leq \bar{\lambda}_{c0} \frac{M_{c,Rd}}{M_{y,Ed}}$$

The radius of gyration $i_{f,z}$ should be obtained for the equivalent compression flange composed of the compression flange plus $1/3$ of the compressed part of the web area, about the minor axis of the section. The slenderness limit $\bar{\lambda}_{c0}$ has to be given in the National Annex, with a recommended value of:

$$\bar{\lambda}_{c0} = \bar{\lambda}_{LT,0} + 0.1$$

so effectively:

$$\bar{\lambda}_{c0} = 0.4 + 0.1 = 0.5$$

If this so-called *stable length method* check fails, the design buckling resistance moment may be taken as :

$$M_{b,Rd} = k_{f\ell}\, \chi M_{c,Rd}$$

with $M_{c,Rd} = W_y f_y / \gamma_{M1}$. Here the reduction factor χ of the equivalent compression flange should be determined with $\bar{\lambda}_f$ using curve c (except for some welded sections). The factor $k_{f\ell}$ accounts for the conservatism of the method and may be taken equal to $k_{f\ell} = 1.10$.

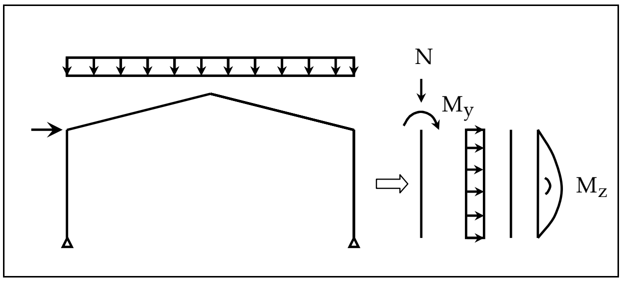

Figure 5.3 Example of extraction of a beam-column for separate verification

This simplified methods seems to be useful mainly for calculation 'by hand' as complicated formulae are no problem in computer-aided design.

Bending and compression

In the former paragraphs the verification format has been presented of isolated elements subjected to either compression or bending (along with some elaborations). Members in portal frames most often are subjected to both. These members are generally called *beam-columns*.

In principle all members in frame structures are beam-columns with the particular cases of beams (where the axial load can be neglected or may be assumed as $N = 0$) and columns (where the bending moment can be neglected or may be assumed as $M = 0$).

In section 5.3.5 is was pointed out that when frame imperfections are allowed for in the global analysis, it is allowed to design the individual elements by considering them as single members. In order to perform this evaluation the member has to be extracted (isolated) from the frame and all direct loads on the member together with the end forces and moments have to be modelled (Figure 5.3) or appropriate buckling lengths have to be used based on the global buckling mode.

This member then can be checked for according to the verification format given in Section 6.3.3 from Eurocode 3. It applies to *uniform members with doubly-symmetric sections* for sections not susceptible to distortional deformations. For class 1 to 3 sections no shift of the centroidal axis will occur and accordingly the verification rule for the member subjected to combined bending and axial compression simplifies to:

$$\frac{N_{Ed}}{\chi_y N_{Rk}/\gamma_{M1}} + k_{yy}\frac{M_{y,Ed}}{\chi_{LT} M_{y,Rk}/\gamma_{M1}} + k_{yz}\frac{M_{z,Ed}}{M_{z,Rk}/\gamma_{M1}} \leq 1$$

$$\frac{N_{Ed}}{\chi_z N_{Rk}/\gamma_{M1}} + k_{zy}\frac{M_{y,Ed}}{\chi_{LT} M_{y,Rk}/\gamma_{M1}} + k_{zz}\frac{M_{z,Ed}}{M_{z,Rk}/\gamma_{M1}} \leq 1$$

In case no lateral load is applied to the member (e.g. when designing a plane frame) the corresponding contribution becomes zero. These interaction formulae are based on the modelling of simply supported single span members with end fork conditions and with or without continuous lateral restraints, which are subjected to compression forces, end moments and/or transverse loads.

The interaction factors k_{ij} are used to check members under coexisting normal forces and moments between points of appropriate restraint. Two different sets of coefficients have been developed separately which originate from different approaches to the beam-column interaction problem:

- Method 1 takes it starting point in the elastic resistance including buckling effects and enhances it by taking account of partial plastification, while
- Method 2 takes the plastic resistance as the basic reference, and reduces it to allow for instability effects.

These methods have been classified in terms of Level 1 and Level 2 formulae.
Level 1 is mainly focused on user-friendly formulae for standard cases of profiles, which allow a good estimate of the effects of the different parameters.
Level 2 is aimed at more comprehensive rules for general cases on the basis of computer-supported formulae.
Level 3 is thought to provide code-related rules for the numerical simulation of the most general cases by means of FE-programs.
In the format of Eurocode 3 all three levels are supported.

Method 1 belongs to the 'higher' Level 2. It has been developed with the primary intent being to obtain accurate estimates for a wide range of situations and to achieve 'maximum transparency' (in the sense that as many parameters as possible should have a clear physical meaning), even if a more complex format could not be avoided.
Generally speaking its formulation is more complex and its coefficients are quite laborious to determine (although this is no objection when implemented in computer-aided design practice). The expressions to determine the interaction coefficient are given in Annex A of EN1993-1-1.

Method 2 on the other hand belongs to the class of the more simple Level 1 formulae.
In its development the focus has been on achieving a format as simple and user-friendly as possible and on limiting the number of parameters involved, though at the expense of a certain degree of accuracy.
The values of the interaction factors can be determined from Annex B of EN1993-1-1.

In determining the interaction factors k_{ij} there is a large dependence on the shape of the bending moment diagram. This is accounted for by so-called *equivalent moment factors* C_m.
It is important to realise that these C_m-factors differ conceptually between Method 1 and Method 2. The first approach refers the actual bending moment distribution between relevant braced points to an *equivalent sinusoidal moment distribution*, while the second approach make reference to an *equivalent uniform bending moment diagram*.
This conceptual difference implies that the C_m-values are not interchangeable between the two methods.
It is remarked here that both methods were developed independently, but in EN1993-1-1 they are poured formally into a common format, despite the different objectives of both methods.

As noted by Gonçalves & Camotim [2004] it is very important to use *accurate* C_m-factors to get an *accurate* and *safe* estimate of the ultimate load capacity of a member. When using *exact* C_m-values Method 1 and Method 2 yield even almost equal results.

5.5 Non-uniform members

So far the formulae presented to verify the stability of members were applicable to *uniform* members only. Cellular beams-columns therefore are clearly outside the scope of application of the rules given to check the member's stability.

To enable the verification of these and other members for which the methods given in Section 6.3.1, 6.3.2 and 6.3.3 do apply, EN1993-1-1 provides in Section 6.3.4 a so-called *general method* which may be used to assess the resistance of such members.
It is stated that the method allows the verification of the resistance to lateral and lateral-torsional buckling for structural components such as

- single members, built-up or not, uniform or not, with complex support conditions or not, or
- plane frames or subframes composed of such member

which are subject to compression and/or mono-axial bending in the plane, but which do not contain rotative plastic hinges.
As this general method may apply to complex structural components of structural components with complex restraint conditions and/or loading, it may require the use of specific software (e.g. using Finite Element Methods)

Two load amplifiers have to be calculated from which the global non-dimensional slenderness for out-of-plane effects for the structural component can be determined:

$$\bar{\lambda}_{op} = \sqrt{\frac{\alpha_{ult,k}}{\alpha_{cr,op}}}$$

and the basic requirement for checking the *out-of-plane buckling resistance* then reads:

$$\frac{\chi_{op}\alpha_{ult,k}}{\gamma_{M1}} \geq 1$$

where:

$\alpha_{ult,k}$	is the minimum load amplifier of the design loads to reach the characteristic resistance of the most critical cross-section of the structural component considering its in-plane behaviour without taking lateral or lateral-torsional buckling into account, however accounting for all effects due to in-plane geometrical deformation and imperfections, global and local, where relevant (GMNIA)
$\alpha_{cr,op}$	is the minimum amplifier for the in-plane design loads to reach the elastic critical resistance of the structural component with regards to lateral or lateral-torsional buckling without accounting for in-plane flexural buckling (LBA)
χ_{op}	is the reduction factor for out-of-plane stability obtained for the non-dimensional slenderness $\bar{\lambda}_{op}$ using the *appropriate* buckling curve (to take into account lateral and/or lateral-torsional buckling)

The reduction factor χ_{op} may either be determined from:

- the minimum value of:
  – χ for lateral buckling
  – χ_{LT} for lateral-torsional buckling
  each calculated for the global non-dimensional slenderness χ_{op}
- a value interpolated between the values χ and χ_{LT} as determined above by using the formula for $\alpha_{ult,k}$ corre–sponding to the critical cross-section

The first method is prescribed in the Dutch National Annex, where the scope is also limited to linear members or frames consisting of such members, which are sufficiently braced laterally (i.e. 'fork' support conditions) such that its lateral or lateral-torsional

buckling behaviour between these restraints can be related to the behaviour of a straight member (either beam- or column-type behaviour).
In fact it is assumed throughout the Sections 5 and 6 of EN1993-1-1 that members can be modelled with sufficient accuracy as line elements for global analysis – i.e. all the member properties (area, inertia, etc.) can be attributed to a single line through the centroids of the consecutive cross-sections.

Contrary to the similar *overall method* found in EN1993-1-6 for the design of shell structures, the *general method* requires to take into account second-order effects when calculating the multiplier for the characteristic resistance. This implies that in-plane buckling has to be included in the determination of $\alpha_{ult,k}$ and thus a lower capacity is obtained than when the full cross-sectional resistance may be used.

That the general method does not simplify to the classical buckling check for simple structures can be seen from the example of a column subjected to pure axial load.
According to the general method:

$$\bar{\lambda}_{op} = \sqrt{\frac{\alpha_{ult,k}}{\alpha_{cr,op}}} = \sqrt{\frac{N_{b,Rd} / N_{Ed}}{N_{cr} / N_{ed}}} = \sqrt{\frac{N_{b,Rd}}{N_{cr}}}$$

which is obviously different from the 'classical' expression given in Section 6.3:

$$\bar{\lambda} = \sqrt{\frac{\alpha_{ult,k}}{\alpha_{cr,op}}} = \sqrt{\frac{A f_y}{N_{cr}}} = \sqrt{\frac{N_{pl}}{N_{cr}}}$$

However, this more conservative approach was adopted because it was shown that using the full plastic cross-section resistance when applied to e.g. hollow sections can lead to unsafe results when compared to full 3D GMNIA calculations. Therefore only the general approach as given above together with taking the minimum of χ and χ_{LT} can be safely applied [ECCS-TC8-2006-015].
From the structure of EN1993-1-1 it follows that non-uniform members like cellular beams and/or columns can only designed according the code regulations by application of this Section 6.3.4. This is affirmed by Access-Steel Resource *General method for out-of-plane buckling in portal frames* [SN032].

However, in the book *Designers' guide to EN1993-1-1* [EC3 Designers' Guide] as well as in the article *The EC3 approach to the design of columns, beams and beam-columns* [Nethercot & Gardner 2005] from the same authors it is pointed that Section 6.3.2.2 *Lateral torsional buckling curves - General case* applies to, for example cellular beams!

This is obviously not correct. Section 6.3.2 is titled *Uniform members in bending* and therefore does not apply to non-uniform members. Moreover Section 6.3.2.2 clause (1) contains the phrase *…for members of constant cross-section…* and therefore explicitly excludes non-uniform members.

The mistake may originate from the difference between the pre-standard prEN1993-1-1:2002 (stage 34 draft) and the final standard EN1993-1-1 as shown in Table 5.6. Besides, the abovementioned phrase was already present in prEN1993-1-1 (opposed to clause (1)).

By the changes made the scope of application of Section 6.3.2.2 is effectively limited (though possibly unintentionally).
Nevertheless is seems reasonable to adopt the approach given in Section 6.3.2.2 also for cellular beams, especially when they are cut from standard hot-rolled beams. It may even be argued that Section 6.3.2.3 *Lateral torsional buckling curves for rolled sections or equivalent welded sections* applies (with the additional reduction factor β) if it could be shown that the global behaviour of cellular beams is very much alike that of plain-webbed uniform beams.

Table 5.6 Overview of changed headings in Eurocode 3-1-1

Section	prEN1993-1-1: 2002	EN1993-1-1: 2005
6.3	Buckling resistance of members	Buckling resistance of members
6.3.1	Compression members	*Uniform* members in compression
6.3.1.1	Buckling resistance of uniform members	Buckling resistance
6.3.1.2	Buckling curves	Buckling curves
6.3.1.3	Flexural buckling	Slenderness for flexural buckling
6.3.1.4	Torsional and torsional-flexural buckling	Slenderness for torsional and torsional-flexural buckling
6.3.2	Lateral-torsional buckling of beams	*Uniform* members in bending
6.3.2.1	Buckling resistance for *uniform* beams	Buckling resistance
6.3.2.2	Lateral torsional buckling curves	Lateral torsional buckling curves – General case
	(2) M_{cr} is based on gross cross-sectional properties and takes into account the loading conditions, the real moment distribution, the lateral restraints *and for non-uniform sections the variation of the cross section.*	(2) M_{cr} is based on gross cross-sectional properties and takes into account the loading conditions, the real moment distribution and the lateral restraints.
6.3.2.3	Lateral torsional buckling curves for rolled sections or equivalent welded sections	Lateral torsional buckling curves for rolled sections or equivalent welded sections
6.3.3	Bending and axial compression	*Uniform* members in bending and axial compression
6.3.4	General method for lateral and lateral-torsional buckling of frames	General method for buckling of *members and* frames

5.6 *Conclusion*

The Eurocodes provides rules for the design of structures. Its various parts (EN1990, EN1991 and the various material-related parts) should be used in conjunction with each other. The rules in EN1993-1-1 are primarily aimed at the design of steel structures whereof the members can be modelled as line elements, or by the wording of Section 1.1.2 clause (6):

> *…structural analysis of structures, in which the members can be modelled with sufficient accuracy as line elements for global analysis.*

For cellular beams a schematisation to a line element satisfies at a global level, but additional checks are required to verify the design of the cross-sectional resistance. If this turns out to be the case for cellular columns also, portal frames may also be analysed by the global analysis strategies of EN1993-1-1.

As the rules given for the element design of beam-columns are almost completely aimed at uniform members , the only direct application of the Eurocode rules is by means of the general method in Section 6.3.4.
It is also possible to perform an advanced second-order elastic-plastic analysis.

For practical design purposes such an analysis is too complex, and simplified design methods may be developed (verified by more accurate analyses) as long as these methods conform to the basic requirement that:

> *the calculation model should reflect the structural behaviour at the relevant limit state with appropriate accuracy and reflect the anticipated type of behaviour of the cross-sections, members, joints and bearings.*

Design of portal frames using cellular members therefore may be based on the Eurocodes, but requires additional effort.

The actual effort needed may be decreased by the development and verification of simplified design methods. Especially the effect on compressive forces on the behaviour of cellular beams-columns is relevant in this context, and therefore requires further research.

PART II

–

NUMERICAL RESEARCH

6 INTRODUCTION

In the literature study, it was concluded that no information is available (in public) regarding the behaviour of cellular members applied as columns, either stand-alone or in portal frame structures. Therefore a numerical study has been performed in order to identify any possible differences in behaviour between plain-webbed columns and cellular members.

For cellular members loaded in compression, flexural buckling of the whole member is an possible additional failure mechanism when compared to beams, loaded in bending.
In the numerical investigation, sections of different geometric proportions were analysed to verify whether the presence of web opening causes local 'tee' buckling at the position of an opening.

Furthermore an simplified expression for checking the flexural buckling capacity of cellular members has been validated.

The second topic that has been investigated numerically, is whether an influence can be identified of the applied axial force on the web-post buckling failure mode. Therefore again sections of different geometric proportions were analysed at increasing axial load level until web-post buckling occurred.

The numerical parameter studies to the above mentioned failure mechanisms are reported in one chapter each. These chapters are preceded by a description of the finite element software SAFIR that has been used in this research, together with its accompanying tools.

7 DESCRIPTION OF THE FINITE ELEMENT SOFTWARE AND TOOLS

7.1 Introduction

The main reason to conduct a part of the research at ArcelorMittal's offices was the availability of a validated finite element tool for the calculation of cellular beams, and a suitable pre-processor. Especially the web-post buckling phenomenon is very sensitive to small deviations from the perfect-shaped structure. It is the pre-processor that introduces the relevant imperfections, such that all possible failure modes are covered by the analysis. The present chapter gives a description of the used software, together with some additional background information on the calculation algorithms.

7.2 Finite element software SAFIR

7.2.1 Capabilities and program structure

SAFIR is a special purpose computer program for studying the behaviour of structures submitted to fire [SAFIR Manual]. It was developed at the University of Liège, Belgium, by Jean-Marc Franssen. The program is based on the finite element method, and can deal with one, two and three-dimensional structures, where the number of dimensions relates to the degrees of freedom.

Using SAFIR, the analysis of a structure exposed to fire may consist of several steps. The first step involves the prediction of the temperature distribution inside the structural members, referred to as *thermal analysis*. For 3D beam elements, a *torsional analysis* may subsequently be carried out to establish the (elastic) torsional stiffness and the warping function (Vlasov theory). The last part of the analysis, termed *structural analysis*, is carried out for the main purpose of determining the response of the heated structure due to the applied loading (static and/or thermal).

As the current investigation deals with ambient temperature conditions only, no thermal analysis has to be carried out. Regarding the torsional analysis, only when a full-blown analysis with 3D beam elements is carried out, the torsional stiffness has to be provided. In that case a torsional analysis may be helpful, though it is also possible to provide a (tabulated) value directly. The torsional constant is subsequently used in the structural analysis.

For the present research, the following features of SAFIR are of interest:

- possibility to analyse both 2D and 3D structures
- various element types, amongst others beam and shell elements
- geometrically as well a materially non-linear calculation
- automatic adaptation of time step until failure occurs
- large displacements and distortions are considered
- local failure of a part of the structure that does not endanger the safety of the whole structure can be handled by means of a dynamic analysis
- both imposed displacements and master-slave relations (forced equal displacements) can be introduced
- residual stresses in beams can be accounted for (using beam elements: fibre model)
- unloading of material is parallel to the elastic-loading branch

The SAFIR program consists of an command-line executable and a library (.DLL) file.

The data for the analysis has to be provided by means of a plain text input (.IN) file. An (abbreviated) example for a structural analysis is provided on the next page. The input file also specifies the type of the analysis (either thermal, torsional or structural). On it's turn the input file refers to separate files for each element type.

Depending of the type of element, the suffices of these files are designated (.TEM) for beam

```
    NPTTOT   4672
     NNODE   628
      NDIM   3
 NDIMMATER   2
   NDDLMAX   6
      FROM   1 TO 628 STEP 1 NDDL 6
  END_NDDL
   DYNAMIC   APPR_NR
   DAMPING   0.
     NLOAD   1
   OBLIQUE   0
  COMEBACK   0.1
 LARGEUR11   537409
 LARGEUR12   253
  RENUMGEO   1
      NMAT   1
  ELEMENTS
     SHELL   584  6
   NGTHICK   2
    NGAREA   2
   NREBARS   0
  END_ELEM
     NODES
      NODE   1     0.00000    0.00000   -0.48250
      NODE   2    -0.00153    0.00000   -0.37726
       ...

FIXATIONS

BLOCK     1   F0    F0    F0    F0   F0   F0
BLOCK     2   F0    F0    F0    F0   F0   F0
 ...

SAME   438   443   NO    YES   NO   NO   NO   NO
SAME   439   443   NO    YES   NO   NO   NO   NO
 ...

END_FIX

NODOFSHELL
ACB_IPE600UF.TSH
 TRANSLATE    1    1
 END_TRANS
 ...

ELEM           1     1     2     13     12     3
ELEM           2     2     3     14     13     3
 ...

PRECISION   1.E-3

LOADS

FUNCTION    F1PS

NODELOAD    448   0   -83.333   0   0   0   0
NODELOAD    509   0   -41.667   0   0   0   0
 ...

END_LOAD

      MASS
   M_SHELL   1   94.20
  GM_SHELL  30   94.20    1
     ...
  END_MASS

MATERIALS
STEELEC32D
210E9   0.3   235E6

TIME
100.   3000.  250.
END_TIME

LARGEDISPL
NOEPSTH

IMPRESSION
TIMEPRINT
250.   2000.
0.1    3000.
END_TIMEPR

PRNNXSHELL
```

Listing 7.1 Structure of an input file for structural analysis

element and (.TSH) for shell elements. These files are the output of the thermal analysis, but they may also be created from scratch (or using a wizard) when no thermal analysis has to be carried out.

For a structural analysis in cold situation these files do not have to include the temperature distribution over the element, which is the output of the thermal analysis.

Besides the possibility to analyse the structural behaviour under elevated temperatures, one of the prime features of SAFIR is the method to deal with non-linear behaviour. For simple structures (e.g. a single compressed column) the maximum on the load-deflection curve is also the 'true' failure load (e.g. the buckling capacity). However, in more complex building structures there is often some redundancy present, which enables the structure to survive when a few elements cease to fulfil their load bearing function. In mathematical terms this corresponds to several local maxima which are present on the load-deflection curve prior to the global maximum. Such local maxima may not only be caused by geometrical non-linear behaviour, but can also be due to non-linear material behaviour (descending branches in $\sigma - \varepsilon$ relationships, formation of plastic hinges) [Franssen 2007].

With the classic algorithm – in which the increment of the applied force ΔF is uniquely related to the incremental displacements Δu – it is usually impossible to reach this global maximum or 'true' failure load. Near the first encountered local maximum the stiffness matrix becomes close to zero which means that it is possible to increase the displacements of the structure without any increase of the load. Mathematically speaking the stiffness matrix is not defined positive anymore.

As a consequence the failure load can be underestimated. Furthermore no insight is gained in the real failure mechanism. Both for research interests and safety reasons (think of rescue operations in case of fire) this knowledge is essential.

Various techniques have been developed to cope with these numerical failures. Unstable elements can be removed from the structures, modified $\sigma-\varepsilon$ relationships, non-tangent stiffness matrices or arc-length type methods can be applied. All these techniques have one or more drawbacks. For example, when members that have failed (buckled) are cut in order to deal with local instabilities, the fact is ignored that even buckled members are able to bear a non-negligible compression force. Due to load redistribution they can even be subjected to an important tensile force in a further stadium. Finite element methods which use an arc-length method calculate an equilibrium solution wherefore the load has to be decreased in order to limit the displacements. Though this may be a mathematically sound solution, in real structures normally no load reduction is observed during failure, and thus it makes no sense.

The approach for non-linearity implemented in SAFIR consists in performing a dynamic analysis. The objective here is that the acceleration term will counterbalance the negative stiffness during the unstable states of the structure. For linear behaviour, the basic equation reads [Franssen & Gens 2004]:

$$\mathbf{K}u + \mathbf{C}\dot{u} + \mathbf{M}\ddot{u} = F$$

where:

$\mathbf{K}$ is the stiffness matrix,
$\mathbf{C}$ is the damping matrix and
$\mathbf{M}$ the mass matrix.

This equation is solved by a step-by-step method of the Newmark family, adapted for non-linear behaviour. In the determination of the mass matrix the contribution from the finite elements has been diagonalised in order to limit memory usage. For the 3D beam finite element, the two masses in rotation about the axes that are perpendicular to the longitudinal axis, are given the same value as the mass in rotation along the longitudinal axis. Thus the need of a coordinate mapping from the local to the global system is avoided. The shell finite element has only the terms in the mass matrix corresponding to displacements.

Furthermore no damping matrix is calculated but the two Newmark parameters are modified, by which a numerical damping is introduced. When using the common solution of Rayleigh damping – where the damping matrix is a linear combination of the stiffness and the mass matrix, with the coefficients of the combination being calculated as a function of the critical damping and the first two eigenfrequencies – a negative stiffness matrix could result in a negative damping matrix, thus making the system unstable.

The above approximations are justified by the fact that the objective is to deal with local instabilities and not to implement a precise modelling of dynamic effects.

It is important to note however that SAFIR is not a toolbox for all kinds of finite element calculations but it is specially geared towards structural and fire engineering calculations for building structures.

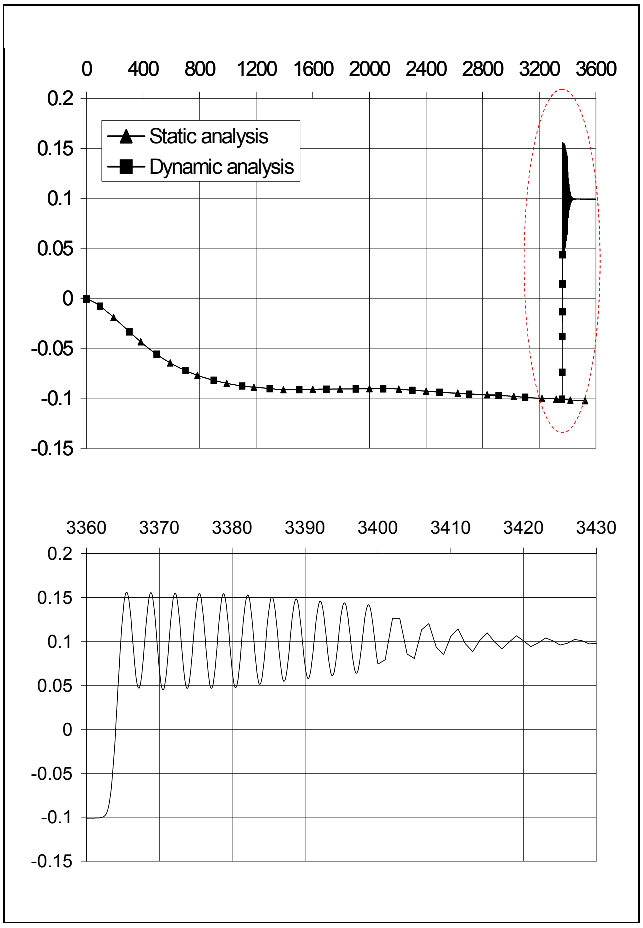

Figure 7.1 Passing through a local failure by the dynamic approach

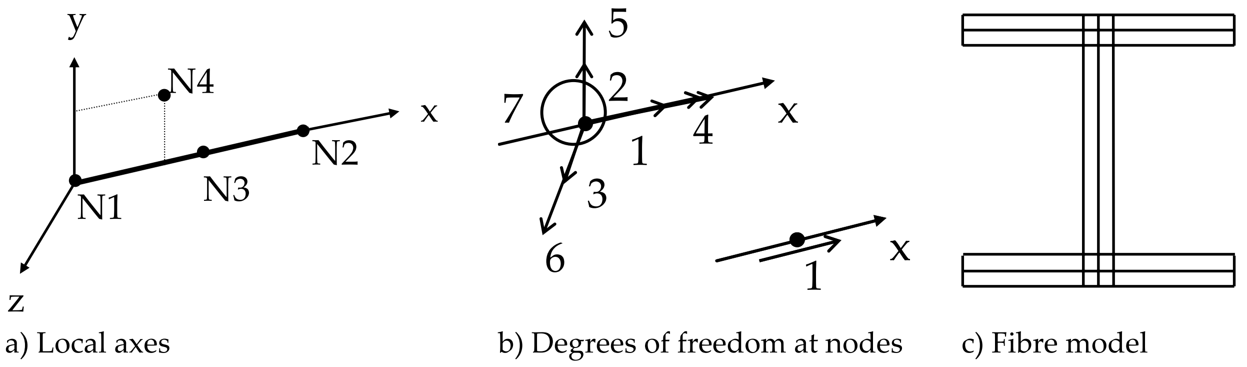

Figure 7.2 Beam element

The dynamic approach enables to predict the influence of a local failure on the global behaviour of the structure and to simulate the complete failure mechanism. Figure 7.1 shows how the dynamic analysis is able to overcome a local stability (buckling of a redundant member, taken from Franssen *et al* [2004]).
By using the dynamic approach the concept of time is introduced for analysis in cold situation. The time step has to be chosen sufficiently small such that dynamic effects due to load application are minimised. Several functions are available and can defined by the user to prescribe the variation of the load application with time.
During the calculation SAFIR adapts the initial time step based on the number of iterations required for obtaining convergence. Choice can be made between a pure Newton-Raphson procedure (recommended for structures made of beam elements) and a modified Newton-Raphson convergence procedure (recommended for structures made of shell elements). If convergence is not obtained, the calculation is repeated from the previously converged point with a reduced time step. The calculation continuous until failure or until the end time (set by the user) is reached. Accordingly, there is no deflection criterion to stop the calculation.
Depending on the kind of analysis (thermal or structural) and the types of elements used, output results like temperatures, reactions, out-of-balance forces, (generalized) displacements, stresses, etc. can be printed.

7.2.2 Element types

SAFIR accommodates various finite element types. However, not all elements are available for every kind of analysis. The solid elements (2D and 3D) are available for thermal analyses only. All other element types can be used for structural analyses as well. They read

- beam elements (2D and 3D)
- shell elements
- truss elements

In the present study only beam and shell elements were used. Therefore only of these elements short descriptions are given here, partly taken from reference [SAFIR Theory].

Beam element

The beam element is straight in its un-deformed geometry. In 2D its position in space is uniquely defined by the two end nodes (N1 and N2). For 3D beam elements an additional node (N4) is needed, which defines the position of the local y axis of the element, and so the orientation of the beam element (strong/weak direction).
The internal node (N3) is used to support an additional degree of freedom (DOF), being the second-order component of the longitudinal displacement. This internal node thus has only one DOF (shown right in Figure 7.2b).
For 2D beam element three DOFs are present at both end nodes: two translations and one rotation. When 3D beams elements are used, seven DOFs are possible for each node: three translations, three rotations and warping (shown left in Figure 7.2b).

To describe the geometry of the cross-section, the fibre model is used. The cross-section of the beam is subdivided into small fibres (triangles, quadrilaterals or both). The material behaviour of each fibre is calculated at the centre of the fibre and it is constant for the whole fibre. Each fibre has it's own material, this allows for the building of composite sections made of different materials. The cross-sectional data of each fibre has to be provided in the (.TEM) file, together with the material number and eventually a value for the residual stress.
Assumptions for beam elements are:

- the Bernoulli hypothesis is considered, i.e. the cross-section remains plane under bending moment
- plastifications are only considered in the longitudinal direction of the member, i.e. uni-axial constitutive models
- non-uniform torsion is considered (3D)

In the input (.IN) file the number of integration points has to be provided. These points are defined according to the scheme of Gauss. For each beam element and at each (Gaussian) integration point, the following quantities can be printed:

- internal forces (normal force and bending moment)
- the stresses in each fibre
- the tangent modulus (in the linear range: the modulus of elasticity)

By a linear interpolation from the integration points to the end of the element, the bending moment will be nearly exactly equal to 0 at simple supports.

Shell element

The shell element is described by it's four nodes. These nodes determine the local reference frame of the element. Each node has six degrees of freedom: three translations and three rotations.
There are four points of integration on the surface of the element, placed according to Gauss' method. The choice of the number of integration points on the thickness has to be made by the user, from 2 to 10, and the integration is also by the method of Gauss.
It is also possible to provide different layers of rebars with varying cross-section, material and angles between the bar direction and the local x-axis. Because the present investigation is limited to steel members and no rebars are used, this possibility is not further explained.
A detailed theoretical description about the development of the shell element, together with some verification examples, can be found in Talamona & Franssen [2005].
The quantities available for print in each element for each surface integration point are:

- stresses (normal and shear stresses) for each integration point over the thickness
- stress resultants (membrane forces and bending moments), together with the principal values and angle
- membrane and bending stiffnesses

In structures with non-rectangular shell elements like a cellular beam, the local reference frame is different for each element. Because most results are expressed in this local frame, which does not coincide with the global reference frame, most values are not easy interpreted.
The principal stress resultants, in combination with the corresponding angles, can be used anyway as they are independent of the chosen reference frame.

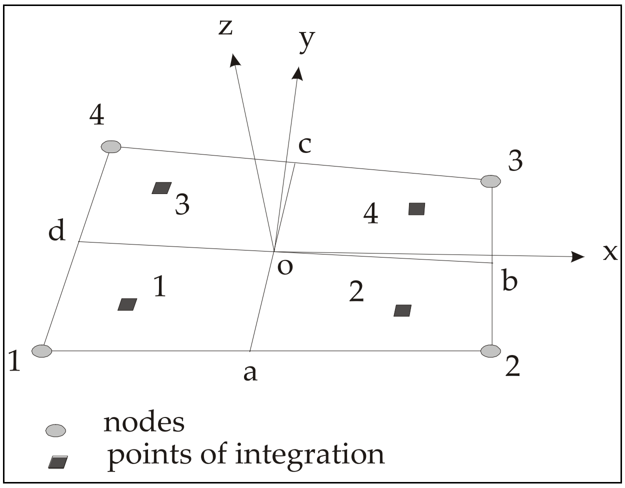

Figure 7.3 Shell element

7.2.3 Material laws

Material properties are already included in the SAFIR code. They are defined according to the Eurocodes for both steel and concrete. The degradation of the material properties with increasing temperatures is also incorporated, For each group of elements, a different material can be specified. It is also possible to provide a user-defined material. Such a material may be linear-elastic, bi-linear, plane stress, with or without the Von Mises criterion, it may have different compression and tensile strengths (for concrete) or it may even not able to carry any load at all (useful for insulation materials, whereof only the thermal properties are of interest).
For shell finite elements the material law for steel according to the Eurocode has been adapted for the two-dimensional material model: plane stress, Von Mises, with non-linear isotropic hardening. Contrary to beam elements, whose material law is one-dimensional (uniaxial deformation of the fibres), an additional parameter is required to be introduced by the user: Poisson's ratio ν.

7.2.4 Safir Shell

For practical purposes, an interface to the SAFIR executable was developed. This interface, designated Safir Shell, allows the user to specify a number of input files at one go. The files are then processed in the given order. Thus the need to start each analysis by hand is avoided and several subsequent analyses can be carried out automatically, e.g. run a temperature analysis first, and then use the results for the next structural analysis.

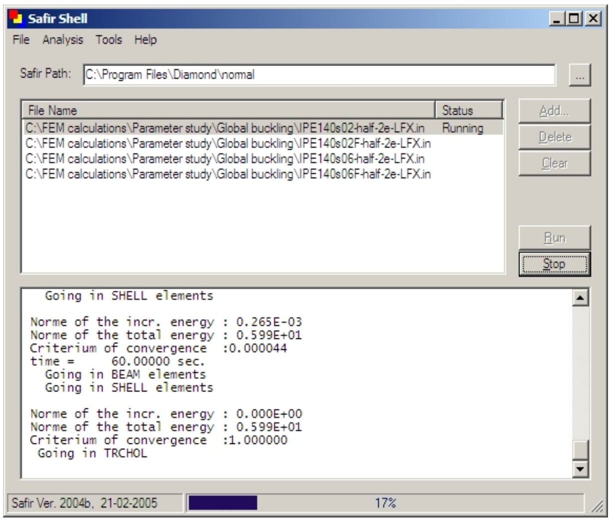

Safir Path: C:\Program Files\Diamond\normal

File Name	Status
C:\FEM calculations\Parameter study\Global buckling\IPE140s02-half-2e-LFX.in	Running
C:\FEM calculations\Parameter study\Global buckling\IPE140s02F-half-2e-LFX.in	
C:\FEM calculations\Parameter study\Global buckling\IPE140s06-half-2e-LFX.in	
C:\FEM calculations\Parameter study\Global buckling\IPE140s06F-half-2e-LFX.in	

```
  Going in SHELL elements

Norme of the incr. energy : 0.265E-03
Norme of the total energy : 0.599E+01
Criterium of convergence  :0.000044
time =     60.00000 sec.
  Going in BEAM elements
  Going in SHELL elements

Norme of the incr. energy : 0.000E+00
Norme of the total energy : 0.599E+01
Criterium of convergence  :1.000000
 Going in TRCHOL
```

Safir Ver. 2004b, 21-02-2005 17%

Figure 7.4 The Safir Shell interface

7.3 Pre-processors

7.3.1 Introduction

While it is possible to predict the structural behaviour considerably more accurate by advanced modelling, it still takes a lot of time to build a proper finite element model, including boundary conditions, loads and input for the thermal analysis, if required.
In order to facilitate this task for single-span cellular beams, the pre-processor Crystal Pro was developed for ARBED (merged into Arcelor, now ArcelorMittal). Furthermore a pre-processor to generate a finite element model for portal frames made of cellular beams is still under development.

7.3.2 Crystal Pro

This pre-processor allows the easy generation of a finite element model of a (composite) cellular beam to simulate the behaviour in case of fire. It basically divides a cellular beam into panels related to the web configuration. The web panel types that are possible are:

- plain sheet panel
- panel with circular opening, that is either filled or not
- panel with half a circular opening, that is either filled or not

All data, including the dimensions and thicknesses of the different plate parts, the number of panels and stiffeners, boundary conditions, anti-buckling supports, material properties, loading, fire exposure conditions, type of analysis etc. have to be provided in a single (.DAT) file. The format of this file is described in the User's Manual [Crystal Pro]. Together with information about the number of finite elements to be used on each panel, the executable can build the (.IN) and (.TSH) files needed for calculation in SAFIR.

Using the Crystal Interface to Crystal Pro, all data can be entered step-by-step in a user-friendly graphical interface (see below). It also allows to import a (.CLB) file created with the software tool ARCELOR Cellular Beams, which contains all beam data, the supports and the loadings. Thus the need to enter all data by hand is avoided and the risk on errors is reduced. The FE model allows the fire engineering design of ACBs and a wider range of beams (fixed supports etc.) can be analysed than in the ACB program.

Supports, loads, etc. are applied such that the real conditions are met most closely. Furthermore and most important, initial imperfections are modelled, consisting of a sine over the profile's height times a cosine over half the beam length, thus enabling the failure modes of web-post buckling and lateral-torsional buckling to occur.
The amplitudes are based on extensive measurements on produced ACBs, and depend on the type of section, the size of the web post and the support conditions.

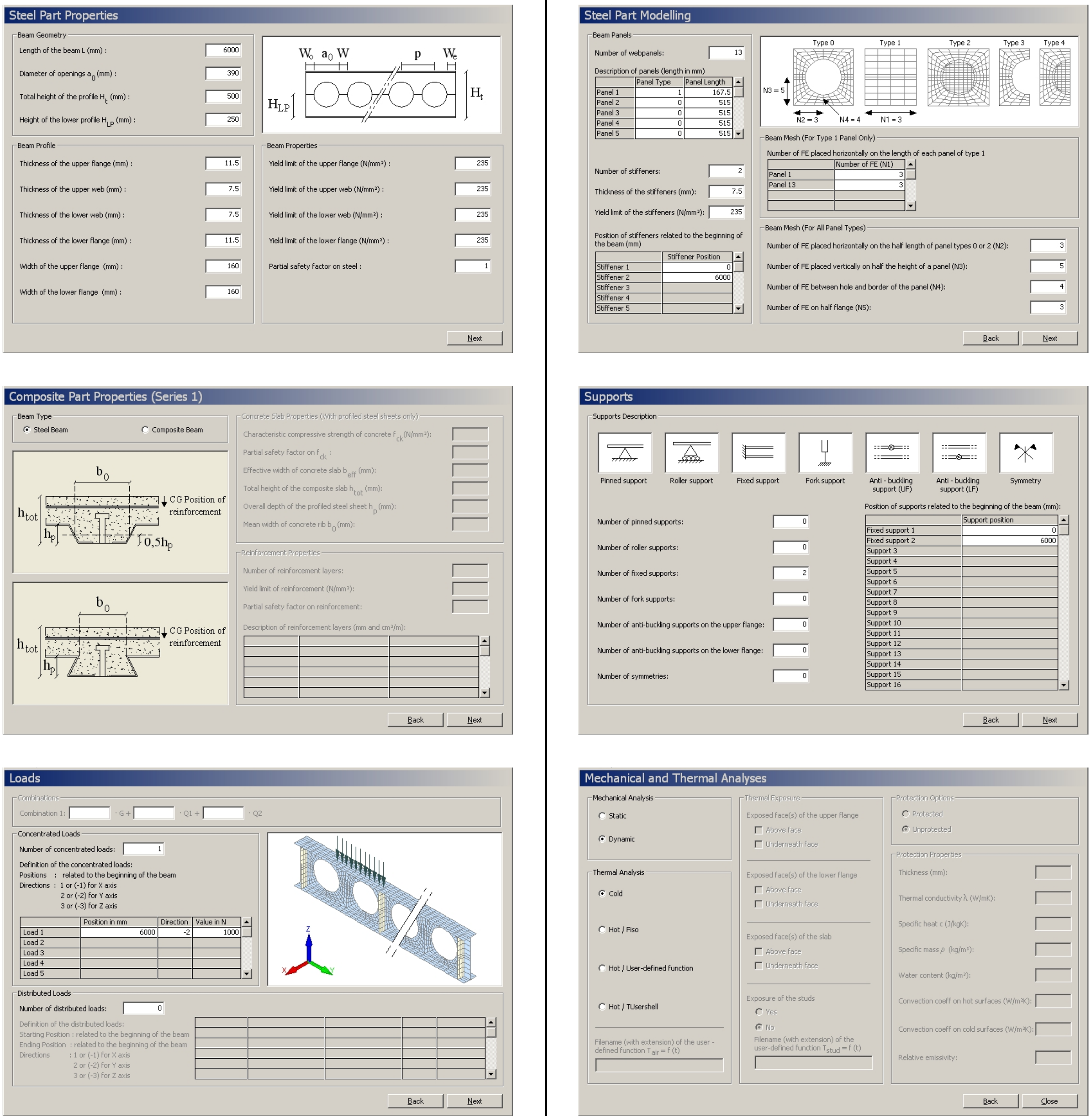

Steel Part Properties

Beam Geometry
Length of the beam L (mm) : 6000
Diameter of openings a_0 (mm) : 390
Total height of the profile H_t (mm) : 500
Height of the lower profile H_{LP} (mm) : 250

Beam Profile
Thickness of the upper flange (mm) : 11.5
Thickness of the upper web (mm) : 7.5
Thickness of the lower web (mm) : 7.5
Thickness of the lower flange (mm) : 11.5
Width of the upper flange (mm) : 160
Width of the lower flange (mm) : 160

Beam Properties
Yield limit of the upper flange (N/mm²) : 235
Yield limit of the upper web (N/mm²) : 235
Yield limit of the lower web (N/mm²) : 235
Yield limit of the lower flange (N/mm²) : 235
Partial safety factor on steel : 1

Steel Part Modelling

Beam Panels
Number of webpanels: 13

Description of panels (length in mm)

	Panel Type	Panel Length
Panel 1	1	167.5
Panel 2	0	515
Panel 3	0	515
Panel 4	0	515
Panel 5	0	515

Number of stiffeners: 2
Thickness of the stiffeners (mm): 7.5
Yield limit of the stiffeners (N/mm²): 235

Position of stiffeners related to the beginning of the beam (mm)

	Stiffener Position
Stiffener 1	0
Stiffener 2	6000
Stiffener 3	
Stiffener 4	
Stiffener 5	

Beam Mesh (For Type 1 Panel Only)
Number of FE placed horizontally on the length of each panel of type 1

	Number of FE (N1)
Panel 1	3
Panel 13	3

Beam Mesh (For All Panel Types)
Number of FE placed horizontally on the half length of panel types 0 or 2 (N2): 3
Number of FE placed vertically on half the height of a panel (N3): 5
Number of FE between hole and border of the panel (N4): 4
Number of FE on half flange (N5): 3

Composite Part Properties (Series 1)

Beam Type
● Steel Beam ○ Composite Beam

Concrete Slab Properties (With profiled steel sheets only)
Characteristic compressive strength of concrete f_{ck} (N/mm²):
Partial safety factor on f_{ck} :
Effective width of concrete slab b_{eff} (mm):
Total height of the composite slab h_{tot} (mm):
Overall depth of the profiled steel sheet h_p (mm):
Mean width of concrete rib b_0 (mm):

Reinforcement Properties
Number of reinforcement layers:
Yield limit of reinforcement (N/mm²):
Partial safety factor on reinforcement:
Description of reinforcement layers (mm and cm²/m):

Supports

Supports Description
Number of pinned supports: 0
Number of roller supports: 0
Number of fixed supports: 2
Number of fork supports: 0
Number of anti-buckling supports on the upper flange: 0
Number of anti-buckling supports on the lower flange: 0
Number of symmetries: 0

Position of supports related to the beginning of the beam (mm):

	Support position
Fixed support 1	0
Fixed support 2	6000
Support 3	
Support 4	
Support 5	
Support 6	
Support 7	
Support 8	
Support 9	
Support 10	
Support 11	
Support 12	
Support 13	
Support 14	
Support 15	
Support 16	

Loads

Combinations
Combination 1: · G + · Q1 + · Q2

Concentrated Loads
Number of concentrated loads: 1
Definition of the concentrated loads:
Positions : related to the beginning of the beam
Directions : 1 or (-1) for X axis
2 or (-2) for Y axis
3 or (-3) for Z axis

	Position in mm	Direction	Value in N
Load 1	6000	-2	1000
Load 2			
Load 3			
Load 4			
Load 5			

Distributed Loads
Number of distributed loads: 0
Definition of the distributed loads:
Starting Position : related to the beginning of the beam
Ending Position : related to the beginning of the beam
Directions : 1 or (-1) for X axis
2 or (-2) for Y axis
3 or (-3) for Z axis

Mechanical and Thermal Analyses

Mechanical Analysis
○ Static
● Dynamic

Thermal Analysis
● Cold
○ Hot / Fiso
○ Hot / User-defined function
○ Hot / TUsershell
Filename (with extension) of the user - defined function $T_{air} = f(t)$

Thermal Exposure
Exposed face(s) of the upper flange
☐ Above face
☐ Underneath face
Exposed face(s) of the lower flange
☐ Above face
☐ Underneath face
Exposed face(s) of the slab
☐ Above face
☐ Underneath face
Exposure of the studs
○ Yes
● No
Filename (with extension) of the user-defined function $T_{stud} = f(t)$

Protection Options
○ Protected
● Unprotected

Protection Properties
Thickness (mm):
Thermal conductivity λ (W/mK):
Specific heat c (J/kgK):
Specific mass ρ (kg/m³):
Water content (kg/m³):
Convection coeff on hot surfaces (W/m²K):
Convection coeff on cold surfaces (W/m²K):
Relative emissivity:

Figure 7.5 The several windows of the Crystal Interface for Crystal Pro

7.3.3 Mailleur Portique

In the framework of an internal research project within Arcelor, another pre-processor has been developed. The project aimed to gain knowledge about the application possibilities and limitations of cellular beams in portal frame structures. However, due to a shift in research priorities the project status is on hiatus now.

In order to ease the generation of the finite element model, the project started with the development of a pre-processor for in-plane (multi-storey) portal frame structures. This pre-processor consists of a single executable, called MPort4. As for Crystal Pro, all data has to be entered in a single (.DAT) file. Basically the input consists of a number of global coordinates, and for each beam or column the dimensions of the separate plate parts. Furthermore it is possible to add intermediate stiffeners, e.g. at joint locations. The pre-processor generates a finite element mesh, the (.IN) file, whereof the parameters (number of elements placed on the height etc.) have to be entered in the input file.

The pre-processor is still in a beta-phase. No user interface is available yet and the only documentation is in the form of a sample input file with elucidatory comments. It does generate a finite element mesh, but quite a lot of modelling afterwards is still required before the analysis can be run.

At present the supports and loadings have to be added by hand. Furthermore no imperfections, either global or local, are taken into account and some errors were encountered also. Some of these are easily corrected (e.g. the timestep parameter is limited to an integer), but others require due attention: the thicknesses of some plate parts are set to zero, web panel nodes do not always match with the nodes of stiffener plates and masses are generated only for the first few elements. When these issues are properly addressed afterwards, the pre-processor can be used to analyse portal frame structures.

In principle it is possible to enter an arbitrary number of nodes (global coordinates), so multi-bay portal frame structures can be processed by MPort4 as well. However, the non-dynamical memory allocation in SAFIR itself, at the start of the analysis, limits the size (i.e. nodes/elements/blocks) of the problem.

7.4 Post-processor Diamond

In finite element analysis it is essential to be able to have different ways to check for errors. The post-processor Diamond provides a means for this. It allows to check the input data (mesh view, modelling of supports, loads, etc.) and it can visualise the results that are stored in the (.OUT) files. The viewpoint can be changed and a selection can be made so that only certain elements/nodes/materials are shown (e.g. to make cut a section).

Depending on the type of analysis and the quantities that have been stored, it is possible to plot the temperature distribution, deformations, generalised stress diagrams (axial and normal force as well as the moment distribution) and shell stress resultants. Furthermore charts can be generated to show the evolution of displacements, bending moments, etc. as a function of time.

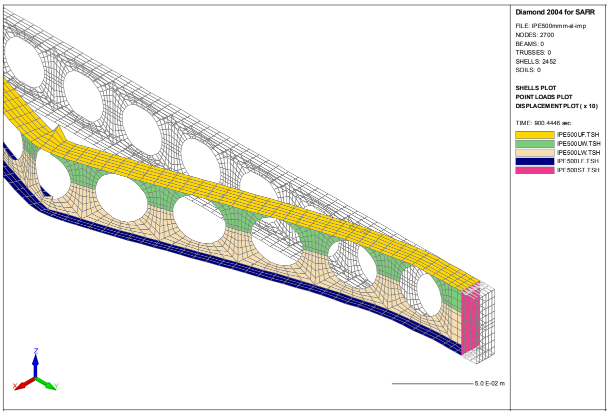

Figure 7.6 Deformation plot in Diamond

8 GLOBAL BUCKLING OF CELLULAR MEMBERS

8.1 Introduction

Cellular members have been used extensively in floor and roof applications. As such beams are primarily loaded in bending, all previous test programmes were designed to investigate the response if loads are applied perpendicular to the beam's system line. Of course some additional normal forces (due to wind loads) may occur in beams, but these will normally not dominate the behaviour.

On the contrary, when cellular members are applied as columns the normal load will govern the element's behaviour, while bending due to transverse loads plays an subordinate part.

As no experimental evidence is available on the flexural buckling behaviour of cellular members, numerical investigations were carried out with the next objectives in mind:

- to verify the similarity of global flexural buckling of cellular members when compared to plain-webbed members, and to provide easy-to-use design expressions for checking the buckling capacity of cellular columns
- to study the influence of the applied axial force on the web-post buckling failure mode

The current chapter present the set-up and results of an extensive parameter study made in order to confirm theoretical results and to validate an easy rule for determining the flexural buckling capacity of cellular columns. Ample attention is given to the modelling of the structure with its supports and the way in which the loads are applied together with the imperfections in use.

In the next chapter the results of the investigation to the influence of an axial force on the web-post buckling behaviour are discussed.

8.2 Theoretical analysis

While cellular beams have been researched quite extensively, no information is available regarding specific studies to the behaviour of cellular columns. However, for castellated beams it has been shown that the lateral-torsional buckling behaviour is similar to that of plain-webbed beams.
Therefore it was expected that the global buckling behaviour of cellular columns is also similar to that of standard hot-rolled sections.

The easiest method to deal with the reduction in flexural stiffness of a cellular column due to the presence of multiple web openings, is to use the properties of the *net section* at the location of an opening in the formulae that are valid for a plain-webbed section.

The slenderness for flexural buckling reads:

$$\bar{\lambda} = \sqrt{\frac{N_{pl}}{N_{cr}}}$$

where:

$$N_{pl} = A f_y$$

$$N_{cr} = \frac{\pi^2 EI}{\ell^2}$$

The amount by which the *plastic capacity* of the net section is reduced is independent of the buckling direction considered.
However, the amount by which N_{cr} is reduced – which is directly related to the reduction factor for buckling χ – *does* depend on the buckling direction that is considered.

For buckling in the weak direction the weak second moment of area I_z applies. This quantity is hardly affected by the presence of a web opening and so N_{cr} remains almost unchanged.

Therefore the slenderness $\bar{\lambda} = \bar{\lambda}_z$ *decreases* with increasing opening diameter, thereby *increasing* the reduction factor $\chi = \chi_z$.

However, it turns out that for practical dimensions the reduction in net area *outweighs* the increase of the reduction factor for buckling, and so the global buckling capacity:

$$N_{b,Rd,z} = \chi_z \cdot N_{pl}$$

is effectively *reduced* indeed due to the presence of web openings.

The second moment of area I_y of the net section, which applies for flexural buckling about the strong axis, is also reduced, but to a stronger extend than I_z. Therefore *qualitatively* the effect of the web openings (a reduction) is the same as for buckling in the weak direction.

Nevertheless, *quantitatively* there is an major difference. For a pinned-pinned column that is not braced at intermediate locations and whereof thus the buckling lengths in both directions are equal, the slenderness $\bar{\lambda}_z$ in the weak direction will be much higher than the slenderness $\bar{\lambda}_y$ in the strong direction.

With increasing slenderness the influence of the opening diameter becomes less apparent, as *not the pure axial capacity but the buckling factor* becomes the governing parameter.

So it follows that the buckling capacity in the strong direction will be much more affected by the presence of web openings than the capacity in the weak direction, because of the already high reduction factor for flexural buckling χ_y in the case of buckling about the strong axis.

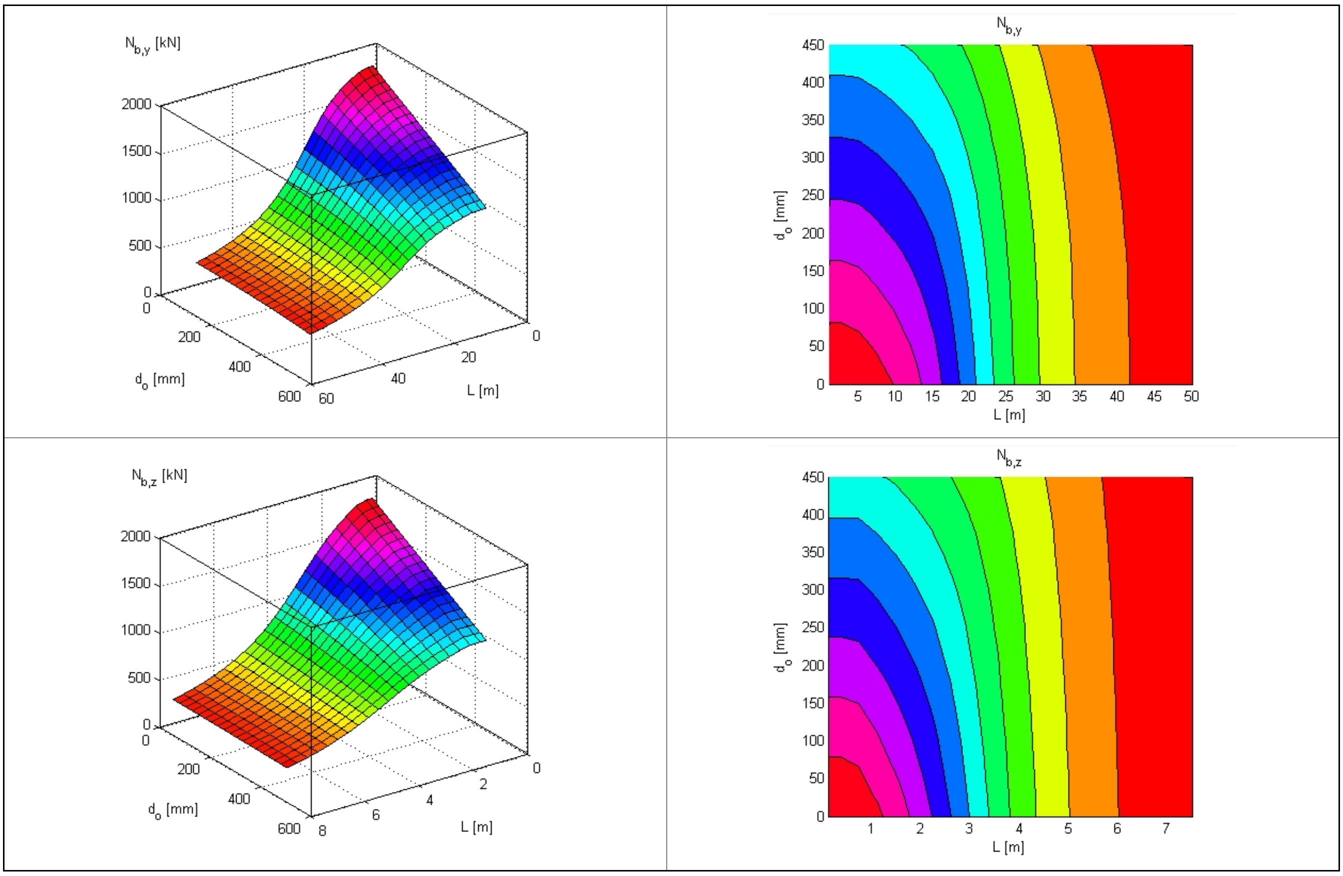

Figure 8.1 Influence of the opening diameter on the buckling load of a cellular beam
Example for a cellular beam cut from a IPE330 profile with h = 500mm.
Top: buckling in strong direction. *Bottom*: buckling in weak direction.

8.3 Finite element model

8.3.1 Introduction

The main goal of this part of the numerical investigation to the behaviour of cellular beam-columns, is to confirm the hypothesis that the global buckling behaviour does not *qualitatively* differ from that of plain-webbed columns. A further objective was to validate the easy approach described above to the verification of the global buckling capacity of cellular columns based on the net-section properties, and to determine its accuracy.

The focus of the research being aimed primarily at global buckling behaviour, numerical simulations have been performed on cellular members loaded axially only.

The finite element tool that was used to perform the calculations, SAFIR, has been described in Chapter 7 already. In the next subsections the modelling of the supports, the applied imperfections and the way of load application are explained.

8.3.2 Support conditions

Flexural buckling of a pin-ended strut is commonly regarded as the most elementary case for flexural buckling of a single column. It would therefore be reasonable to investigate this specific case.

In 2D finite element simulations using beam elements this is quite easy to achieve. At the supports, only the translations have to be prevented (i.e. prescribed value equal to zero), while rotations are allowed to occur freely. However, in a full 3D analysis using shell elements a correct modelling of pinned supports is far more difficult to obtain.

In plain-webbed columns the flange area constitutes the biggest part of the total area of a cross-section. For cellular columns this holds even more. Therefore the largest part of the axial force will be carried by the flanges.

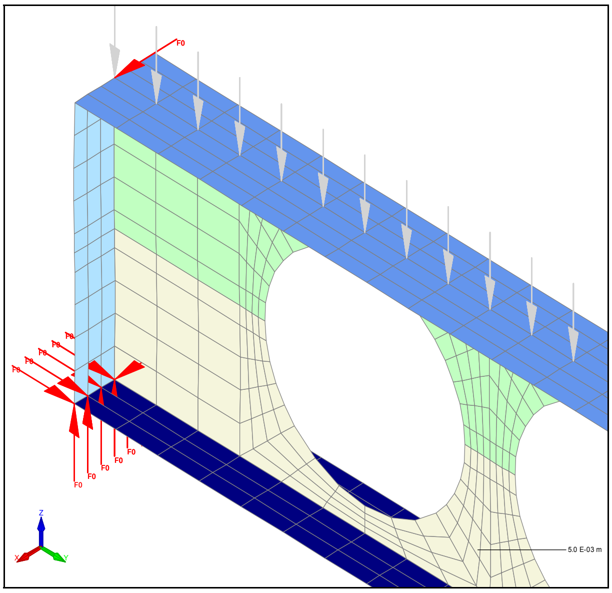

Figure 8.2 Finite element modelling of pinned supports for beams

In order to transmit this force to its supporting structure, whether it be a beam, another column or the foundation structure, the nodal points representing the flanges thus have to be fixed axially.

The prime difficulty then is that the fixation of the flange nodes automatically prevents the rotations of the cellular members at the supports, about both axes. This cannot be avoided even partially by fixing the web only, as high local deformations due to the force transfer from the flanges to the web would then limit the ultimate capacity, and the column would fail even before reaching its flexural buckling capacity. The goal being to investigate global member buckling, such local failures have to be prevented.

For beams this problem also exists, but to a lesser extent. At the supports the primary load transfer is by shear, which is carried mainly by the web. When investigating practical applications – in which sense SAFIR is used mostly at ArcelorMittal's offices – the modelled supports have to resemble practice as closely as possible. In Figure 8.2 the fixations applied by Crystal Pro for a pinned fork support are shown.

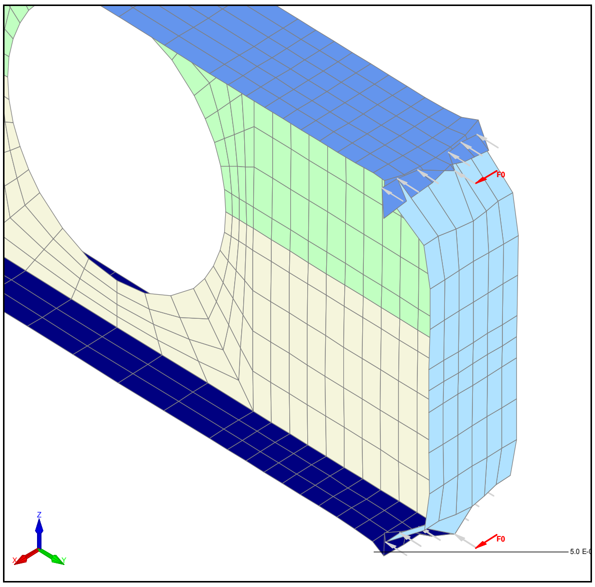

Figure 8.3 Failure behaviour when equal displacements are prescribed for each flange

Still when performing numerical analyses to investigate the theoretical problem of lateral-torsional buckling it may be a problem that the rotation about the beam axis is also partly restrained by this way of modelling.
A workaround is to add stiffening elements, like beam elements which connect the flange nodes and the web nodes respectively, see for example Maljaars *et al* [2004].
Comparatively one may think of methods to overcome the described problem for simply supported (pinned-pinned) columns.

Firstly, just like for beams (i.e. members in bending) *beam elements* can be added to the end cross-sections. This approach however was not applied in the present investigation, as it requires a lot of manual adaptation of the automatic generated finite element mesh, together with a thorough evaluation of the geometric properties which should be assigned to these connecting elements.

Secondly, *thick plate elements* can be added as stiffening elements. It is a fairly easy method as the thickness of the stiffener plate is just one parameter which can be directly edited. Nevertheless he limits of application of the shell elements have to be kept in mind. By definition the thickness of a shell element is far less than the two other dimensions and so should be the thickness of the stiffening plate. Moreover in the SAFIR formulation for the shell element, no shear transfer is allowed in the out-of-plane direction, thus the element is not suitable to very thick end plates.

Thirdly, an attempt has been made to model a pinned support by *prescribing that the beam end rotates as a whole*. This can be implemented by using the SAME command. Each degree of freedom, e.g. the displacement of a certain node, can be defined to be equal to that of another node. However, this approach also has its problems.

For example, it is straightforward to prescribe equal *displacements* for all nodes at the beam end that are connected to one particular flange. But then, the support will actually behave as clamped in the out-of-plane direction. Therefore the approach with equal displacements can only be applied to problems where only an in-plane response is expected and/or possible. Even then this additional support may be unwanted.

Furthermore, due to load introduction at the flanges, the beam end will deform heavily (see Figure 8.3). As the web is not stressed, it does not deform along with the flange. Therefore in addition equal displacements for every single node-line have to be prescribed. And still this would not suffice as the end plate is not forced to rotate as a single body (which is what happens in elementary beam theory).

For that reason it is necessary to enforce that all *rotations* of the end plate are equal also. Even then the behaviour is not satisfactory. It's even more difficult to model a support that really behaves as pinned in both directions, as no equal displacements can be prescribed for each node-line anymore.

Fourthly, it has been considered not to model these pinned supports as such, but instead to fix the middle of the member and to apply *symmetry conditions for the ends*. Although this approach seems attractive, it was not applied as it turned out that applying symmetry conditions is very costly in terms of computing time. Furthermore the results of a few preliminary calculations by this approach differed up to 10% from the expected theoretical result, where the method described next proved more successful.

Finally, it was decided that in order to eliminate all kinds of problems with trying to model a pinned support, not a pinned-pinned column, but one with *clamped supports* would be analysed. Therefore all rotations have been *fully restrained* at both sides. This implies that the elastic buckling length of the member is not equal to the system length anymore.
In order to acquire the same slenderness the beam length thus has to be increased, which requires additional computation effort. However, for symmetric problems like a column only loaded by an axial force, it is possible to define a symmetry condition half-way the beam. Thus the model size and the computation time are reduced considerably.

8.3.3 Use of imperfections

When performing finite element calculations to determine ultimate loads for the flexural buckling mechanism, the use of the appropriate shape and size of imperfections is of primary importance. Usually *equivalent geometric imperfections* are applied, which account for the combined effect of:

- geometrical imperfections of members as governed by geometrical tolerances in product standards or the execution standard
- structural imperfections due to fabrication and erection
- residual stresses
- variation of the yield strength

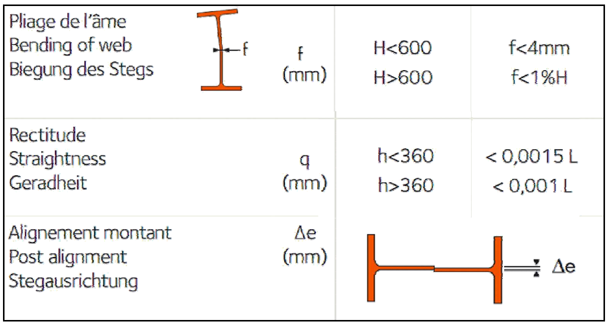

Pliage de l'âme Bending of web Biegung des Stegs	f	f (mm)	H<600 H>600	f<4mm f<1%H
Rectitude Straightness Geradheit		q (mm)	h<360 h>360	< 0,0015 L < 0,001 L
Alignement montant Post alignment Stegausrichtung		Δe (mm)	Δe	

Figure 8.4 Tolerances for ACBs

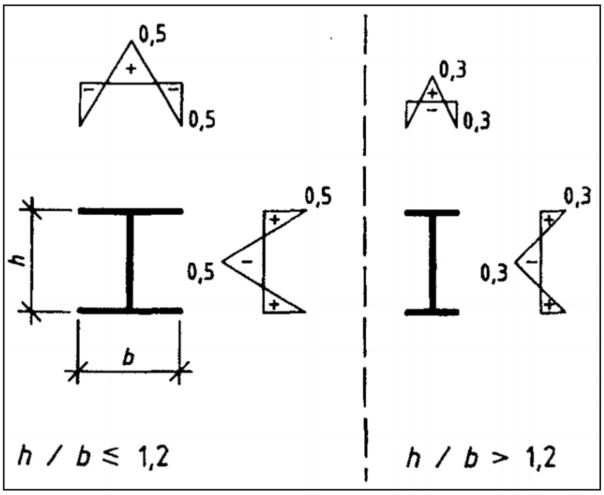

Figure 8.5 Residual stress patterns for rolled I-section profiles [NEN]

For a column loaded by an axial force only, a sine imperfection over the length (in one or both directions) constitutes the most appropriate shape, as it represents the worst possible condition (initial bow). In the present investigation this shape was adopted also, although ultimately fixed supports were applied. Preliminary tests showed that the obtained results differ less than 0.1 percent. The amplitude of the equivalent imperfection depends among others on the fabrication tolerances. For ARCELOR Cellular Beams the relevant tolerances for flexural buckling are given in Figure 8.4.

It can be seen that for more stocky sections the deviation from the perfect straight member is most severe. Furthermore the residual stresses will be larger in stocky sections as the cooling down phase will take a longer time. Therefore, if residual stresses are explicitly modelled in finite element analysis the Dutch

steel standard requires a more severe residual stress pattern to be applied for stocky sections than for more slender sections. The transition for which this stress pattern applies, was set on the value $h/b = 1.2$ (see Figure 8.5), and this value has been adopted in the current investigation also.
The same limit value of $h/b = 1.2$ is also used in Eurocode 3 in the table for the selection of buckling curves. The prescribed initial local bow imperfections in EN1993-1-1 are based on the applicable buckling curve, and thus it appears that EN1993-1-1 uses the same value for the transition limit ($h/b = 1.2$) for the size of the initial imperfections.

In 3D problems modelled using beam elements the imperfection has to be applied for both directions. Normally no extra torsional imperfection is needed, even not in lateral-buckling simulations.

Both effects of geometric and material non-linearity have been combined in the so-called *equivalent* geometric imperfection. Therefore the amplitude of the imperfection is not determined directly from the tolerances, but a simple rule is used that relates the size of the imperfection to the member's characteristic buckling length.

In beam finite element models that take account of *both* geometric and material non-linearity it is common use to apply a sine imperfection with an amplitude equal to 1/1000 of the member's length:

$$e^* = \ell/1000$$

This is somehow less than the design values for initial local bow imperfections as given in EN1993-1-1 Section 5.3 (EC3 Table 5.1).

It turns out that these values in EC3 are too conservative when a more advanced modelling is applied. The explicit modelling of residual stresses already belongs to such 'more advanced' methods.

Table 8.1 Imperfection amplitudes

	$h/b < 1.2$	$h/b \geq 1.2$
weak	$2.0 \cdot L/1000$	$1.5 \cdot L/1000$
strong	$0.25 \cdot L/1000$	$0.25 \cdot L/1000$

The limits in EC3 are primarily geared at finite element models using 'standard beam elements' without explicitly modelling the 'fibres'. This suffices for most applications used in daily practise, but in parameter studies is has become common use to discretise the cross-section by modelling the fibres itself, as it is a far more convenient way to take into account residual stresses and material non-linearity (plasticity).
The initial imperfections given by EN1993-1-1 are *equivalent* geometric imperfections however, allowing for the effects of the residual stresses already.

Even more conservative is the use of these equivalent imperfections in finite element calculations using shell elements.
Finite element models using 3D shell elements are already more sensitive to imperfections than models with beam elements. Therefore first a number of test runs were performed to determine a suitable imperfection amplitude. The *goal* has been to acquire finite element results for plain-webbed beams that match the prediction of the buckling load according to EN1993-1-1 Section 6.3 as close as possible. These values were taken to be representative for the true ultimate load, as it concerns a fairly basic case which has been researched extensively in the past and thereby has lead to rather accurate design expressions.

It appears that to initiate global buckling in the *weak* direction an amplitude

$$e^* = 1.5 \cdot L/1000$$

suffices for most cases. This value accounts for all kinds of imperfections, geometric and material, except an inclination of the column (sway imperfection).

When the lateral movements are prohibited, only a small imperfection is needed to initiate buckling in the *strong* direction:

$$e^* = 0.25 \cdot L / 1000$$

These imperfection amplitudes are summarized in Table 8.1.

Furthermore it was mentioned already that for finite element modelling of the web-post buckling the initial imperfections over the web are of primary importance.
The basic finite element mesh was generated using the pre-processor Crystal Pro.

This proprietary program applies a web imperfection that consists of a sine over the profile's height times a half cosine bow over the beam length. Figure 8.6 shows an exaggerated view of this imperfection, together with its distribution over the beam length.

The imperfection to initiate global buckling was applied manually afterwards by modifying the generated (.IN) file by a shift of the nodes according to its position along the length of the column and the appropriate imperfection amplitude.

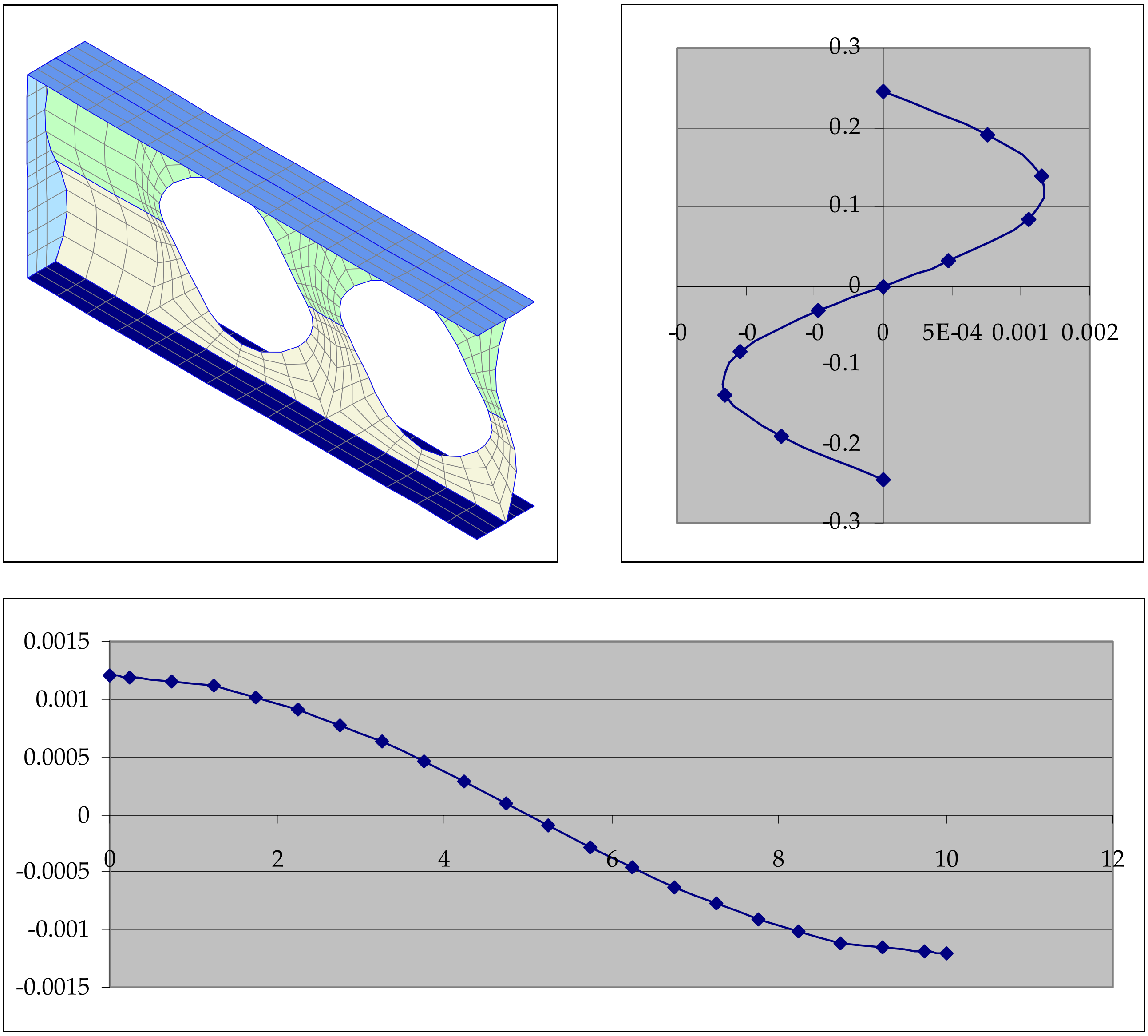

Figure 8.6 Web-post imperfection for an ACB cut from IPE330 as applied by Crystal Pro. Sine over the height (upper right), half cosine over the length (bottom).

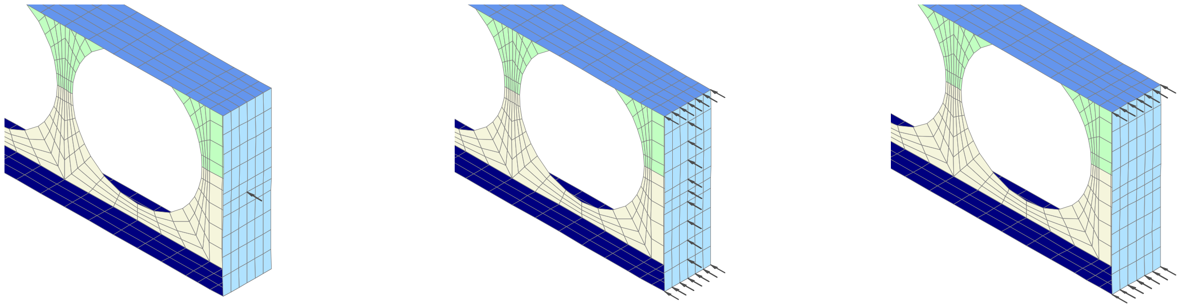

Load application by one single point load

Load application at web and flanges

Load application at flanges

Figure 8.7 Several ways of axial load introduction

8.3.4 Load application

In the preliminary stage of the research it was also investigated how to apply the axial loads at best, such that the global behaviour is not affected. As the axial load has to be transmitted mainly by the flanges, the introduction of this load should match the corresponding stress pattern as close as possible. Therefore the axial force cannot be introduced simply by one single point load. Besides causing a severe local deformation of the beam end, this would nevertheless introduce a disrupting additional stress flow from the point of load application to the flanges.

Probably the best option is to distribute the load over the section minus the web hole area according to their respective areas:

$$N_{\text{flange}} = \frac{b\,t_f}{A - d_o t_w} \cdot N_{Ed}$$

$$N_{\text{web outstand}} = \frac{d_t\,t_w}{A - d_o t_w} \cdot N_{Ed}$$

$$N_{Ed} = 2 \cdot \left(N_{\text{flange}} + N_{\text{web part}}\right)$$

However, as the area of both flanges easily constitutes more than 75% of the total area at an opening location, for convenience the loads were applied to the flanges only.

No deviating behaviour due to this way of load application has occurred throughout.

8.4 Parameter study

8.4.1 Set-up

The main concern in the part of the research that is presented here, has been to verify whether a simplified design rule applies to determine the flexural buckling capacity of a cellular column, based on the section properties of the *net* section.

In order to maximise the possibility of occurrence of deviating results due to the presence of web openings, the opening size was maximised for each section analysed, while at the same time the web-post width was minimised (within the fabrication limits).

Five hot-rolled sections were selected which served as base profiles for as much cellular beam-columns. Thus the whole range of available standard hot-rolled sections has been covered. The dimensions of the analysed ACBs are given in Table 8.2.

The precise choice of the dimensions of the sections was made using the program ARCELOR Cellular Beams (as described earlier). This ensures that all geometric limits are met, and enables the resulting file (.CLB) to be imported into the pre-processor Crystal Pro, for easy mesh generation. Furthermore the relevant imperfection for web-post buckling is added automatically.

Table 8.2 Section data of the cellular beams analysed (dimensions in mm)

base profile	**IPE140**	**IPE330**	**IPE600**	**HE200A**	**HE650M**
base height	140	330	600	190	668
opening diameter	97	427	787	196	877
resulting height	172	535	984	276	1097
flange width	73	160	220	200	305
flange thickness	6.9	11.5	19	10	40
web thickness	4.7	7.5	12	6.5	21
root radius	7	18	24	18	27
web-post width	50	50	62	50	70
ratio height expansion	1.23	1.62	1.64	1.45	1.64
ratio area	0.746	0.589	0.533	0.786	0.603
ratio I_y	0.959	0.862	0.832	0.952	0.866
ratio I_z	0.998	0.998	0.997	1.000	0.996

As the Crystal Pro pre-processor is aimed at cellular *beams*, it does not apply an initial bow imperfection to the member. However, this imperfection is needed to enable the onset of geometrical non-linear behaviour. Therefore the input files were edited by hand afterwards to apply a sine imperfection along the beam length, see section 8.3.3.

For each section at least 4×3 beam-columns with different lengths were analysed. These lengths have been chosen such that the non-dimensional slenderness of the member with respect to the *gross section* (i.e. at a web-post location) successively was equal to:

- $\bar{\lambda} = 0.2$ (limit for onset of buckling)
- $\bar{\lambda} = 0.6$ (intermediate value)
- $\bar{\lambda} = 1.4$ (quite high value)

It is noted that this choice for the *gross slenderness* implies that the *net slenderness* is somewhat less, because the net area decreases due to the presence of the web opening while the second moment of area is hardly affected. Therefore in the graphs in the next subsections, the bar representing the result for the *net* section is placed somewhat to the left of the bar representing the result for the *gross* section with the same length. This shift can be remarkable: e.g. for base section IPE600 with $\bar{\lambda}_z = 1.4$ for the *gross* section, this slenderness becomes about $\bar{\lambda}_z = 1.0$ for the *net* section!

The ultimate load capacity of a fixed-fixed column subjected to an axial force was determined for the beam-column *with* and *without* web-openings, for each of the three chosen slenderness values. This analysis was made *both* for buckling about the weak axis and for buckling about the strong axis.
The analyses for the beam-columns with uniform section (without web-openings, thus referred to as the *gross section*) were made in order to be able to assess the accuracy of the analyses by comparing the results with the buckling capacity according to Eurocode 3. These analyses thus amount to 2×2 analyses per slenderness value.

For some cases other slenderness values (like $\bar{\lambda} = 1.3$) were analysed also, when it appeared that – due to software limits – the analysis could not be made in a completely analogous way for a slenderness equal to $\bar{\lambda} = 1.4$ (i.e. with a very large length of the member, thus with many nodes and elements).

However, it was possible to reduce the number of horizontal restraints – by which the memory usage of the FEM model is reduced, as for longer beams the spacing between these support can be reduced without affecting the failure mode of flexural buckling.

The beams with uniform section have been modelled in two different ways:

- using filled openings ('F')
- using a rectangular mesh ('R')

In most cases the more refined mesh was used with added filler plates ('F') for the web holes. As this sometimes caused the mesh to go beyond the limits of the version of SAFIR used, some analyses were made using a rectangular mesh ('R') – which requires less elements and nodes.

For each section, the results of the runs with slenderness values which are common for all sections (i.e. $\bar{\lambda} = 0.2$, $\bar{\lambda} = 0.6$ and $\bar{\lambda} = 1.4$) were compared to the predicted EC3-buckling capacities, which are referred to as the 100%-values. For the cellular members the EC3-buckling load was calculated using the method as described in section 8.2, based on the dimensions and properties of the *net section* at the location of a web opening.

In order not to bias the comparison of the EC3-buckling load with the computed FEM-result, the calculation of the EC3-buckling loads was performed using the *FEM modelled* dimensions instead of using (exact) tabulated dimensions for the base profile.

The difference between the 'tabulated dimensions' and the FEM modelled dimensions is caused by the fact that in the FEM model, the section is modelled by the centrelines of the flanges and the web. This implies that the overlap of the web area and the flanges is double-counted. On the other hand, the root fillets are not modelled at all.

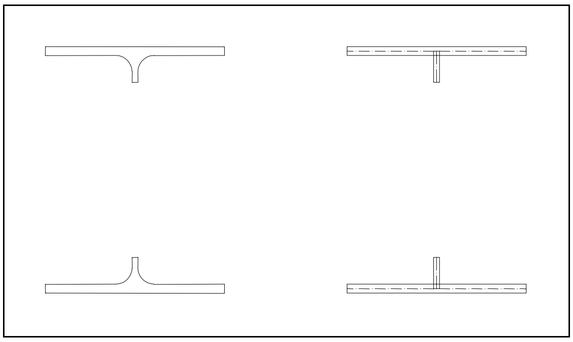

Figure 8.8 Differences between 'tabulated dimensions' and FEM model for base profile HE200A
Left : $A = 4668.1\text{mm}^2$
Right : $A = 4455.0\text{mm}^2$

See for illustration Figure 8.8 above, for base profile HE200A. This observation holds both for the section with and without web holes.

The neglect of the root radii can have different effects, and is related to the geometrical properties of the base section (flange and web thickness, radius of the fillets).
The geometrical quantities like area, second moment of area and radius of gyration, may either increase of decrease, depending on whether the double-counting of the part of the web that overlaps the flanges, outweighs the reduction in area caused by neglecting the root fillets.
For the *net section*, these differences vary from about 95.5% to 102.5% of the quantity based on the 'tabulated dimensions', see Figure 8.9.

The combined effect on the ultimate buckling load also depends on the slenderness, which in turn affects the buckling factor χ. Due to the hyperbolic nature of the relationship between this factor χ and the slenderness $\bar{\lambda}$ (which itself is non-linearly influenced by the ratio between the second moment of area, and the area itself), the total effect on the ultimate buckling load $N_{b,Rd} = \chi \cdot N_{pl} = \chi \cdot A \cdot f_{yd}$ is non-linear also.

This is illustrated in Figure 8.10, from which it can be seen that for the *net section* the influence varies from about 95.0% to 101.0% of the quantity based on the 'tabulated dimensions'.

It is noted furthermore that while the comparison has been based on the FEM dimensions, the beam lengths are determined such that exactly $\bar{\lambda}=0.2$, $\bar{\lambda}=0.6$ and $\bar{\lambda}=1.4$, based on the 'tabulated dimensions'. Consequentially these non-dimensional slenderness values are no longer equal to respectively $\bar{\lambda}=0.2$, $\bar{\lambda}=0.6$ and $\bar{\lambda}=1.4$, but these values have been altered somewhat. These changes have been considered throughout in making the comparison.

The analyses being performed for buckling about the weak axis are designated as *w02* for buckling about the *weak* axis of a beam with slenderness $\bar{\lambda}=0.2$, etc. Accordingly the analyses performed for buckling about the *strong* axis are designated *s02* etc.

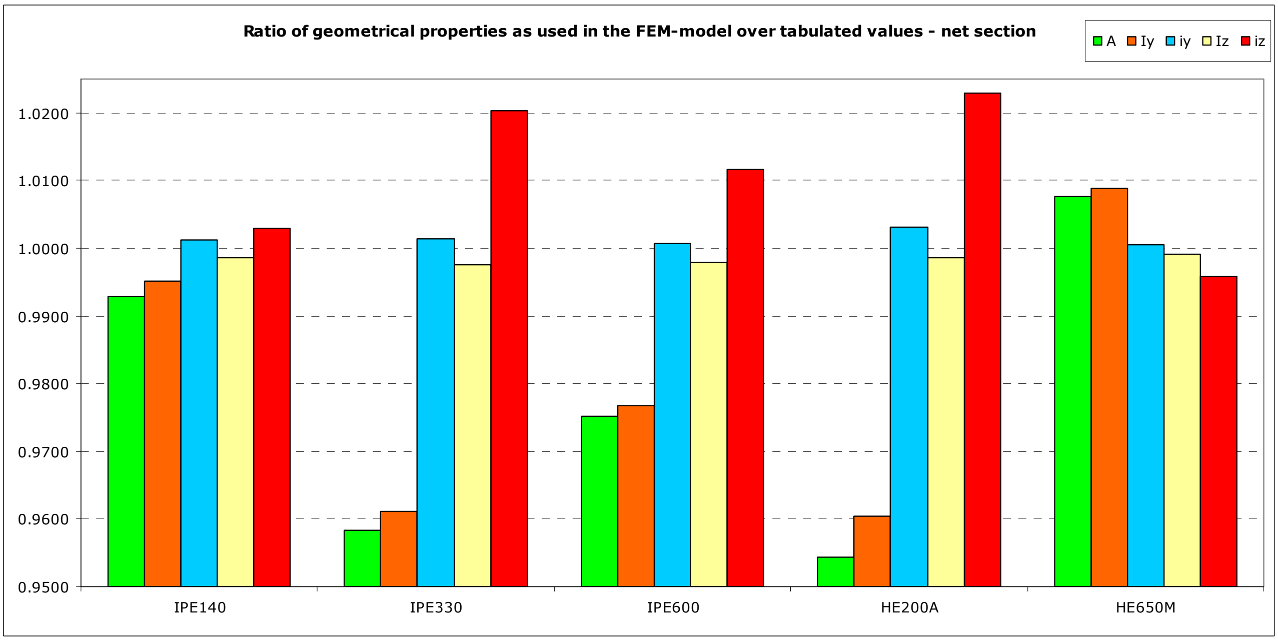

Figure 8.9 Geometrical properties according to the FEM-model vs. tabulated values (net section)

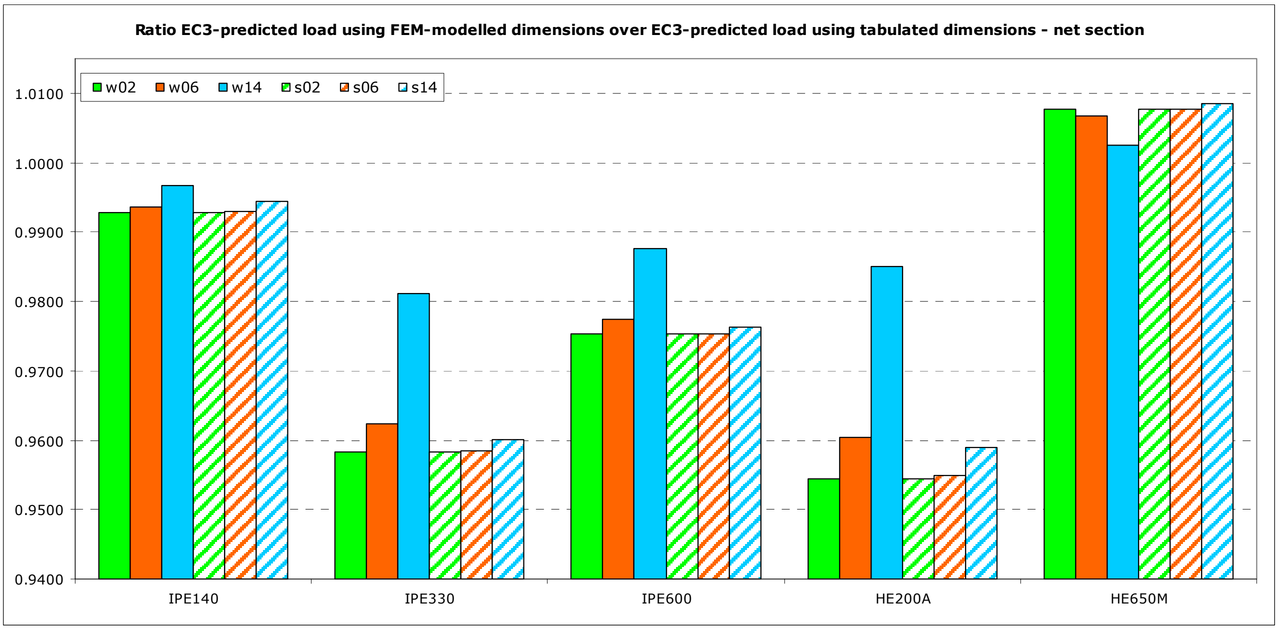

Figure 8.10 Comparison of the EC3-predicted ultimate buckling load based on the net section properties with dimensions according to the FEM-model vs. tabulated values

The abbreviation *LFX* which is used in the filenames stands for *laterally fixed* (i.e. against lateral buckling).

From the comparison of the results for the cellular member and the plain-webbed member, it could be verified whether there is an influence of the presence of web openings on the global buckling mechanism, and the proposed method for calculating the global buckling resistance could be tested.
Generally the results from the FEM analysis were more or less equal to the predicted EC3 result. However, sometimes additional lateral supports were needed to prevent local buckling to become the failure mechanism. Nevertheless, in a few cases some kind of local plate buckling could not be averted.

In the following subsections the results for each base profile are discussed. The complete results are presented in Annex B by means of load-deflection graphs and tables for each analysis performed, together with explanations there where required.

If not mentioned otherwise, the default steel grade is S235 throughout this section.

8.4.2 Base profile IPE140

The minimum depth of the base profile for an ACB is 140 mm, because of fabrication limits. Therefore an IPE140 is the smallest possible section from the IPE-range.
In total 16 different analyses have been performed for beams using this base section. The results of the runs with the slenderness values which are common for all runs (i.e. $\bar{\lambda} = 0.2$, $\bar{\lambda} = 0.6$ and $\bar{\lambda} = 1.4$) are presented in Figure 8.11, together with the curves depicting the flexural buckling capacity according to Eurocode 3. These predicted EC3 buckling capacities are referred to as 100%-values, to which the FEM results are compared. In the Annex also results are presented for $\bar{\lambda} = 1.3$ (3x) and for a rectangular mesh for *s02* (1x).

That the failure mechanism is indeed flexural buckling was inspected by observation of the deformed configuration as well as by inspection of the load-deformation behaviour until the moment of collapse (ultimate load).

In Figure 8.12 this is illustrated for a beam with slenderness $\bar{\lambda} = 0.2$, which is not supported laterally in between. As an initial lateral imperfection was applied to the beam, it displaces sideways with increasing axial load. The load displacement diagram is shown for the upper middle node. After each load increment, the response is determined. The FEM simulation stops when the system of equations cannot be solved anymore for the increased load. The ultimate load then is defined as the load that was applied in the last successful performed run.

One first observation that can be made from the bar graphs is that the FEM ultimate loads of both the cellular section and the plain-webbed section indeed show a *qualitative and quantitative similarity* with the predicted EC3 buckling loads, using the method as described in section 8.2: EC3 buckling load on basis of the properties of the *net section* at the location of an web opening.

Furthermore it can be seen that the difference between the EC3-predicted value and the FEM result for the *net* section is more or less proportional to the difference between these values for the *gross* section.
For example: the result for *w06* (net section) lies approximately 6 percent above the predicted EC3 value, and so does the result for *w06F* (gross section).

The similarity is not for all tested sections as pronounced as for this particular one, but in global terms the results are proportionally. When the result for the *gross* section is below the predicted EC3 value, so is the result for the *net* section, and vice versa.

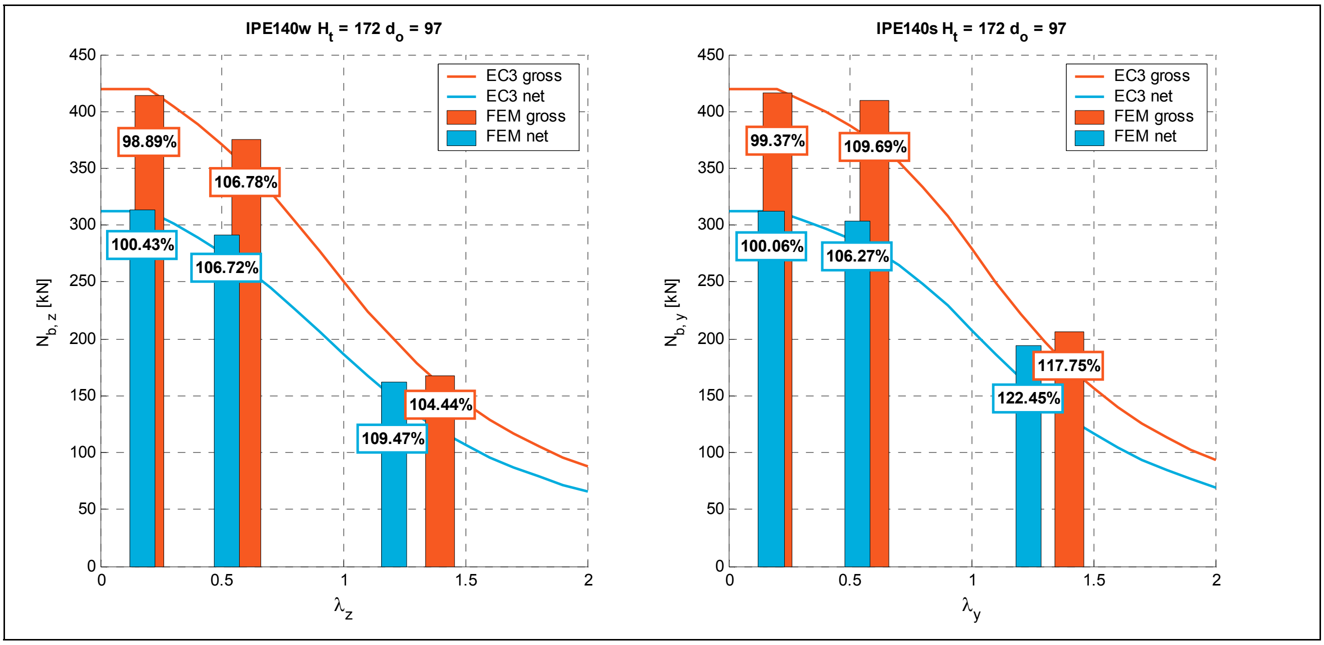

Figure 8.11 Flexural buckling loads for ACBs cut from a IPE140 section with/without web holes

Table 8.3 Relative error of buckling loads for ACBs cut from a IPE140 section with/without web holes

IPE140	**w02**		**w06**		**w14**		**s02**		**s06**		**s14**	
	gross	net	gross	net	gross	net	gross	net	gross	net	gross	net
EC3	419.1	312.0	351.1	273.5	160.5	148.0	419.1	312.0	373.0	285.5	175.2	158.9
FEM	414.4	313.3	374.9	291.8	167.6	162.1	416.5	312.2	409.2	303.4	206.3	194.6
Δ [%]	-1.1	+0.4	+6.8	+6.7	+4.4	+9.5	-0.6	+0.1	+9.7	+6.3	+17.8	+22.4

Another relationship that can be observed most times, is that when for buckling about the weak axis the result for the *gross* section is larger than that for the *net* section (as relative to the predicted EC3 value), this is also the case for buckling about the *strong* axis.

For example: for buckling about the *weak* axis it is observed that the relative 'error' for *w14* (net section) is bigger than that of *w14F* (gross section). Similarly it can be seen that for buckling about the *strong* axis the relative difference is bigger for *s14* (net section) than for *s14F* (gross section).

These observations confirm the expected behaviour. After all it is reasonable that the behaviour of a section that is modelled in FEM once, is similar for buckling in either of the directions (at the same slenderness).

A last observation is that for the lower slenderness values the deviation from the predicted EC3 value turns out to be lower than for sections with a high slenderness. This behaviour seems reasonable as well, as the buckling curve tends to 'runaway' for higher slenderness values. Therefore an only small disturbance – either caused by the numerical implementation, or by a possibly somewhat too big initial imperfection – already may have a rather big influence.

Concluding it can be said that for the more commonly used range of slenderness values (i.e. for $\bar{\lambda} = 0.2$ and $\bar{\lambda} = 0.6$) it appears that when the numerical results are compared to the values predicted by the method as described in section 8.2 – EC3 buckling load using the properties of the net section, at the location of an web opening – that:

- the differences are either small (less than 1.1%), or
- for larger deviations, the predicted values (labelled EC3) constitute a safe estimation of the ultimate flexural buckling load

These conclusions are supported by the results given in Table 8.3. Consequently the proposed method yields safe results for columns cut out of a IPE140 section for the tested range of slenderness values.

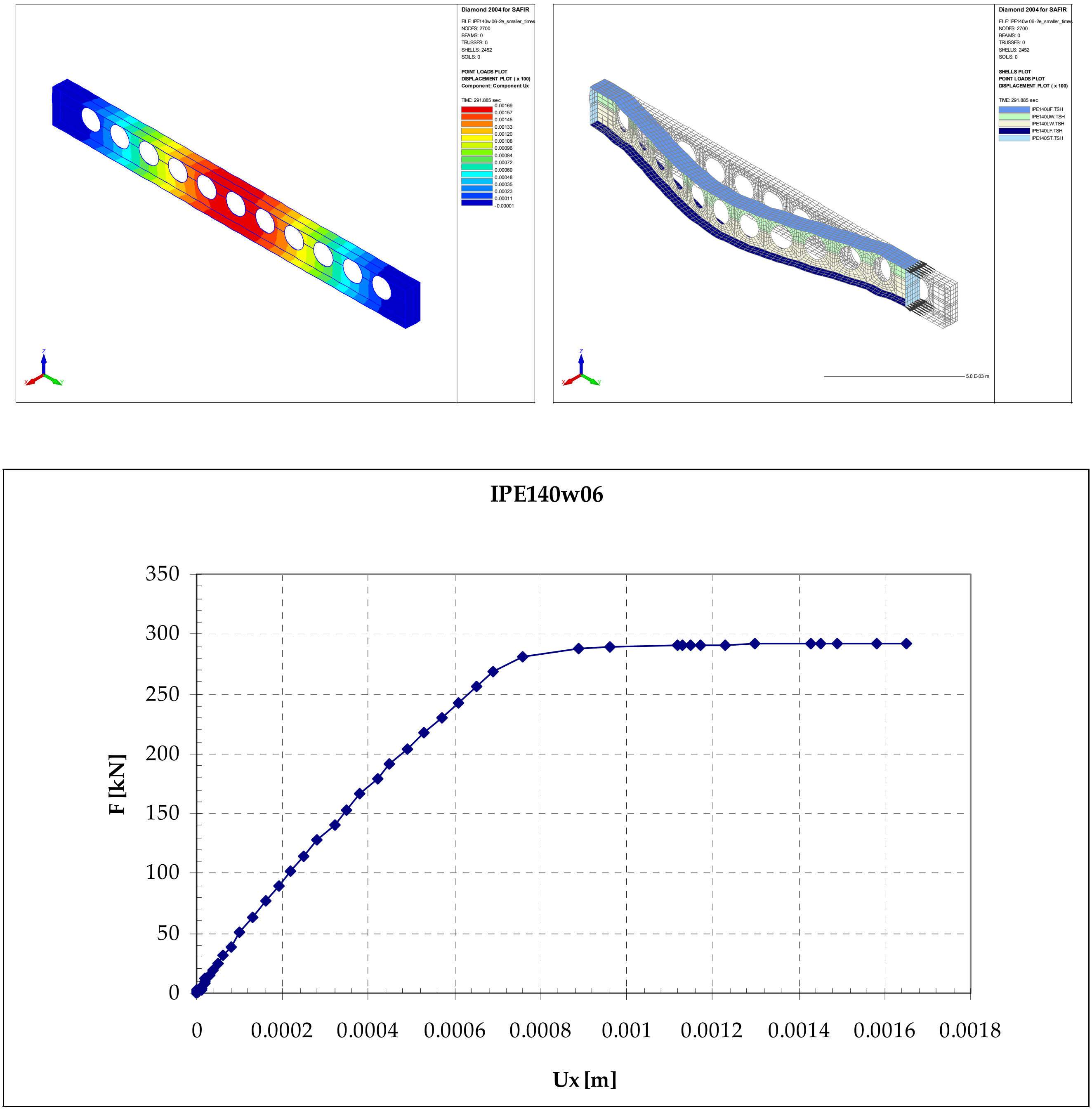

Figure 8.12 Flexural buckling of an ACB cut from a IPE140 section, slenderness: $\lambda = 0.6$
Top left : Coloured view of the lateral displacement
Top right : Top view of the deformed configuration
Bottom : Load displacement diagram for the upper middle node

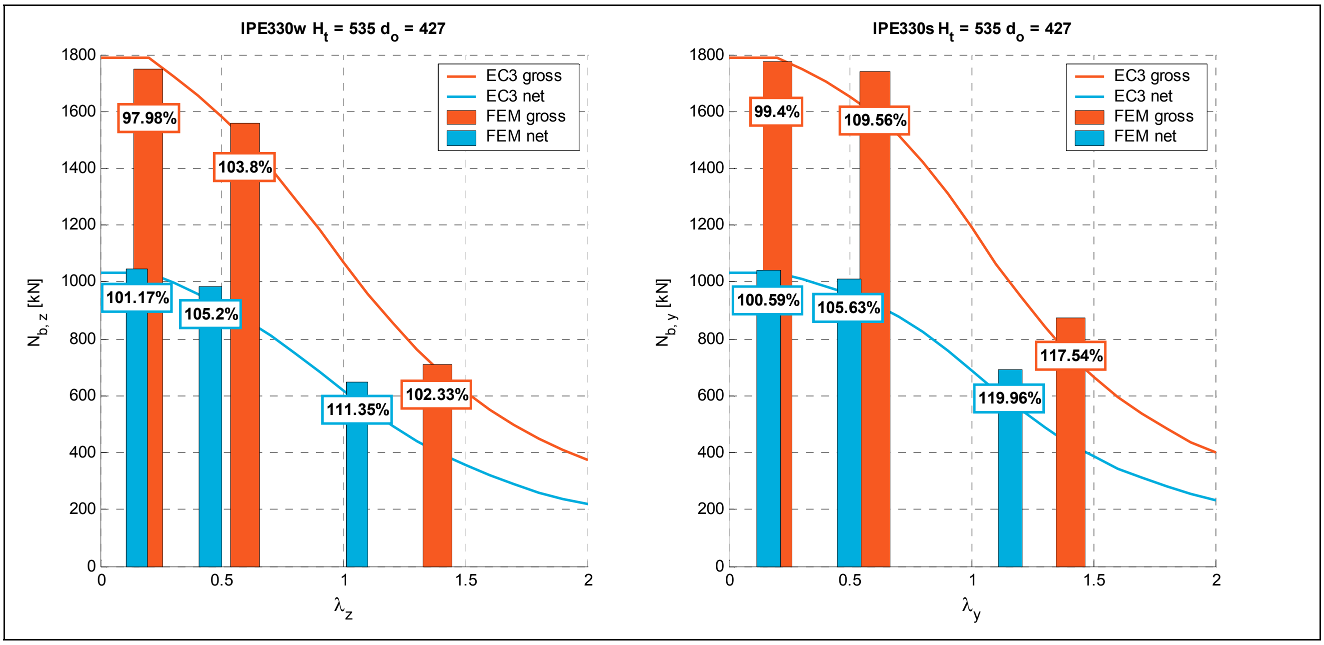

Figure 8.13 Flexural buckling loads for ACBs cut from a IPE330 section with/without web holes

Table 8.4 Relative error of buckling loads for ACBs cut from a IPE330 section with/without web holes

IPE330	w02		w06		w14		s02		s06		s14	
	gross	net	gross	net	gross	net	gross	net	gross	net	gross	net
EC3	1787	1035	1502	937	694	583	1787	1035	1589	958	741	578
FEM	1751	1047	1559	985	710	649	1776	1041	1741	1012	871	694
Δ [%]	-2.0	+1.2	+3.8	+5.2	+2.3	+11.3	-0.6	+0.6	+9.6	+5.6	+17.5	+20.0

8.4.3 Base profile IPE330

The next section whereof the buckling capacity was investigated, is based on an IPE330 base section. With a resulting height of 535 mm, this section is 'medium-sized', referring to the whole range of possible ACBs cut from an IPE base section. As such, it served for a number of additional analysis, to compare the results for differently modelled meshes. A number of 18 different analyses have been made to investigate the global buckling behaviour of cellular members with the aforementioned geometrical properties.

The results of the analyses with slenderness values $\bar{\lambda}=0.2$, $\bar{\lambda}=0.6$ and $\bar{\lambda}=1.4$ are presented in Figure 8.13 and Table 8.4.
In general terms the results for the current base section IPE330 show the same characteristics as the results for base section IPE140:

- for the small slenderness value 0.2 the FEM result is slightly lower than the EC3 prediction
- for the medium slenderness value 0.6 the FEM result is less than 10 percent above the EC3 prediction
- for the higher slenderness value 1.4 the FEM analyses return a fairly bigger ultimate load capacity than predicted by the EC3 method based on the net section

These observations hold for buckling about the weak axis, as well as for buckling about the strong axis.

The $18-2\cdot(3\cdot2)=6$ extra analyses – on top of the results summarised in Figure 8.13 and Table 8.4 – were made for different reasons:

- 3x an additional analysis was made for the plain-webbed section, so that that the result of a mesh with *filled holes* could be compared against the result of a *rectangular mesh*

- 2x additional SAME commands were defined in order to prevent prior failure in a plate buckling mode (for *w02F-2e* and *s02F-half-2e-LFX*)
- 1x the support conditions were defined in the middle instead of at the ends (for the *w06* section)

Concerning the first point noted, it appears that if the comparison is not troubled by prior occurrence of plate buckling of a mesh, both the mesh with *filled holes* and the *rectangular mesh* delivers nearly the same result.
Indeed the additional SAME commands did prevent the section to fail by plate buckling before attainment of the flexural buckling capacity, as confirmed by inspection of the deformed configuration, see for illustration Figure 8.14.

The extra analysis with different support conditions, defined in the middle of the member instead of at the ends, was made as a check on the correctness of the modelling. Now the load was applied to *both* ends.
As the ultimate load thus obtained agrees with that of the usual modelling, it can be concluded that no side effects are present due to the fixations of the DOFs at the ends.

With respect to the aim of this part of the numerical research, it thus turns out that:

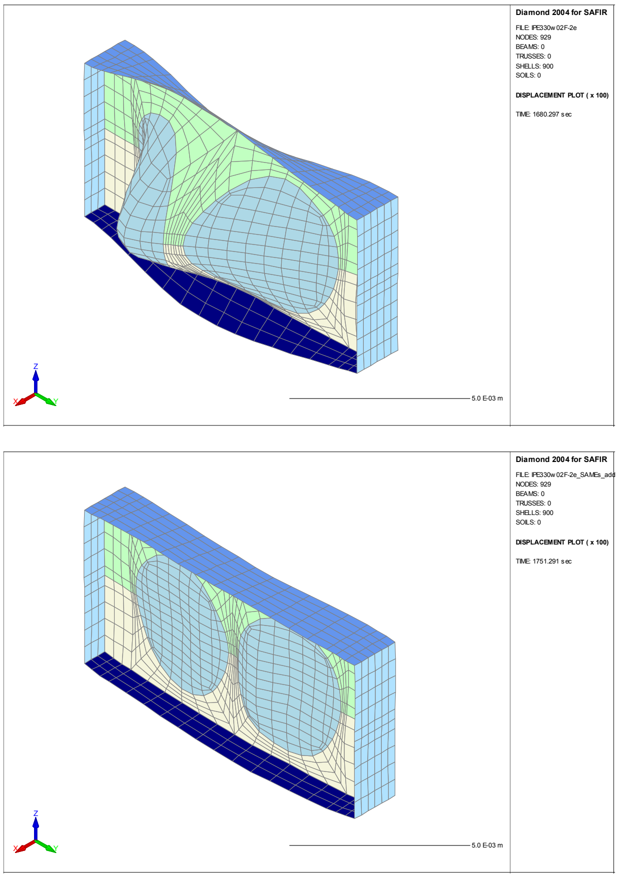
Diamond 2004 for SAFIR
FILE: IPE330w02F-2e
NODES: 929
BEAMS: 0
TRUSSES: 0
SHELLS: 900
SOILS: 0
DISPLACEMENT PLOT (x 100)
TIME: 1680.297 sec
5.0 E-03 m
Z
X
Y
Diamond 2004 for SAFIR
FILE: IPE330w02F-2e_SAMEs_add
NODES: 929
BEAMS: 0
TRUSSES: 0
SHELLS: 900
SOILS: 0
DISPLACEMENT PLOT (x 100)
TIME: 1751.291 sec
5.0 E-03 m
Z
X
Y

Figure 8.14 Displacement plots with (bottom) and without (top) additional restraints for an IPE330w02F-2e section (magnification: 100x)

- the differences between the EC3 predicted values, and the FEM results are either small (less than 2.0%) , or
- for larger deviations, the EC3 predicted constitute a safe estimation of the ultimate flexural buckling load

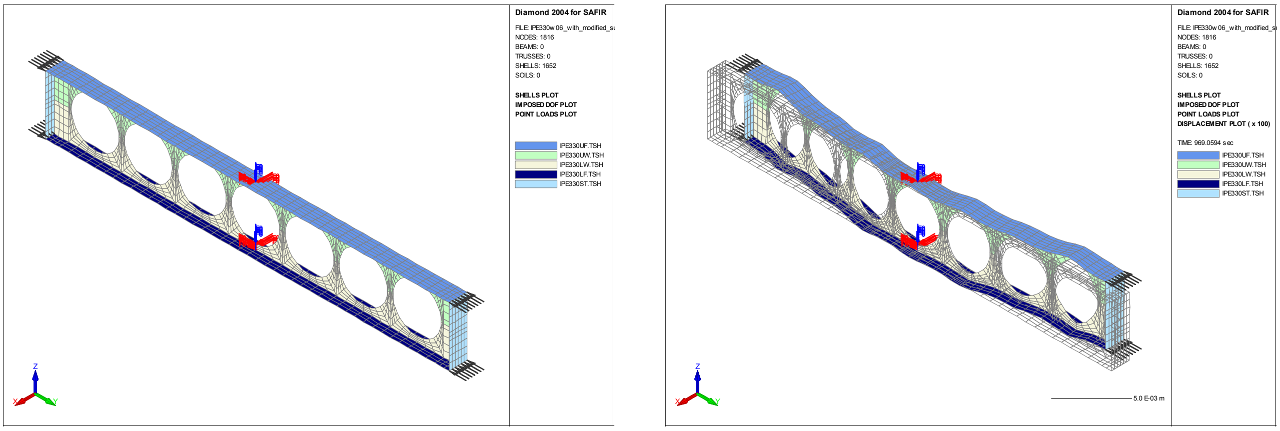
Diamond 2004 for SAFIR
FILE: IPE330w06_with_modified_s
NODES: 1816
BEAMS: 0
TRUSSES: 0
SHELLS: 1652
SOILS: 0
SHELLS PLOT
IMPOSED DOF PLOT
POINT LOADS PLOT
IPE330UF.TSH
IPE330UW.TSH
IPE330LW.TSH
IPE330LF.TSH
IPE330ST.TSH
Z
X
Y
Diamond 2004 for SAFIR
FILE: IPE330w06_with_modified_s
NODES: 1816
BEAMS: 0
TRUSSES: 0
SHELLS: 1652
SOILS: 0
SHELLS PLOT
IMPOSED DOF PLOT
POINT LOADS PLOT
DISPLACEMENT PLOT (x 100)
TIME: 969.0594 sec
IPE330UF.TSH
IPE330UW.TSH
IPE330LW.TSH
IPE330LF.TSH
IPE330ST.TSH
5.0 E-03 m
Z
X
Y

Figure 8.15 Applied support conditions (left) and displacement plot (right) for an IPE330w06 section with modified support conditions in the middle (magnification: 100x)

8.4.4 Base profile IPE600

The last base section from the IPE range whereof the global buckling behaviour was investigated, is an IPE600 – the biggest section from the 'normal' IPE range. This time 28 analyses were carried out, meaning that some $28-2\cdot(3\cdot 2)=16$ extra analyses were made. Partly these were required for excluding failure mechanisms other than global buckling of the whole member (i.e. by preventing these to happen), but also quite a few additional cases were analyzed. These results are also discussed hereafter.

From the results presented in Figure 8.16 and Table 8.5 a qualitatively equal behaviour emerges as for the earlier tested sections.

- for the small slenderness value 0.2 the FEM result is somehow lower than the EC3 prediction
- for the medium slenderness value 0.6 the FEM result is less than 10 percent above the EC3 prediction
- for the higher slenderness value 1.4 the FEM analyses return a fairly bigger ultimate load capacity than predicted by the EC3 method based on the net section

The relative 'error' of as much as -4.7% for the result of the gross section of *w02* is the biggest relative 'error' on the *unsafe* side. However, from analysing the displacement pattern at the ultimate load it becomes clear that failure still occurs due to plate buckling prior to attainment of the flexural buckling load, but in a higher mode due to the applied additional restraint. It turned out that these extra restraints were unable to prevent plate buckling to happen completely, as is illustrated in Figure 8.17 on the next page.

These figures show a coloured representation of the lateral displacement Ux.

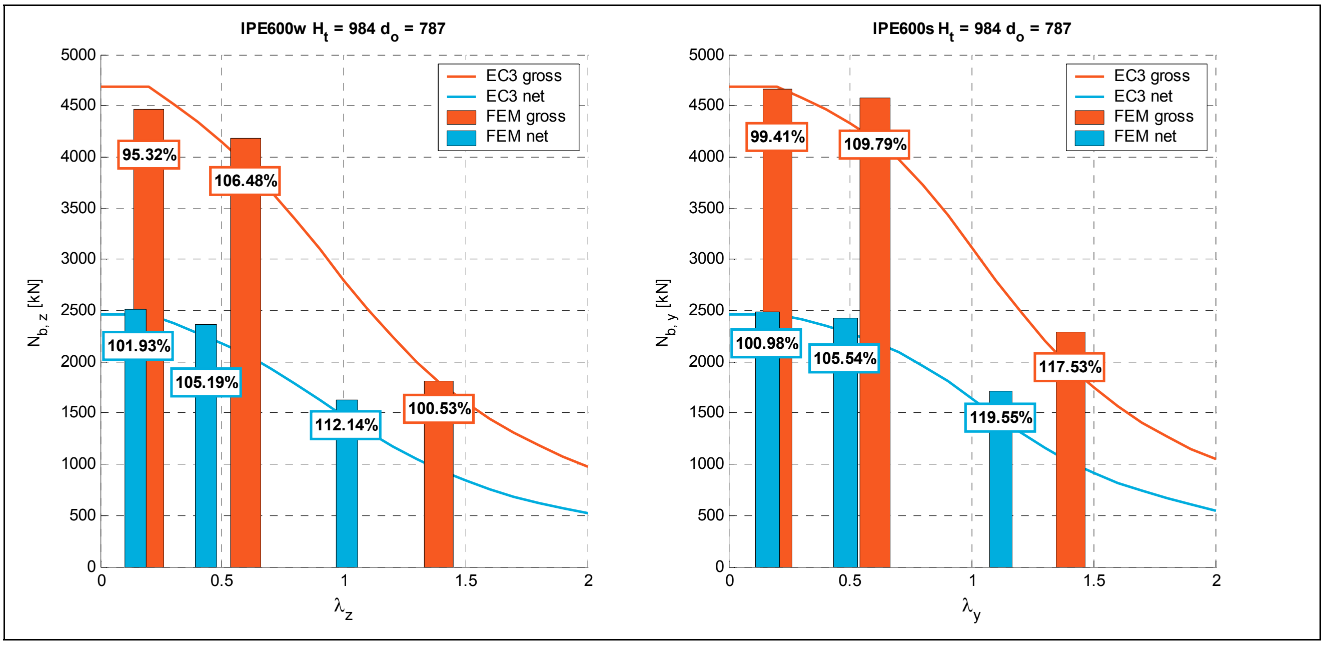

Figure 8.16 Flexural buckling loads for ACBs cut from a IPE600 section with/without web holes

Table 8.5 Relative error of buckling loads for ACBs cut from a IPE600 section with/without web holes

IPE600	w02		w06		w14		s02		s06		s14	
	gross	net	gross	net	gross	net	gross	net	gross	net	gross	net
EC3	4686	2467	3930	2251	1804	1454	4685	2467	4167	2295	1948	1438
FEM	4466	2514	4185	2368	1814	1631	4657	2491	4575	2422	2290	1719
Δ [%]	-4.7	+1.9	+6.5	+5.2	+0.5	+12.1	-0.6	+1.0	+9.8	+5.5	+17.5	+19.5

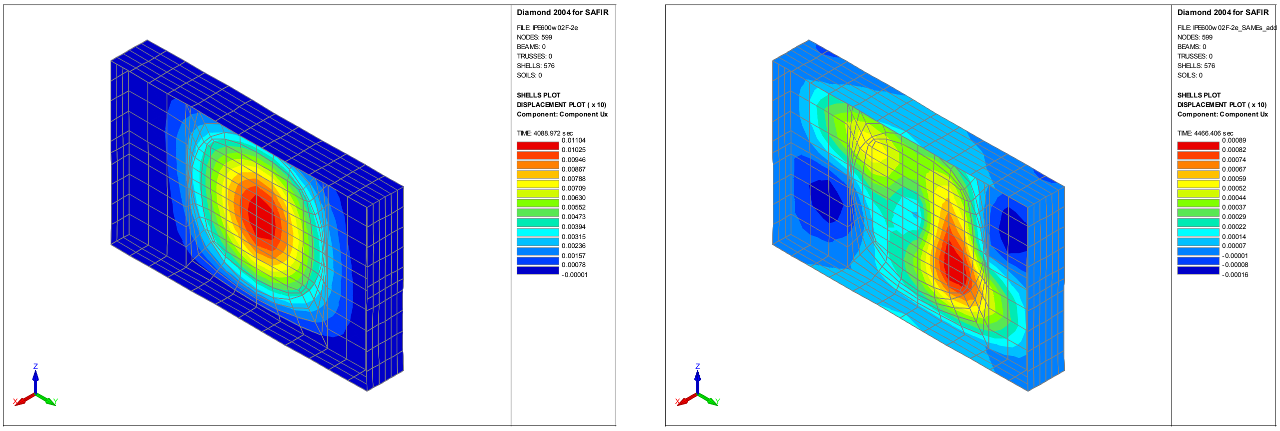
Diamond 2004 for SAFIR
FILE: IPE600w02F-2e
NODES: 599
BEAMS: 0
TRUSSES: 0
SHELLS: 576
SOILS: 0
SHELLS PLOT
DISPLACEMENT PLOT (x 10)
Component: Component Ux
TIME: 4088.972 sec
0.01104
0.01025
0.00946
0.00867
0.00788
0.00709
0.00630
0.00552
0.00473
0.00394
0.00315
0.00236
0.00157
0.00078
-0.00001
Diamond 2004 for SAFIR
FILE: IPE600w02F-2e_SAMEs_add
NODES: 599
BEAMS: 0
TRUSSES: 0
SHELLS: 576
SOILS: 0
SHELLS PLOT
DISPLACEMENT PLOT (x 10)
Component: Component Ux
TIME: 4466.406 sec
0.00089
0.00082
0.00074
0.00067
0.00059
0.00052
0.00044
0.00037
0.00029
0.00022
0.00014
0.00007
-0.00001
-0.00008
-0.00016
Z
Y
X

Figure 8.17 Lateral displacement Ux for IPE600w02F: failure in a plate buckling mode. Left: without additional restraints; right: with additional restraining conditions.

In the left figure the displacement is shown for the section without additional restraints. The right figure shows the pattern again but now with additional lateral restraints. Instead of one big half period of a sinusoidal displacement field, now a complete period is shown – implying by the required additional strain energy that a higher failure load is obtained, as confirmed by Table 8.6. However, the plate buckling mode still dominates the behaviour, which explains that the ultimate load value is below the EC3 predicted value for failure in a flexural buckling mode of the I-shaped member.

The same behaviour has been observed from an additional series of runs for a section with a slightly higher slenderness value of 0.25, see Table 8.7.

The results for the model with a rectangular mesh show a similar behaviour and were not investigated further therefore.

Also for slenderness value 0.6 plate buckling played an important part, which could be eliminated however by adding further restraining conditions, see Table 8.8 and Figure 8.20 and Figure 8.21.

For each section all results have been presented in such tables (and with accompanying figures) in Annex B, from which these tables are reproduced.

Table 8.6 Flexural buckling load for ACBs cut from a IPE600 section with slenderness 0.2

flexural buckling load [kN]	**EC3**	**FEM**	**Δ [%]**
IPE600w02F-2e	4685.9	4089.0	-12.7
IPE600w02F-2e_SAMEs_added	4685.9	4466.4	-4.7
IPE600w02R-2e	4685.9	4075.9	-13.0
IPE600w02-2e	2466.6	2514.1	+1.9

Table 8.7 Flexural buckling load for ACBs cut from a IPE600 section with slenderness 0.25

flexural buckling load [kN]	**EC3**	**FEM**	**Δ [%]**
IPE600w025F-2e	4604.9	4100.7	-10.9
IPE600w025F-2e_SAMEs_added	4604.9	4439.1	-3.6
IPE600w025R-2e	4604.9	4035.6	-12.4
IPE600w025-2e	2466.6	2498.5	-1.3

Table 8.8 Flexural buckling load for ACBs cut from a IPE600 section with slenderness 0.6

flexural buckling load [kN]	EC3	FEM	Δ [%]
IPE600w06F-2e	3974.8	3795.1	-4.5
IPE600w06F-2e_SAMEs_added	3974.8	4184.9	+5.3
IPE600w06R-2e	3974.8	3791.0	-4.6
IPE600w06R-2e_SAMEs_added	3974.8	4214.7	+6.0
IPE600w06-2e	2302.7	2367.6	+2.8

Table 8.9 Flexural buckling load for ACBs cut from a IPE600 section with slenderness 1.4

flexural buckling load [kN]	EC3	FEM	Δ [%]
IPE600w14F-2e	1804.2	1813.7	+0.5
IPE600w14-2e	1454.2	1630.8	+12.1

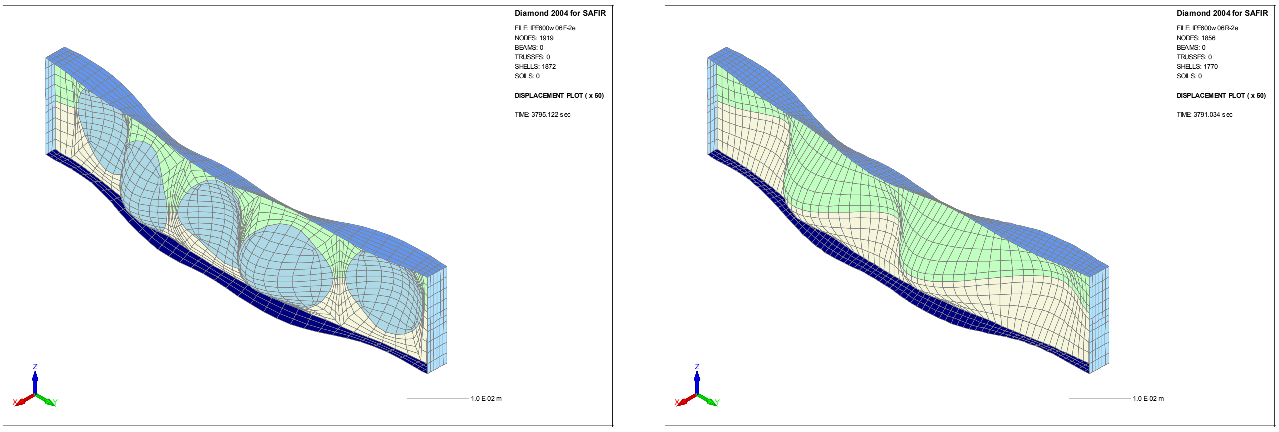
Diamond 2004 for SAFIR
FILE: IPE600w06F-2e
NODES: 1919
BEAMS: 0
TRUSSES: 0
SHELLS: 1872
SOILS: 0
DISPLACEMENT PLOT (x 50)
TIME: 3795.122 sec
1.0 E-02 m
Z
X
Y
Diamond 2004 for SAFIR
FILE: IPE600w06R-2e
NODES: 1856
BEAMS: 0
TRUSSES: 0
SHELLS: 1770
SOILS: 0
DISPLACEMENT PLOT (x 50)
TIME: 3791.034 sec
1.0 E-02 m
Z
X
Y

Figure 8.18 Deformation plot for IPE600w06F *without* additional restraints (magnification 50x)

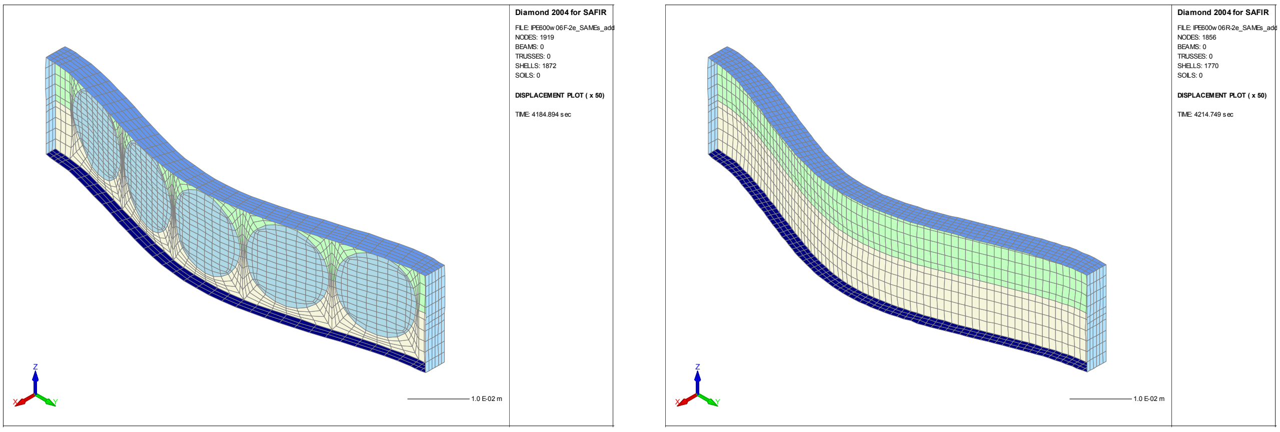
Diamond 2004 for SAFIR
FILE: IPE600w06F-2e_SAMEs_add
NODES: 1919
BEAMS: 0
TRUSSES: 0
SHELLS: 1872
SOILS: 0
DISPLACEMENT PLOT (x 50)
TIME: 4184.894 sec
1.0 E-02 m
Z
X
Y
Diamond 2004 for SAFIR
FILE: IPE600w06R-2e_SAMEs_add
NODES: 1856
BEAMS: 0
TRUSSES: 0
SHELLS: 1770
SOILS: 0
DISPLACEMENT PLOT (x 50)
TIME: 4214.749 sec
1.0 E-02 m
Z
X
Y

Figure 8.19 Deformation plot for IPE600w06F *with* additional restraints (magnification 50x)

For slenderness value 1.4 flexural buckling turned out to be the governing failure mode, even without additional lateral restraints.

The buckling behaviour of this member about the strong axis turned out to be completely similar: while for *s02F* plate buckling could not be eliminated completely – as was the case for *w02F* – this was possible indeed for the other tested slenderness values.

It is noted here that the results for *s14* are about 20% on the safe side. However, this load is reached by a lateral displacement of up to 1% of the member length – which will be most often not acceptable in practice.

Therefore, apart from the prior failure due to plate buckling of the gross sections with slenderness 0.2 (either with respect to the weak or strong direction), these results confirm that the EC3 method indeed yields safe estimates of the flexural buckling load for cellular sections cut from an IPE600.

As noted at the start of this paragraph, a number of additional analyses has been carried out for this section as well. These amount to 16 extra analyses:

- 2x the usual analyses were performed for slenderness $\bar{\lambda} = 0.25$ (additional to the slenderness values of $\bar{\lambda} = 0.2$, $\bar{\lambda} = 0.6$ and $\bar{\lambda} = 1.4$) in order to investigate whether the plate buckling *even after adding additional restraints* could be prevented for this slightly higher slenderness – these results have been discussed before
- 2x the usual analyses were performed for a section with slenderness $\bar{\lambda} = 0.6$ *referred to steel grade S355 instead of S235* – with no difference in behaviour observed
- 3x an additional analysis was made for the plain-webbed section, so that that the result of a mesh with *filled holes* could be compared against the result of a *rectangular mesh*
- 8x additional SAME commands were defined in order to prevent prior failure in a plate buckling mode
- 1x an investigation was made where a *cosine* imperfection was applied instead of the usual *sine* imperfection shape (for the *s02* section) – which delivered a result that differs less than 0.1 percent with the section given an sine imperfection

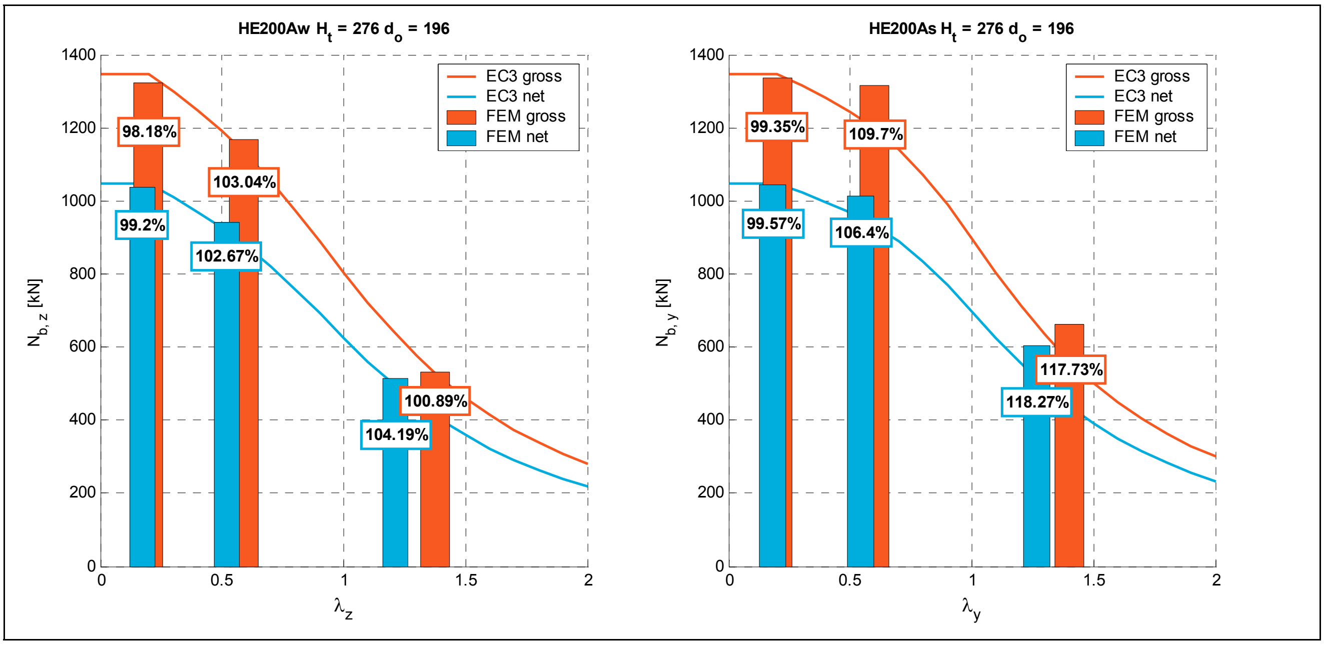

Figure 8.20 Flexural buckling loads for ACBs cut from a HE200A section with/without web holes

Table 8.10 Relative error of buckling loads for ACBs cut from a HE200A section with/without web holes

HE200A	w02		w06		w14		s02		s06		s14	
	gross	net	gross	net	gross	net	gross	net	gross	net	gross	net
EC3	1346	1047	1134	916.3	528.0	493.1	1346	1047	1198	952.9	561.8	511.6
FEM	1322	1039	1168	940.8	532.7	513.8	1338	1042	1314	1014	661.3	605.0
Δ [%]	-1.8	-0.8	+3.0	+2.7	+0.9	+4.2	-0.7	-0.4	+9.7	+6.4	+17.7	+18.3

8.4.5 Base profile HE200A

Besides ACBs cut from IPE sections, two sections for which a HEA section served as a base profile were investigated as well.
The first one was a HE200A section, with a $h/b-$ratio (of the base profile) of $0.95<1.2$.
The second base profile was a HE650M, with a $h/b-$ratio of $2.19>>1.2$, which is discussed in the next subsection.
Due to the fact that profiles from the HE range are more stocky than IPE profiles, and therefore are less prone to buckling about the weak axis, longer member lengths are required to meet the pre-defined slenderness values of $\bar{\lambda}=0.2$, $\bar{\lambda}=0.6$ and $\bar{\lambda}=1.4$.

From Figure 8.20 and Table 8.10 it is clear that for buckling about the *weak* axis the results from the FEM analysis show quite some similarity with the EC3 predicted values:

- the biggest deviation on the *unsafe* side (for the *net* section) is only -0.8%, and
- the biggest relative 'error' on the positive side is $+4.2\%$

The first result (for buckling about the weak direction), where the deviation is less for the *net* section (-0.8%) than for the *gross* section (-1.8%), indicates that the behaviour even has improved something.

For buckling about the *strong* axis it is immediately clear that the results are far higher than the EC3-predicted values.
This may have been caused by an inadequate choice of the initial imperfection.
Nevertheless, it *is* possible to compare the results for the *gross* and the *net* section with each other. Only for *s06* a decrease from *gross* to *net* is seen, for which reference is made to the conclusive section 8.5.

Regarding *s02* and *s14* the conclusion is that the EC3-predicted values constitute a safe lowerbound. The biggest error is only -0.4%.

Three additional analyses were made for this section, for which the results are presented in Annex B. There from it follows that:

- for *w14* the whole member length (instead of the half member length) was modelled also with exactly the same result as given in Table 8.10, and
- for *s13* the results ($+20.2\%$ for both the *gross* and the *net* section) resemble the other results

Therefore, these results show that the EC3 method also yields safe estimates of the flexural buckling load for cellular sections cut from an HE200A.

8.4.6 Base profile HE650M

Another series of analyses was carried out on cellular sections cut from base profile HE650M. The results are displayed in both Figure 8.21 and Table 8.11 on the next page.

In qualitative terms these results are similar to those of base profile HE200A.
For buckling about the *weak* axis all results for the cellular section are higher than the predicted EC3-values, the biggest relative 'error' being $+5.6\%$ (on the positive side).
It turned out that for *w02* it was necessary to define extra restraining conditions to prevent plate buckling to occur.

Again for buckling about the *strong* axis, a considerably higher result was obtained than predicted, which are probably caused by an inappropriate (too low) initial imperfection, though it's noted that the lateral displacement is quite high at the reach of this failure load.

It is therefore affirmed again that the method of predicting ultimate buckling loads based on the EC3-formulae applied to the net section, yields safe estimates.

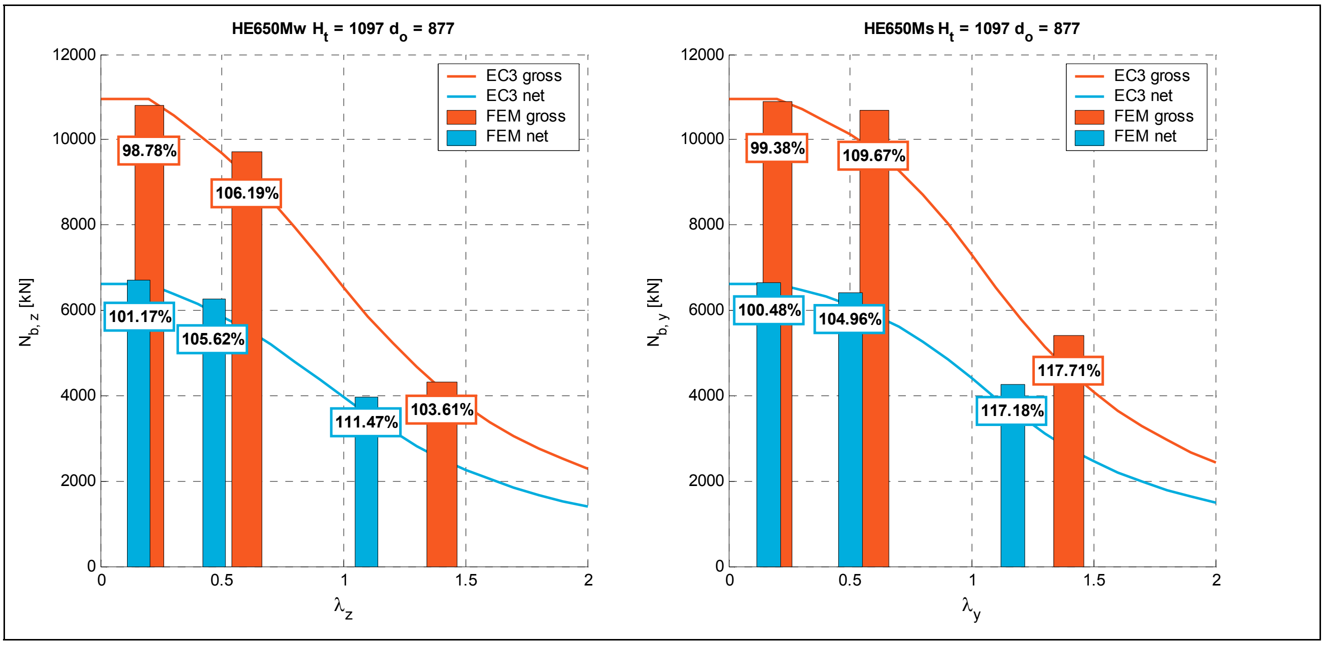

Figure 8.21 Flexural buckling loads for ACBs cut from a HE650M section with/without web holes

Table 8.11 Relative error of buckling loads for ACBs cut from a HE650M section with/without web holes

HE650M	**w02**		**w06**		**w14**		**s02**		**s06**		**s14**	
	gross	net	gross	net	gross	net	gross	net	gross	net	gross	net
EC3	10948	6622	9157	5946	4162	3570	10950	6622	9750	6120	4588	3648
FEM	10815	6700	9724	6280	4313	3979	10883	6654	10692	6424	5400	4275
Δ [%]	-1.2	+1.2	+6.2	+5.6	+3.6	+11.5	-0.6	+0.5	+9.7	+5.0	+17.7	+17.2

8.5 Conclusion

From the results presented in the preceding paragraphs for each base section, it follows that the proposed simplified method for checking the ultimate flexural buckling loading capacity is safe, though sometimes conservative.

The observed relative errors on the *unsafe* side (i.e. less than zero) as compared to the EC3-predicted buckling load, appeared to be maximum for section *IPE600w02F*: -4.7% . However, in this case it wasn't global failure that governed the member behaviour, as the occurrence of plate buckling could not be prevented completely.
Apart from this section (as the plate buckling failure mode should be checked for separately in design where relevant), the relative error on the *unsafe* side was never greater than -2.0% .

Therefore the hypothesis that generally *safe* results are obtained by the proposed method for checking the flexural buckling load capacity of cellular members by means of an EC3-check based on the *net section* properties, is confirmed.
This method sometimes returns admittedly quite conservative predictions. As this occurs especially for higher member lengths – with large displacements – this might indicate that the imperfection amplitude is not appropriate for these high slenderness values.

However, the results are still valuable, as the results for the *gross* and the *net* section can be compared to *each other*. Thereby it is also possible to assess the accuracy of the FEM analyses. After all, only by this comparison it can be determined whether the perforated section behaves *relatively* better or worse than the plain-webbed section.

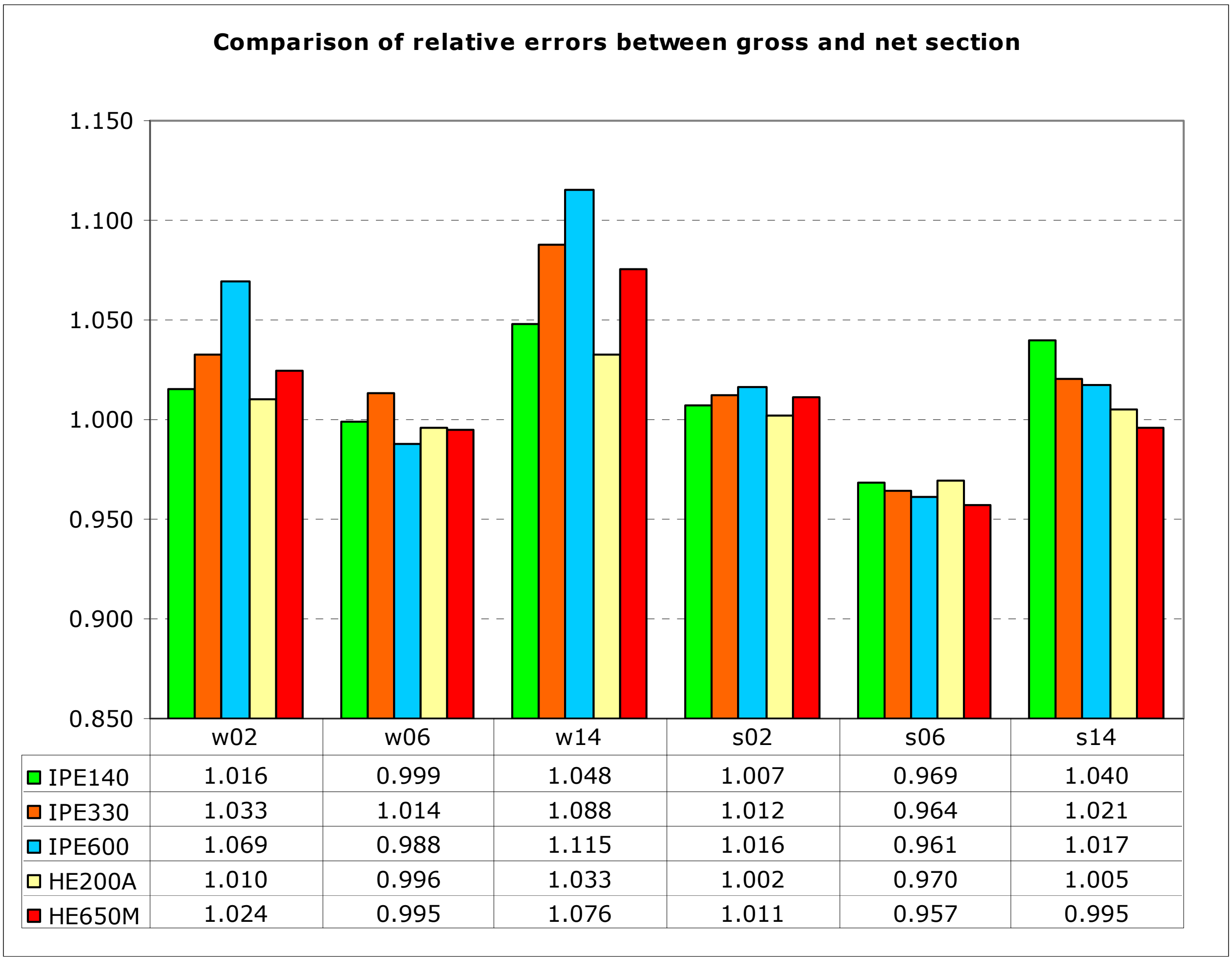

	w02	w06	w14	s02	s06	s14
🟩 IPE140	1.016	0.999	1.048	1.007	0.969	1.040
🟧 IPE330	1.033	1.014	1.088	1.012	0.964	1.021
🟦 IPE600	1.069	0.988	1.115	1.016	0.961	1.017
🟨 HE200A	1.010	0.996	1.033	1.002	0.970	1.005
🟥 HE650M	1.024	0.995	1.076	1.011	0.957	0.995

Figure 8.22 Comparison of relative errors between gross and net section

Therefore in Figure 8.22 above the results of this comparison are displayed, according to the formula mentioned hereunder:

$$\frac{\text{relative error for net section}}{\text{relative error for gross section}} = \frac{1+\Delta_{\text{net}}}{1+\Delta_{\text{gross}}}$$

whereby the relative error Δ should be expressed as a number instead of a percentage, i.e. $\Delta = \Delta[\%]/100$.

From the figure, it is immediately clear that all sections s06 behave *relatively* worse than s06F. However all *s06* sections (with web openings) performed better than expected $(\geq +5.0\%)$ on basis of the EC3-prediction. The sections *s06F* (without web holes) performed still better though $(\geq +9.5\%)$. Therefore the main point of interest here is that the plain webbed sections behaved better in the FEM simulation than expected. This somehow stiffer response might be attributed to a too low initial imperfection. It seems reasonable after all that the perforated section behaves relatively less stiff than the plain webbed section, as additionally shear-type deformations can occur. Still the results are on the safe side.

Almost all other sections behaved relatively better, once even up to 11.5%. These large values occur for the higher (weak) slenderness values. It turns out that the sections with openings performed far better than expected, while the sections with filled openings just performed satisfactory. It is interested to note that for all *w14* sections except *HE200A* an imperfection factor for buckling about the weak axis $\alpha_z = 0.21$ instead of $\alpha_z = 0.34$ would have resulted in a closer match.

It is furthermore possible to state a few general quantitative observations about the comparison of relative errors:

- for buckling about the *weak* axis:
  $(\text{w14} > \text{w02} > 1) > (\text{w06} < 1)$
  except for IPE330: *w06* = 1.014
- for buckling about the *strong* axis:
  $(\text{s14} > \text{s02} > 1) > (\text{s06} < 1)$
  except for HE650M: *w14* = 0.996

These exceptions are minor differences however, order of magnitude 1.5%.

From the results presented in this chapter it therefore follows indeed that the proposed simplified method for checking the ultimate flexural buckling loading capacity is safe, though sometimes conservative.

9 WEB-POST BUCKLING IN COMPRESSED CELLULAR MEMBERS

9.1 Introduction

In the former chapter it was concluded that the global behaviour of axially loaded cellular members is not notably influenced by the presence of web openings.

As so far no experimental evidence is available structural behaviour of cellular members loaded in axial compression, the next objective of the here presented research has been to study the influence of an applied axial force on the web-post buckling failure mechanism.

The main difference in behaviour between beams and columns lies in the presence of an not-negligible axial (compression) force, which might influence the web-post buckling capacity.
As this concerns *local buckling* behaviour, another model is required than that which was used to study the *global buckling* failure mode.

First an analytical analysis was made of both described approaches for checking the web-post buckling capacity, in order to evaluate whether they can allow for the presence of an axial force. This theoretical investigation is followed – and affirmed – by the subsequent numerical evaluation.

9.2 Theoretical analysis

9.2.1 LWO model

As seen in section 4.2.10 in the model the loading is solely represented by the effective shear force:

$$V_{h,eff} = V_h \pm 2M_h / d_o$$

which delivers the design compressive stress in the narrowest part of the web-post:

$$\sigma_c = \frac{V_{h,eff}}{s_o t_w}$$

Note that this stress is not the occurring compressive stress but rather a design quantity, for simplicity taken equal to the horizontal shear stress. The effects of stress concentrations are taken into account by the calibration of the effective length of the web-post used in the buckling model.

For symmetric cellular beams under bending and shear force, the web-post moment $M_h = 0$ and the horizontal shear force at the centre-line of the opening is given by:

$$V_h = \Delta T = T_2 - T_1 = \frac{M_2 - M_1}{h - 2y_e} = \frac{V_{Ed}\, s}{h - 2y_e}$$

(The last equality in this formula is only exact for a constant shear force).

If a constant normal force N_{Ed} is applied to the centre-line of a symmetric cellular beam, the axial forces in the tee-sections will be either increased or decreased:

$$N_t = \frac{M_{Ed}}{h - 2y_e} \pm \frac{N_{Ed}}{2}$$

but the difference $\Delta T = T_2 - T_1$ will not change. Therefore the horizontal shear force is not affected. Neither is a web-post moment introduced due to the (centrally) applied normal force. It thus follows that according to the LWO model the web-post buckling phenomenon is *not* influenced by the presence of an axial force.

The additional bending effect of an axial force which is not applied to the centre-line of the beam can be easily incorporated by a *shift* in the bending moment line.

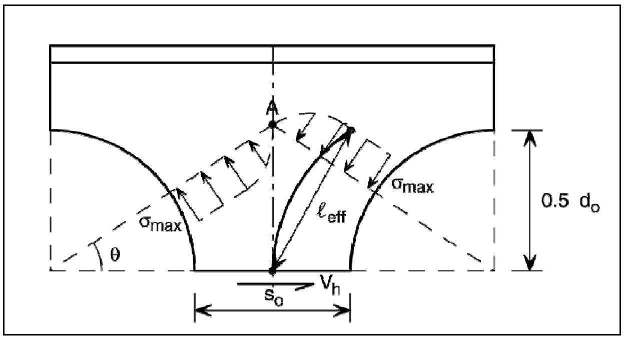

Figure 9.1 Compression strut model for web-post buckling in the LWO model

It must be noted however that this method, which uses an effective length for the compression strut in the web post, is only a rough representation of the true behaviour. The horizontal shear force V_h is used only to *represent* the compressive stress in the strut, but the real stress state is quite complex.

In the development of the LWO model, the effective lengths to be used, were calibrated against a number of test results and finite element simulations.

For these finite element simulations, a model of a single web-post was subjected to only a vertical shear force. As bending will utilise some capacity of the flanges already, the part of the axial load that is transmitted by the webs of the tee sections will increase.

This effect is not accounted for in the LWO model. In the calibration of the effective lengths, compressive stresses in the web occurred only due to the bending moment caused by the vertical shear load.

Furthermore it is remarked that the LWO web-post buckling model has been shown to be rather conservative, with model factors ranging from 1.19 to 1.90.
Therefore it is unlikely that the use of this model will or can reveal (substantial) differences in behaviour and capacity in the finite element simulations.

9.2.2 Arcelor's model

Just like for the LWO model, the main parameter concerning the loading is the horizontal shear force V_h, wherefrom the principal compressive stress $\sigma_{w,Sd}$ at the critical section is calculated, according to:

$$\sigma_{w,Sd} = \frac{6M_{c,Sd}}{\ell_w^2 t_w \left(1-4\left[d_w/d_o\right]^2\right)}$$

in which for a symmetrical cellular beam:

$$M_{c,Sd} = V_{h,Sd} d_w \pm \cancel{M_{h,Sd}} = V_{h,Sd} d_w$$

Furthermore is was already discussed in section 4.3.4 that there is also a dependency of the resistance on the loading. This dependence is given by the relation for the critical principal stress for instability:

$$\sigma_{w,Cr} = \alpha_{Cr} \cdot \sigma_{w,Sd}$$

This stress is used to calculate the slenderness:

$$\bar{\lambda} = \sqrt{\frac{\xi f_y}{\sigma_{w,Cr}}}$$

which is needed to calculate the buckling factor χ. Thereupon the principal compressive resistance is given by:

$$\sigma_{w,Rd} = \chi \, \xi \, f_y / \gamma_{M1}$$

The method to calculate the critical principal stress uses a *multiplier* called α_{Cr} to the applied load configuration (not to be confused with $\alpha_{cr} = F_{cr}/F_{Ed}$).

The advantage of using a multiplier is that the approach is valid for different load cases and support conditions. It is also to possible to obtain the value of the multiplier by using appropriate finite element models.

In the model from Arcelor explicit expressions to determine α_{Cr} are given *for the case of a cellular beam subjected to bending*.
These contain the axial forces *in the web* $N_{m,up}$ and $N_{m,low}$ which are directly linked to the axial forces N_t and N_b that act *on the tee-sections* (see 4.3.4).

For the compressed upper web-post:

$$\alpha_{Cr,up} = \max\left(\beta_{Cr,up}\,;\,\frac{2\beta_{Cr,up}\,\beta_{Cr,low}}{\beta_{Cr,up}+\beta_{Cr,low}}\right)$$

where:

$$\beta_{Cr,up} = \frac{1}{\dfrac{V_h}{V_{h,Cr,up}} + \dfrac{N_{m,up}}{N_{m,up,Cr}}}$$

$$\beta_{Cr,low} = \frac{1}{\dfrac{V_h}{V_{h,Cr,low}} - \dfrac{1}{2}\dfrac{N_{m,low}}{N_{m,low,Cr}}}$$

Thereupon it follows from the model that the presence of an axial load results in a decrease of $\beta_{Cr,up}$ and a (relatively less) increase of $\beta_{Cr,low}$ value, leading to a decrease of $\alpha_{Cr,up}$.

As the principal compressive stress $\sigma_{w,Sd}$ is not affected by a constant axial force (because $V_h = \Delta T$ keeps equal) the value of the critical principal stress for instability will decrease also. Therefore a higher slenderness will be found, resulting in a lower principal compressive resistance $\sigma_{w,Rd}$.

So according to Arcelor's model the web-post buckling phenomenon is indeed modified by the presence of an axial force. Numerical calculations however show that the influence is quite small, even for large axial forces.

Further it may be noted here that the program ARCELOR Cellular Beams is already able to take account of an axial force.
However, the applied axial compressive force N_{Ed} is limited such that it may not exceed 10% of the design resistance $N_{b,Rd}$ for flexural buckling in the plane of the web.
This buckling resistance is calculated considering the second moment of area of the *net section* and using buckling curve 'c' according to Eurocode 3-1-1.
Apart from this limitation of the axial force, only lateral-torsional buckling and the local cross-sectional resistance is checked for.

The limit was applied because of two reasons:

- the ACB program is specifically aimed at the design of *beams* primarily subjected to bending moments
- no sufficient test data has been available to ensure the applicability of the method for cellular *columns* (especially regarding stability)

9.2.3 Comparison and conclusion

In both models the main parameter that represents the load is given by the horizontal shear force $V_h = \Delta T = T_2 - T_1$.
For a symmetrical cellular beam this value is not modified by the presence of an constant axial force. Actually it is the difference in forces between the upper and lower parts of the beams that counts.

Therefore, according to both models, the inclusion of the normal force N_{Ed} in the calculation of the axial forces acting at the tee-sections, will have little to no effect on the web-post buckling stability. The horizontal shear force V_h however is used only to *represent* the compressive stress in the strut, but the real stress state is quite complex.

While in the LWO model the resistance to web-post buckling does *not* depend on the applied axial load, in the ACB model the axial force *does* affect this resistance.

It seems reasonable indeed that there is a dependency, as the compressive stress in the web of the upper tee section will increase due to the applied axial load.
The ACB model does make allowance for the effect of axial load on the web-post buckling resistance. In the calculation of the multiplier α_{Cr} the axial force acting at the tee-sections is explicitly included.

But although an effect is present, it seems to be quite small. In the next section this will be researched numerically.
As the LWO model (which is less advanced than Arcelor's model) has been shown to be conservative, it seems unlikely that using the present model will reveal differences in behaviour and capacity in the finite element simulations. Neither it is expected to result in unsafe designs. One goal of the numerical simulations that have been performed for this chapter has been to confirm this.

9.3 Finite element model

9.3.1 Introduction

For the verification of the described web-post buckling behaviour in the presence of an axial force, a new FEM model was developed.
This model basically consists of a simply supported cellular beam, loaded by a combination of a point load 2F in the middle and an axial force N at both outer ends.
The beam length is chosen such that there are two circular web openings with a single web-post in between on each half of the beam.

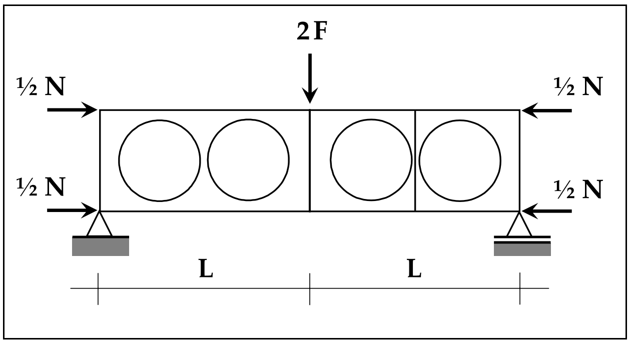

Figure 9.2 Loading configuration

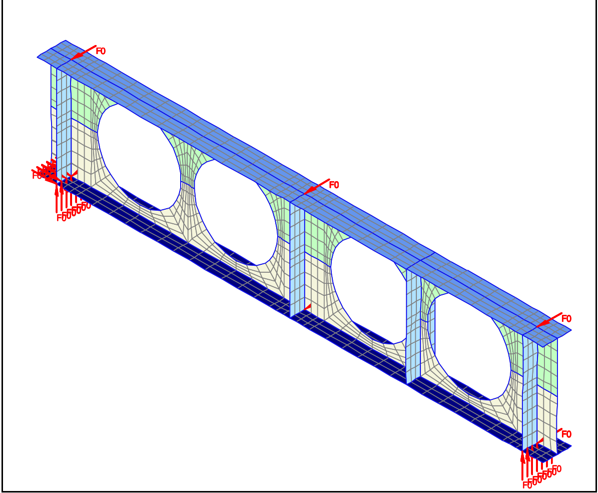

Figure 9.3 FEM model for the verification of the influence of an axial force on the web-post buckling capacity

As this investigation concerns a *local* failure mechanism, there is no need of varying the length to obtain failure loads for difference slenderness values.
In order not to bias the results by simultaneous buckling of the web-post at each beam half, at one side a stiffener was added.
Furthermore stiffeners were added at the supports and halfway the beam where the vertical point load is applied.
At both sides of the free span of 2L, the beam was a little extended, because otherwise these points of load introduction might limit the ultimate load instead of the beam section itself.
This extension of the beam length removed the need for additional SAME commands for the translations and rotations of the beam ends, that would otherwise be required in order to ensure an uniform introduction.

9.3.2 Support conditions

At the left support all translations are fixed at the level of the lower flange. The right support is free to move in the longitudinal direction, but is restrained vertically.
By means of a few lateral supports (at the beam ends and in the middle) the possibility of lateral-torsional buckling was prevented to occur. No more restraints were applied.

9.3.3 Use of imperfections

Due to the set-up of the FEM model, and the way it is loaded, basically failure can occur due to either:

- buckling of the web-post between the two circular openings
- yielding of the tee-section at the location of the opening most near to the support

In order to initiate web-post buckling, an imperfection was applied by the pre-processor Crystal Pro. This imperfection consists of a sine bow over the height of the profile and a cosine along the length of the member, and has been described already in section 8.3.3.

9.3.4 Load application

Web-post buckling can occur due to the horizontal shear force that has to be transmitted by the web-post, and is therefore mainly dependent on the vertical shear force. Yielding of the tee-section can occur due to an internal tension or compression force, either due to bending moment or axial load.
Therefore, the load application consists of:

- a vertical point load 2F at the middle of the member, causing a linear bending moment diagram along the halve length of the beam and an uniform shear force diagram of size F
- a compressive axial force applied at both beam ends

The influence of the axial force on the web-post buckling capacity then can be determined by investigating various combinations of the vertical and the axial load.

9.4 Parameter study

9.4.1 Set-up

In order to validate and illustrate the theoretical analysis as described in section 9.2, a series of calculations have been conducted. For these analyses, the same set of five hot-rolled sections (base profiles) was selected, as for the parameter study into the global buckling behaviour of cellular members. For each base section, two web-post widths have been researched numerically. The first time with the minimum web-post width according to the geometrical limitations of the ARCELOR Cellular Beams, and the second time with a web-post width twice as big.
It may be noted here, that these values are many times out of the scope of application for the LWO method, as this method was only validated for a certain geometrical range. Furthermore, the models with double web-post width may be unsuitable to be produced by the technique of cutting and welding as described in section 2.2.
In all simulations, the steel grade used is S235.

The simulations are carried out to determine the ultimate vertical load for a *given* axial load. In the FEM calculation, first the axial load is applied in a few steps. Then the vertical load is increased until failure occurs.

In the following subsections the results for each base profile are presented by means of a combined graph of the FEM results versus the ACB en LWO prediction of the ultimate load. At the horizontal axis, the applied axial force N is shown, while at the vertical axis the shear force F is plotted. Note that this shear force is a half of the applied vertical point load.
For each graph, at least 6 FEM analyses were conducted in order to provide a smooth curve.

In Annex C these graphs are given separately for the ACB en LWO model, such that it can be seen clearly whether the FEM result matches with the ultimate load prediction of that specific theoretical model.

These ultimate load predictions are based on the following criteria:

- web-post buckling
- Vierendeel bending and/or yielding of the net section (axial force only)
- shear capacity of the web-post

These checks have been described extensively in Chapter 4 for both (ACB and LWO) models.

Web-post buckling is dependent mainly on the horizontal shear force $V_{h,eff} = V_h \pm 2M_h / d_o$ which for symmetric sections (where $M_h = 0$) reduces to V_h, which is also limited directly by the shear capacity of the web-post.

In the ACB model, the Vierendeel bending capacity is checked at each opening location for each section inclined at angle ϕ to the vertical by increments of $1°$. For each inclined section the section properties are calculated, and the forces acting on the inclined section are determined from equilibrium.
When both normal load and bending moment act on the inclined tee-section, *linear interaction* is considered:

$$M_{pl,t,red} = M_{pl,t}\left(1 - \left[N_t / N_{pl,t}\right]\right)$$

Allowance for the influence of a high shear force is made also.

In the LWO model, the check against Vierendeel action is carried out by considering the additional local bending that occurs across the openings. For circular holes the effective opening length for Vierendeel action is given by $\ell_{v,eff} = 0.45d_o$ (see also section 2.4).

The total applied Vierendeel moment of $M_v = V_{Ed}\ell_{v,eff}$ should be less than the bending capacity of both tee-sections: $2M_{b,red} + 2M_{t,red}$.
However, as for an axially compressed beam the normal forces in the upper and lower tee-sections will vary, the compressed tee-section will limit the shear force that can be transferred: $V_t \leq 2M_{t,red} / \ell_{v,eff}$.

It is possible that redistribution of the shear force occurs from the compressed top tee to the less compressed (or even tensioned) bottom tee, but this was not further considered. The effect of this would also be to introduce a web-post moment and thus increase the effective horizontal shear force $V_{h,eff}$ which governs web-post buckling.

For simultaneous axial and bending action on the tee-sections, the LWO model considers *quadratic interaction* according to:

$$M_{pl,t,red} = M_{pl,t}\left(1 - \left[N_t / N_{pl,t}\right]^2\right)$$

and will therefore provide an enhanced moment capacity for a given axial force as compared with the ACB model.
However, as the formulation of the check on Vierendeel bending is entirely different between the two models, this may or may not result in an higher Vierendeel resistance.

One important thing to note is that in the comparison of the FEM ultimate load with those resulting from the described theoretical models, there is a small discrepancy due to the modelling of the section by it's centrelines and the neglect of the root radii in the FEM model.

In the calculation using the theoretical models, these root radii *were* taken into account.
Not doing so would result in an under-estimation of the ultimate load capacity (especially concerning axial load) and therefore provide an overly safe, and therefore unrealistic, estimation of the margin between the FEM result and the theoretical results.
Therefore the pure plastic axial capacity (so without vertical point load) from the FEM model is a little less than that predicted from the theoretical models, as can be seen from the graphs for high axial load. However, for usual structures flexural buckling will be rather control the design.

While in beam-column structures it can also occur that the bending moment changes sign between the two opening locations left and right from the web-post being studied, this case was not investigated here. Indeed, in general these moments (where the bending moment diagram passes through the zero-point) are relatively small and therefore this case will not be decisive for the design.

9.4.2 Base profile IPE140

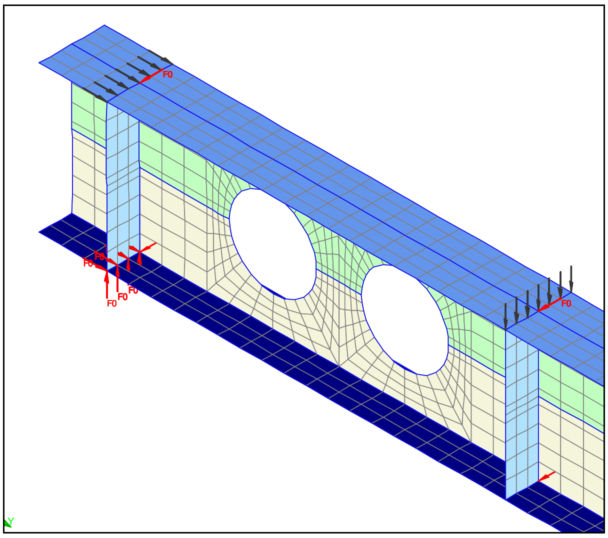

Figure 9.4 IPE140 with s_0 = 50 mm

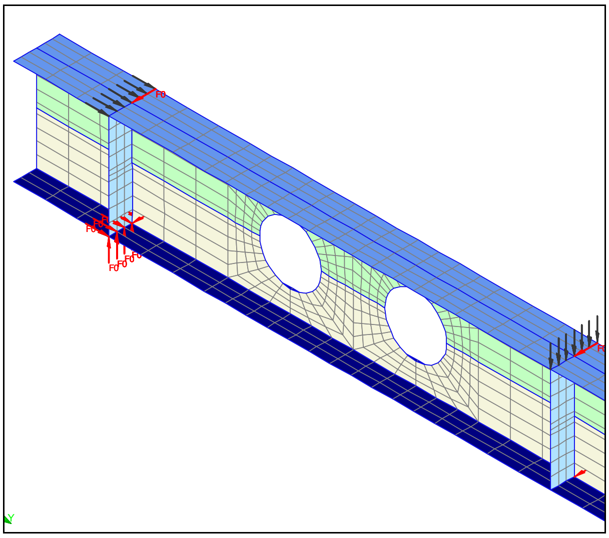

Figure 9.5 IPE140 with s_0 = 100 mm

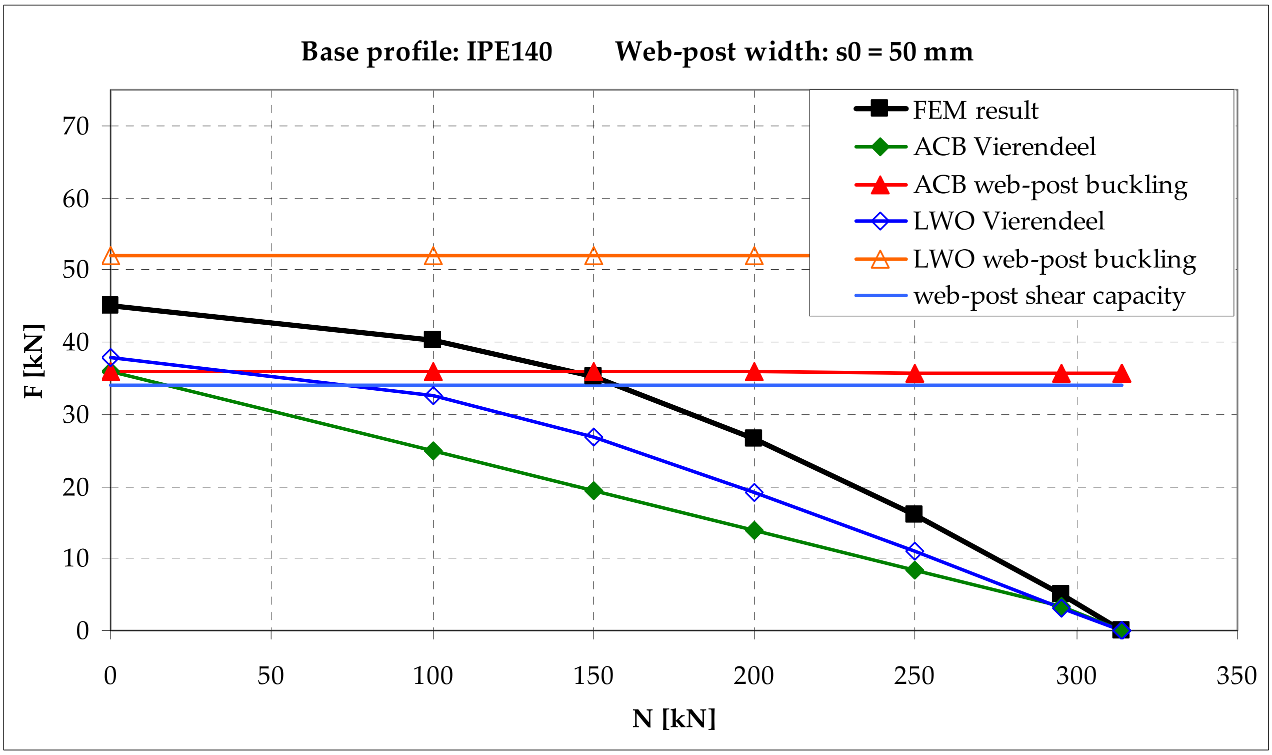

Figure 9.6 Results for web-post buckling parameter study: IPE140 with s_0 = 50 mm

From the figures of the FEM model it is already clear that the width of the web-post is relatively big compared to the opening diameter. The results confirm the minor importance of web-post buckling in this case. The ultimate load is rather limited by the shear capacity of the web-post and by Vierendeel bending.

For increasing axial load, the Vierendeel action even becomes dominant. Indeed Arcelor's model shows an almost linear dependence on the axial load, while the curve from the LWO model is of a quadratic order. For both models, at every point the ultimate load prediction is lower than acquired in the FEM simulation.

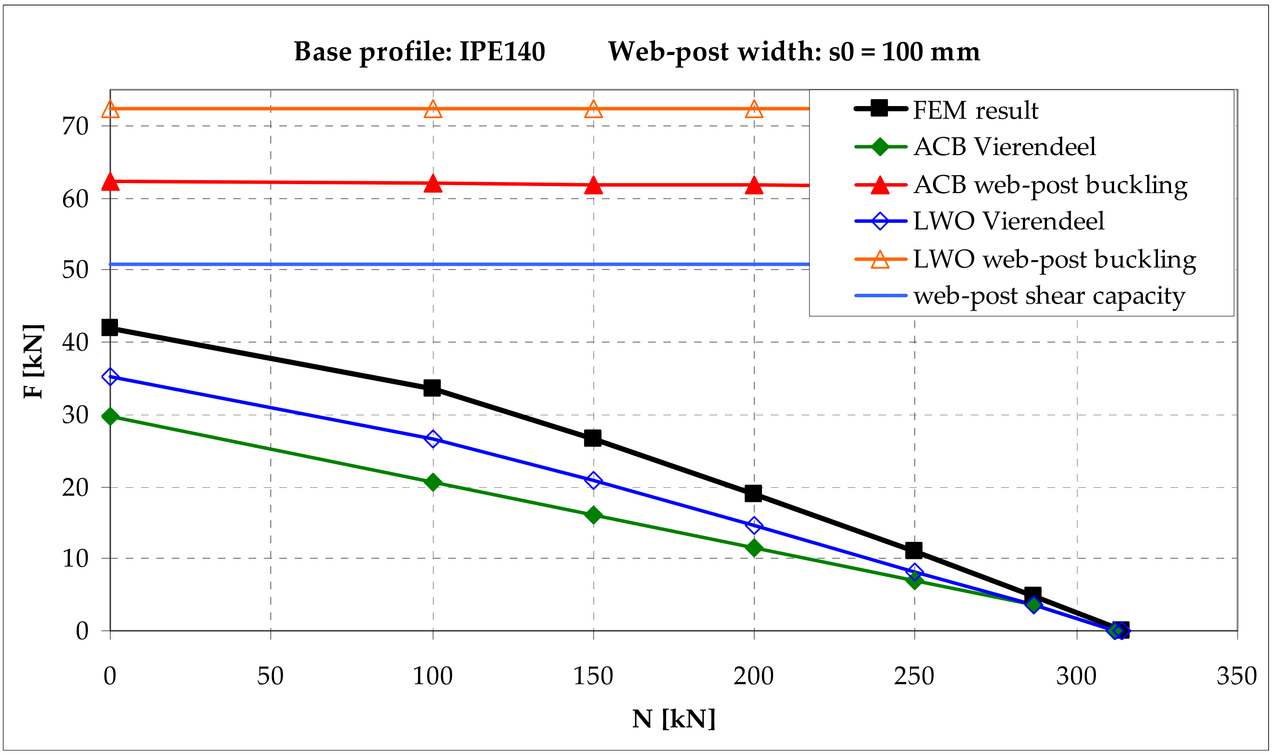

Figure 9.7 Results for web-post buckling parameter study: IPE140 with s_0 = 100 mm

This pattern is even more clear for the model with double web-post width. The ultimate load now is solely controlled by Vierendeel action.
Just like for the smaller web-post width, the LWO curve for web-post buckling is above that of Arcelor's model. The contrary is true for the curves for the Vierendeel bending capacity.

It is concluded that both models return safe results for this case.

9.4.3 Base profile IPE330

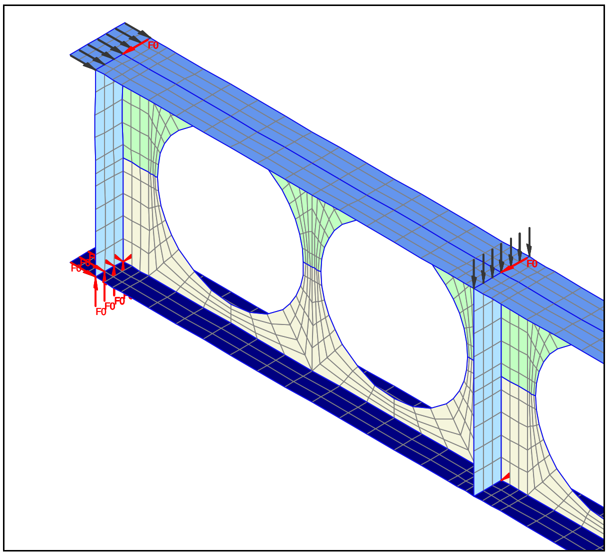

Figure 9.8 IPE330 with s_0 = 50 mm

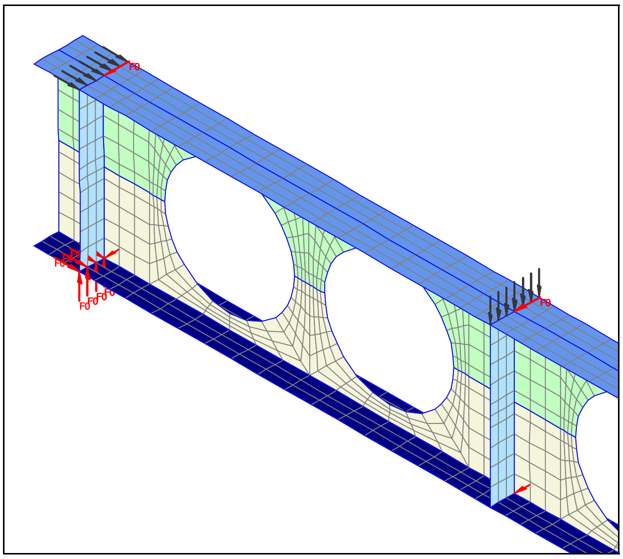

Figure 9.9 IPE330 with s_0 = 50 mm

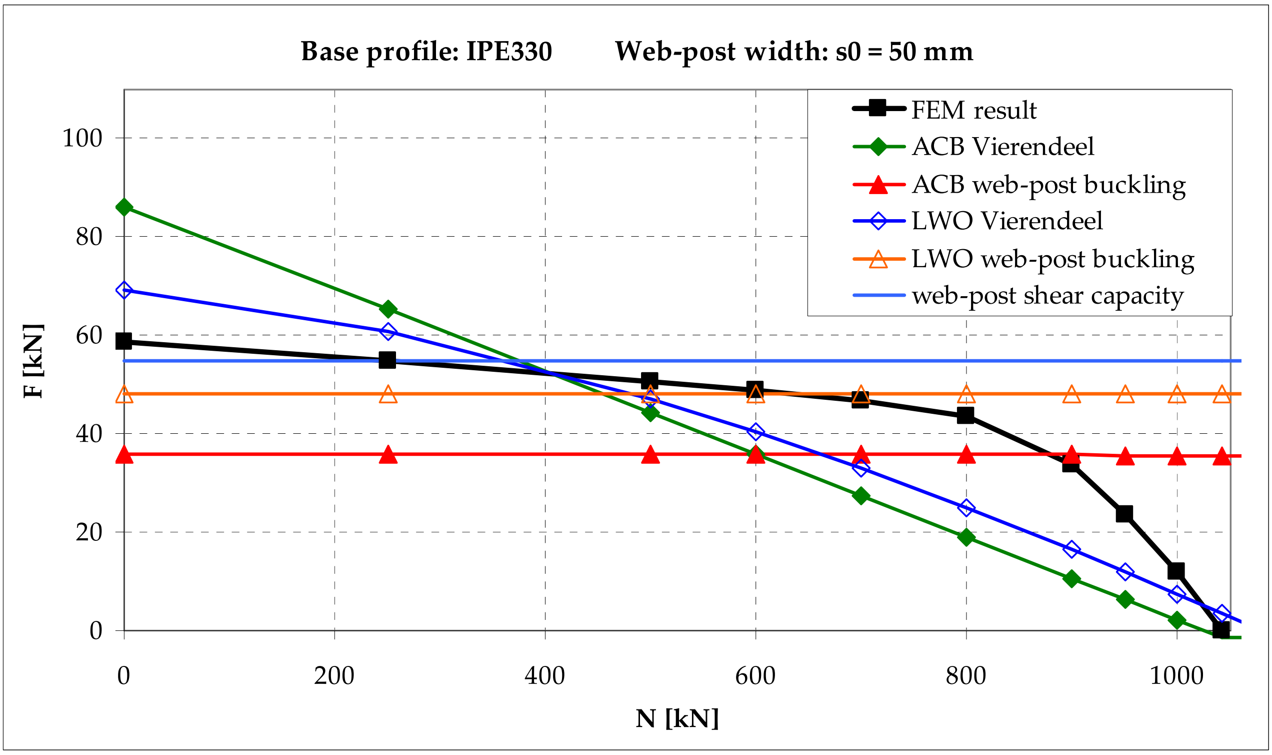

Figure 9.10 Results for web-post buckling parameter study: IPE330 with s_0 = 50 mm

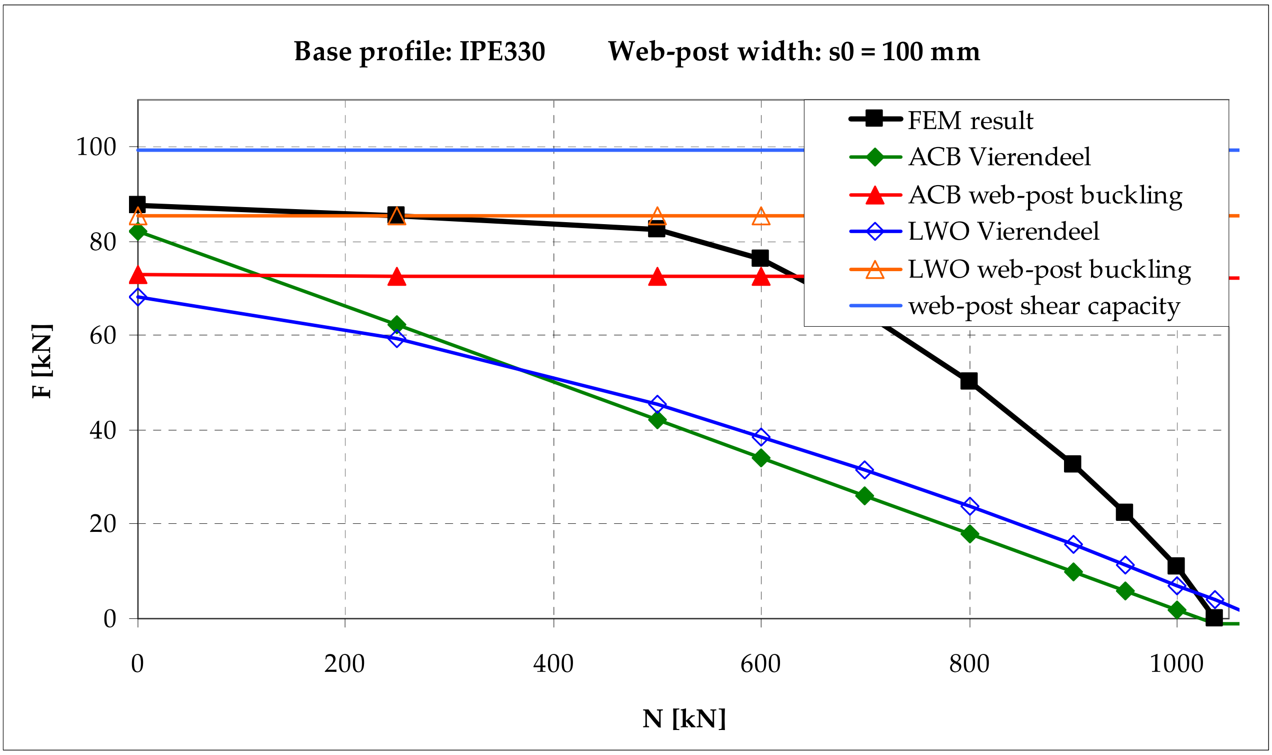

Figure 9.11 Results for web-post buckling parameter study: IPE330 with s_0 = 100 mm

For base profile IPE330 web-post buckling is much more likely to occur. Now for low axial force, web-post buckling does govern the design, while for higher normal load Vierendeel action becomes decisive. Again the FEM results are above the predictions of both models, which are thus safe. Especially for the double web-post width the models are rather

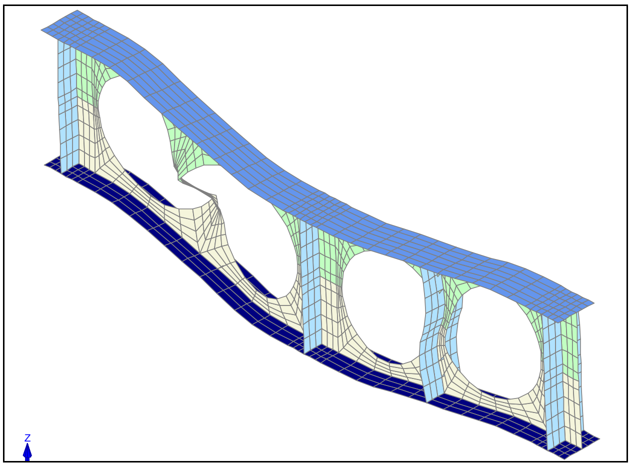

Figure 9.12 Web-post buckling for base profile IPE330 with s_0 = 50 mm, N=500 kN

conservative, given the margin seen between the FEM result and the predictions from the theoretical models.

Furthermore a small influence can be seen of the axial load on the ultimate load capacity. For low values of the axial load, where the Vierendeel bending capacity is higher than the web-post buckling capacity, the FEM curve is approximately linear decreasing.

This effect is not visible in the theoretical predictions. In the theoretical analyses a qualitative influence was spotted for Arcelor's model, but numerically this can be hardly noticed. Still the predicted ultimate load is below the acquired FEM results.

From the figure on the left it is clear that web-post buckling only occurred at the left post. As expected, the stiffened web-post did not buckle.

9.4.4 Base profile IPE600

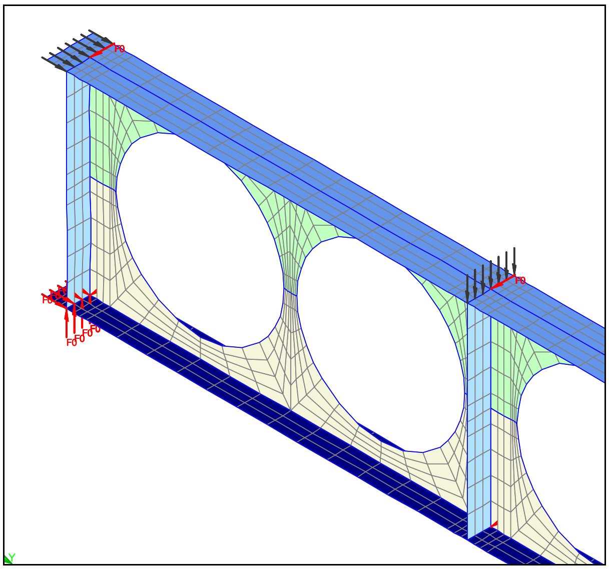

Figure 9.13 IPE600 with s_0 = 62 mm

For base profile IPE600 the web-post is relatively even more slender. In this case the prediction of the web-post buckling load is almost equal for both Arcelor's and the LWO model. Clearly this failure mechanism does govern the design, until the axial force reaches about 60% of it's ultimate value, when Vierendeel bending behaviour becomes dominant.

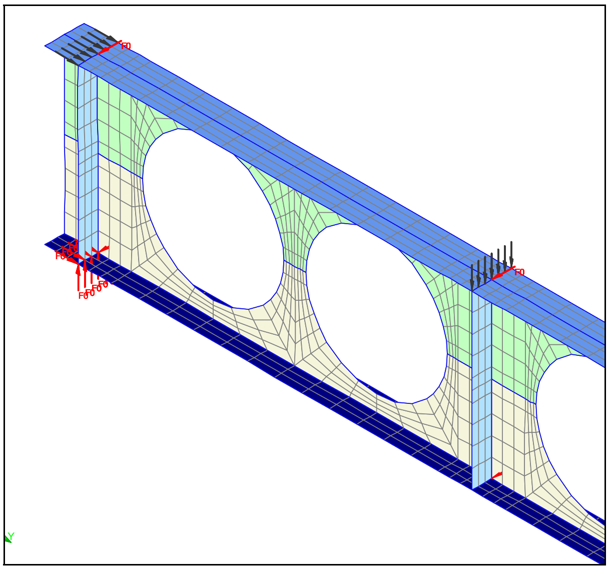

Figure 9.14 IPE600 with s_0 = 124 mm

Remarkably the FEM curve for the smaller web-post width (s_0 = 62 mm) is also above the curve for the pure plastic web-post shear capacity. This indicates that further plastic redistribution has occurred in the web-post, before failure occurred by web-post buckling. Indeed it follows from the stress results of the FEM analysis, that at ultimate horizontal shear force, the principal stresses already fully satisfy the Von Mises yield criterion, but that these stresses do not increase further.

For both web-post widths the LWO web-post buckling prediction again is above the ACB one. The LWO Vierendeel curve starts below the ACB curve, but due to it's quadratic (instead of linear) nature it later passes through, predicting an enhanced Vierendeel bending capacity. The governing curves are always below the FEM curve and thus safe.

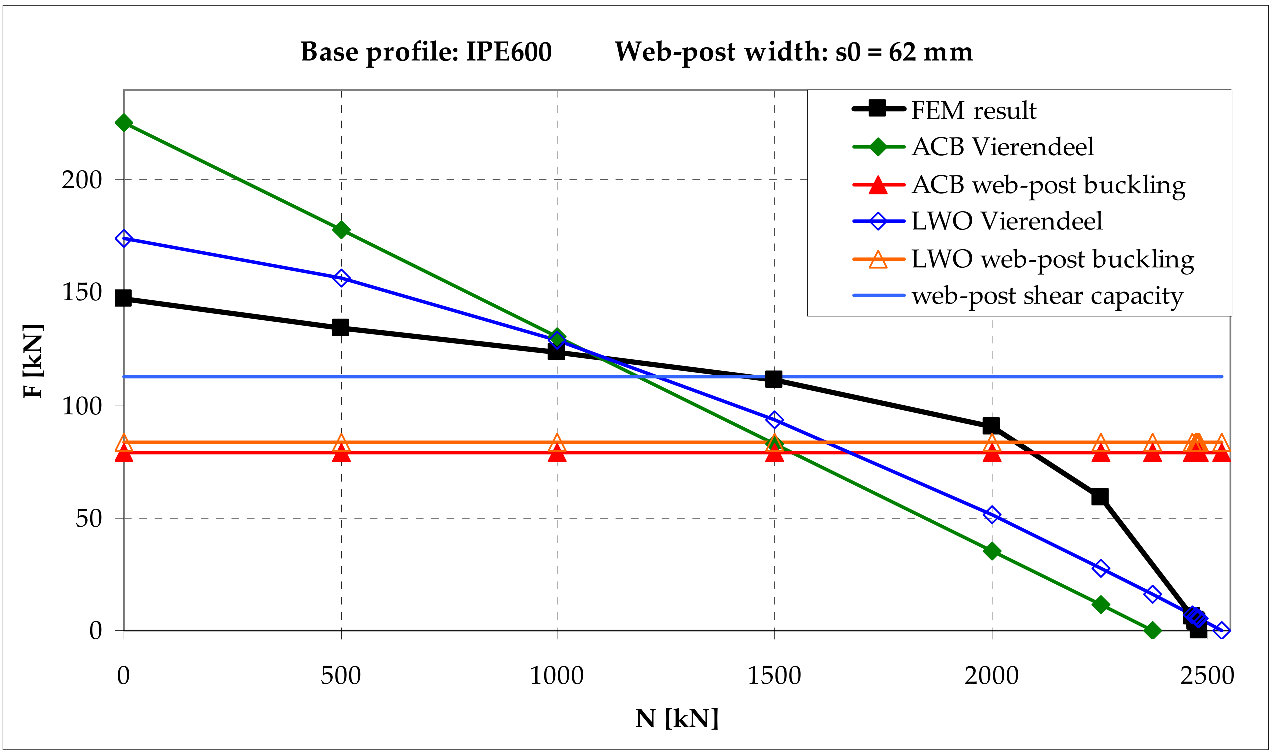

Figure 9.15 Results for web-post buckling parameter study: IPE600 with s_0 = 62 mm

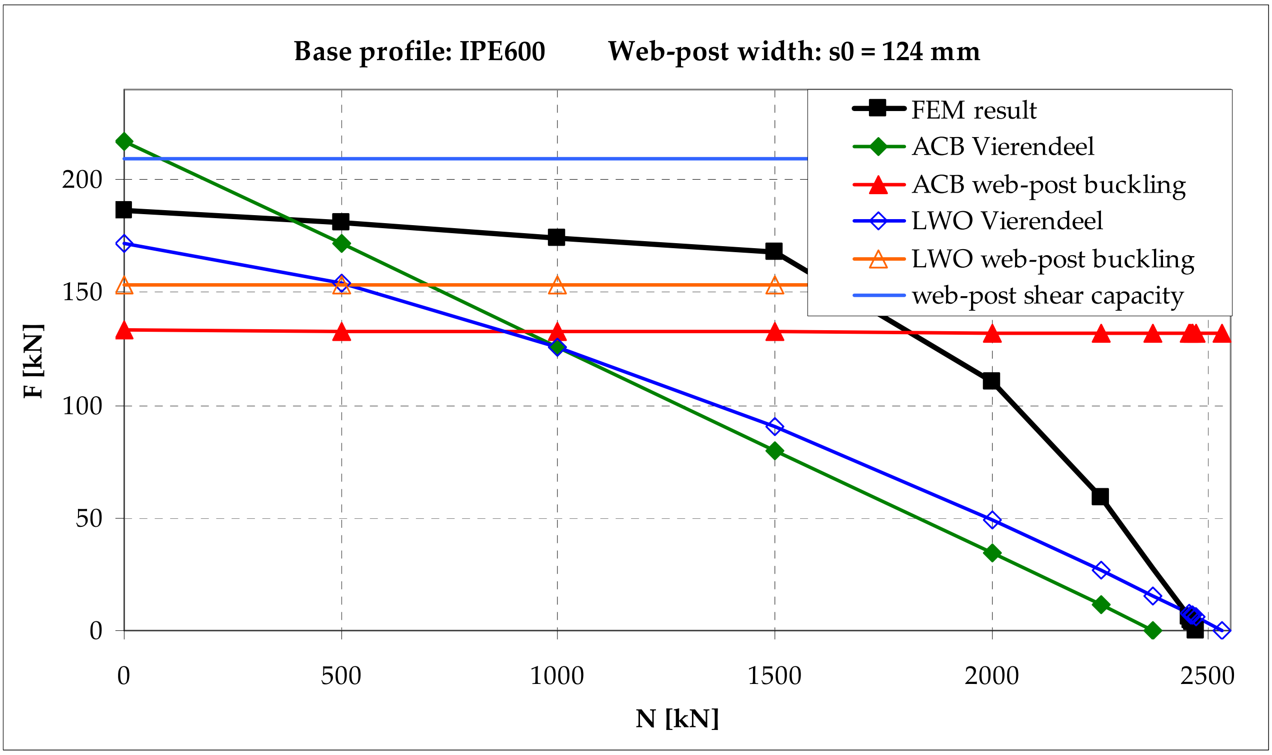

Figure 9.16 Results for web-post buckling parameter study: IPE600 with s_0 = 124 mm

9.4.5 Base profile HE200A

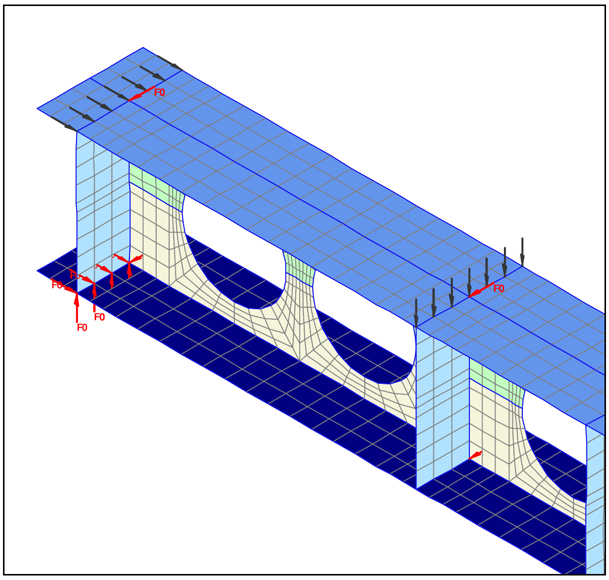

Figure 9.17 HE200A with s_0 = 50 mm

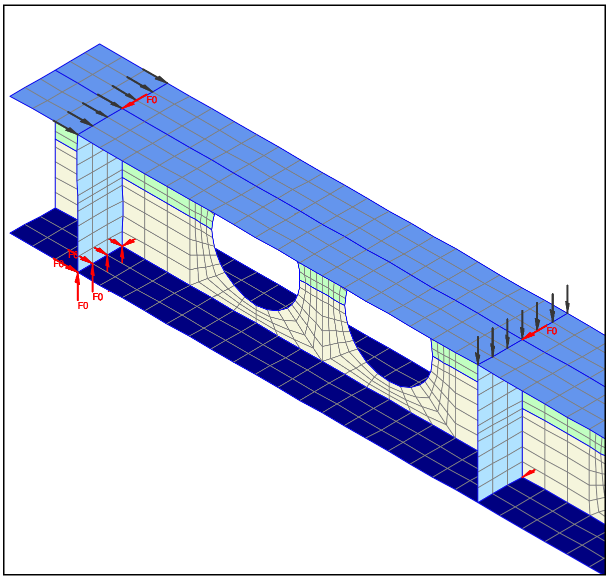

Figure 9.18 HE200A with s_0 = 100 mm

The first base section that was chosen from the HE-range has relatively wide flanges. Therefore the axial forces in the tee-sections are rather high, in comparison with sections like IPE330 which have a bigger height.
As the horizontal shear force that has to be transferred by the web-post depends on the difference in axial force on the tee-sections, caused by bending, it is to be expected that this profile will be susceptible to web-post buckling. For web-post width s_0 = 50 mm this was indeed observed from the FEM analyses, but seems to be initiated by reaching the ultimate web-post shear capacity first.

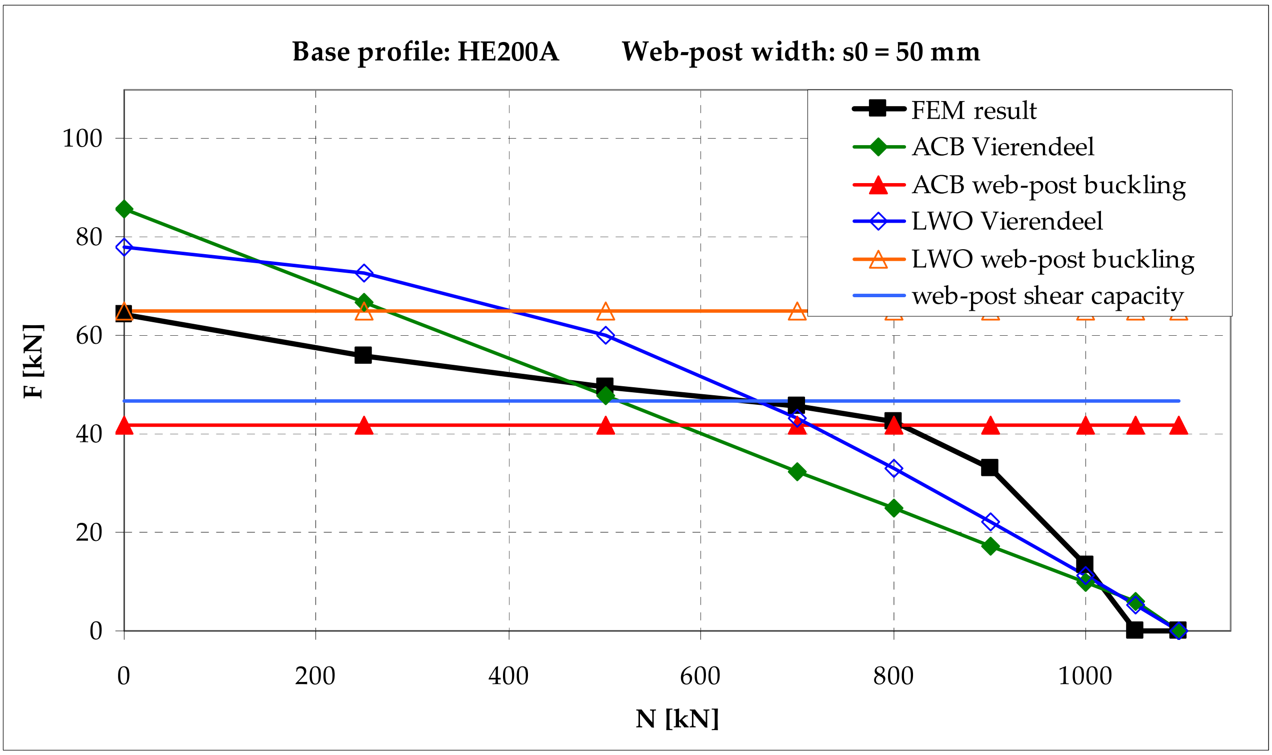

Figure 9.19 Results for web-post buckling parameter study: HE200A with s_0 = 50 mm

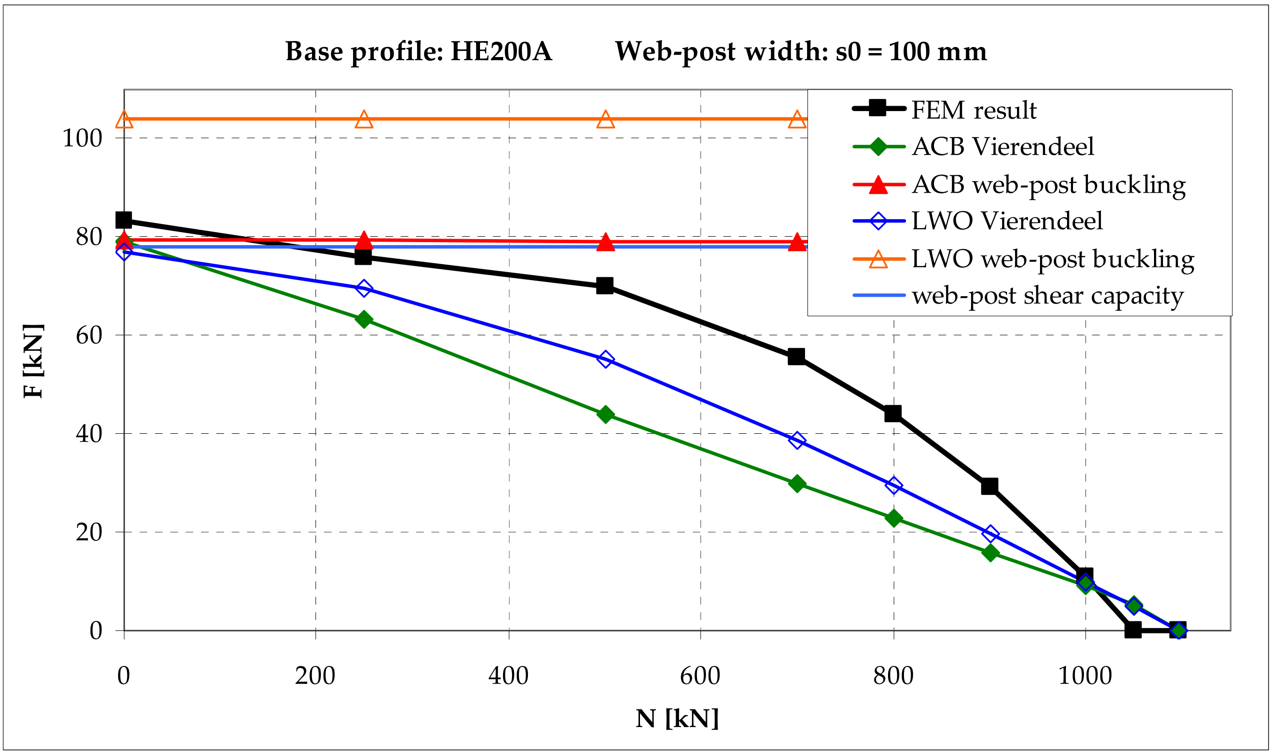

Figure 9.20 Results for web-post buckling parameter study: HE200A with s_0 = 100 mm

For the double web-post width, the web-post not longer does govern the design, but rather it is controlled by Vierendeel bending. This is also predicted by both theoretical models.

The two trends that have been seen so far, are also confirmed here: the ACB web-post buckling prediction is lower than calculated by the LWO method, and the LWO method predicts an enhanced Vierendeel capacity for higher axial forces.

Apart from the somewhat higher pure plastic load prediction due to the neglect of the root radii in the FEM model (see section 9.4.1), the theoretical results are on the safe side.

9.4.6 Base profile HE650M

Finally base section HE650M was considered also. Due to it's large web opening size, this section looks rather slender. Nevertheless it's flanges are no less than 40 mm thick.

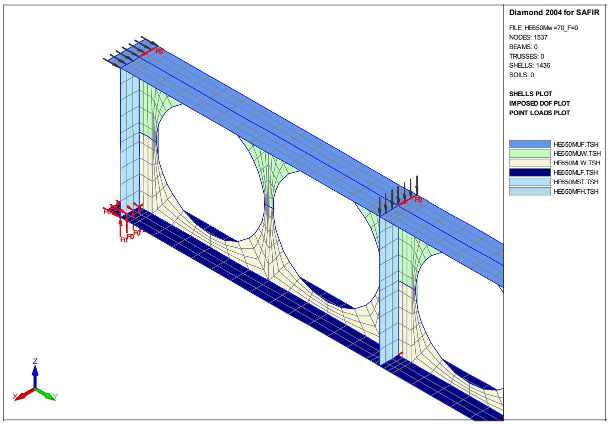
Diamond 2004 for SAFIR
FILE: HE650Mw =70_F=0
NODES: 1537
BEAMS: 0
TRUSSES: 0
SHELLS: 1436
SOILS: 0
SHELLS PLOT
IMPOSED DOF PLOT
POINT LOADS PLOT
HE650MUF.TSH
HE650MUW.TSH
HE650MLW.TSH
HE650MLF.TSH
HE650MST.TSH
HE650MFH.TSH

Figure 9.21 HE650M with s_0 = 70 mm

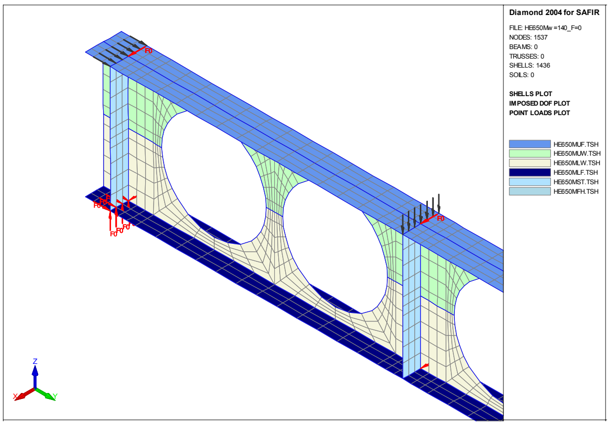
Diamond 2004 for SAFIR
FILE: HE650Mw =140_F=0
NODES: 1537
BEAMS: 0
TRUSSES: 0
SHELLS: 1436
SOILS: 0
SHELLS PLOT
IMPOSED DOF PLOT
POINT LOADS PLOT
HE650MUF.TSH
HE650MUW.TSH
HE650MLW.TSH
HE650MLF.TSH
HE650MST.TSH
HE650MFH.TSH

Figure 9.22 HE650M with s_0 = 140 mm

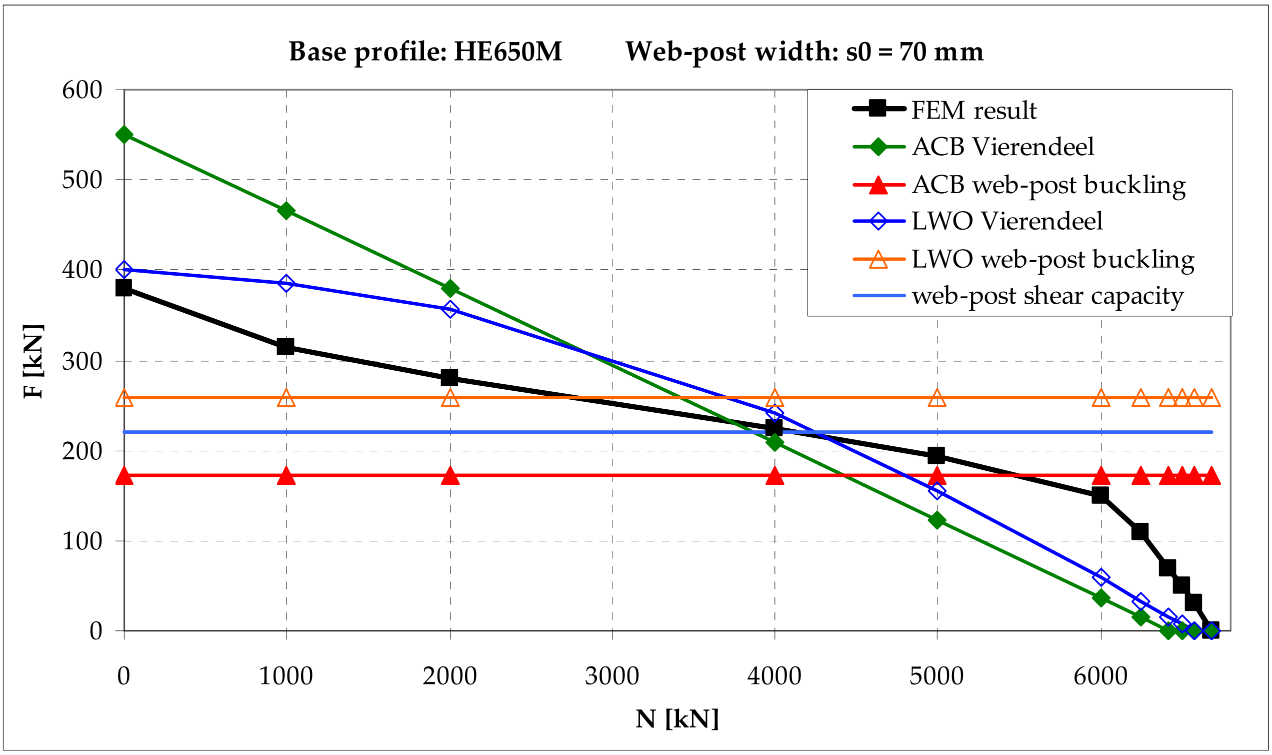

Figure 9.23 Results for web-post buckling parameter study: HE650M with $s_0 = 70$ mm

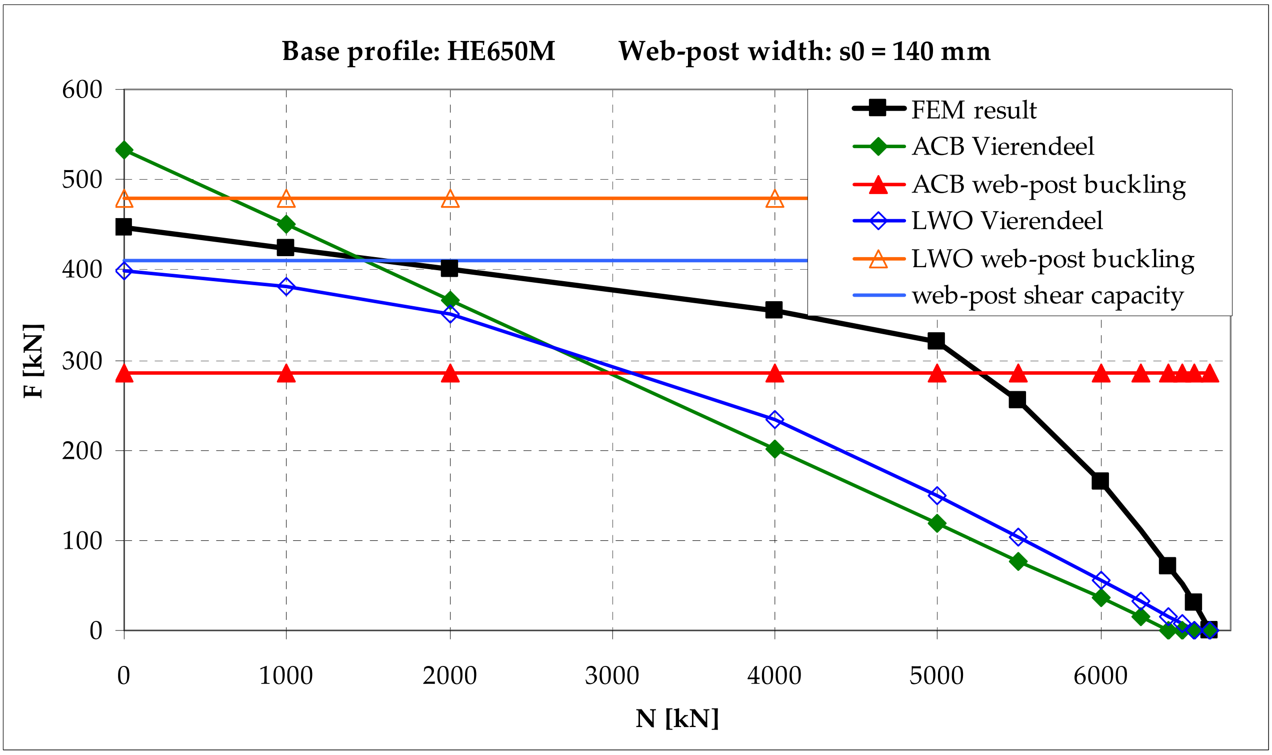

Figure 9.24 Results for web-post buckling parameter study: HE650M with $s_0 = 140$ mm

For the smaller web-post width, again the FEM result was higher than predicted on basis of the shear capacity of the web-post. Possibly a part of the force transfer has been realized by global Vierendeel bending of the beam, in which only the web-post halfway the beam and the tee-sections play a role.

It is interesting to see here that the LWO prediction of the ultimate load with respect to

Vierendeel bending for N = 0 almost coincides with the obtained FEM result. Furthermore the intersection of the web-post shear capacity curve and the LWO Vierendeel curve lies at the FEM curve.

On the other hand the ACB curve for Vierendeel bending is far too optimistic for low axial force (where actually web-post shear and/or buckling is decisive). This is due to the consideration of the *inclined* tee-section, thus with increased height where the local bending moment acts (see also section 4.3.2).
In the LWO approach with an effective opening length for Vierendeel bending, the tee-section of the (perpendicular) net section is used instead.

Nevertheless, the resulting predictions of both theoretical models are safe also for this case.

9.5 Conclusion

From the analyses presented in the preceding paragraphs for each base section considered, the following conclusions may be drawn:

- an approximately linear relation has been observed for the influence from an axial force on the web-post buckling capacity of cellular members
- while the effect of an axial force is qualitatively included in Arcelor's model, this influence is numerically negligible
- after reach of the web-post shear capacity, web-post buckling is initiated but due to plastic redistribution the load can increase further
- the LWO model gives web-post buckling predictions which are both higher than the ACB curve, and more close to the FEM curve
- while for low axial force the LWO Vierendeel curve is below the ACB curve, due to the quadratic M-N interaction for the tee-sections (instead of linear in the ACB model), for higher axial force the LWO curve predicts an enhanced capacity
- for low axial force where web-post shear and/or buckling governs, the ACB Vierendeel prediction seems overly optimistic, whereas the LWO prediction is more close to the FEM curve
- the LWO model always predicts an lower capacity than the calculated FEM-results
- the governing equation of the ACB model is more conservative in all cases

Therefore, despite the influence of axial force is not (effectively) accounted for in the theoretical models, these models still return valid results in the researched range of sections, and thus can be applied safely in design. The LWO methods seems to provide the most realistic failure load prediction.

PART III
–
CASE STUDY

10 PORTAL FRAME STRUCTURES USING CELLULAR MEMBERS

10.1 Introduction

In the preceding numerical research part, isolated cellular members were analysed in order to identify differences in behaviour due to the presence of web openings.
It was concluded that flexural buckling occurs in a similar way as for plain-webbed members. Regarding web-post buckling, it turned out that although an influence of axial force could be identified, the current calculation models can be applied safely in design.

In practice, steel members can occur either isolated or as part of a building frame. Portal frame structures are a examples of such a building frame. If cellular members are to be applied in portal frame structures, the most probable reason seems to be of esthetical nature.

In this last chapter, the conclusions from the former part of the literature study and the numerical research are illustrated by and applied to the design of portal frames using cellular members.

10.2 Design using the LWO method

10.2.1 Structure of the Excel tool

In order to be able to design quickly a portal frame, an Excel tool has been developed using Visual Basic for Applications. In this tool the LWO method is used to check the capacity of the cross-section at each opening position in an automated way.
Furthermore the in-plane stability (flexural buckling) is checked using the rules from Eurocode 3-1-1, based on the net section properties and the web-post buckling phenomenon is assessed.

As the out-of-plane behaviour of cellular members is not significantly different from that of plain-webbed sections, the Excel tool has been limited to in-plane behaviour only.

First all geometric data have to be entered. On the basis of the given system lines of the portal frame and the sectional data of the cellular members, the positions of the web openings in the real frame are calculated.

The user then has to enter the value of the value of the permanent load per unit area (e.g. selfweight of the roof structure).
All variable loadings are generated automatically according to the provisions of the Eurocodes, only the peak velocity pressure for wind loading has to be entered by the user.

Finally a load combination can be selected – or the user can enter all loading data by hand – and the analysis can be started.

10.2.2 Analysis procedure

The actual analysis of the portal frame structure consists of a number of steps:

- determination of the design forces at each opening location, including the appropriate initial imperfections and incorporation of sway effects
- cross-section checks at each opening location according to the LWO method, together with a check on web-post buckling
- flexural buckling checks of the cellular members

The output of all checks are presented in a table format, together with the calculated displacement values.

Determination of design forces and moments
In this first step, the load distribution has to be determined accounting for second-order effects and imperfections where relevant. The actual finite element code for this calculation has been set up completely in Excel.

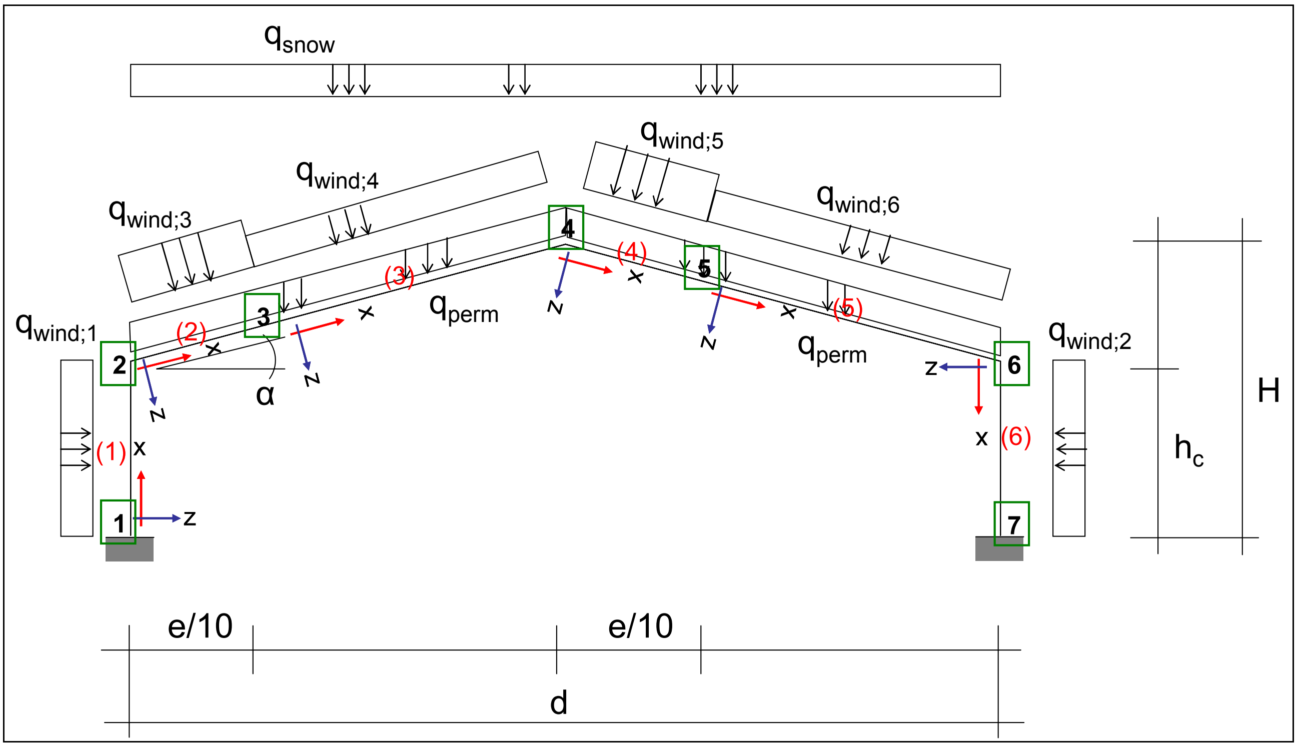

Figure 10.1 Node and element numbering for the finite element model in the Excel tool

The supports at node number 1 and 7 can be set to either “clamped” of “pinned”.

The rafters have been subdivided in two parts, as the Eurocode prescribes two wind pressure areas for each side of the roof of a ‘middle’ frame (i.e. not near the ends op the building). This subdivision makes it easier to apply the distributed loads.

The section properties which are used in the analysis, are calculated on basis of the net section geometry.

Global sway imperfections are accounted for by the possibility for the user to define an initial inclination of the whole structure. Second-order effects have been included in the analysis by means of the amplified sway method (see section 5.3.5). Therefore first (an approximation of) the critical buckling factor α_{cr} is determined, by which the ‘sway effects’ have to be multiplied.

In order to calculate α_{cr}, the (linearised) second-order global stiffnes matrix of the whole frame is assembled. The minimum value of the critical elastic load multiplier is calculated by solving the generalised eigen-value problem [MSA]:

$$\left(\mathbf{K}_E+\alpha_{cr}\mathbf{K}_G\right)u=0$$

in which:

$\mathbf{K}_E$ is the linear elastic stiffness matrix,
$\mathbf{K}_G$ is the geometric stiffness matrix,
and u is the displacement vector.

The entries of the geometric stiffness matrix depend on the axial forces in the elements, which are calculated in advance by first-order theory.

The amplified sway method only requires to multiply the so-called sway effects. These are determined by the following procedure:

- first a global linear-elastic analysis is carried out for the sway frame in order to determine the moments, axial forces and shear forces in each member (“sway case”)

- then another analysis is carried out for the same structure, but with an extra horizontal support at the top of the portal frame ("propped case")
- the moments induced in the members from the propped case are then subtracted from the moments determined from the sway case – the resultant moments are those induced by "pure sway" (see Figure 10.2)
- the "pure sway" moments are then amplified by $\alpha_{cr}/(\alpha_{cr}-1)$ and added to the moments which have been obtained from the analysis of the propped structure, resulting in the design moments which each member must be able to resist

This procedure for the calculation of α_{cr} and the determination of the design forces is therefore repeated for every load combination. The approximate second-order displacements are also calculated by this method.

The results of this step are the design forces and moments at each opening position. All opening locations are calculated in accordance with the real geometry of the frame, based on the system lines, such that the geometry fully coincides with the modelled portal frame in the analysis with shell elements.

Cross-section checks at each opening location
For each opening position, the capacity of the cellular member is checked according to the LWO method as described in section 4.2. Dependent of the cross-section classification, either the plastic of the elastic ultimate capacities are used.

The results of these checks are summarised in a table on the output sheet in the format of unity-checks, and the maximum unity-check value is presented to the user as well.

For each opening the full coordinates of it's position are printed for easier reference.

Member flexural buckling checks
Finally the in-plane stability of all members is checked according to Section 6.3.3 from Eurocode 3-1-1. In section 5.5 *Non-uniform members* it was concluded out that the rules in Section 6.3.3 do not *directly* apply to cellular members. However, as it has been shown in the parameter study of chapter 8, the flexural buckling capacity of cellular members can be calculated safely by using 'substitutive' members with section properties based on the net section.

The interaction factors k_{ij} to be used in the following expressions are calculated from Annex B of EN1993-1-1:

$$\frac{N_{Ed}}{\chi_y N_{Rk}/\gamma_{M1}}+k_{yy}\frac{M_{y,Ed}}{\chi_{LT} M_{y,Rk}/\gamma_{M1}}+k_{yz}\frac{M_{z,Ed}}{M_{z,Rk}/\gamma_{M1}}\leq 1$$

$$\frac{N_{Ed}}{\chi_z N_{Rk}/\gamma_{M1}}+k_{zy}\frac{M_{y,Ed}}{\chi_{LT} M_{y,Rk}/\gamma_{M1}}+k_{zz}\frac{M_{z,Ed}}{M_{z,Rk}/\gamma_{M1}}\leq 1$$

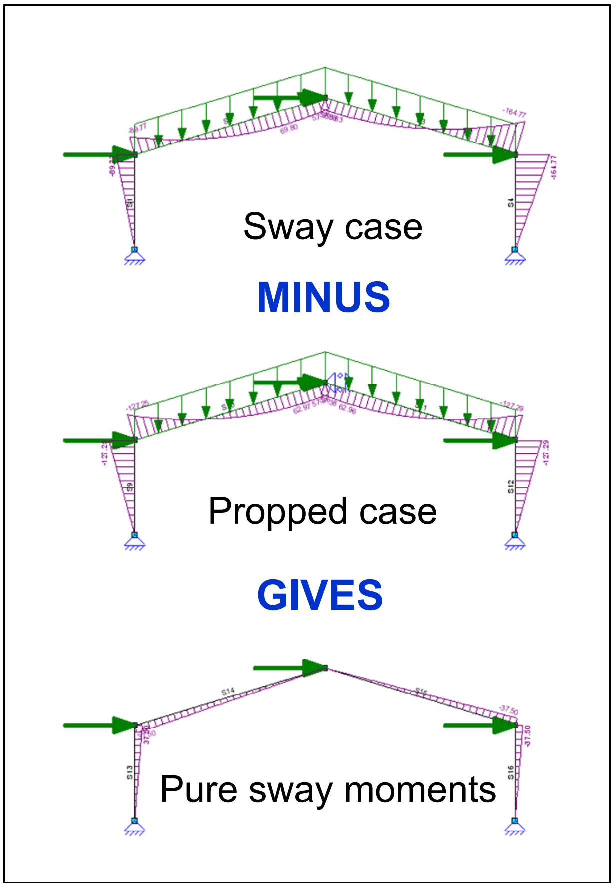

Figure 10.2 Determination of pure sway forces "to be amplified"

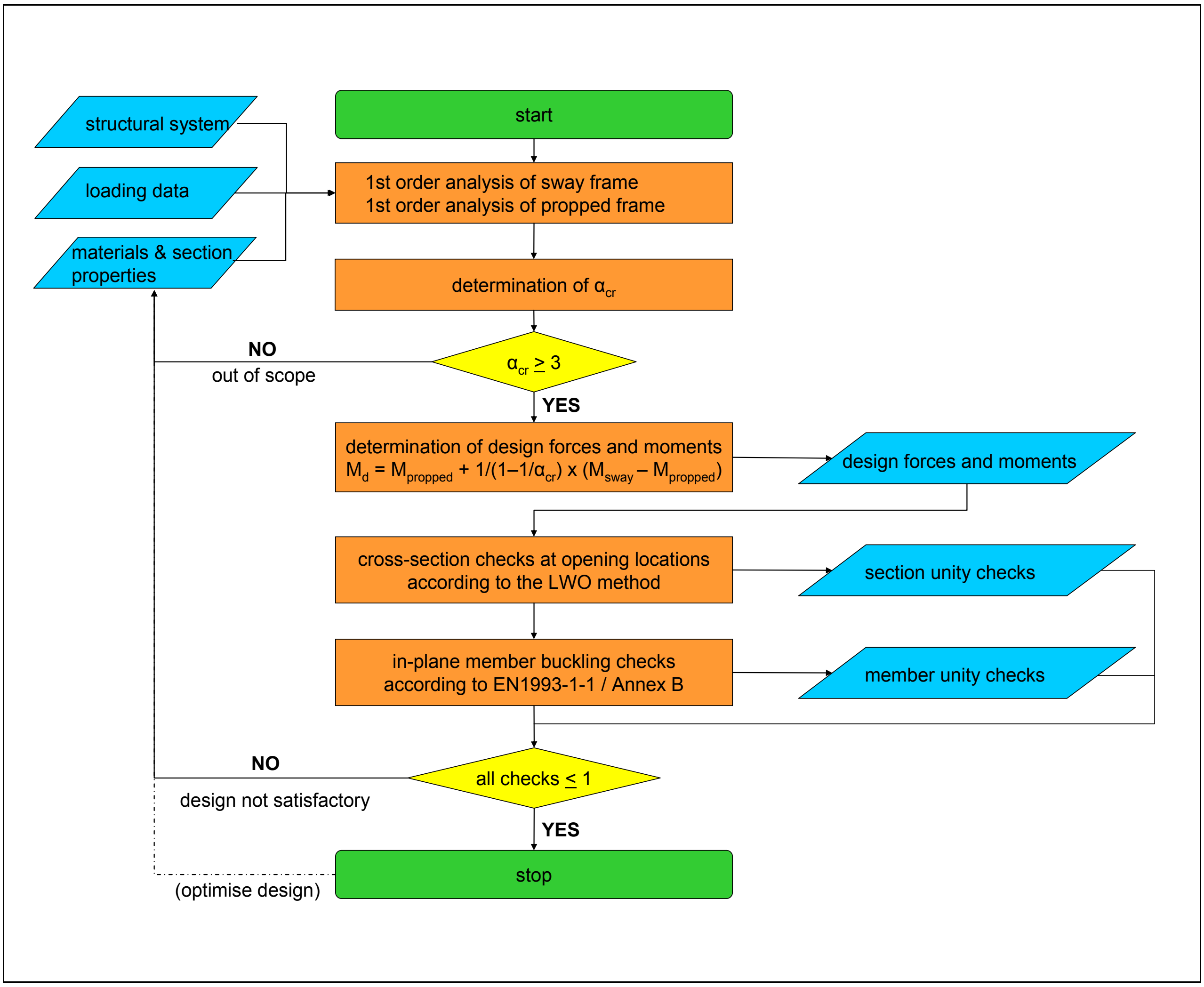
structural system
loading data
materials & section properties
start
1st order analysis of sway frame
1st order analysis of propped frame
determination of α_{cr}
NO
out of scope
$\alpha_{cr} \geq 3$
YES
determination of design forces and moments
$M_d = M_{propped} + 1/(1-1/\alpha_{cr}) \times (M_{sway} - M_{propped})$
design forces and moments
cross-section checks at opening locations according to the LWO method
section unity checks
in-plane member buckling checks according to EN1993-1-1 / Annex B
member unity checks
NO
design not satisfactory
all checks ≤ 1
YES
stop
(optimise design)

Figure 10.3 Flow chart for portal frame design tool in Excel using cellular members

Depending on the type of loading and the moment distribution along the member (either column or rafter), the equivalent moment factor C_{my} is calculated.

As second-order effects already have been accounted for in the global analysis (by means of the amplified sway method), in this stage of the calculation the member is supposed to be non-sway.
Therefore the C_{my} – factor is *calculated* and not just taken equal to 0.9 as given by Table B.3 for members with sway buckling mode *not* susceptible to torsional deformations (so with either sufficient rotational stiffness or lateral restraints).
The braced points are the member ends, in which the rafter is considered as a whole (not separately for the subdivisions).

For each of the four members, these results are also summarised on the output sheet.

Limitations
The analysis has been limited to the in-plane behaviour of symmetrical pitched-roof portal frame structures, whereof the members cross sections are doubly symmetrical as well.
As both out-of-plane flexural buckling and lateral-torsional buckling are no new phenomena for cellular members, and neither fundamentally different from plain-webbed members, no out-of-plane behaviour has been considered. For similar reasons no connection design is included.
These items therefore should be checked separately in real design. In many practical design cases it is easy to provide sufficient restraints to prevent out-of-plane buckling.

10.3 Design using FEA in SAFIR

10.3.1 Introduction

In order to illustrate the application of the LWO method to portal frame structures, a representative example portal frame structure has been analysed for a number of load cases.

The analysis was performed in three ways:

- using the Excel design tool, based on the net section properties with cross-sectional checks according to the LWO method and in-plane member buckling checks according to EN1993-1-1
- using a second-order non-linear in-plane finite element analysis in SAFIR with 2D beam elements, based on a discretation of the net section
- using a second-order non-linear 3D finite element analysis in SAFIR with shell elements, based of the modelled real geometry of the portal frame structure including the web openings as generated by the pre-processor *Mailleur Portique* ("mesh generator for portal frames")

The remainder of this section discusses some details of the finite analyses made in SAFIR.

10.3.2 Second-order non-linear in-plane analysis with 2D beam elements

Just like the finite element analysis implemented in the Excel design tool, the finite element analysis in SAFIR with 2D beam elements is based on the net section properties. The beam element was described in section 7.2.2 already. For the generation of the fibre discretisation of the net cross-section, use is made of a specially developed mesh generator in Excel, see Figure 10.4.
As out-of-plane buckling has been decided to be left out from the case study, only in-plane behaviour is considered.

The material model is elasto-plastic, thus even after a plastic hinge is formed, the frame can sustain a further loading increase (if statically indeterminate).

It is very important to realise here that a finite element analysis can deliver results only *which can be described with the modelled structure* (thus depending on the degrees of freedom). Obviously out-of-plane flexural buckling or lateral-torsional buckling cannot be described by the (non-linear!) finite element analysis with 2D beam elements. However, this also holds for the failure modes Vierendeel bending, web-post shear and web-post buckling!

In the analysis with beam elements, the Bernoulli hypothesis is considered, i.e. cross-sections remain plane under bending moment. This proposition is no longer fulfilled at the location of an opening. Therefore additional to the geometrically and materially non-linear in-plane frame analysis, the mentioned failure mechanisms have to be checked for separately – which is precisely that what is done by the Excel design tool based on the LWO method.

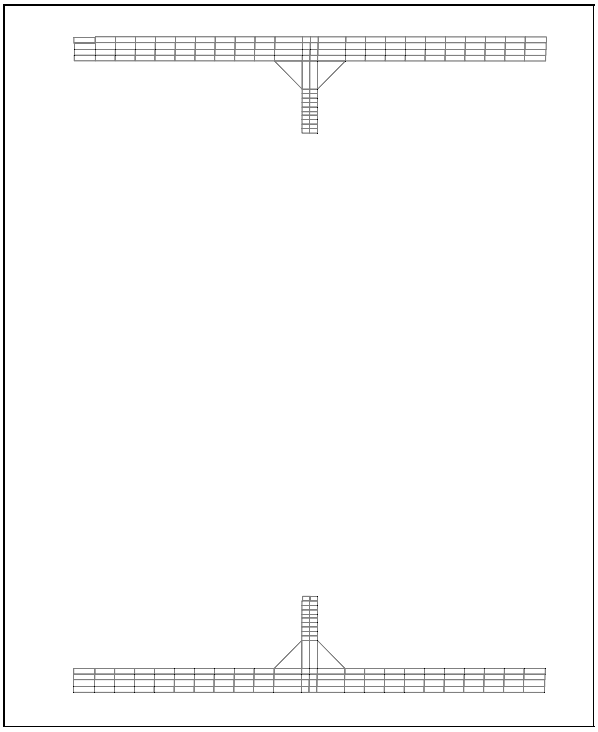

Figure 10.4 Fibre discretisation of the cross-section at an opening position

10.3.3 Second-order non-linear 3D finite element analysis with shell elements

The most 'advanced' analysis where the other results are compared with, is the full three-dimensional finite element analysis of the whole frame modelled with shell elements. The basic geometry has been generated with the pre-processor *Mailleur Portique*, which was developed within the scope of an internal research project of ArcelorMittal. Due to a number of deficiencies in it's implementation (which is still in beta-status), the preparation of the input files before the analysis can be run requires a lot of adaptation by hand (see also section 7.3.3).

The 3D modelling of the structure permits out-of-plane displacements and therefore can describe all possible failure modes. Within the scope of the case study, both flexural buckling and lateral-torsional buckling have been prevented by adding appropriately placed lateral supports to the flanges.

Both geometrically and materially, the analysis is non-linear, with material behaviour modelled according to EN1993-1.

Loads can be applied the easiest to nodes instead of surfaces. Therefore distributed loads have to be translated to point loads.

In section 8.3.2 the modelling of the supports was discussed. Here again fully clamped supports were applied, as these can be modelled more easy and reliable than theoretically pinned supports.

Just like for the other analyses, connection design itself has not been addressed.

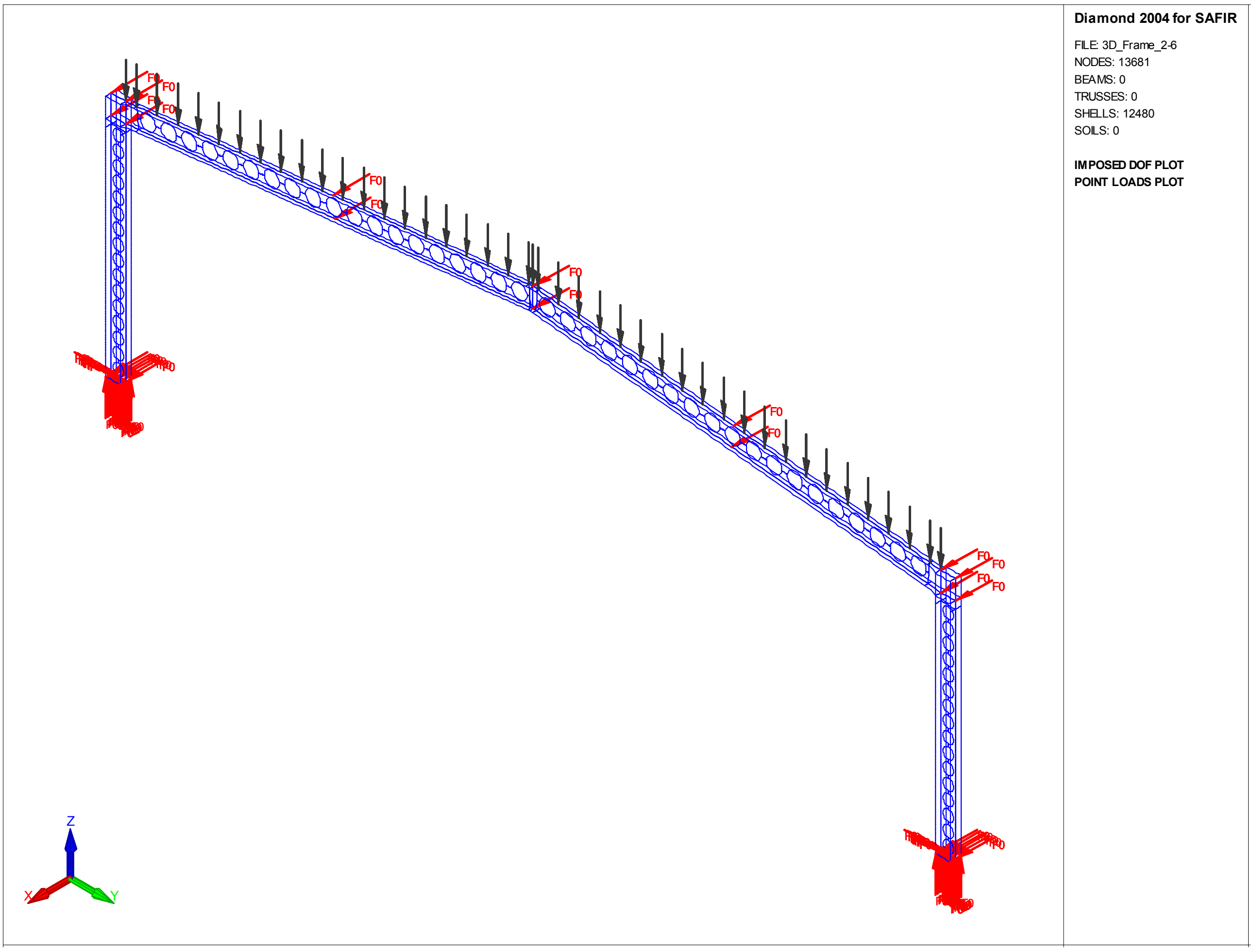

Figure 10.5 Example model of a portal frame with loading and supports; the 'red arrows' indicate restrained displacements

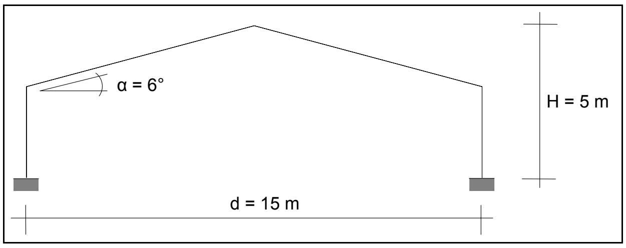

Figure 10.6 Case study: structural system

10.4 Case study

10.4.1 Structural system

The frame considered is described by the following characteristics:

span	d = 15 m
top height	H = 5 m
roof inclination	$\alpha = 6°$

The members have been chosen as:

- columns ACB from HE200A with:
  $H_t = 275;\quad d_0 = 195;\quad s_0 = 50 \quad [\text{mm}]$
- rafters ACB from IPE240 with:
  $H_t = 360;\quad d_0 = 275;\quad s_0 = 100 \quad [\text{mm}]$

The support conditions have been chosen as fully clamped. In practise pinned supports may be encountered more frequently, but in 3D finite element calculations clamped supports are easier to model.
Lateral supports have been added to prevent out-of-plane flexural buckling an lateral-torsional buckling to occur.
Hereafter the results for a number of simplified load cases are discussed and compared.

10.4.2 Load case 1: distributed vertical load

From the analysis with 2D beam elements it follows that failure occurs when the plastic capacity of the rafter at both ends is reached. The frame is able to resist an increase loading, although with reduced stiffness, until another plastic hinge has been formed.

In the analysis with 3D shell elements, the frame responds less stiff than indicated by the 2D analysis. This is due to the fact that the Bernoulli hypothesis does not hold for the member with web holes. The amount of the additional deformation sums up to about 32% in this case! From the graphs of Figure 10.8 it is clear however, that the predicted failure behaviour is almost equal: the same bend is present, though smoother for the 3D analysis.

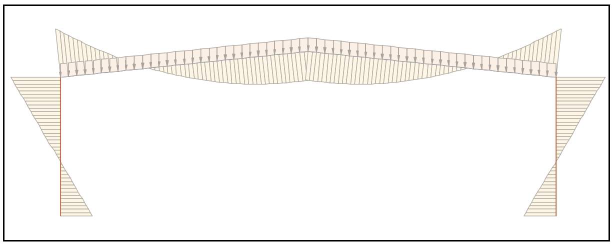

Figure 10.7 LC 1: distributed vertical load

When compared with the results generated by the Excel design tool, it appears that not the pure bending resistance, but rather the Vierendeel bending resistance governs design. For increased load this would also occur at the next openings in the rafter (and subsequently in the columns) if only the bending moment could increase at the eaves.
Failure finally occurs when the web-post shear capacity in the columns in reached, as no redistribution of these forces is possible.

The fact that the Excel design tool predicts a far higher load at which the first plastic hinge in the rafter is formed, is explained by the fact that this tool takes into account that at the position of the eaves there is no opening present. If the properties of the net section were used in the check on the bending moment capacity, then the results would have been equal to the 2D finite element analysis.

The calculated displacements by the Excel tool are equal to those calculated by the 2D finite element analysis – as long as the behaviour is linear-elastic.

It is concluded that the Excel design tool in this case is well able to describe the structural behaviour until the first failure mode occurs. The frame analysis then is still in the elastic range, but plastic section properties may be used for class 2 or better cross-sections.

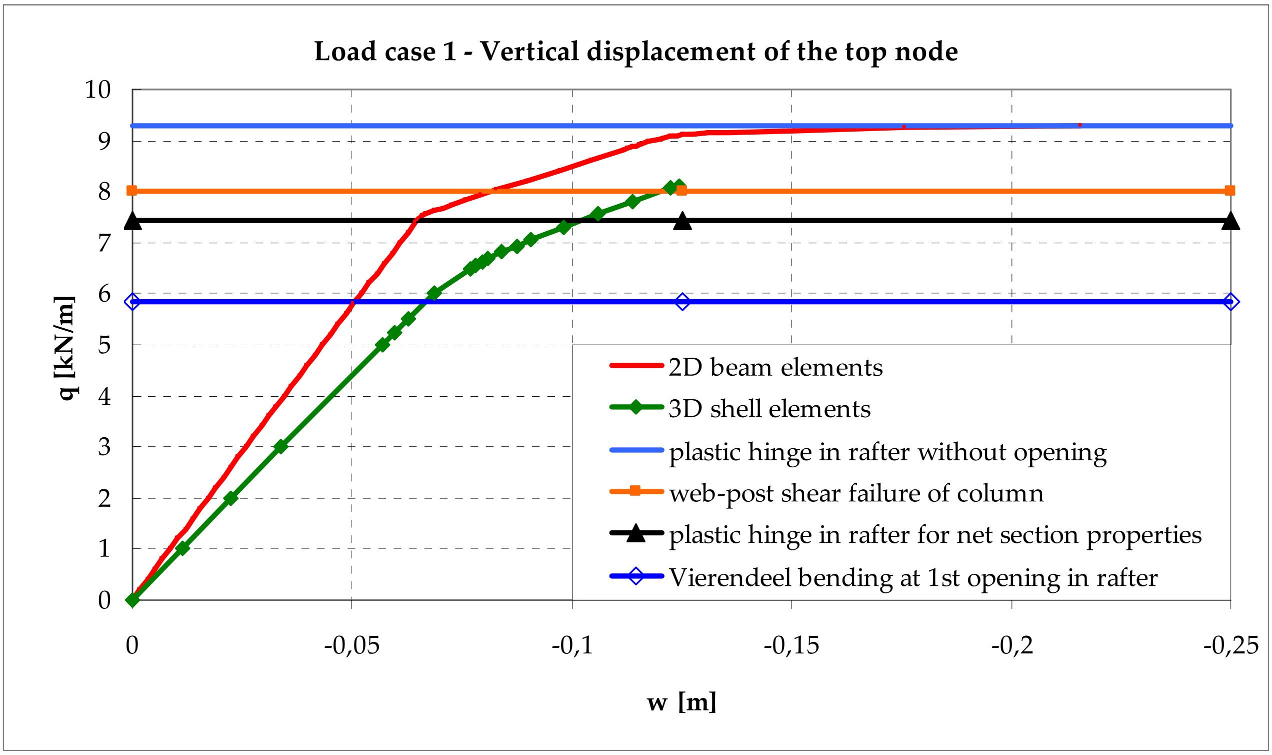

Figure 10.8 Load case 1: Load-displacement graphs for vertical displacement of the top node

10.4.3 Load case 2: horizontal point loads

The second load case is loaded solely by *two equal horizontal point loads F at the eaves,* representing e.g. wind loading.
Again from the 2D finite element analysis with beam elements it follows that failure is caused by plastification of the cross-section, with corresponding loss of stiffness after each plastic hinge that has been formed. In fact, the 2D finite element model can only describe a few failure mechanisms: plastification of the cross-section due to axial load or bending moment and in-plane instability.
This time the maximum moment is located at the support positions, which is therefore the location where the first plastic hinge develops.

Due to the statically indeterminate nature of this portal frame, the load thus can be further increased. According to the 2D finite element model, failure occurs finally when another pair of plastic hinges – allowing for interaction of shear and axial load – is formed at the ends of the rafters – which causes the frame to be kinematically indeterminate, thus initiating collapse of the portal frame.

However, from both the analysis using the Excel design tool and the 3D finite element analysis with shell elements, if follows that before the plastic moment resistance of the column can be reached, the Vierendeel bending resistance at the first opening of the column is exceeded. Afterwards the frame starts to loose stiffness until failure finally occurs due web-post shear.

The displaced structure of the 3D analysis seems to suggest that failure is due to web-post buckling, see Figure 10.11.
From a closer look it yet becomes clear that the web-posts do not displace perpendicular to the web, but the deformation is wholly in-plane, thus due to exceeding the web-post shear resistance.

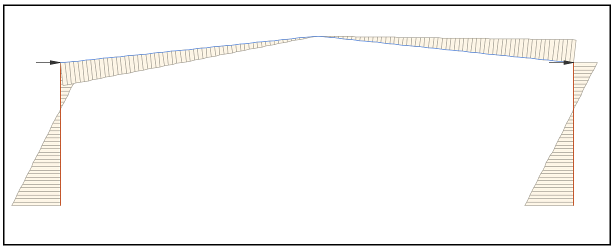

Figure 10.9 LC 2: horizontal point loads

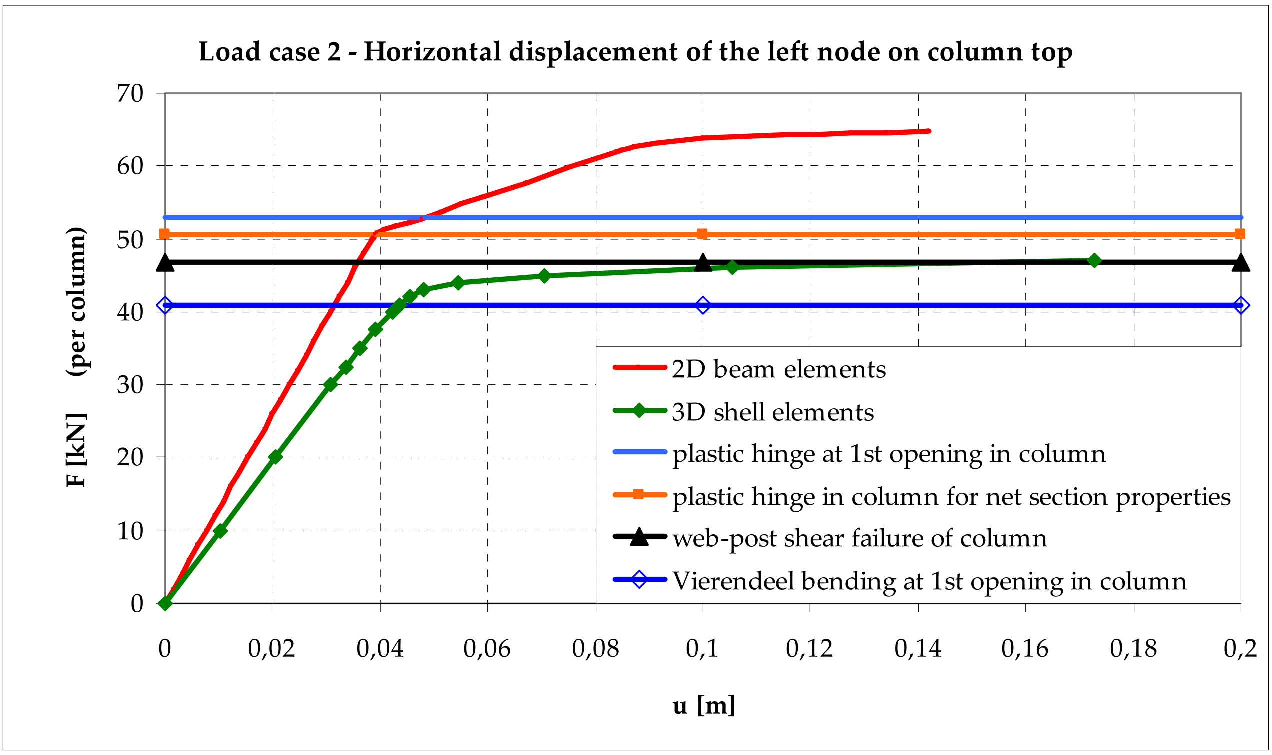

Figure 10.10 Load case 2: Load-displacement graphs for horizontal displacement of left node on column top

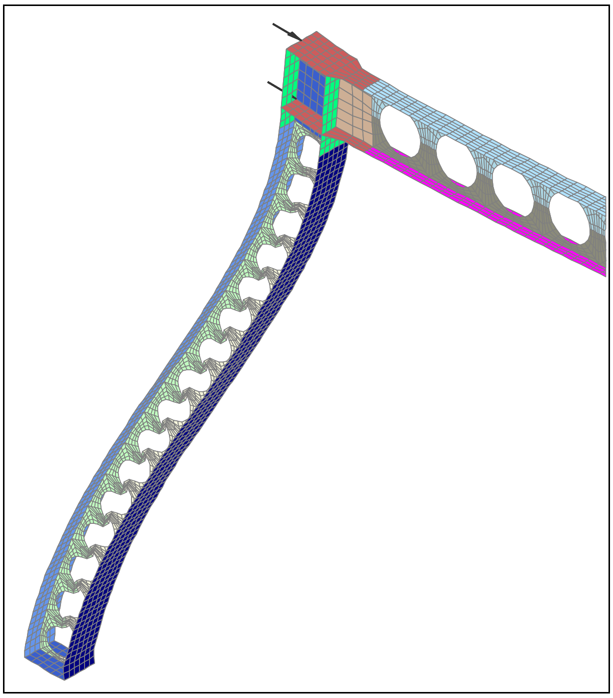

Figure 10.11 Final failure mechanism of load case 2: web-post shear

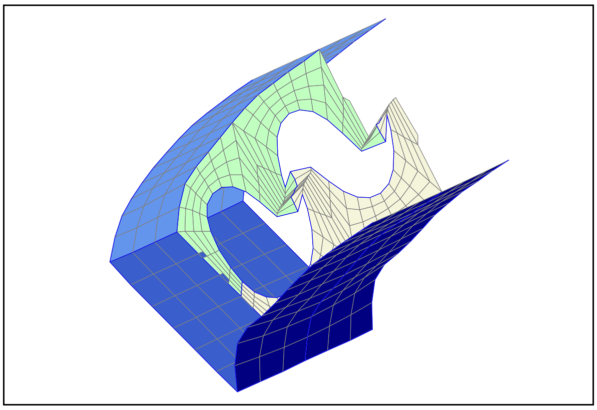

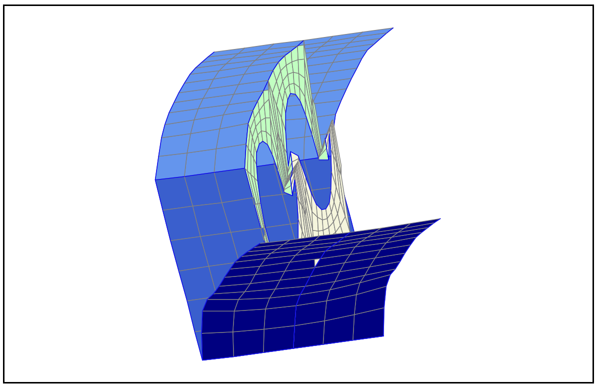

In Figure 10.10 two lines are drawn which indicate the load at which the first plastic hinge is formed calculated by the Excel design tool. The lowest value is obtained if based on the fictitious net section properties, which coincides with the obtained 2D frame result.

However, because the first opening actually is located at some distance from the support, the 'real' load at which the plastic hinge is formed is somewhat higher – thus not at the support position but at the first opening location. This result is given by the second line.

This time again the frame modelled in 3D with shell elements responds less stiff than the 2D frame analysis with beam elements by a percentage of circa 37.5%.

The same conclusion as for load case 1 therefore holds also here, i.e. that the Excel design tool is well able to describe the structural behaviour until the first failure mode occurs, based on a linear-elastic frame analysis.

10.4.4 Load case 3: combination of both vertical and horizontal point load

In the last load case considered, the frame is subjected to a combination of a *vertical point load F* on top of the frame together with a *horizontal point load of double magnitude 2F* acting on top of the left column.

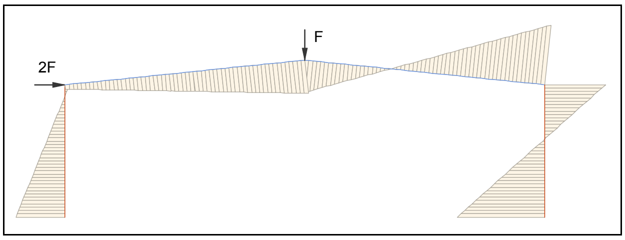

Figure 10.12 LC 3: combination of both vertical and horizontal point load

Due to the asymmetric loading, the maximum bending moment and shear force occurs at the bottom of the right column. The 2D finite element analysis with beam elements therefore predicts that at this position the first plastic hinge will be formed.

From the calculations with the Excel design tool nevertheless is appears that prior to attaining the plastic moment capacity, the additional moments caused by Vierendeel action at the first opening position of the right column limits the design load. The web-post shear capacity is only a little higher – all these checks being based on the load distribution determined by a linear-elastic frame analysis.

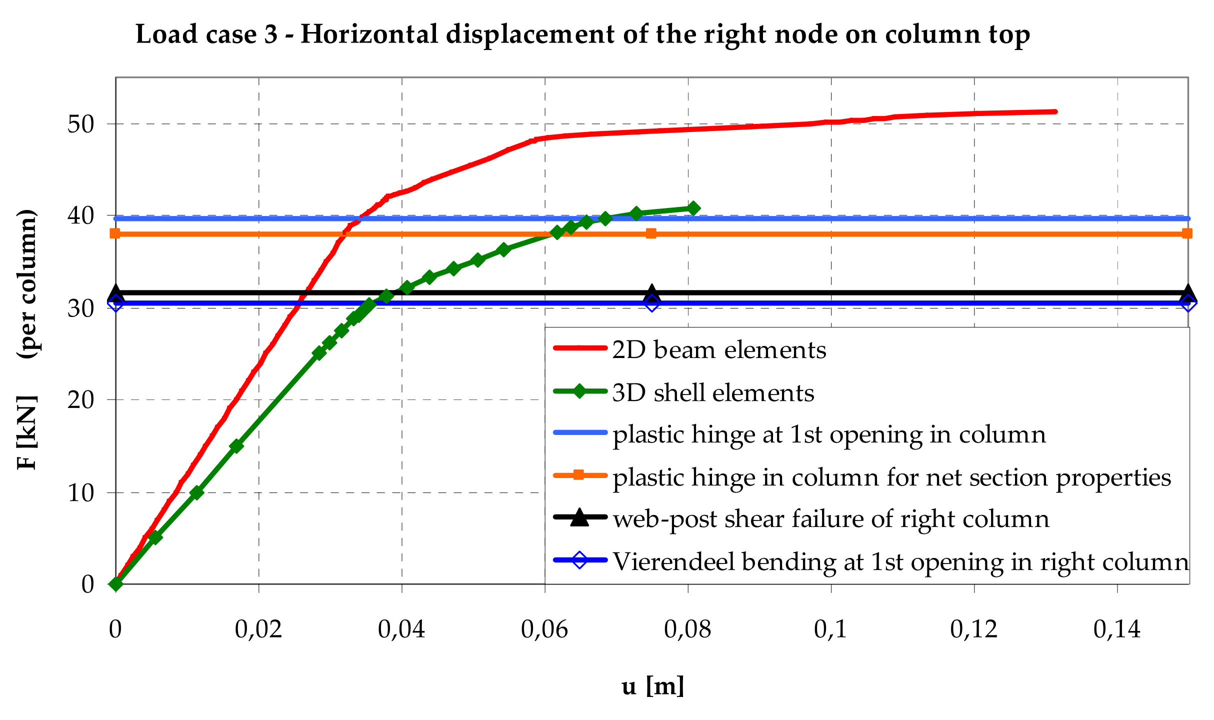

Figure 10.13 Load case 3: Load-displacement graphs for horizontal displacement of right node on column top

The graph depicting the load-displacement behaviour calculating with the 3D finite element analysis – see Figure 10.13 – indeed confirms that the Vierendeel capacity is reached first. However, the load can be increased further, even beyond the web-post shear capacity of the right column.
This is explained by the redistribution of loads that is possible for this statically undeterminate portal frame structure: the left column is able to transmit further horizontal load.

With the Excel design tool it is not possible to further analyse the structural behaviour after the plastic capacity is reached at one location, as the implemented finite element analysis is based on linear elastic behaviour.

Based on the first elastic part of the portal frame response, it appears again that the additional deformation due to the presence of the circular web openings is significant: 39%.

Full details of all analyses have been included on the data-dvd accompanying this report; see also Annex D.

10.5 Conclusion

In this chapter the application of the LWO method for circular beam-columns has been illustrated for a number of load cases. All load cases were analysed by 2D and 3D finite element analyses, and using the Excel design tool specially developed.

It appears that the structural behaviour in the elastic range can be predicted well with this Excel design tool. As the tool is based on a linear-elastic frame analysis, possibly additional load carrying capacity might be present even after the governing ultimate failure load is reached. However, this will be accompanied by increased deformations which often limit the design.

It is noted furthermore that the calculated Vierendeel bending capacity does not allow for the possible redistribution of the shear force over the bottom and top tee.

In many cases Vierendeel action appeared to be the governing failure load, even before the plastic moment capacity of the net section is reached. Therefore it may be considered to fill one or more openings at the position of high shear force and/or bending moment. The modelling of these filled openings is however not included in the present beta-version of the pre-processor *Mailleur Portique*.

From the comparison with 3D finite element analyses with shell elements, it is illustrated that the Excel design tool really gives the lowest ultimate failure load, so the design tool delivers safe results.

While the ultimate load predictions are rather accurate, the calculated values of the displacements based on the net section properties overestimate the stiffness of the portal frame.
In the present case study, it appeared that due to 'shear deformation' of the members, an additional displacement component of 30-40% must be added to the calculated values.
This value is higher than usually encountered in beam structures and therefore might need further research.

11 CONCLUSIONS AND RECOMMENDATIONS

11.1 Introduction

The present chapter summarizes the most important conclusions that are drawn from the research work performed, and gives recommendations for further research.

11.2 Conclusions

The main conclusions are listed hereafter.

- At present two design methods exists for the design of cellular *beams*:
    1. LWO design method, as developed in the RFCS-project *Large web openings for service integration in composite floors*, offers an detailed procedure for the design of beams with web openings, that is consistent with the Eurocodes.
       The method of analysis is based on calculating the additional effects caused by the presence of web openings by means of an effective opening length approach for Vierendeel bending.
       Web-post buckling is accounted for by means of a simplified compressed strut model.
    2. The ACB program by ArcelorMittal forms an convenient way to analyse cellular beams.
       In this method, Vierendeel bending is checked for by means of an analysis of an inclined section at regular angle increments.
       For the capacity check on web-post buckling, a more advanced model has been set up using data from an extensive test program.
- In-depth analysis of cellular beams can be performed conveniently by the finite element software *SAFIR* (using plane shell elements), in combination with the pre-processor *Crystal Pro* (which implies an initial imperfection along the beam length and the web-post height in order to initiate web-post buckling).

Global buckling behaviour

- From an extensive parameter study using finite element analysis it has been shown that the global buckling behaviour of cellular *columns* is similar to that of plain-webbed columns.
- An simplified design rule has been proposed for checking the ultimate flexural buckling load capacity of cellular columns, based on the *net section* properties. This design rule has been shown to be safe, though sometimes conservative.

Web-post buckling behaviour

- Both mentioned design models do not purposely include the influence of the presence of an axial load on the web-post buckling capacity of cellular members.
- From the parameter study performed, it follows however that there exists an approximately linear relation between the web-post buckling capacity and an applied axial force.
- In all cases the LWO model predicts an lower (thus safe) ultimate capacity than the calculated FEM results. The governing equation of the ACB model is more conservative in all cases.
- Although the influence of axial force is not (effectively) accounted for in both design models, these models still return valid results in the range of sections investigated. Both existing models therefore can be applied safely.

- Cellular *columns* therefore can be analysed similar to cellular beams, but with an *modified flexural buckling check*.

- For use of cellular members in *portal frame structures*, an Excel tool using Visual Basic for Applications has been developed which enables the quick design of a complete portal frame structure for different support and loading conditions. It automatically takes initial imperfections and second-order effects into consideration and is able to check both cross-sections and web-post buckling according to the LWO method. Furthermore flexural buckling of members is checked for according to the proposed design rule.
- From a comparison with 3D FEM calculations it follows that the structural behaviour until the first failure occurs can be predicted well with the Excel tool developed.
- While the failure behaviour itself is similar, a significant *difference in stiffness* between the 2D model based on elementary beam theory (using reduced section properties because of the openings) and the 3D model with shell elements has been observed.

11.3 Recommendations

On basis of the research performed, the following recommendations are given for further research.

- Perform an in-depth market study to identify any constraints on the application of cellular beams in the current building practise.
- Prepare guidance manuals and software for the design of cellular beam-columns, targeted at the local situation (at a national level).

- Extend the LWO model for web-post buckling to also include the effect of an applied axial force.
- Finish the beta version of the pre-processor *Mailleur Portiques*, with special attention to easy modelling supports and initial imperfections.

- Further investigate how to model pinned supports in 3D finite element models with shell elements.
- Investigate global buckling behaviour of cellular columns when loaded both in bending and by axial load.
- Further investigate the reduction in stiffness due to the presence of web-openings.
- Extend the investigation to include the behaviour in fire conditions, or when using asymmetrical sections, or considering composite action between the steel beam and the concrete slab.

REFERENCES

Brochures

ACB 2006	*Arcelor Cellular Beams – The intelligent solution for long spans.* Arcelor Commercial Sections S.A, Luxembourg. Edition 2006-1.
BmS 2002	*Brandveilige verdiepingbouw met staal.* Bouwen met Staal, Rotterdam. 2002.

Software

ACB program	*ARCELOR Cellular Beams v2.31.* Developed by Centre Technique Industriel de la Construction Metallique. October 2005.
ACB DTD	*ARCELOR Cellular Beams – Detailed Technical Description.* Developed by Centre Technique Industriel de la Construction Metallique. Version 2.31. May 2006.
Crystal Pro	Franssen, J.M. and Majkut, S. *User's manual for CRYSTAL_PRO – A computer program building data files for the analysis of ARBED Cellular Beams with SAFIR 2004*. University of Liège. September 2004.
Crystal Interface	Majkut, S. and Pintea, D.I. *Crystal_Interface v1.5.3.* University of Liège. Build: 20-9-2006.
LTBEAM	Galéa, Y. *Lateral torsional buckling of beams*. CTICM. Version 1.0.7. 2002. Partly funded by ECSC (developed in the frame of the LTB research project).
SAFIR Manual	Franssen, J.M., Kodur, V.K.R. and Mason, J. *User's manual for SAFIR 2004 – A computer program for analysis of structures subjected to fire.* University of Liège. March 2005.
SAFIR Theory	Franssen, J.M., Kodur, V.K.R. and Mason, J. *Elements of theory for SAFIR 2002 – A computer program for analysis of structures subjected to the fire.* University of Liège. Augustus 2002.

Standards

Eurocodes

EN1991-1-1	Eurocode 1: Actions on structures – *Part 1-1: General actions – Densities, self-weight, imposed loads for buildings*. CEN – European Committee for Standardization. April 2002.

EN1991-1-3	Eurocode 1: Actions on structures – *Part 1-3: General actions – Snow loads*. CEN – European Committee for Standardization. July 2005.
EN1991-1-4	Eurocode 1: Actions on structures – *Part 1-4: General actions – Wind actions*. CEN – European Committee for Standardization. April 2005.
ENV1993-1-1	Eurocode 3: Design of steel structures – *Part 1-1: General rules and rules for buildings*. CEN – European Committee for Standardization. April1992.
Annex N	Eurocode 3: Design of steel structures – *Part 1-1: General rules and rules for buildings. Amendment A2: Annex N* – Openings in webs (draft). British Standards Institution. 1993.
EN1993-1-1	Eurocode 3: Design of steel structures – *Part 1-1: General rules and rules for buildings*. CEN – European Committee for Standardization. May 2005.
EN1993-1-5	Eurocode 3: Design of steel structures – *Part 1-5: Plated structural elements.* CEN – European Committee for Standardization. October 2006.
NEN-EN1993-1-1/NB	Eurocode 3: Design of steel structures – *Part 1-1: General rules and rules for buildings*. National Annex (Dutch: Nationale Bijlage). Nederlands Normalisatie Instituut. December 2006.

TGB1990 series (Dutch Standards)

Building Decree 2003	Building Decree (Dutch: Bouwbesluit 2003). Implementation regulation to the Dutch Housing Act. 2003.
NEN6702	Technical principles for building structures - TGB 1990 - Loadings and deformations (Dutch: Technische grondslagen voor bouwconstructies - TGB 1990 - Belastingen en vervormingen). Nederlands Normalisatie Instituut. 2007.
NEN6770	TGB 1990 - Steel structures - Basic requirements and basic rules for calculation of predominant statically loaded structures (Dutch: Staalconstructies. Basiseisen en basisrekenregels voor overwegend statisch belaste constructies). Nederlands Normalisatie Instituut. 1997 + A1, 2001.
NEN6771	TGB 1990 - Steel structures - Stability (Dutch: Staalconstructies. Stabiliteit). Nederlands Normalisatie Instituut. 2000 + A1, 2001.

Other standards

Hong Kong Steel Code	Code of Practice for the Structural Use of Steel. Buildings Department Hong Kong. August 2005.

Access Steel resources

SF002	*Flow chart: Frame analysis.* Approved 17/07/06.
SF020	*Flow chart: Elastic analysis of a portal frame.* Approved 25/07/06.
SN003	*NCCI: Elastic critical moment for lateral torsional buckling.* Approved 21/04/06.
SN019	*NCCI: Design rules for web openings in beams.* Approved 12/07/06.
SN032	*NCCI: General method for out-of-plane buckling in portal frames.* Approved 11/07/06.
SN033	*NCCI: Simple methods for second order effects in portal frames.* Approved 08/07/06.
SS005	*Scheme development - Service integration in buildings.* Approved
SS015	*Scheme development: Web openings in beams in multi-storey buildings.* Approved 26/04/06.
SX016	*Example: Determination of loads on a building envelope.* Approved 11/07/06.
SX029	*Example: Elastic design of a single bay portal frame.* Approved 18/09/06.

Books and reports

PhD Kerdal	Kerdal, D. *Lateral-torsional buckling strength of castellated beams*. Dissertation. University of Sheffield. November 1982.
Handbook castellated beams	Das, P.K. and Srimani, S.L. *Handbook for the design of castellated beams.* A.A. Balkema, Rotterdam. 1985.
CIRIA/SCI P068	Lawson, R.M. *Design for openings in the webs of composite beams.* CIRIA Special Publication and SCI Publication 068. CIRIA/The Steel Construction Institute. 1987.
SCI P100	Ward, J.K. *Design of composite and non-composite cellular beams.* SCI Publication P100. The Steel Construction Institute, UK. 1990.

Darwin 1990	Darwin, D. *Steel and Composite Beams with Web Openings*. Steel design guide series no. 2. American Institute of Steel Construction. Chicago, IL, USA. 1990.
FABSEC Design Guide	*Design of FABSEC Cellular Beams in non-composite and composite applications. For both normal temperature and fire engineering conditions.* Prepared for FABSEC by The Steel Construction Institute. Revised April 2006.
UMIST	*Indicative fire test on a cellular and a solid web steel beam.* Manchester Centre for Civil and Structural Engineering, UMIST. May 2003.
LTB	*Lateral torsional buckling in steel and composite beams.* Final report for ECSC Research Contract 7210-PR-183. 2002.
LWO	*Large web openings for service integrations in composite floors.* Final report for ECSC Research Contract 7210-PR-315. 2003.
LWO+	*Large web openings for service integrations in composite floors.* Final report for ECSC Research Contract RFS-CT-2005-00037. 2006.
	This project is a follow-up on the LWO project, and aims to promote the knowledge gained to a wider audience, especially to practitioners.
MSA	McGuire, W., Gallagher, R.H. and Ziemian, R.D. *Matrix Structural Analysis*, 2nd Edition, John Wiley & Sons, Inc. 2000.
EC3 Designers' Guide	Gardner, L. and Nethercot, D.A. *Designers' guide to EN1993-1-1 Eurocode 3: Design of steel structures. General rules and rules for buildings.* Thomas Telford Publishing. 2005.
Thesis Rini	Rini, D.T. *Critical behaviour of long span cellular beams in fire.* MSc Thesis. University of Maryland. 2006.
SCI RT1085	Newman, G. and Simms, W.I. *Guidance on the use of intumescent coatings for the fire protections of beams with web openings.* SCI RT1085v04. The Steel Construction Institute, UK. March 2007.
Vibration Guide	Feldmann, M., Heinemeyer, Ch. and Völling, B. *Design guide for floor vibrations.* RWTH Aachen University. Prepared for ArcelorMittal. 2007.
ECCS-TC8-2006-015	Snijder, B., Greiner, R. and Jaspart, J.-P. *Field and limits of the General Method.* ECCS TC8 Stability, Reportnr. ECCS-TC8-2006-015. 2006.
BmS Constr A	Man, G. de. (samenst.) and Eldik, C.H. van (red.) *Overspannend staal – Deel 2 Construeren A*. Bouwen met Staal, Rotterdam, The Netherlands. 2001.

Scientific articles

Gibson & Jenkins 1957	Gibson, J.E. and Jenkins, W.M. *An investigation of the stresses and deflections in castellated beams.* The Structural Engineer, Vol. 35, No. 12. 1957
Toprac & Cooke 1959	Toprac, A.A. and Cooke, B.R. *An experimental investigation of open-web beams.* Welding Research Council Bulletin Series, No. 47. February 1959.
Kolosowski 1964	Kolosowski, J. *Stresses and deflexions in castellated beams.* The Structural Engineer; Vol. 42, No. 1. 1964.
Halleux 1967	Halleux, P. *Limit analysis of castellated steel beams.* Acier-Stahl-Steel, Vol. 32, No. 3. March 1967.
Redwood 1973	Redwood, R.G. *Design of beams with web holes*. Canadian Steel Industries Construction Council, 1973.
Stahlbau 1970s	Schweizerische Zentralstelle für Stahlbau. *Bauen in Stahl*. Zürich. 1974. Nos. 1-8, 1975: Nos. 16-18, 1976: No. 23, 1977: No. 31, 1978: Nos. 32-33. Cited in Redwood 2000.
Horne 1975	Horne, M.R. *An approximate method for calculating the elastic critical loads of multi-storey plane frames*. The Structural Engineer, Vol. 53, No. 6. 1975.
Uenoyo & Redwood 1977	Uenoyo, M. & Redwood, R.G. *Buckling of webs with openings.* Computers & Structures, Vol. 9, No. 2. 1978.
Nethercot & Kerdal 1982	Nethercot, D.A. and Kerdal, D. *Lateral-torsional buckling of castellated beams.* The Structural Engineer, Vol. 60B, No. 3. 1982.
Kerdal & Nethercot 1984	Kerdal, D. and Nethercot, D.A. *Failure modes of castellated beams* Journal of Constructional Steel Research, No. 4. 1984.
Thevendran & Shanmugam 1990	Thevendran, V. and Shanmugam, N.E. *Lateral buckling of doubly symmetric beams containing openings.* Journal of Engineering Mechanics, Vol. 117, No. 19. 1990.
ASCE 1992	ASCE Task Committee on Design Criteria for Concrete Structures in Steel and Concrete. *Proposed Specification for Structural Steel Beams with Web Openings*. Journal of Structural Engineering, Vol. 118, No. 12. December 1992.
Zaarour & Redwood 1996	Zaarour, W. and Redwood, R. *Web buckling in thin-webbed castellated beams.* Journal of Structural Engineering. Vol. 122, No. 8. 1996.
Redwood & Demirdjian 1998	Redwood, R. and Demirdjian, S. *Castellated beam web buckling in shear.* Journal of Structural Engineering, Vol. 124, No. 10. 1998.
Redwood & Cho 1993	Redwood, R.G. and Cho, S.H. *Design of steel and composite beams with web openings*. Journal of Constructional Steel Research, No. 25. 1993.

Darwin 2000	Darwin, D. *Design of composite beams with web openings.* Progress in Structural Engineering and Materials, Vol. 2, No. 2. 2002.
Redwood 2000	Redwood, R.G. *Behaviour of composite castellated beams.* Progress in Structural Engineering and Materials, Vol. 2, No. 2. 2002.
Chung & Lawson 2001	Chung, K.F. and Lawson, R.M. *Simplified design of composite beams with large web openings to Eurocode 4*. Journal of Constructional Steel Research, No. 57. 2001.
Chung *et al* 2001	Chung, K.F., Liu, T.C.H. and Ko, A.C.H. *Investigation on Vierendeel mechanism in steel beams with circular web openings*. Journal of Constructional Steel Research, No. 57. 2001.
Chung 2002	Chung, K.F. *Composite beams and floor systems fully integrated with building services.* Progress in Structural Engineering and Materials, Vol. 4, No. 2. 2002. doi:10.1002/pse.116.
Ko & Chung 2002	Ko, C.H. & Chung, K.F. *A review of recent developments on design of perforated beams.* Advances in Steel Structures, Vol. 1. 2002.
TN 2002	Technical Note. *Fire engineering of cellular beams using intumescent coatings.* The Structural Engineer. 1 October 2002.
King 2003	King, C.M. *Improved economy of Eurocode 3 for portal frames – Draft for consultation*. The Steel Construction Institute. 2003. Cited in Lim *et al* 2005.
Liu & Chung 2003	Liu, T.C.H. and Chung, K.F. *Steel beams with large web openings of various shapes and sizes: finite element investigation.* Journal of Constructional Steel Research, No. 59. 2003.
Chung *et al* 2003	Chung, K.F. Liu, C.H. and Ko, A.C.H. *Steel beams with large web openings of various shapes and sizes: an empirical design method using a generalised moment-shear interaction curve*. Journal of Constructional Steel Research, No. 59. 2003.
Gonçalves & Camotim 2004	Gonçalves, R. and Camotim, D. *On the application of beam-column interaction formulae to steel members with arbitrary loading and support conditions.* Journal of Constructional Steel Research, No. 60. 2004. doi: 10.1016/S0143-974X(03)00122-6
Franssen *et al* 2004	Franssen, J.M., Gens, F., Vassart, O. and Cajot, L.G., *Dynamic approach of structural fire calculation with FEM software.* 5th International Conference on Performance-Based Codes and Fire Safety Design Methods. Luxembourg 2004.
Maljaars *et al* 2004	Maljaars, J., Stark, J.W.B. and Steenbergen, H.M.G.M. *Buckling of coped steel beams and steel beams with partial endplate.* HERON, Vol. 49, No. 3. 2004.
Bailey 2004	Bailey, C. *Indicative fire tests to investigate the behaviour of cellular beams protected with intumescent coatings.* Fire Safety Journal; Vol. 39, No. 8. 2004. doi:10.1016/j.firesaf.2004.06.007

Nethercot & Gardner 2005	Nethercot, D.A. and Gardner, L. *The EC3 approach to the design of columns, beams and beam-columns.* Steel and Composite Structures, Vol. 5, No. 2-3. 2005.
Lawson & Hicks 2005	Lawson, R.M. and Hicks, S.J. *Developments in composite construction and cellular beams.* Steel and Composite Structures, Vol. 5, No. 2-3. 2005.
Lim *et al* 2005	Lim, J.B.P, King, C.M., Rathbone, A.J., Davies, J.M. and Edmondson, V. *Eurocode 3 and the in-plane stability of portal frames.* The Structural Engineer, Vol. 83, No. 21. 2005.
Talamona & Franssen 2005	Talamona, D. and Franssen, J.M. *A quadrangular shell finite element for concrete and steel structures subjected to fire.* Journal of Fire Protection Engineering, Vol. 15, No. 4. 2005. doi: 10.1177/1042391505052769
Lawson *et al* 2006	Lawson, R.M., Lim, J., Hicks, S.J. and Simms, W.I. *Design of composite asymmetric cellular beams and beams with large web openings.* Journal of Constructional Steel Research, No. 62. 2006.
Nadjai *et al* 2007	Nadjai, A., Vassart, O., Ali, F., Talamona, D., Allam, A. and Hawes, M. *Performance of cellular composite floor beams at elevated temperatures.* Fire Safety Journal, Vol. 42, No. 6-7. 2007. doi:10.1016/j.firesaf.2007.05.001
Franssen 2007	Franssen, J.M. *Modeling the behavior of structures – Current capabilities and future trends.* Presentation held at the National Workshop on Structures in Fire. East Lansing, 10-12 June 2007.

Websites

www.arcelor.com/sections

Arcelor Commercial Sections S.A.

www.bouwtechniek.nl

IBT Ingenieurs in Bouwtechniek

www.iicbm.org

International Institute of Cellular Beam Manufacturers

lwo.steel-sci.org

Website of the RFCS funded project: Large Web Openings for Service Integration in Composite Floors (ECSC 7210-PR-315).

www.access-steel.com

Website with supporting documentation to the use of the upcoming Eurocodes for steel construction.

ANNEXES

A EUROPEAN STANDARDS

A.1 Introduction

The Eurocodes result from an action programme by the Commission of the European Community, whereof the twofold objective was to eliminate technical obstacles to trade and to harmonize the technical specifications. Now, more than 30 years later, through the intermediate phase of publication of the ENV-pre-standards, most of the final EN-versions have been published.

The Eurocodes are expected to come into force within a few years and then will coexist for a limited period of time together with the national standards. Following the final withdrawal of these national standards, all structural designs have to comply with the Eurocodes. Table A.1 gives an overview of the standards from the structural Eurocode programme that are of particular relevance for the design of steel structures consisting of (or containing) cellular members.

A general property of the European standards is that they provide common structural design rules for everyday use for the design of whole structures and component products.

As a consequence, for unusual forms of construction or design conditions that are not specifically covered, additional expert consideration will be required by the designer.

Cellular members are a typical example of such a case. As already mentioned in chapter 2, a draft annex, Annex N, to the pre-standard ENV1993-1-1 was prepared that addressed the design for (single) web openings, but this was not converted to the final version in order to limit its volume.

Furthermore the underlying philosophy of the Eurocodes is to give the general principles and basic design rules, and not to provide detailed receipts for structural analysis of all kinds of structures – which is regarded as 'textbook-material' by some of the participating countries.

Because the current project concerns the research into the behaviour of steel cellular beam-columns, no further attention is paid to Eurocodes 0 and 1. The next sections provide an overview of the structure and contents of Part 1-1 and Part 1-5 of Eurocode 3.

Table A.1 Overview of the relevant parts of the Eurocode programme

Main package	Relevant parts	Abbreviation
Eurocode (0): Basis of structural design	Not subdivided	EN1990
Eurocode 1: Actions on structures	Part 1-1: General actions – Densities, self-weight, imposed loads for buildings	EN1991-1-1
	Part 1-3: General actions – Snow loads	EN1991-1-3
	Part 1-4: General actions – Wind actions	EN1991-1-4
Eurocode 3: Design of steel structures	Part 1-1: General rules and rules for buildings	EN1991-1-1
	Part 1-5: Plated structural elements	EN1991-1-5
(pre-standard)	Part 1-1: General rules and rules for buildings	ENV1993-1-1
	Annex N: Openings in webs (draft Amendment A2)	Annex N

A.2 Eurocode 3: Part 1-1

Part 1-1 of Eurocode 3 gives basic design rules for steel structures with material thicknesses $t \geq 3$ mm, made of low alloy structural steels. After a foreword and a general first section, additional clauses to the basis of design given in EN1990 are provided in Section 2.
Section 3 deals with material properties and Section 4 gives general rules for durability.
Section 5 applies to structures in which the members can be modelled with sufficient accuracy as line elements for global analysis. It gives rules and limits for the application of the different means of global analysis (first-order or second-order, elastic or plastic) and provides both member and frame (equivalent) imperfections to take into account.
Furthermore the classification of cross-sections is introduced and the limits are given for the assignment of cross-sections into the different classes.
The largest section by far is Section 6 which gives detailed rules for the ultimate limit state design of cross-sections and members. This section covers the resistance of cross-sections, the buckling resistance of members and uniform built-up compression members.
Although rules are provided for checking the resistance against various kinds of buckling, Eurocode 3 does normally not provide design expressions for buckling resistances (normal force or moment), thus leaving the designer at his own. Section 6 also provides a general method for lateral and lateral-torsional buckling of members and frames, which is to be discussed hereafter.
Finally Section 7 deals with serviceability limit states, referring to EN1990.
The informative annexes A and B give interaction factors for the so-called Methods 1 and 2. These interaction factors are used to check members under coexisting normal forces and moments between points of appropriate restraint.
The two methods were developed separately by research teams of different countries and originate from two different approaches to the beam-column interaction problem [EC3 Designers' Guide]:

- Method 1 takes it starting point in the elastic resistance including buckling effects and enhances it by taking account of partial plastification, while
- Method 2 takes the plastic resistance as the basic reference, and reduces it to allow for instability effects.

The *National Annex* may give a choice for one of these methods. The Dutch annex indeed specifies that Method 2 shall be used, and not Method 1, thus making Annex B normative while it prohibits the use of Annex A [NEN-EN1993-1-1/NB] (Dutch: *Nationale Bijlage*).
The informative Annex AB gives some additional design provisions and Annex BB, which is also informative, gives information about buckling of components of buildings structures.

A.3 Eurocode 3: Part 1-5

Part 1-5 of Eurocode 3 gives design requirements of stiffened and unstiffened plates subjected to in-plane forces. It covers effects due to shear lag, in-plane load introduction and plate buckling for I-section girders and box girders. Furthermore it covers plated structural components subject to in-plane load. Out-of-plane loading effects are explicitly excluded from the scope of the document.
In line with the other Eurocodes, Section 2 gives a basis for the design and modelling. It states that effective width models may be used to include the effects of shear lag and of plate buckling. As an alternative, the reduced stress method may be used. The models are applicable to (nearly) rectangular panels of uniform members with parallel flanges, whereof the diameter of the cut outs is less than 5 percent of the width of the panel. For non-uniform members, the calculation may be performed by means of a finite element analysis. Also, basic rules are provided for members with corrugated webs.

Section 3 deals with shear lag in member design and Section 4 give rules to account for plate buckling effects. Effective widths and cross-section areas are given, together with verification rules.

Section 5 covers the calculation of the shear buckling resistance of plates, and Section 6 gives rules for determining the design resistance to transverse forces.

Then Section 7 gives interaction rules for assessing the combined effect of shear force or transverse force, bending moment and axial force.

Section 8 gives criteria which should be met to prevent flange induced buckling and in Section 9 the design of stiffeners is dealt with.

Finally Section 10 presents the reduced stress method to determine stress limits, as an alternative to the effective width method.

The annexes comprise four informative annexes and one normative annex.

In Annex A expressions are provided of critical stresses for stiffened plates.

Annex B deals with to non-uniform members. It states that the rules in Section 10 (reduced stress method) also apply to the webs of members with non-parallel flanges and to webs with regular or irregular openings and non-orthogonal stiffeners.

For the determination of the critical load multipliers, use may be made of finite element methods. Annex C gives guidance on this use (and also on other uses).

Annex D covers design rules for I-shaped plate girders with corrugated webs.

Annex E, which is the only normative annex, provides alternative methods for determining effective cross-sections.

B FEM RESULTS OF PARAMETER STUDY INTO GLOBAL BUCKLING

B.1 Introduction

This Annex presents the results of the parameter study into the global buckling behaviour of cellular members loaded by a compressive axial force, both in graphical and tabulated form.
The graphs show the displacement of the *top node at half-span* with respect to the applied axial force. As the members are forced to deform symmetrically, this single displacement is a reasonable measure of the element's behaviour. These results have been discussed in Chapter 8.
For all cases at least three values for slenderness (in both directions) were considered, i.e. $\bar{\lambda}=0.2$, $\bar{\lambda}=0.6$ and $\bar{\lambda}=1.4$. The results of some additional analyses are also presented in this Annex.

B.2 Base profile IPE140

B.2.1 Buckling about the weak axis

Slenderness 0.2

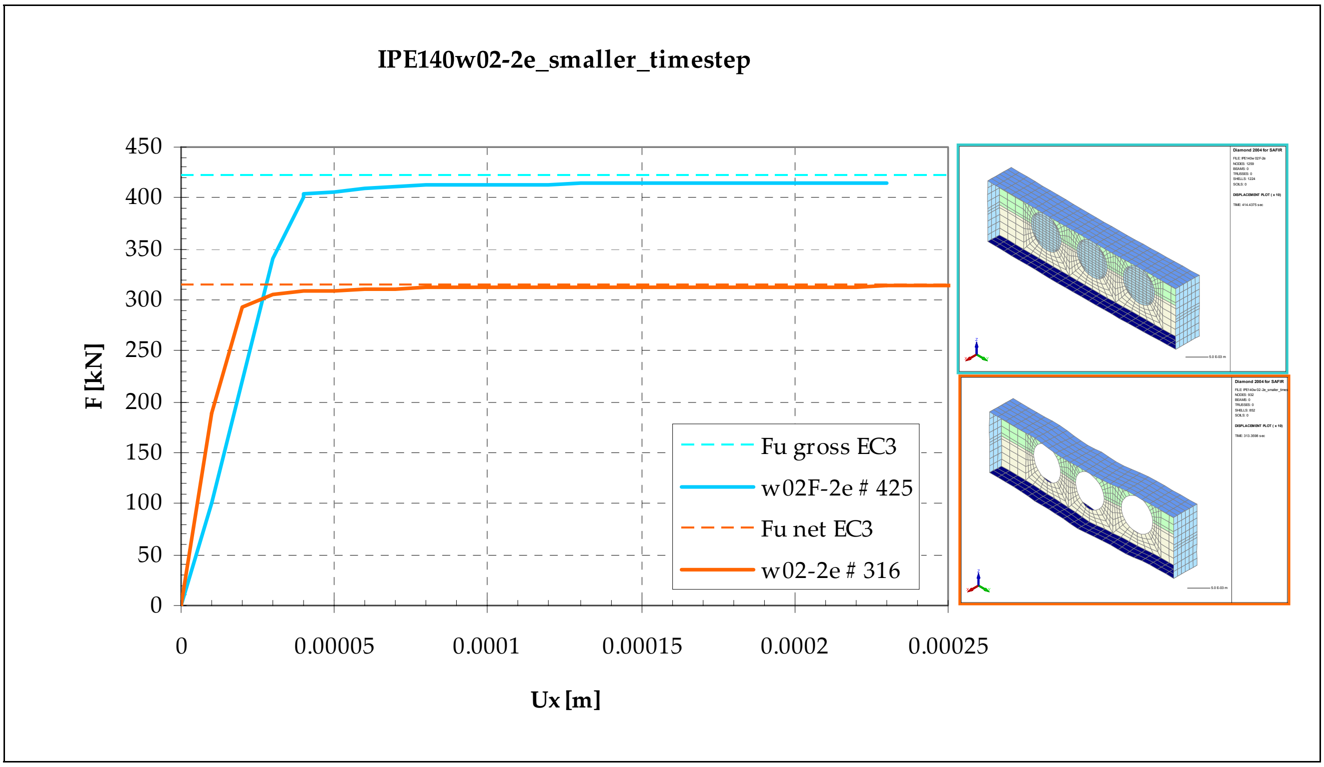

Note: The seemingly initial stiffer response of the net section is caused by a different initial load increment (step size).

flexural buckling load [kN]	EC3	FEM	Δ [%]
IPE140w02F-2e	419.1	414.4	-1.1
IPE140w02-2e_smaller_timestep	312.0	313.3	0.4

Slenderness 0.6

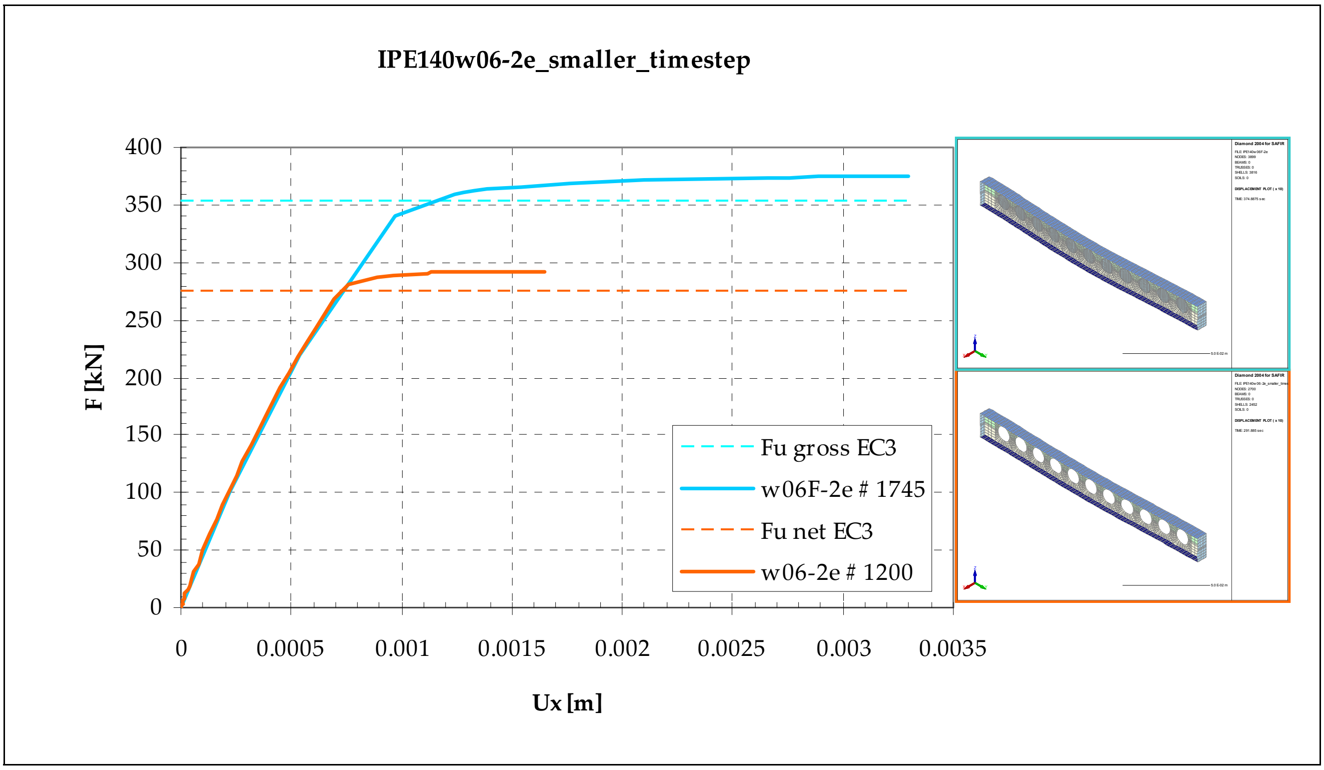

flexural buckling load [kN]	**EC3**	**FEM**	**Δ [%]**
IPE140w06F-2e	351.1	374.9	+6.8
IPE140w06-2e_smaller_timestep	273.5	291.8	+6.7

Slenderness 1.4

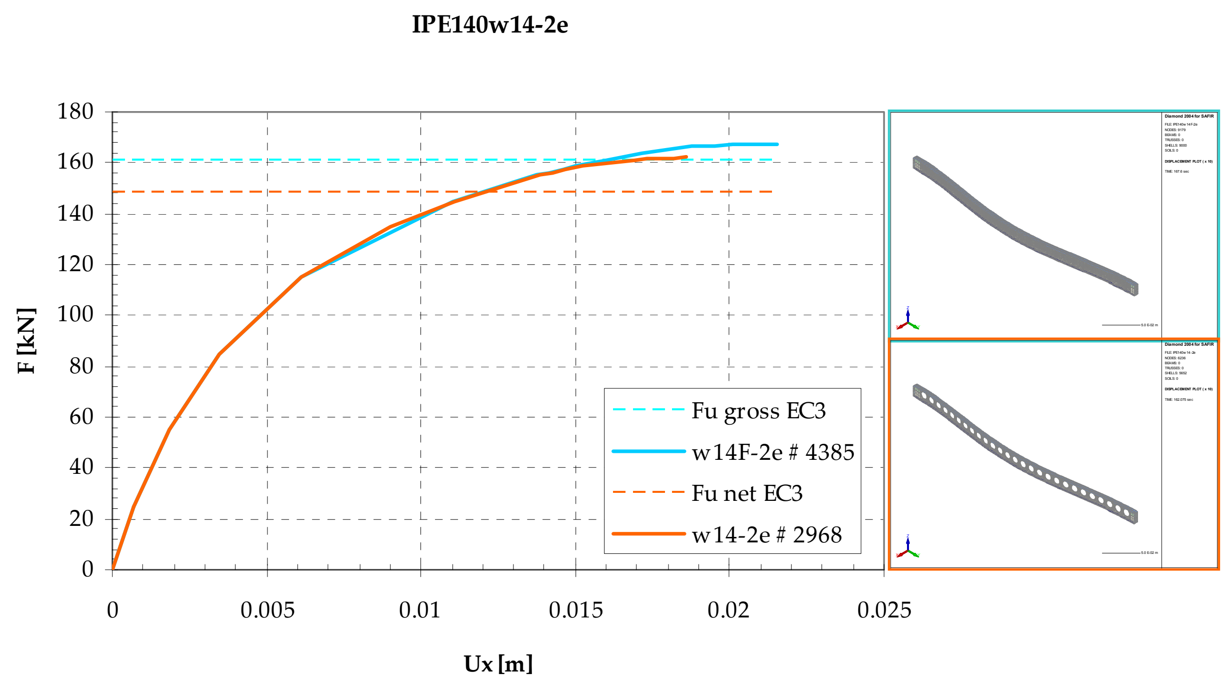

flexural buckling load [kN]	**EC3**	**FEM**	**Δ [%]**
IPE140w14F-2e	160.5	167.6	+4.4
IPE140w14-2e	148.0	162.1	+9.5

B.2.2 Buckling about the strong axis

Slenderness 0.2

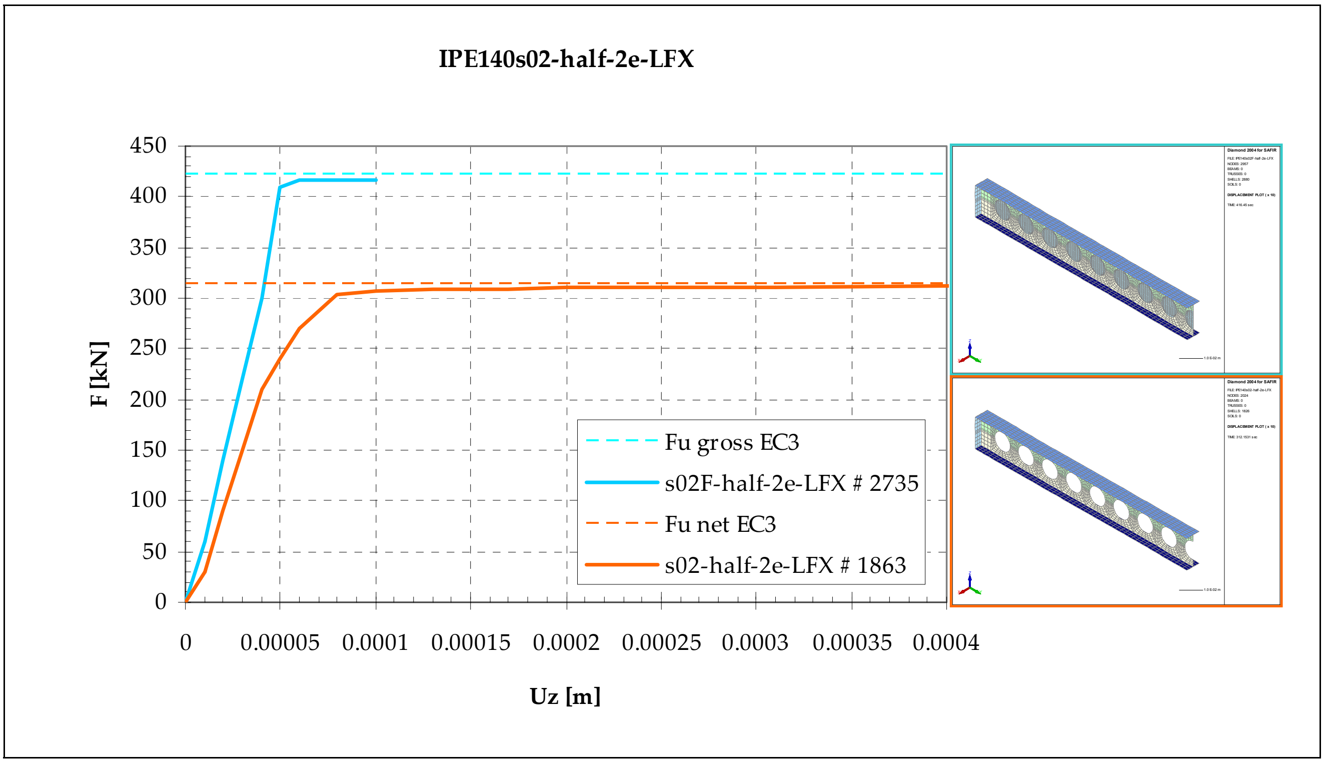

flexural buckling load [kN]	**EC3**	**FEM**	**Δ [%]**
IPE140s02F-half-2e-LFX	419.1	416.5	-0.6
IPE140s02R-half-2e-LFX	419.1	416.5	-0.6
IPE140s02-half-2e-LFX	312.0	312.2	+0.1

It is remarked here, that the analysis for the plain section has been made twice:

- once modelled with filled holes (s02F)
- once modelled with a rectangular mesh (s02R)

Both analyses returned exactly the same ultimate load in this case.
The mesh of both is shown below.

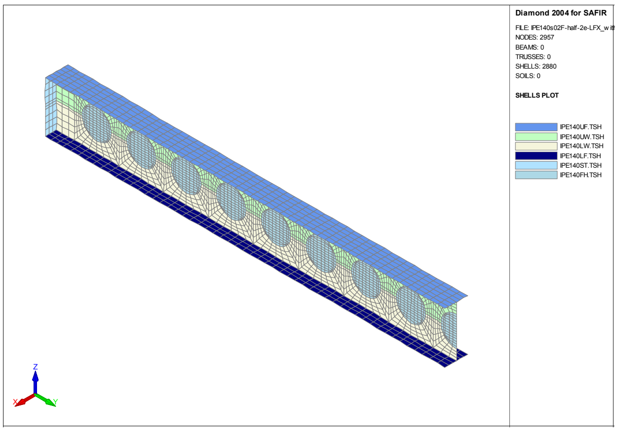
Diamond 2004 for SAFIR
FILE: IPE140s02F-half-2e-LFX_w
NODES: 2957
BEAMS: 0
TRUSSES: 0
SHELLS: 2880
SOILS: 0
SHELLS PLOT
IPE140UF.TSH
IPE140UW.TSH
IPE140LW.TSH
IPE140LF.TSH
IPE140ST.TSH
IPE140FH.TSH

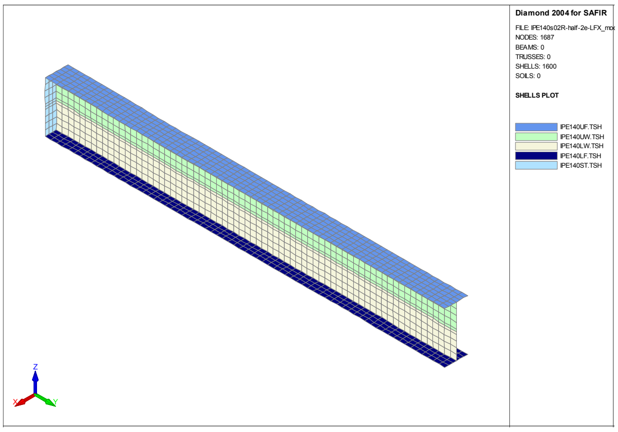
Diamond 2004 for SAFIR
FILE: IPE140s02R-half-2e-LFX_mo
NODES: 1687
BEAMS: 0
TRUSSES: 0
SHELLS: 1600
SOILS: 0
SHELLS PLOT
IPE140UF.TSH
IPE140UW.TSH
IPE140LW.TSH
IPE140LF.TSH
IPE140ST.TSH

Slenderness 0.6

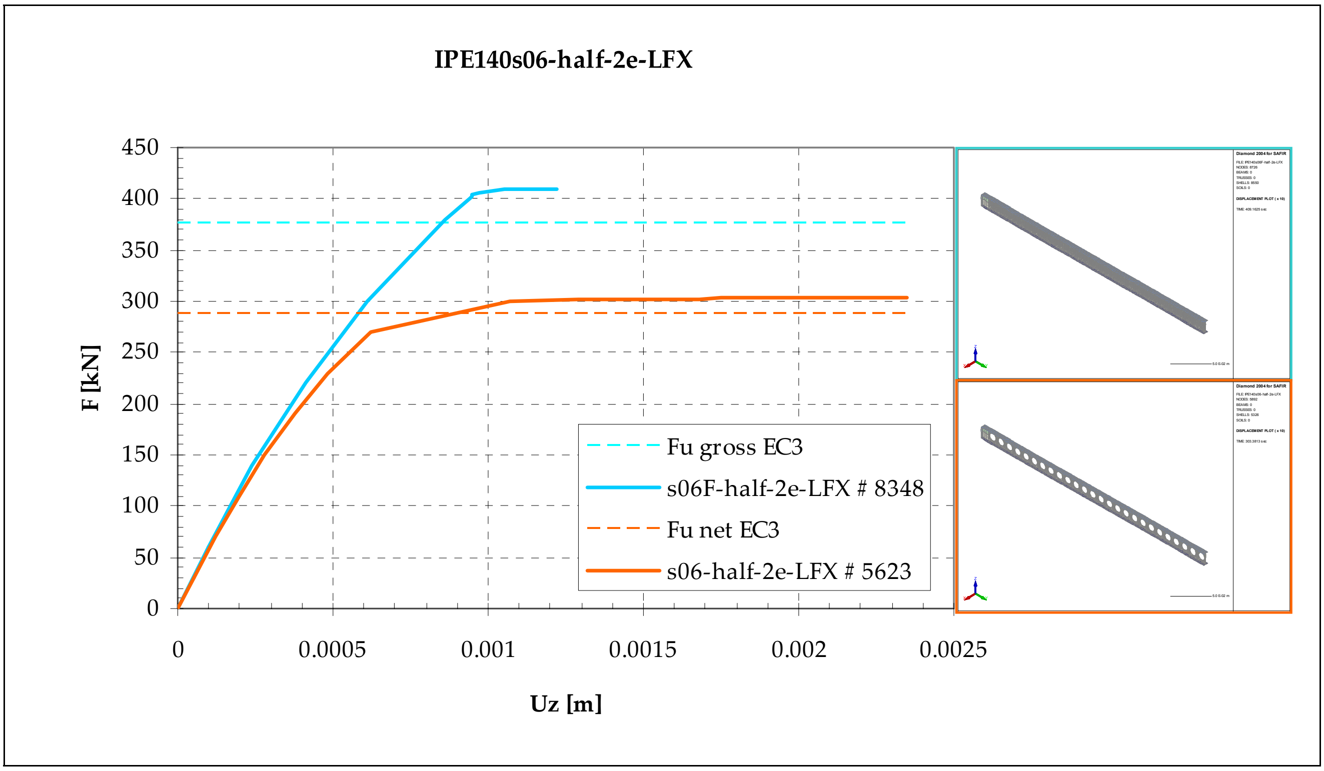

flexural buckling load [kN]	**EC3**	**FEM**	**Δ [%]**
IPE140s06F-half-2e-LFX	373.0	409.2	+9.7
IPE140s06-half-2e-LFX	285.5	303.4	+6.3

Slenderness 1.3

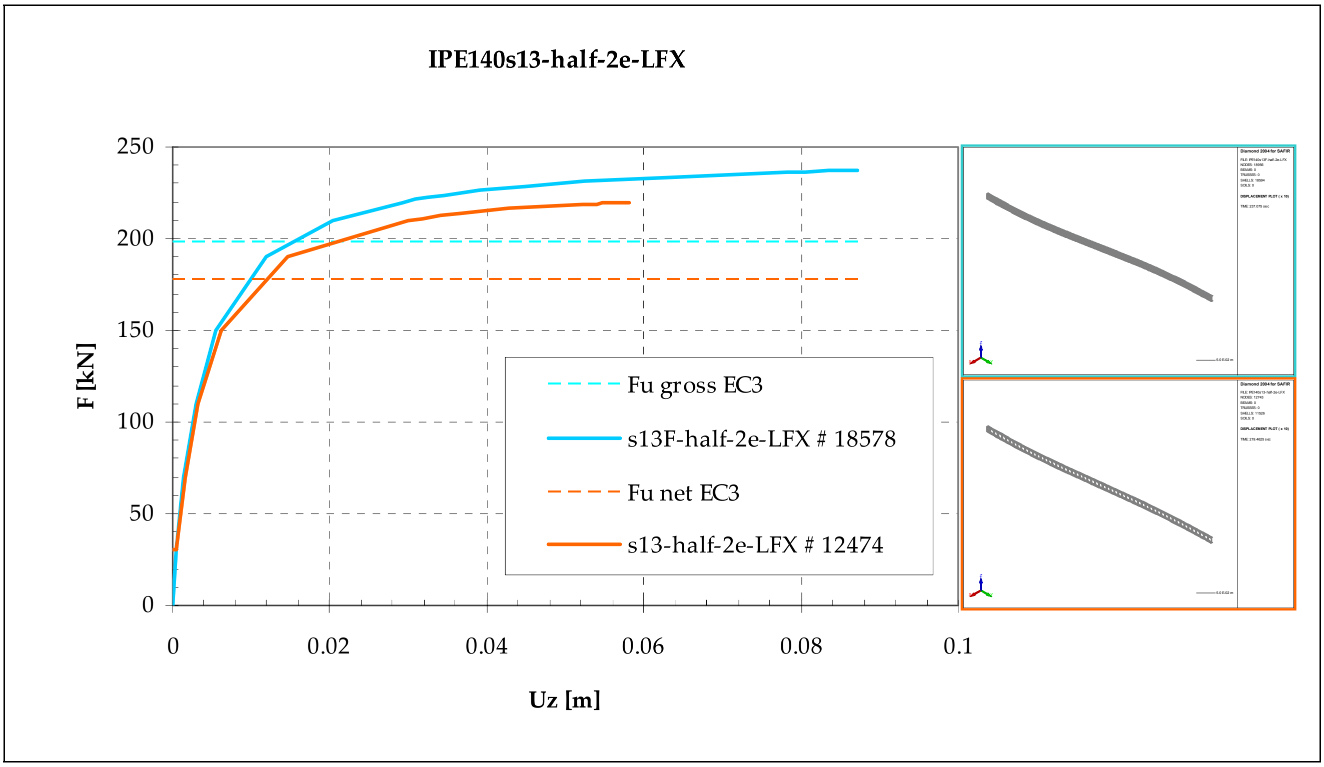

flexural buckling load [kN]	EC3	FEM	Δ [%]
IPE140s13F-half-2e-LFX	197.2	237.1	+20.2
IPE140s13R-half-2e-LFX	197.2	237.0	+20.2
IPE140s13-half-2e-LFX	176.4	219.5	+24.4

Slenderness 1.4

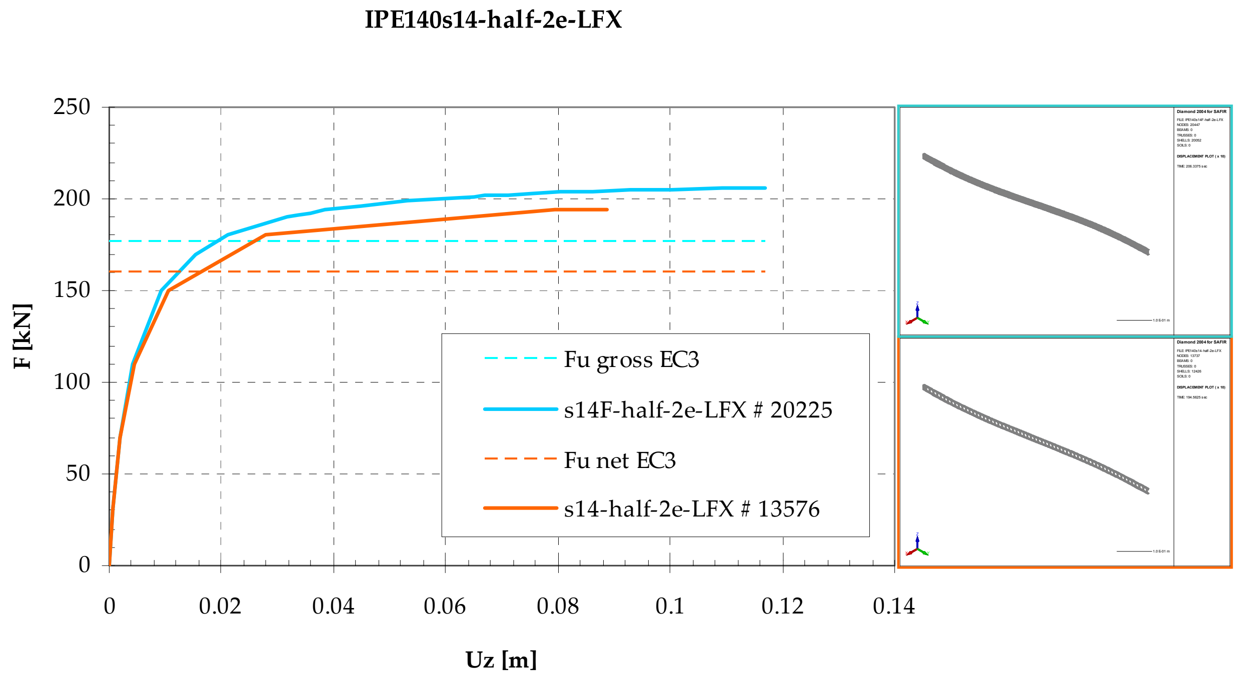

flexural buckling load [kN]	**EC3**	**FEM**	**Δ [%]**
IPE140s14F-half-2e-LFX	175.2	206.3	+17.8
IPE140s14-half-2e-LFX	158.9	194.6	+22.4

B.3 Base profile IPE330

B.3.1 Buckling about the weak axis

Slenderness 0.2

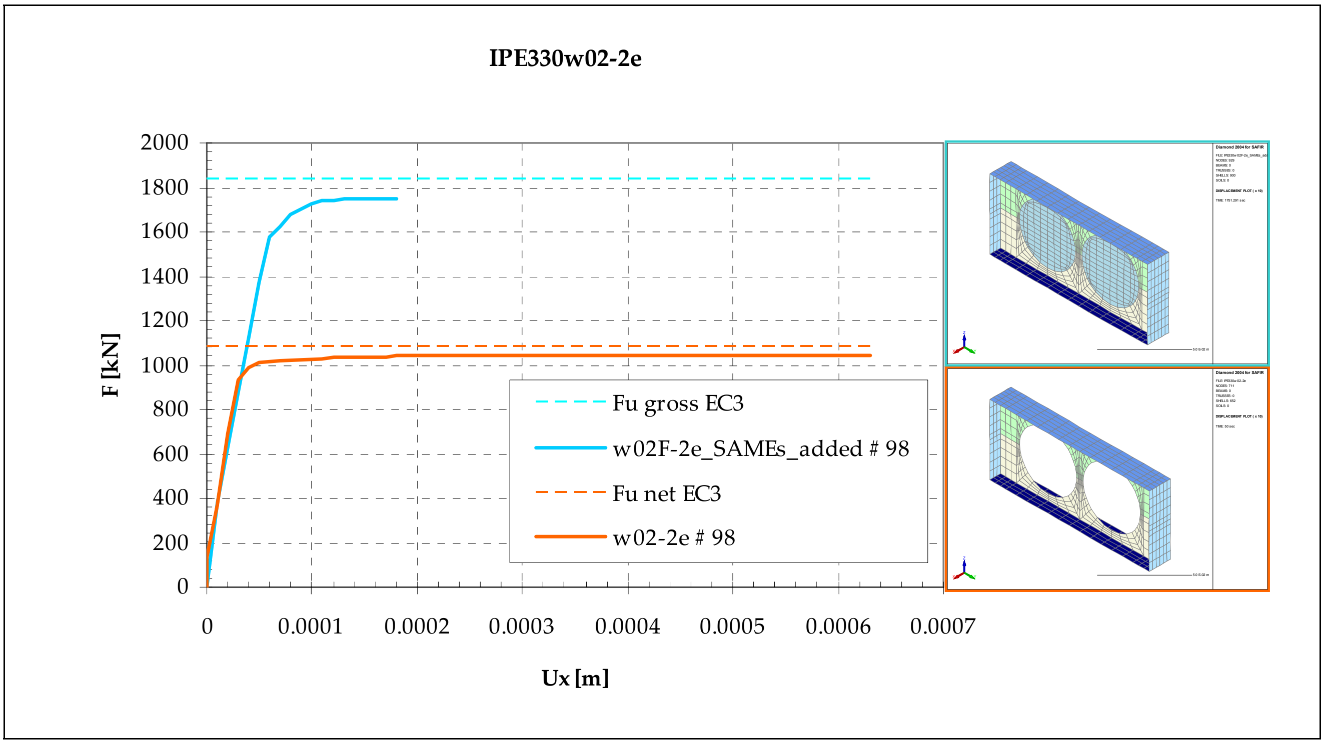

flexural buckling load [kN]	EC3	FEM	Δ [%]
IPE330w02F-2e	1787.5	1680.3	-6.0
IPE330w02F-2e_SAMEs_added	1787.5	1751.3	-2.0
IPE330w02R-2e	1787.5	1699.1	-4.9
IPE330w02-2e	1034.9	1047.0	+1.2

It is remarked here, that the analysis for the plain section has been made thrice:

- once modelled with filled holes (w02F)
- once modelled with filled holes (w02F + SAMEs_added)
- once modelled with a rectangular mesh (w02R)

The analysis was first performed on for the mesh with filled holes. Because of the discrepancy between the expected and the obtained result, the deformation was further examined. It turned out that prior to yielding (as at a slenderness of 0.2 (almost) no flexural buckling takes place yet), the web failed in a plate buckling mode. In order to prevent this, further restraining conditions were added by implying that nodes on a vertical line should displace equally perpendicular to the plane of the web (SAME conditions) – although still some minor plate buckling was observed.

The mesh with rectangular web elements was not modified to prevent plate buckling to happen, as the behaviour shown was just equal to that of the mesh with filled holes.

The effect of the added SAME conditions can be seen below in the displacement plots of the mesh with filled holes, with and without these extra restraining conditions (magnification: 100x).

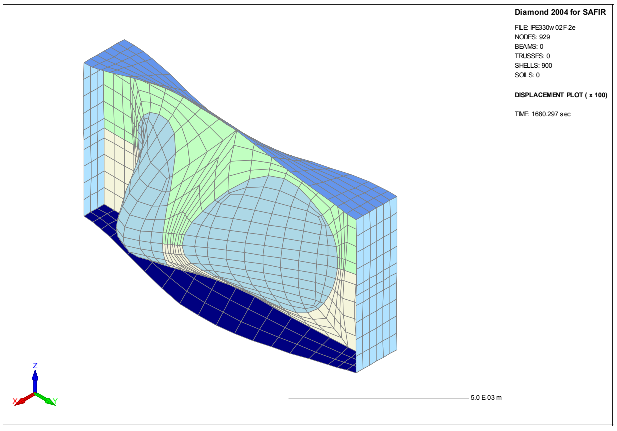
Diamond 2004 for SAFIR
FILE: IPE330w 02F-2e
NODES: 929
BEAMS: 0
TRUSSES: 0
SHELLS: 900
SOILS: 0
DISPLACEMENT PLOT (x 100)
TIME: 1680.297 sec
Z
X
Y
5.0 E-03 m

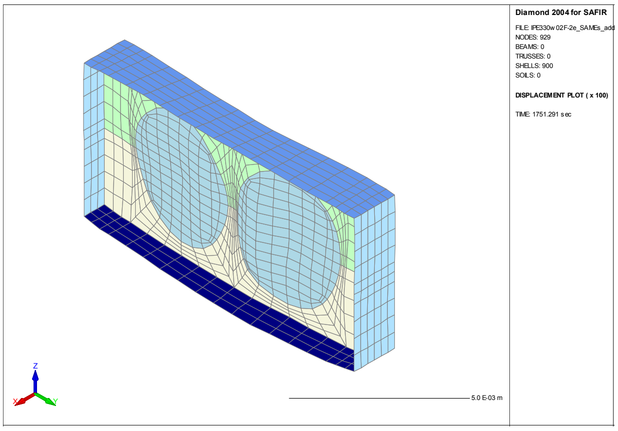
Diamond 2004 for SAFIR
FILE: IPE330w 02F-2e_SAMEs_add
NODES: 929
BEAMS: 0
TRUSSES: 0
SHELLS: 900
SOILS: 0
DISPLACEMENT PLOT (x 100)
TIME: 1751.291 sec
Z
X
Y
5.0 E-03 m

Furthermore shown are the deformation plots of the rectangular mesh and the mesh with holes (also with magnification factor 100).

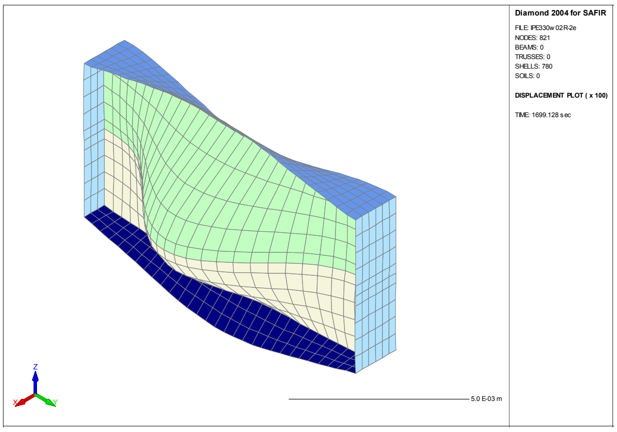
Diamond 2004 for SAFIR
FILE: IPE330w 02R-2e
NODES: 821
BEAMS: 0
TRUSSES: 0
SHELLS: 780
SOILS: 0
DISPLACEMENT PLOT (x 100)
TIME: 1699.128 sec
Z
X
Y
5.0 E-03 m

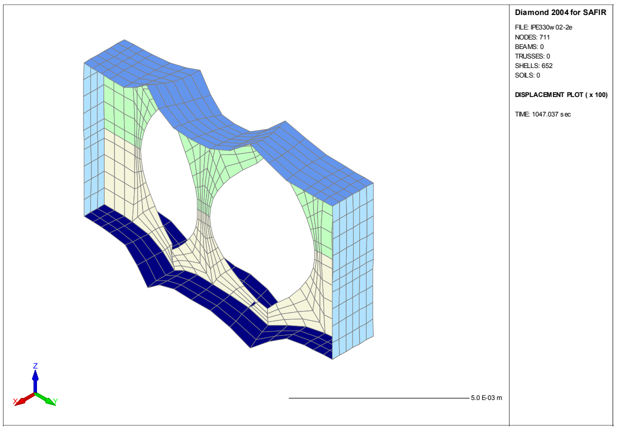
Diamond 2004 for SAFIR
FILE: IPE330w 02-2e
NODES: 711
BEAMS: 0
TRUSSES: 0
SHELLS: 652
SOILS: 0
DISPLACEMENT PLOT (x 100)
TIME: 1047.037 sec
Z
X
Y
5.0 E-03 m

From the plot of the mesh with holes, it is clear that failure of the cellular members is not influenced by some kind of plate buckling (which is indeed absent). Instead it turns out that a kind of buckling occurs of the two tee-sections constituting the net section, just prior to attainment of the flexural buckling capacity of the net section.

Slenderness 0.6

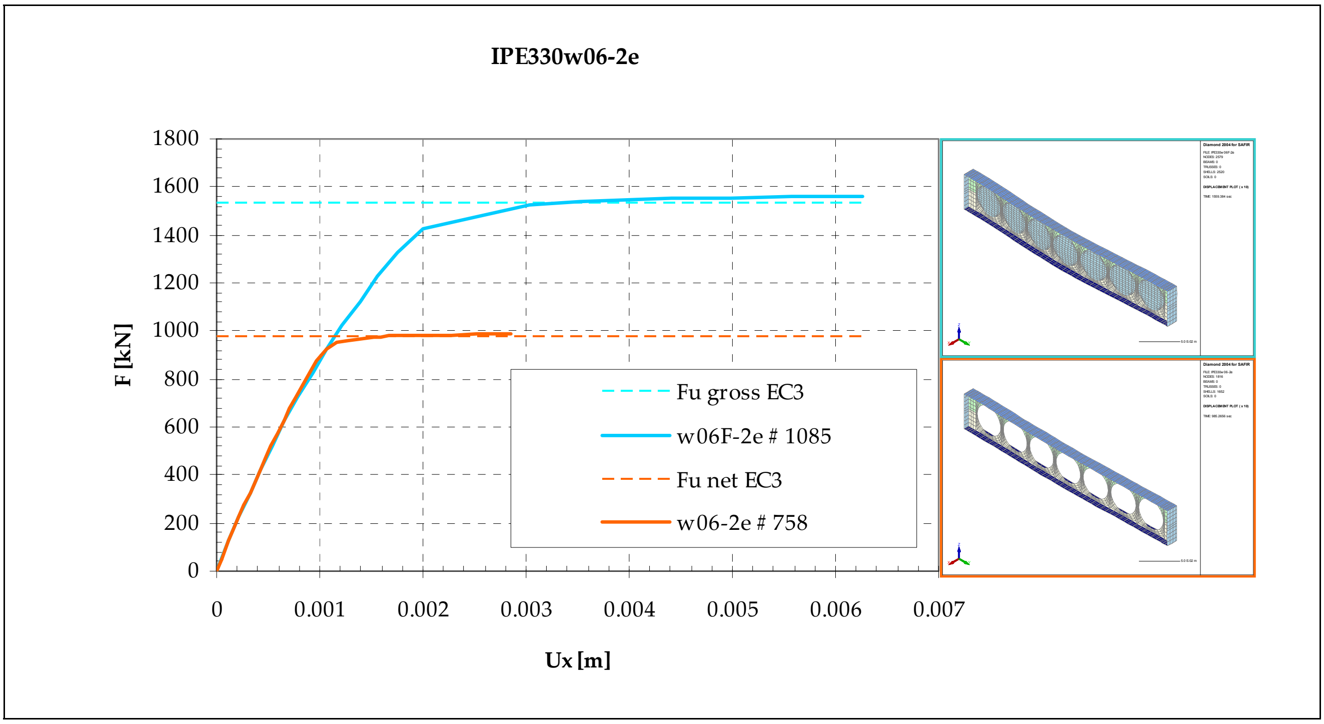

flexural buckling load [kN]	**EC3**	**FEM**	**Δ [%]**
IPE330w06F-2e	1502.2	1559.4	+3.8
IPE330w06-2e	936.5	985.3	+5.2
IPE330w06_with_modified_ support_conditions_in_the_middle	936.5	969.1	+3.5

The last entry in the table above refers to an extra analysis, which was made with different support conditions. In this run the supports were defined in the middle, while symmetry conditions were applied to the ends. The load now had to be applied to *both* ends also. The ultimate load thus acquired agrees with the one with supports at the end only.

See below for a the applied supports, and the deformation plot (magnification: 100x). It can be seen that now the ends displace laterally, instead of the middle of the beam when the usual modelling is applied.

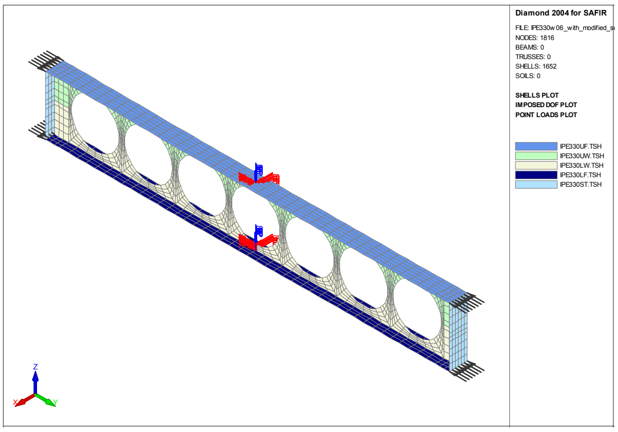
Diamond 2004 for SAFIR
FILE: IPE330w 06_with_modified_s
NODES: 1816
BEAMS: 0
TRUSSES: 0
SHELLS: 1652
SOILS: 0
SHELLS PLOT
IMPOSED DOF PLOT
POINT LOADS PLOT
IPE330UF.TSH
IPE330UW.TSH
IPE330LW.TSH
IPE330LF.TSH
IPE330ST.TSH
Z
X
Y

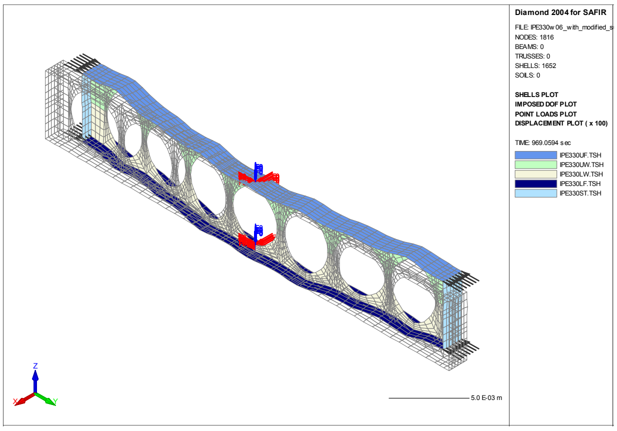
Diamond 2004 for SAFIR
FILE: IPE330w 06_with_modified_s
NODES: 1816
BEAMS: 0
TRUSSES: 0
SHELLS: 1652
SOILS: 0
SHELLS PLOT
IMPOSED DOF PLOT
POINT LOADS PLOT
DISPLACEMENT PLOT (x 100)
TIME: 969.0594 sec
IPE330UF.TSH
IPE330UW.TSH
IPE330LW.TSH
IPE330LF.TSH
IPE330ST.TSH
5.0 E-03 m
Z
X
Y

Slenderness 1.4

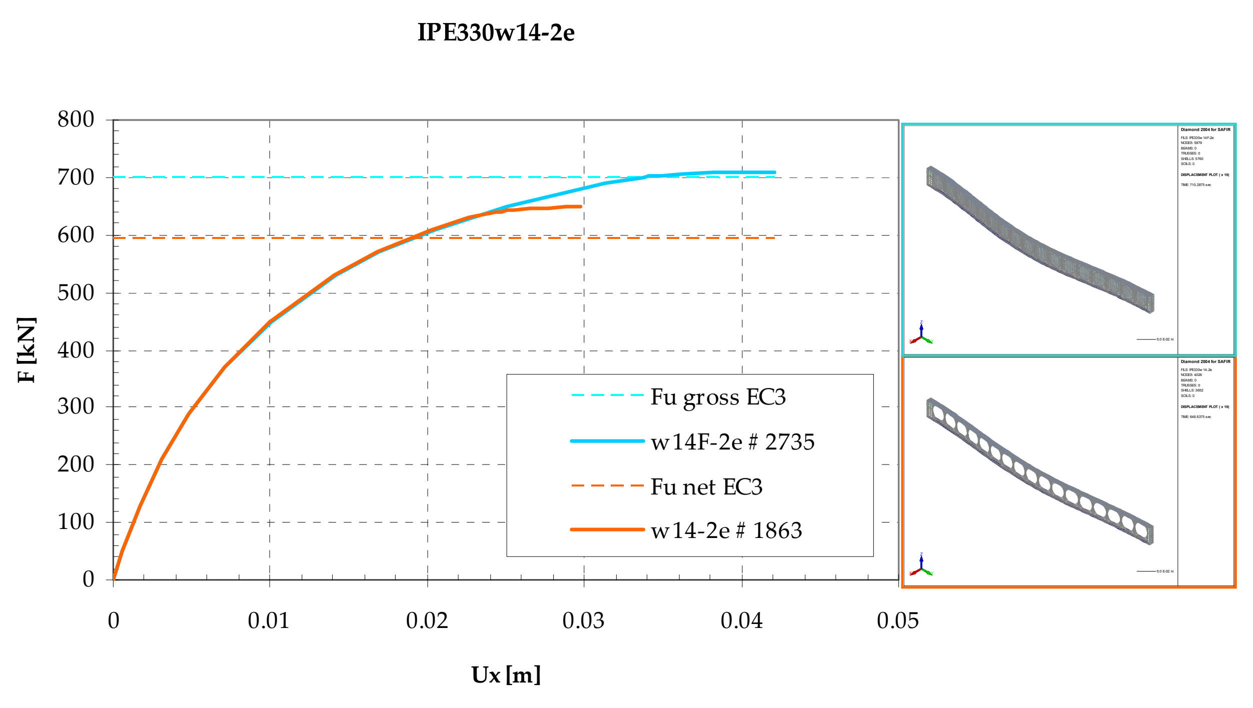

flexural buckling load [kN]	EC3	FEM	Δ [%]
IPE330w14F-2e	694.1	710.3	+2.3
IPE330w14-2e	582.5	648.6	+11.3

B.3.2 Buckling about the strong axis

Slenderness 0.2

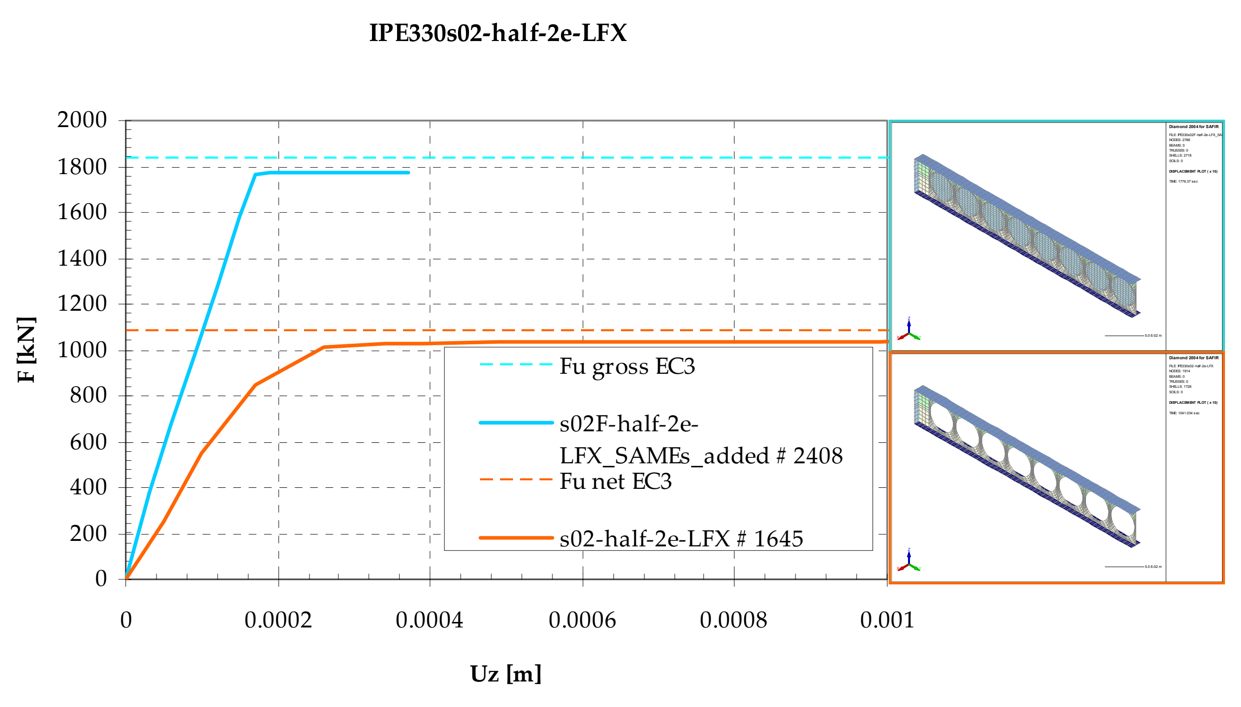

flexural buckling load [kN]	**EC3**	**FEM**	**Δ [%]**
IPE330s02F-half-2e-LFX	1787.1	1762.5	-1.4
IPE330s02F-half-2e-LFX_SAMEs_added	1787.1	1776.4	-0.6
IPE330s02-half-2e-LFX	1034.9	1041.0	+0.6

Just like for flexural buckling about the *weak* axis of the ACB cut from a IPE330 section with slenderness 0.2, even so for flexural buckling about the *strong* axis some plate buckling occurs, unless additional restraints (SAME conditions) are defined – though less apparent.

Slenderness 0.6

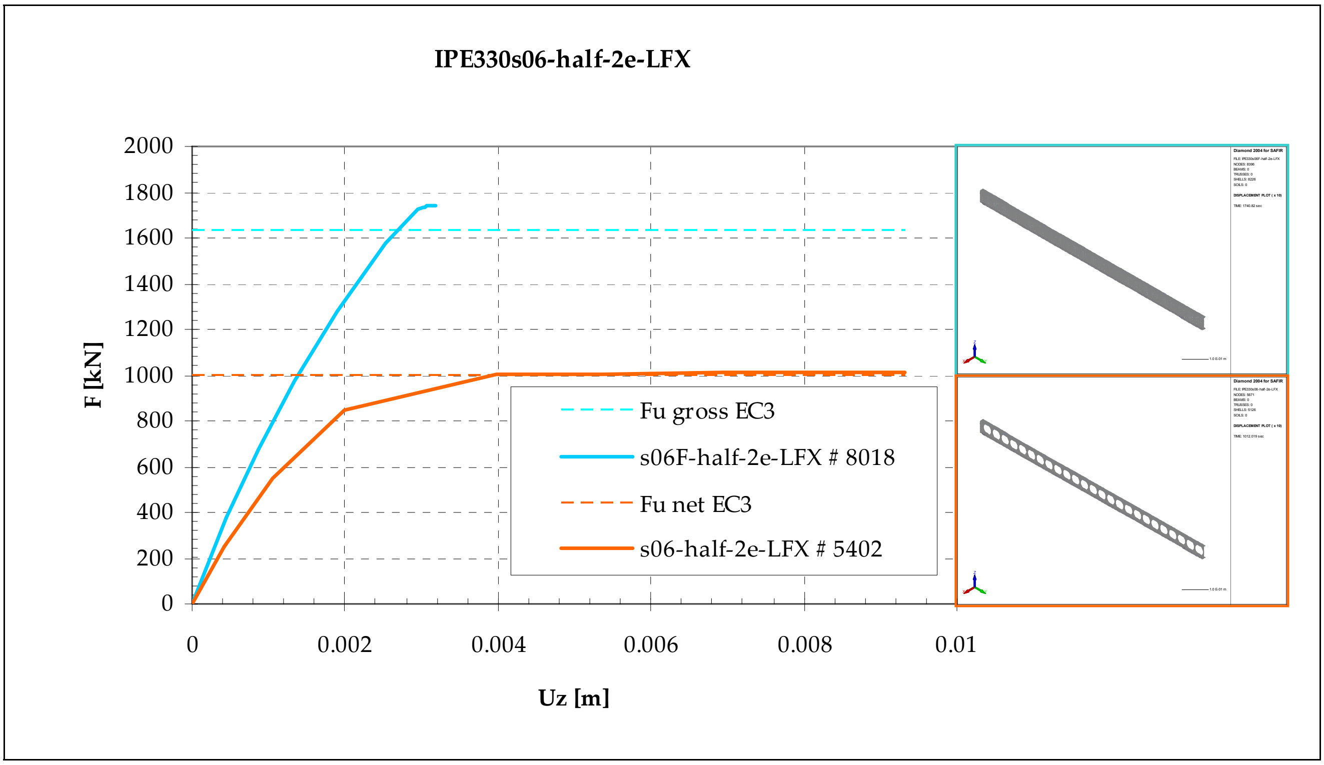

flexural buckling load [kN]	**EC3**	**FEM**	**Δ [%]**
IPE330s06F-half-2e-LFX	1589.0	1740.8	+9.6
IPE330s06R-half-2e-LFX	1589.0	1743.8	+9.7
IPE330s06-half-2e-LFX	958.0	1012.0	+5.6

Slenderness 1.4

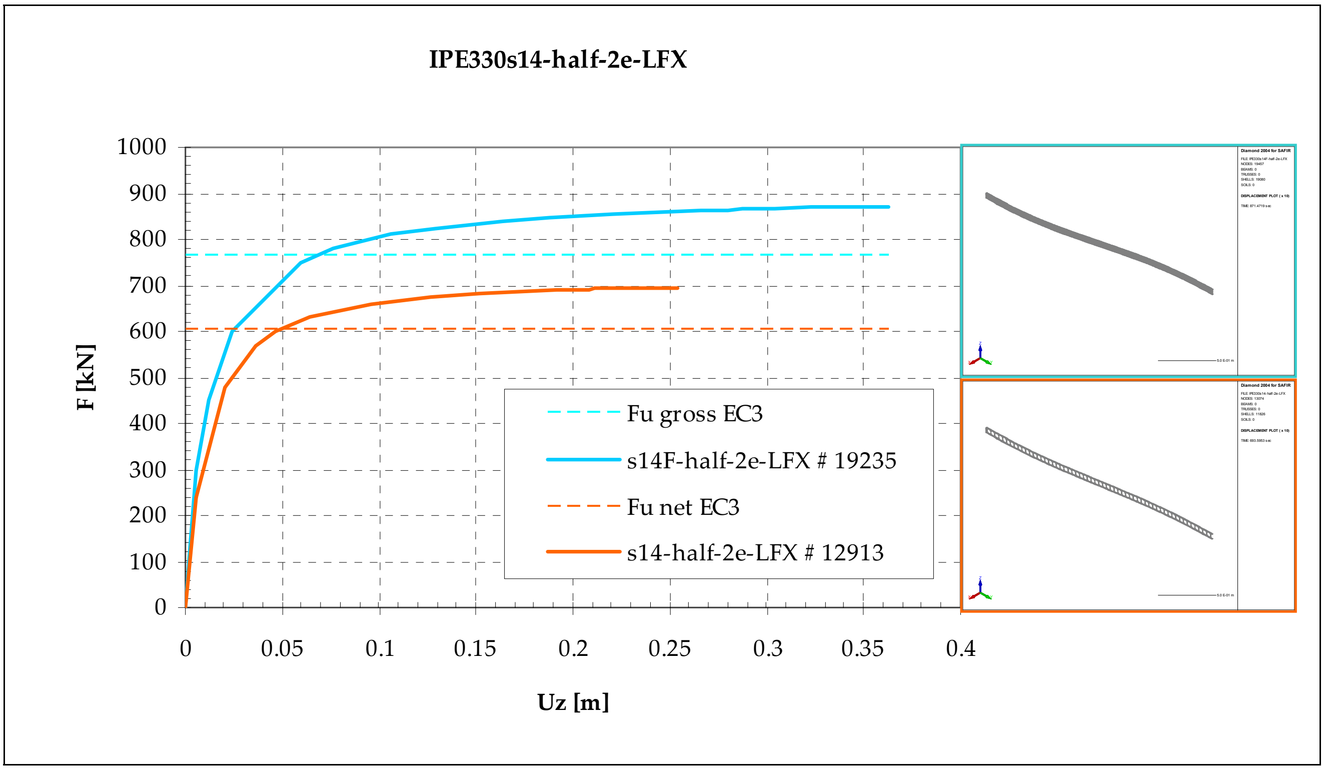

flexural buckling load [kN]	**EC3**	**FEM**	**Δ [%]**
IPE330s14F-half-2e-LFX	741.4	871.5	+17.5
IPE330s14R-half-2e-LFX	741.4	872.0	+17.6
IPE330s14-half-2e-LFX	578.2	693.6	+20.0

B.4 Base profile IPE600

B.4.1 Buckling about the weak axis

Slenderness 0.2

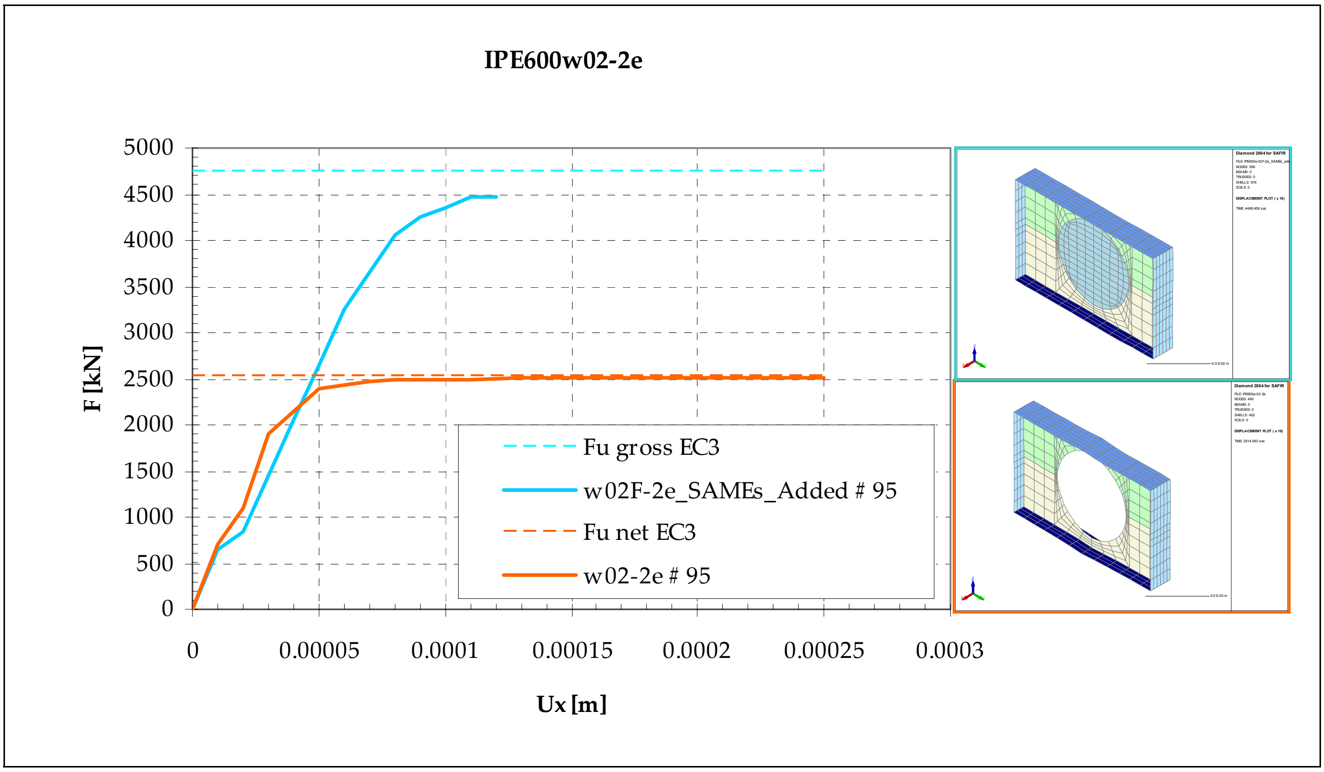

flexural buckling load [kN]	**EC3**	**FEM**	**Δ [%]**
IPE600w02F-2e	4685.9	4089.0	-12.7
IPE600w02F-2e_SAMEs_added	4685.9	4466.4	-4.7
IPE600w02R-2e	4685.9	4075.9	-13.0
IPE600w02-2e	2466.6	2514.1	+1.9

For this case with a relatively high and slender web, plate buckling appeared to be a major failure mode. Even with additional restraints it could not be avoided completely, though the difference can be seen clearly in the figures below (coloured presentation of the lateral displacement Ux).

Left: without additional restraints.

Right: with additional restraining conditions.

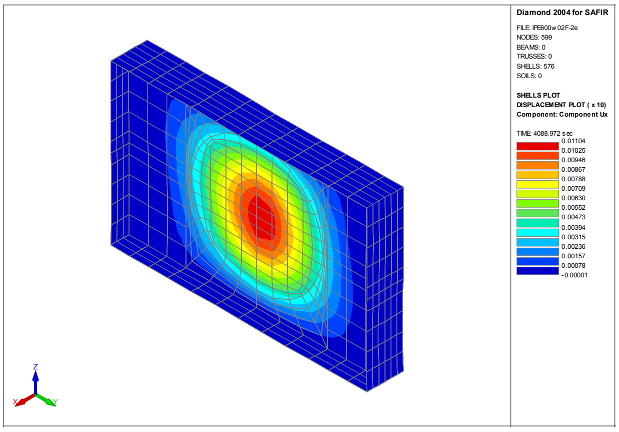
Diamond 2004 for SAFIR
FILE: IPE600w02F-2e
NODES: 599
BEAMS: 0
TRUSSES: 0
SHELLS: 576
SOILS: 0
SHELLS PLOT
DISPLACEMENT PLOT (x 10)
Component: Component Ux
TIME: 4088.972 sec
0.01104
0.01025
0.00946
0.00867
0.00788
0.00709
0.00630
0.00552
0.00473
0.00394
0.00315
0.00236
0.00157
0.00078
-0.00001
Z
X
Y

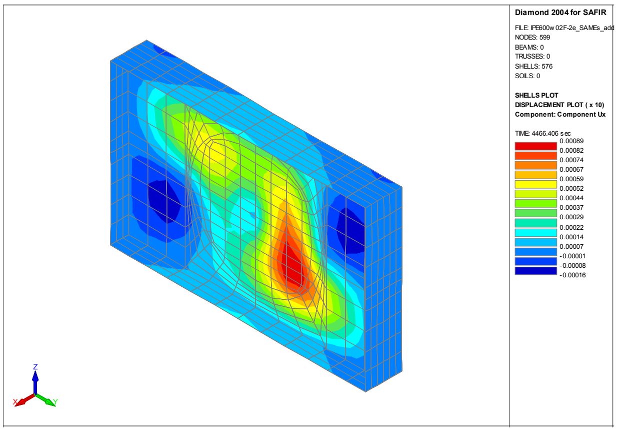
Diamond 2004 for SAFIR
FILE: IPE600w02F-2e_SAMEs_add
NODES: 599
BEAMS: 0
TRUSSES: 0
SHELLS: 576
SOILS: 0
SHELLS PLOT
DISPLACEMENT PLOT (x 10)
Component: Component Ux
TIME: 4466.406 sec
0.00089
0.00082
0.00074
0.00067
0.00059
0.00052
0.00044
0.00037
0.00029
0.00022
0.00014
0.00007
-0.00001
-0.00008
-0.00016
Z
X
Y

It can be seen that plate buckling occurs in a higher, but is not completely eliminated.

Slenderness 0.25

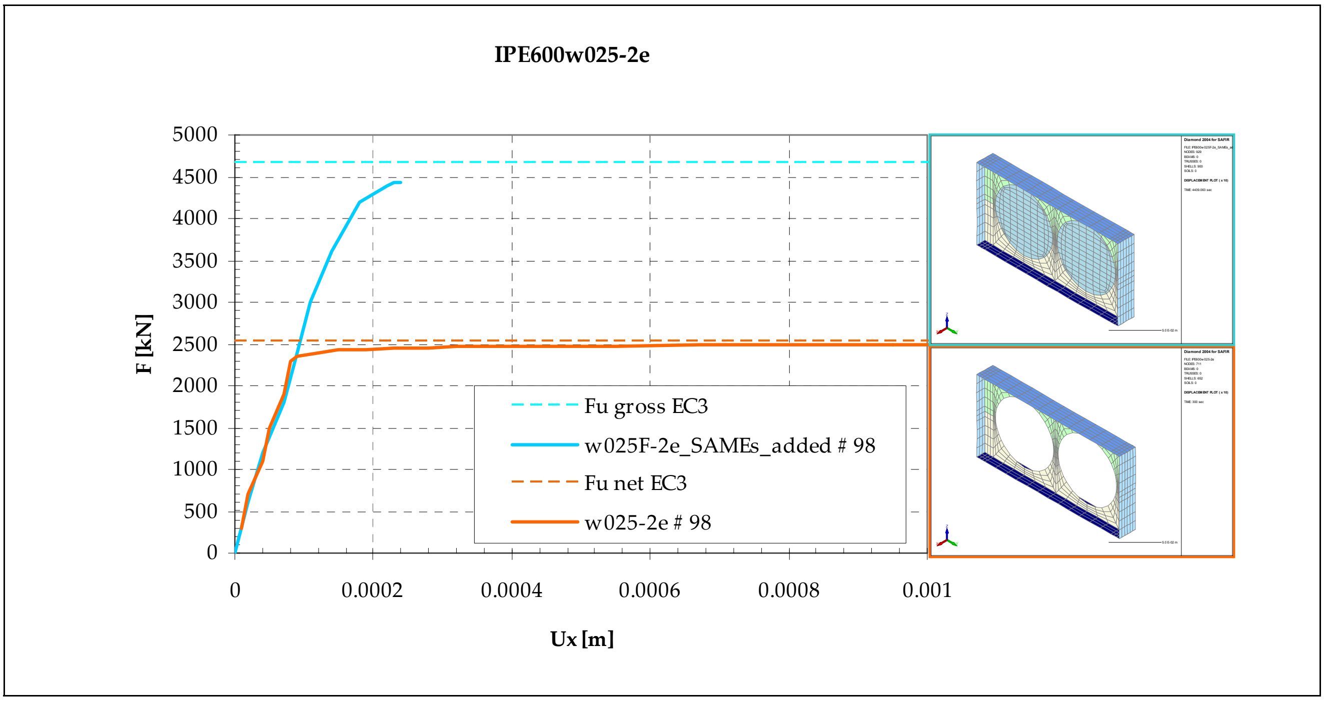

flexural buckling load [kN]	EC3	FEM	Δ [%]
IPE600w025F-2e	4604.9	4100.7	-10.9
IPE600w025F-2e_SAMEs_added	4604.9	4439.1	-3.6
IPE600w025R-2e	4604.9	4035.6	-12.4
IPE600w025-2e	2466.6	2498.5	+1.3

For this case, failure by buckling in a plate mode also could not be avoided completely by adding stiffeners in order to restrain the web from buckling.

Slenderness 0.6

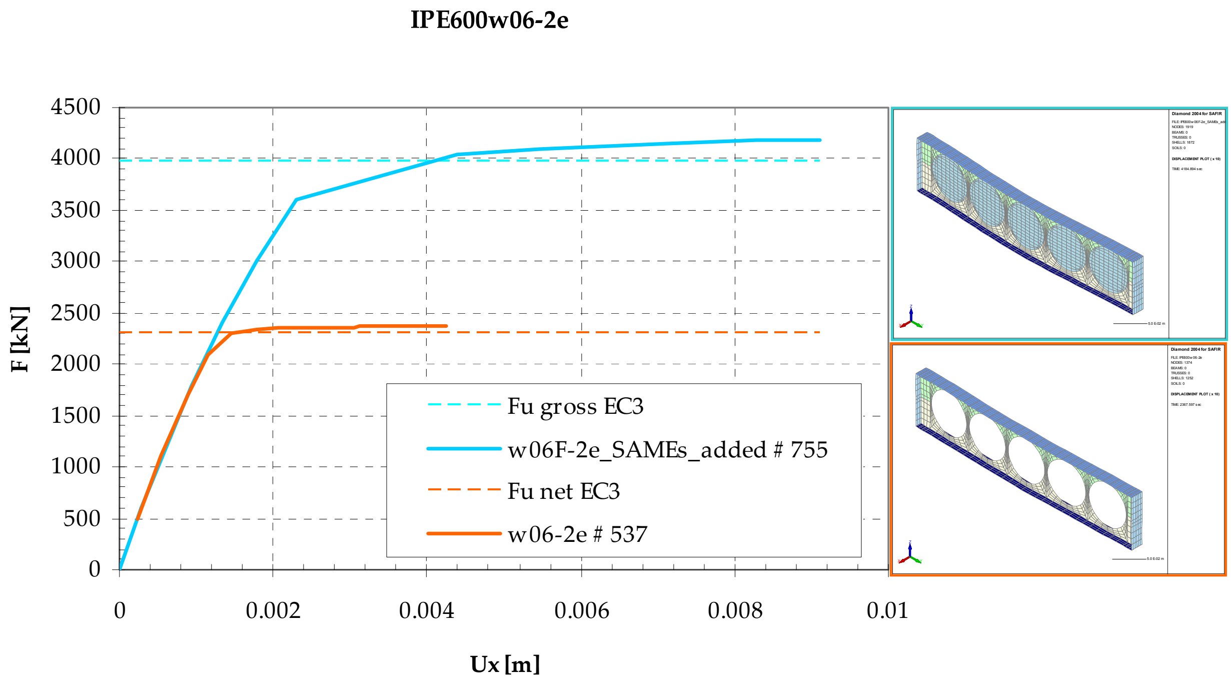

flexural buckling load [kN]	**EC3**	**FEM**	**Δ [%]**
IPE600w06F-2e	3930.2	3795.1	-3.4
IPE600w06F-2e_SAMEs_added	3930.2	4184.9	+6.5
IPE600w06R-2e	3930.2	3791.0	-3.5
IPE600w06R-2e_SAMEs_added	3930.2	4214.7	+7.2
IPE600w06-2e	2250.8	2367.6	+5.2

Again additional restraints were necessary – which allowed flexural buckling to become the governing failure mechanism for the plain-webbed member, see figures below.

Deformation plot (magnification 50x) without additional restraints:

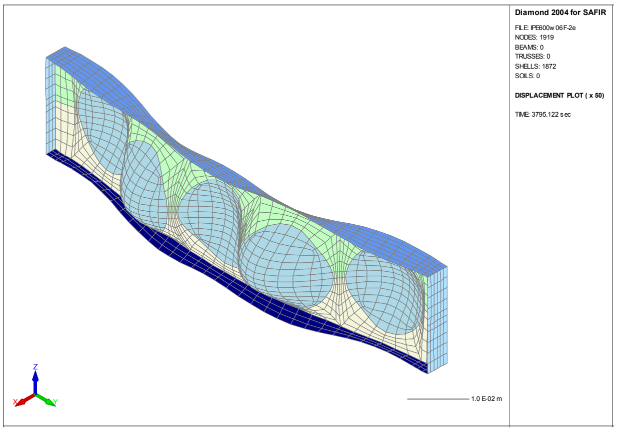
Diamond 2004 for SAFIR
FILE: IPE600w06F-2e
NODES: 1919
BEAMS: 0
TRUSSES: 0
SHELLS: 1872
SOILS: 0
DISPLACEMENT PLOT (x 50)
TIME: 3795.122 sec
1.0 E-02 m
Z
X
Y

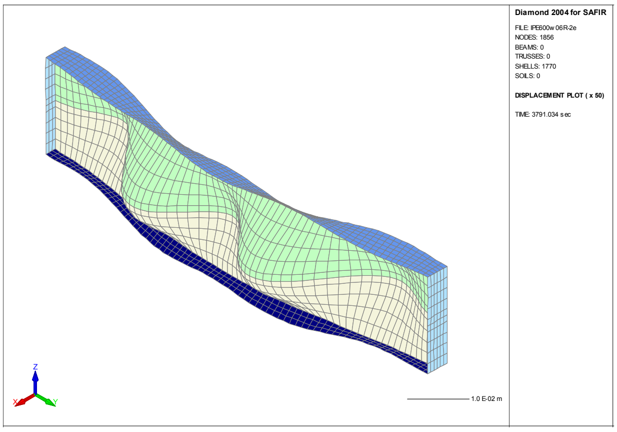
Diamond 2004 for SAFIR
FILE: IPE600w06R-2e
NODES: 1856
BEAMS: 0
TRUSSES: 0
SHELLS: 1770
SOILS: 0
DISPLACEMENT PLOT (x 50)
TIME: 3791.034 sec
1.0 E-02 m
Z
X
Y

Deformation plot (magnification 50x) with additional restraints:

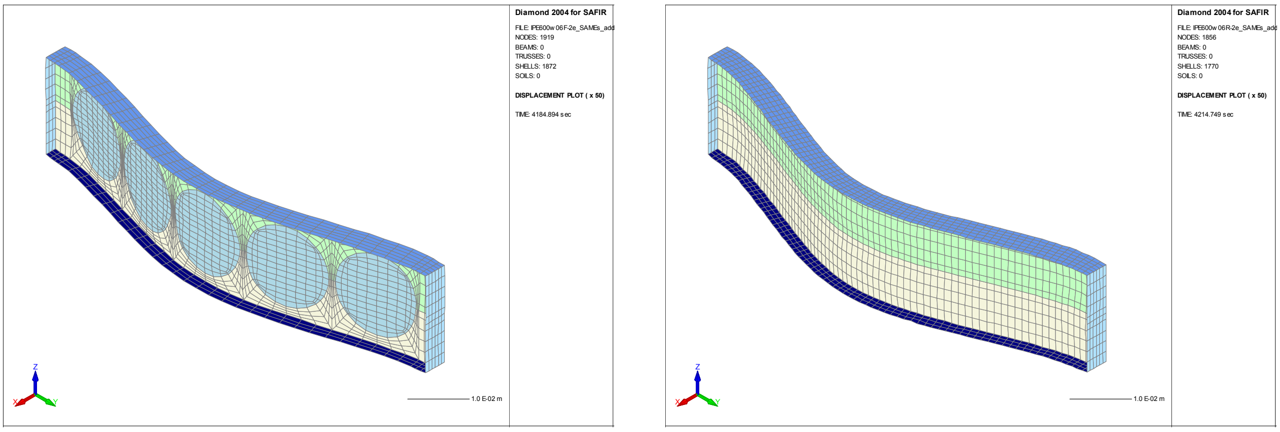
Diamond 2004 for SAFIR
FILE: IPE600w06F-2e_SAMEs_add
NODES: 1919
BEAMS: 0
TRUSSES: 0
SHELLS: 1872
SOILS: 0
DISPLACEMENT PLOT (x 50)
TIME: 4184.894 sec
1.0 E-02 m
Diamond 2004 for SAFIR
FILE: IPE600w06R-2e_SAMEs_add
NODES: 1856
BEAMS: 0
TRUSSES: 0
SHELLS: 1770
SOILS: 0
DISPLACEMENT PLOT (x 50)
TIME: 4214.749 sec
1.0 E-02 m

Slenderness 1.4

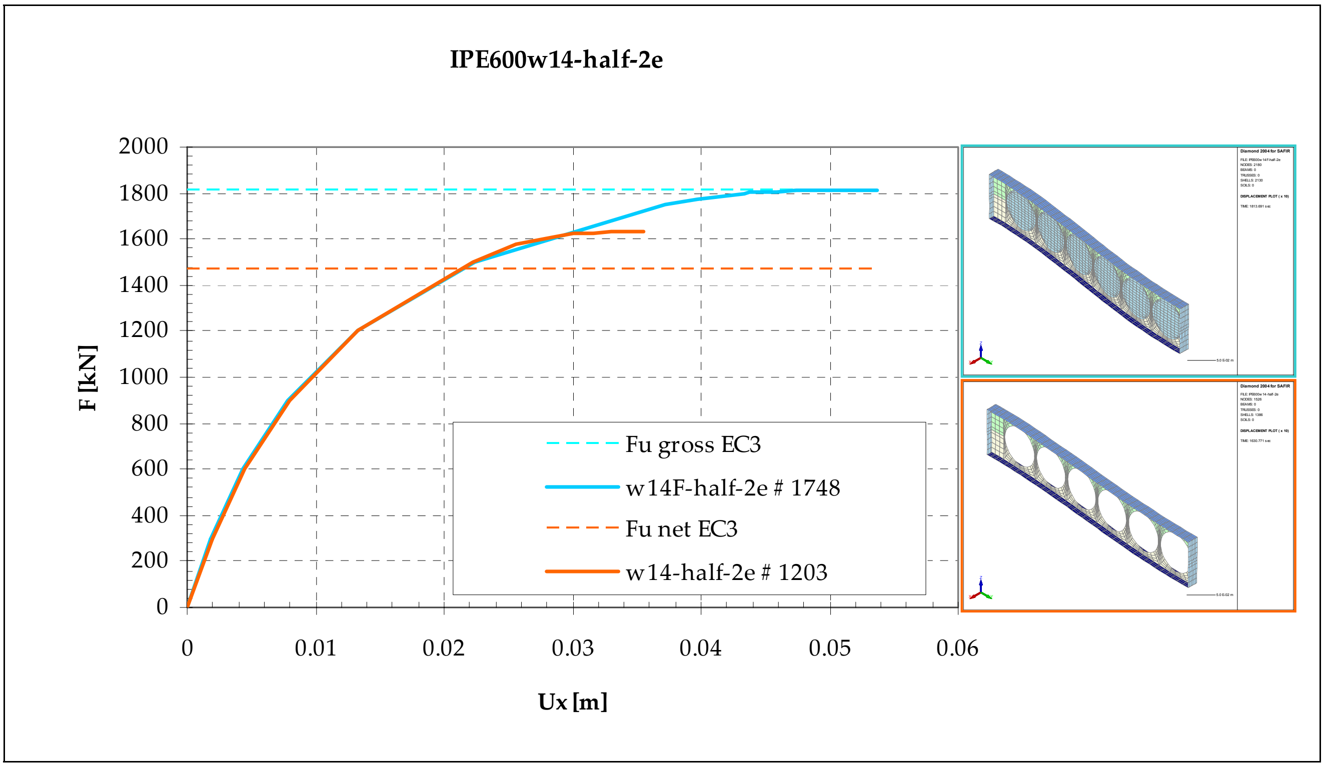

flexural buckling load [kN]	EC3	FEM	Δ [%]
IPE600w14F-2e	1804.2	1813.7	+0.5
IPE600w14-2e	1454.2	1630.8	+12.1

For this relatively long length the flexural buckling mode is predominant.

B.4.2 Buckling about the strong axis

*Slenderness 0.2**

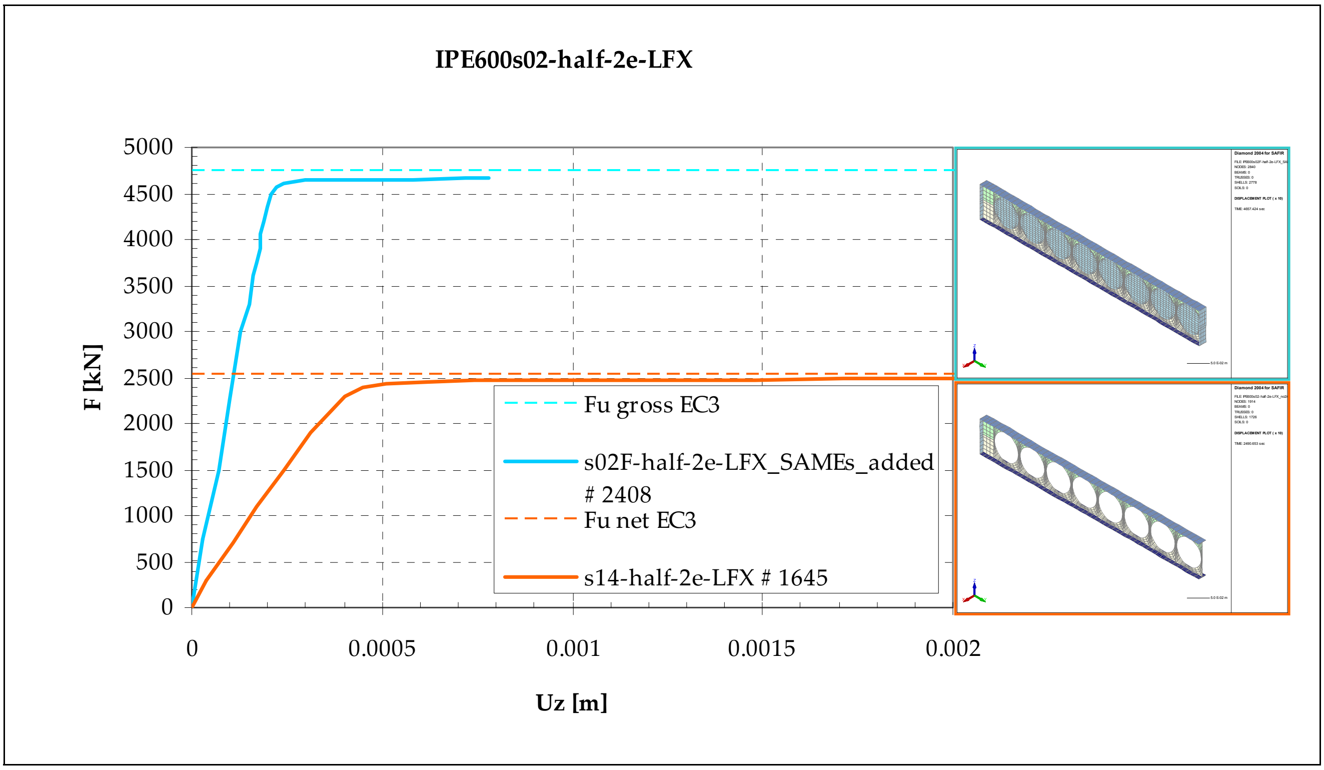

flexural buckling load [kN]	**EC3**	**FEM**	**Δ [%]**
IPE600s02F-half-2e-LFX	4685.3	3947.8	-15.7
IPE600s02F-half-2e-LFX_SAMEs_added	4685.3	4657.4	-0.6
IPE600s02-half-2e-LFX	2466.6	2490.7	+1.0
IPE600s02-half-2e-LFX_cosinebow	2466.6	2488.8	+0.9

Again additional restraints were necessary to allow flexural buckling to become the governing failure mechanism (for the plain-webbed member). Plate buckling near the support could not be prevented completely by these added restraints however.

Furthermore it was noted (as seen earlier) that prior to attainment of the flexural buckling capacity of the net section, the section failed by a kind of buckling of the two tee-sections constituting the net section.

For comparison, the analysis of the cellular member was performed also for a cosine imperfection (maxima at supports and mid-span) instead of the usual sine imperfection. It turned out that the result differs less than 0.1 percent.

* **Note:** the term 'no2ndstiffener' has been omitted in the table for sake of brevity, although the stiffener itself *is* present in the runs for the plain-webbed section (and also in the top figure).

Slenderness 0.6

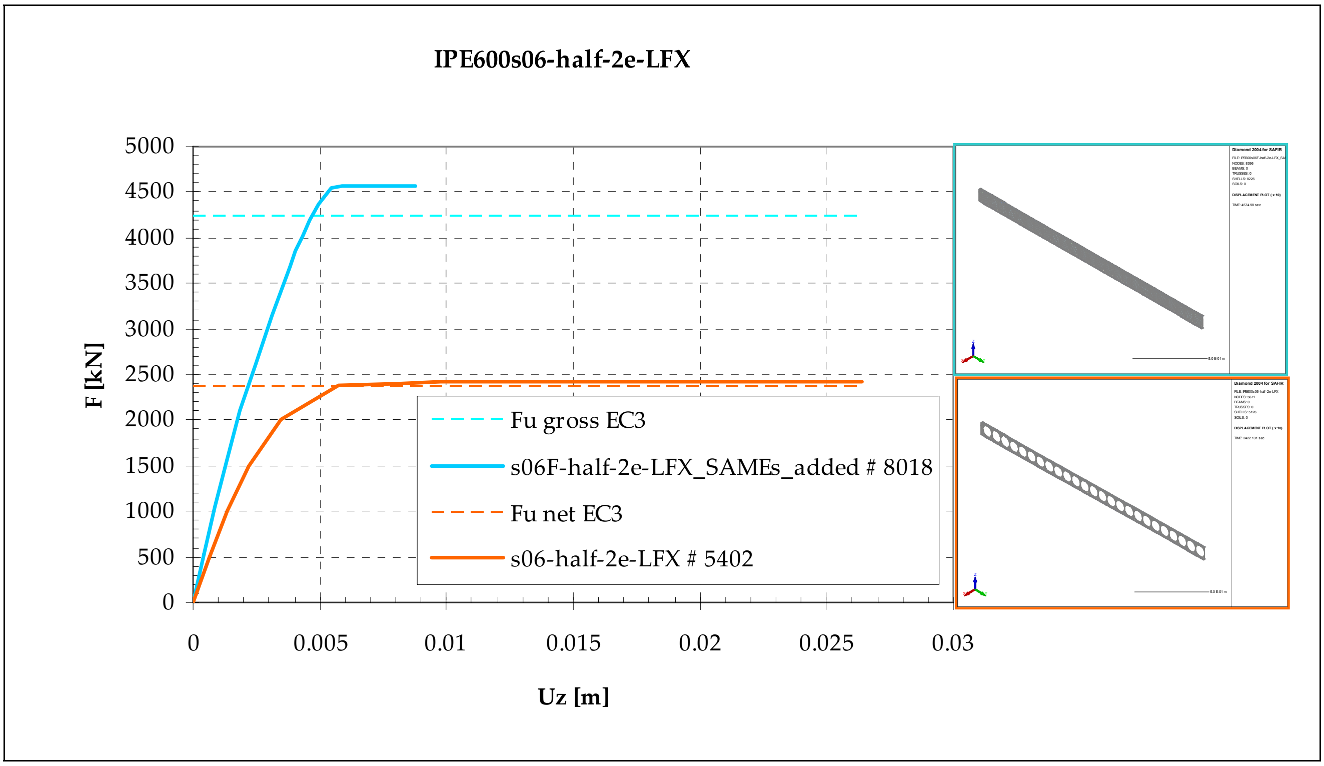

flexural buckling load [kN]	**EC3**	**FEM**	**Δ [%]**
IPE600s06F-half-2e-LFX	4167.1	3576.6	-14.2
IPE600s06F-half-2e-LFX_SAMEs_added	4167.1	4575.0	+9.8
IPE600s06-half-2e-LFX	2295.0	2422.1	+5.5
IPE600s06S355F-half-2e-LFX	6295.0	4210.9	-33.1
IPE600s06S355F-half-2e-LFX_SAMEs_added	6295.0	6934.6	+10.2
IPE600s06S355-half-2e-LFX	3467.0	3653.3	+5.4

By adding additional restraints the plate buckling mode could be eliminated.

For comparison, an additional series of analyses was performed for a cellular member with a gross slenderness (about the strong axis) of $\overline{\lambda} = 0.6$ *as referred to steel grade S355 instead of S235*. It turns out that the behaviour is qualitatively and quantitatively similar.

Slenderness 1.4

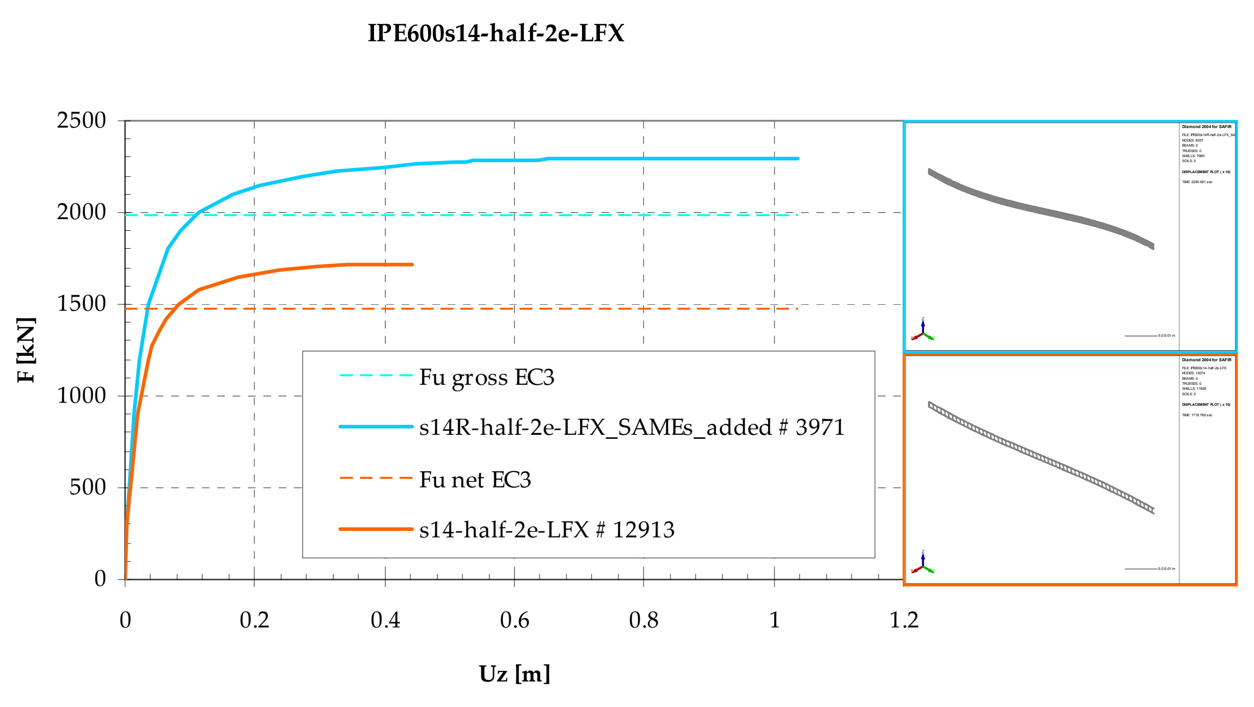

flexural buckling load [kN]	EC3	FEM	Δ [%]
IPE600s14R-half-2e-LFX	1948.2	2289.8	+17.5
IPE600s14R-half-2e-LFX_SAMEs_added	1948.2	2290.1	+17.5
IPE600s14-half-2e-LFX	1437.7	1718.8	+19.6

Again, by adding additional restraints the plate buckling mode could be eliminated.

It is noted here that the displacements are quite high – lateral displacement up to 1.0% of the member length – caused by the relatively high slenderness of the member, which is most often not acceptable in practice.

B.5 Base profile HE200A

B.5.1 Buckling about the weak axis

Slenderness 0.2

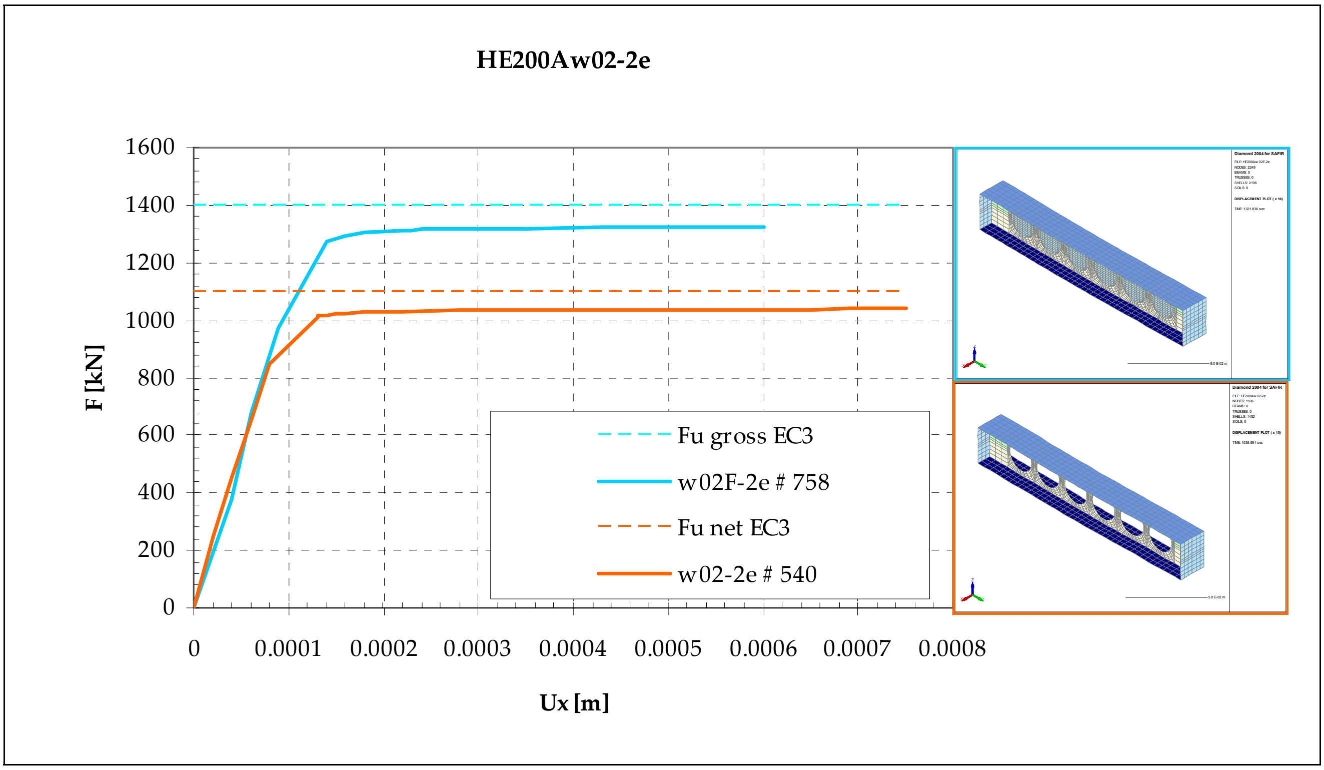

flexural buckling load [kN]	EC3	FEM	Δ [%]
HE200Aw02F-2e	1346.3	1321.8	-1.8
HE200Aw02-2e	1046.9	1038.6	-0.8

Slenderness 0.6

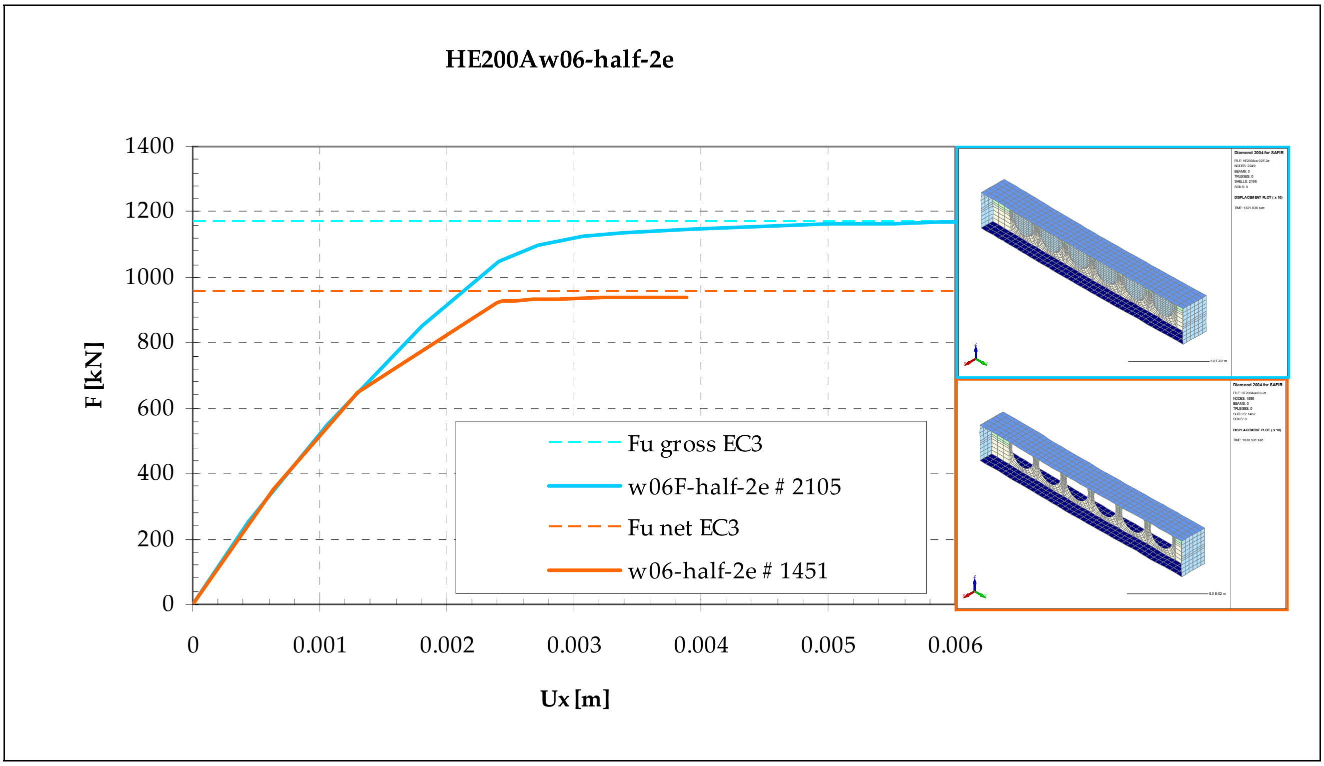

flexural buckling load [kN]	**EC3**	**FEM**	**Δ [%]**
HE200Aw06F-half-2e	1134.0	1168.5	+3.0
HE200Aw06-half-2e	916.3	940.8	+2.7

Slenderness 1.4

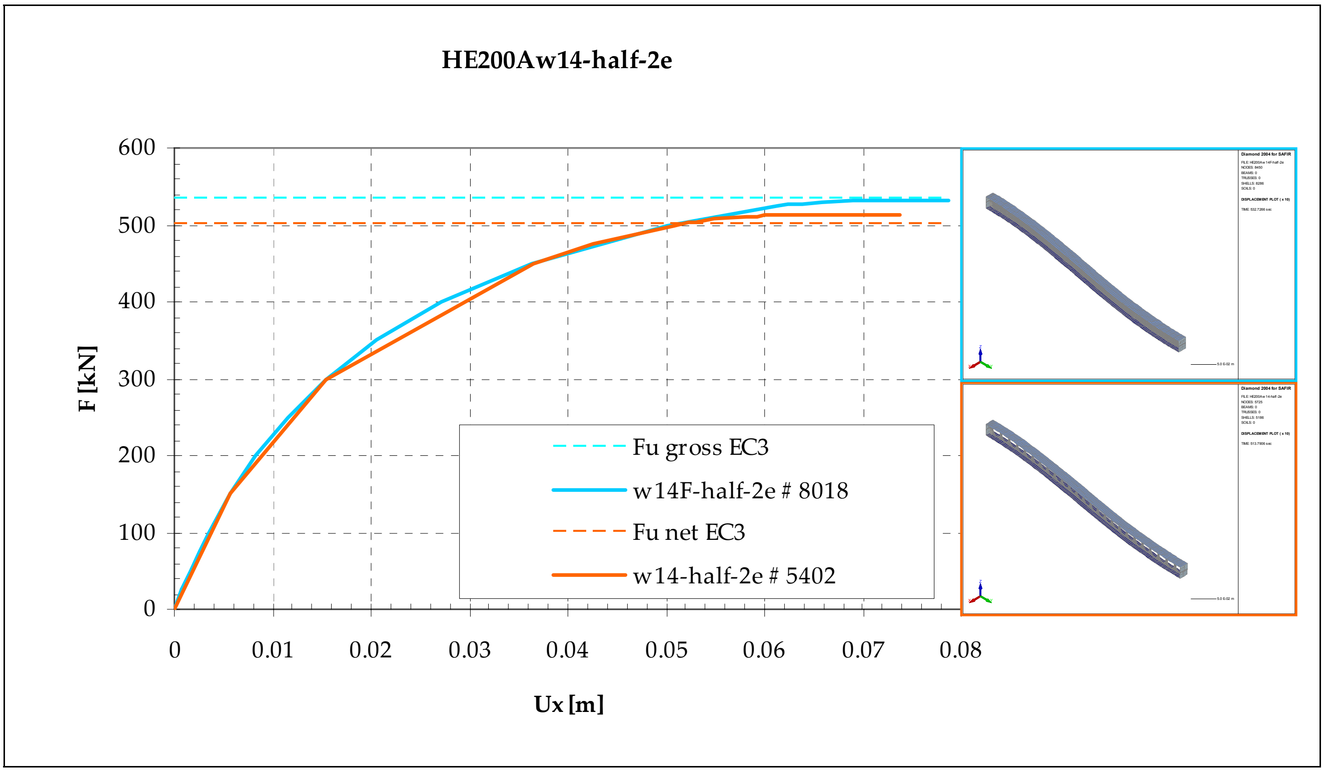

flexural buckling load [kN]	**EC3**	**FEM**	**Δ [%]**
HE200Aw14F-half-2e	528.0	532.7	+0.9
HE200Aw14-half-2e	493.1	513.8	+4.2
HE200Aw14-2e	493.1	513.6	+4.2

The latter – with the whole member modelled instead of a half member – could not be modelled with filled openings, as this would make the model size beyond limits. It turns out that the results of both runs for the cellular member are practically equal.

B.5.2 Buckling about the strong axis

Slenderness 0.2

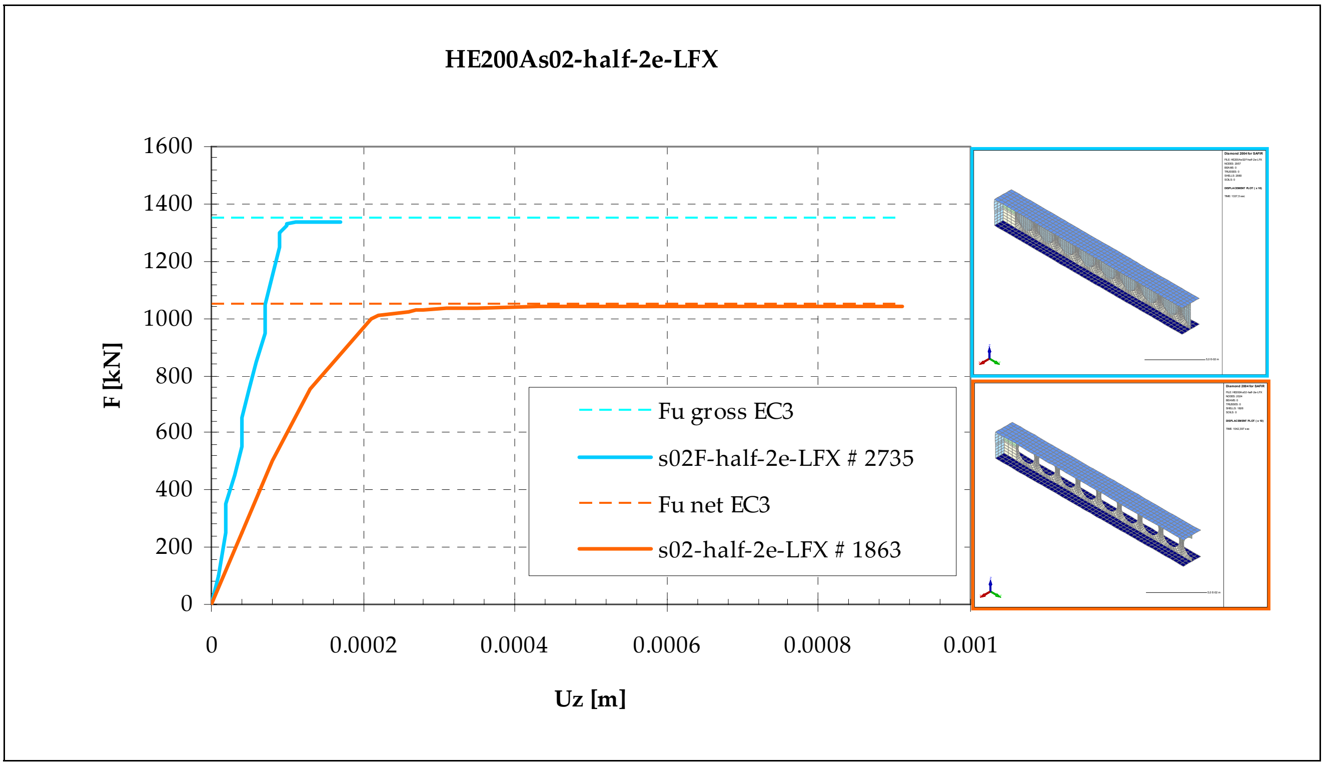

flexural buckling load [kN]	**EC3**	**FEM**	**Δ [%]**
HE200As02F-half-2e-LFX	1346.3	1337.5	-0.7
HE200As02-half-2e-LFX	1046.9	1042.4	-0.4

Slenderness 0.6

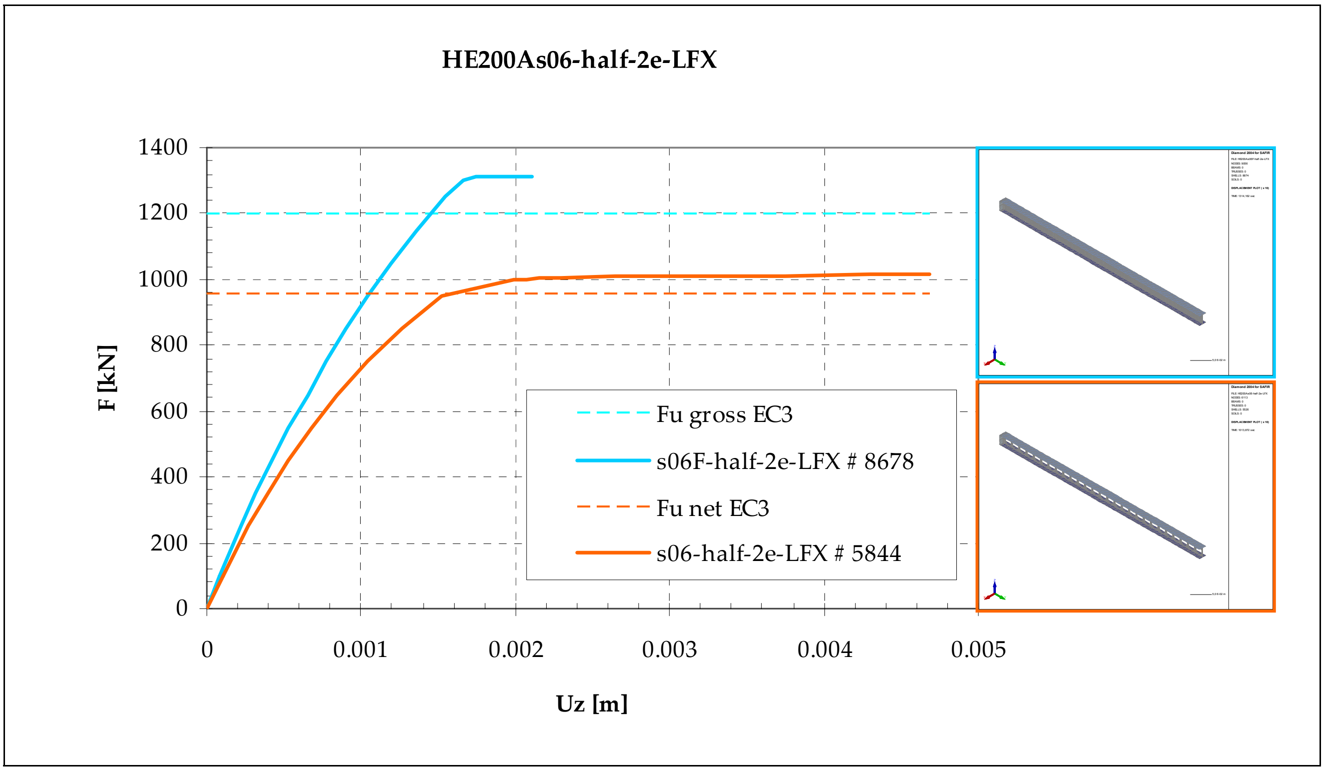

flexural buckling load [kN]	**EC3**	**FEM**	**Δ [%]**
HE200As06F-half-2e-LFX	1197.9	1314.2	+9.7
HE200As06-half-2e-LFX	952.9	1013.9	+6.4

Slenderness 1.3

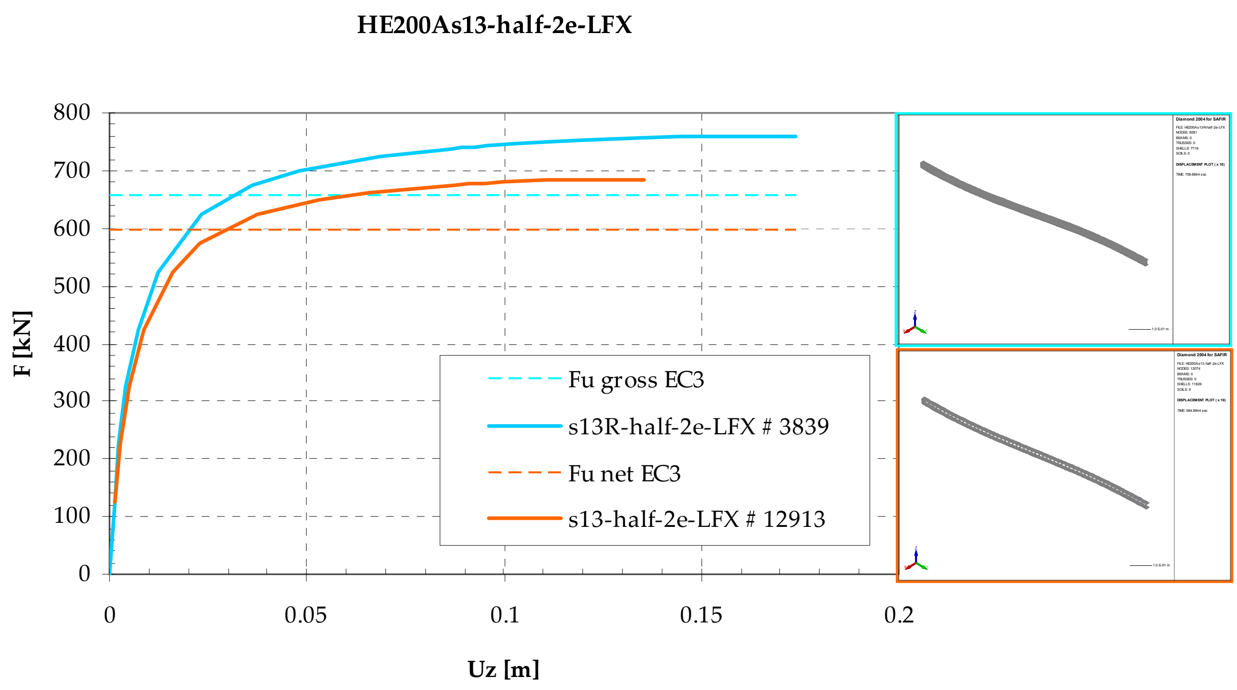

flexural buckling load [kN]	**EC3**	**FEM**	**Δ [%]**
HE200As13R-half-2e-LFX	632.3	759.9	+20.2
HE200As13-half-2e-LFX	569.9	684.9	+20.2

Slenderness 1.4

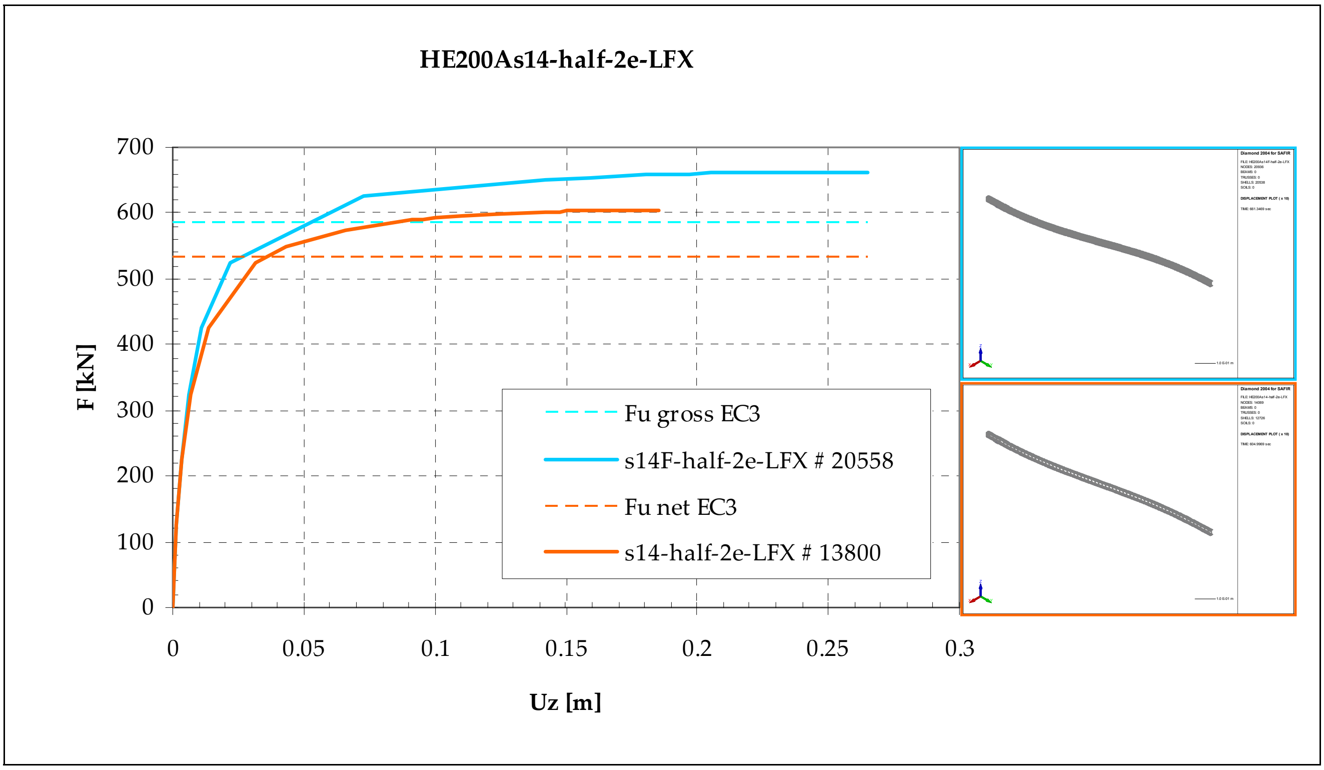

flexural buckling load [kN]	**EC3**	**FEM**	**Δ [%]**
HE200As14F-half-2e-LFX	561.8	661.3	+17.7
HE200As14-half-2e-LFX	511.6	605.0	+18.3

B.6 Base profile HE650M

B.6.1 Buckling about the weak axis

Slenderness 0.2

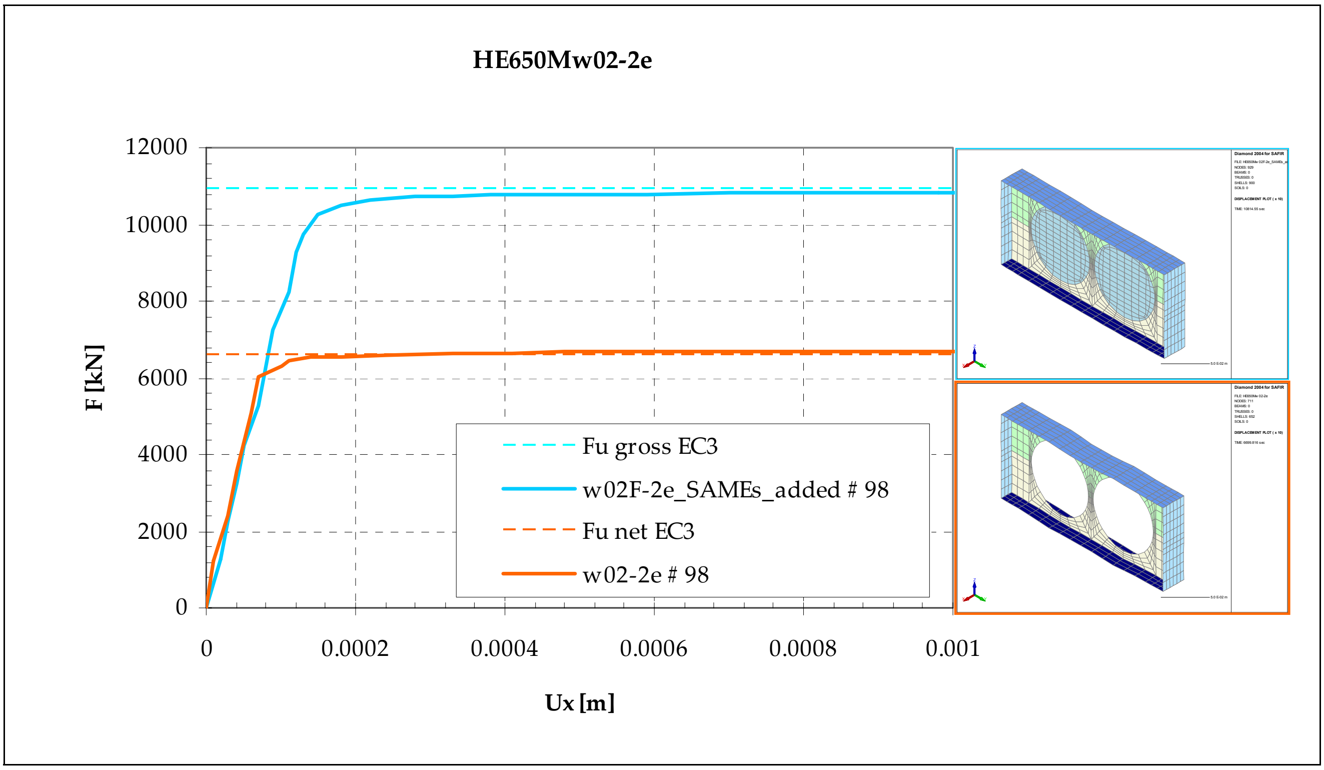

flexural buckling load [kN]	EC3	FEM	Δ [%]
HE650Mw02F-2e	10948.2	10786.1	-1.5
HE650Mw02F-2e_SAMEs_added	10948.2	10814.6	-1.2
HE650Mw02-2e	6622.3	6699.8	+1.2

The additional restraints prevented plate buckling to occur.

Slenderness 0.6

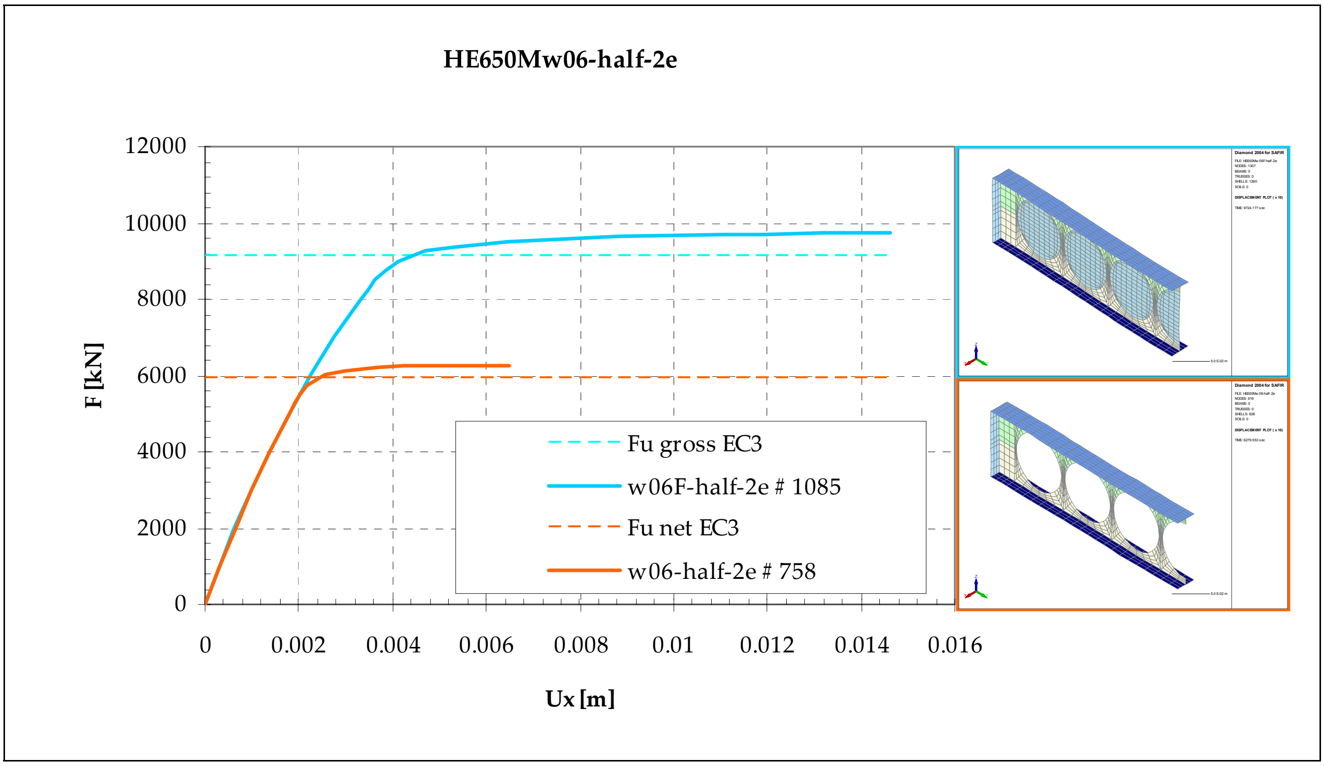

flexural buckling load [kN]	EC3	FEM	Δ [%]
HE650Mw06F-half-2e	9157.1	9724.2	+6.2
HE650Mw06-half-2e	5945.7	6279.6	+5.6

Slenderness 1.4

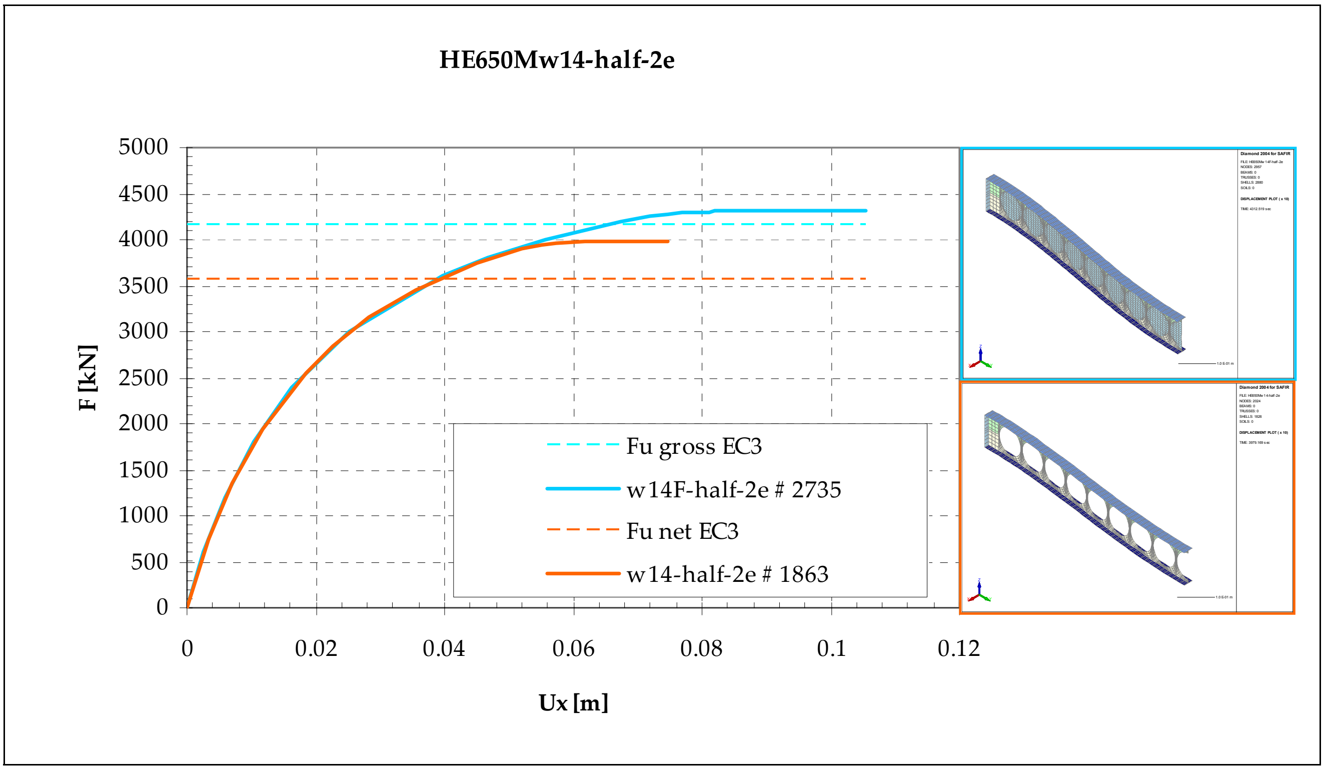

flexural buckling load [kN]	EC3	FEM	Δ [%]
HE650Mw14F-half-2e	4162.3	4312.5	+3.6
HE650Mw14-half-2e	3569.7	3979.2	+11.5

B.6.2 Buckling about the strong axis

Slenderness 0.2

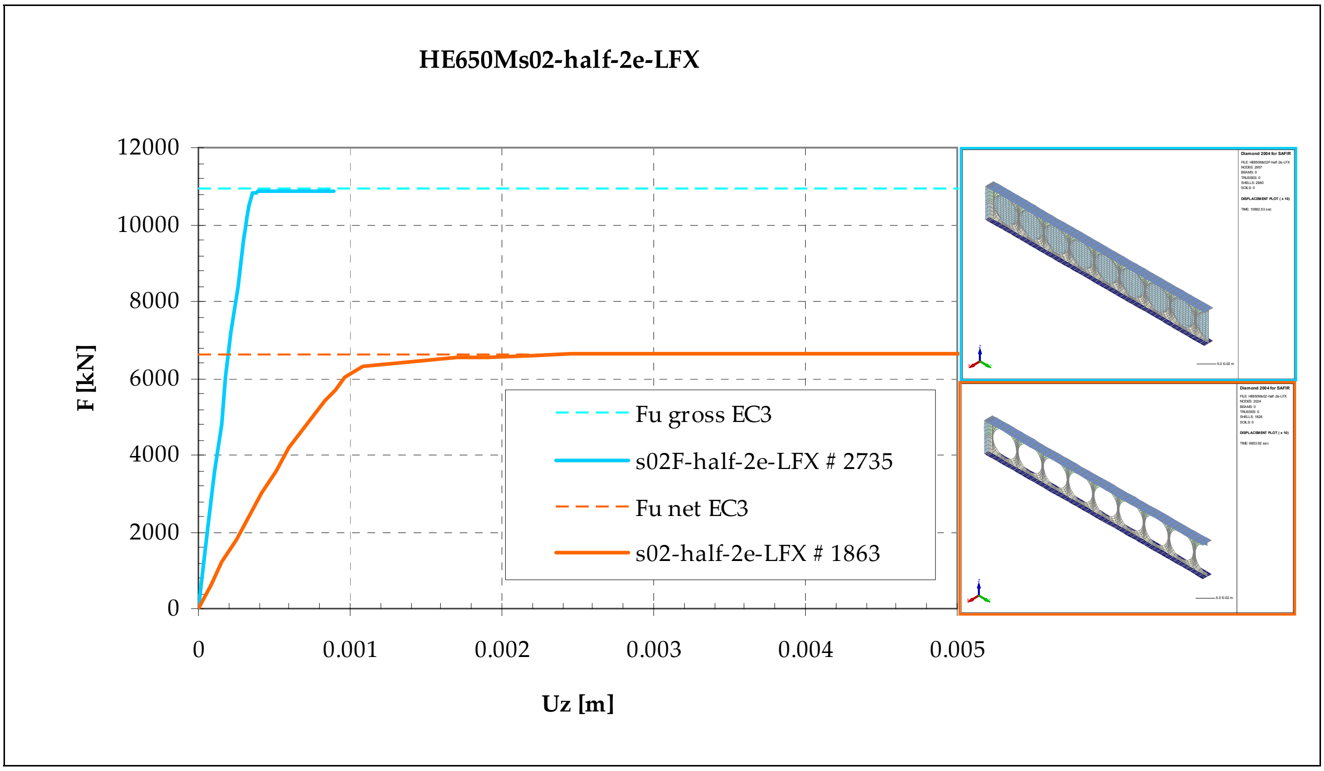

flexural buckling load [kN]	**EC3**	**FEM**	**Δ [%]**
HE650Ms02F-half-2e-LFX	10950.3	10882.5	-0.6
HE650Ms02-half-2e-LFX	6622.3	6653.9	+0.5

Slenderness 0.6

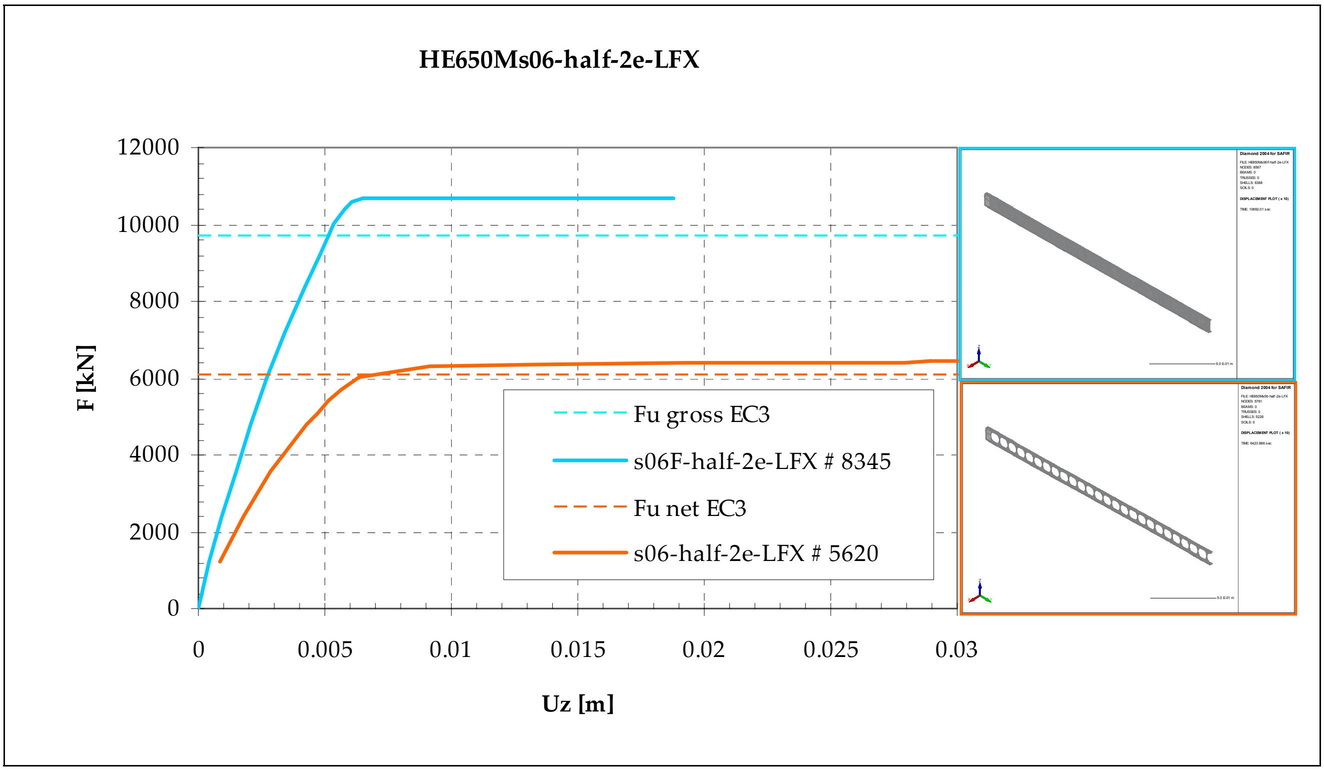

flexural buckling load [kN]	**EC3**	**FEM**	**Δ [%]**
HE650Ms06F-half-2e-LFX	9749.5	10692.0	+9.7
HE650Ms06-half-2e-LFX	6120.2	6423.9	+5.0

Slenderness 1.4

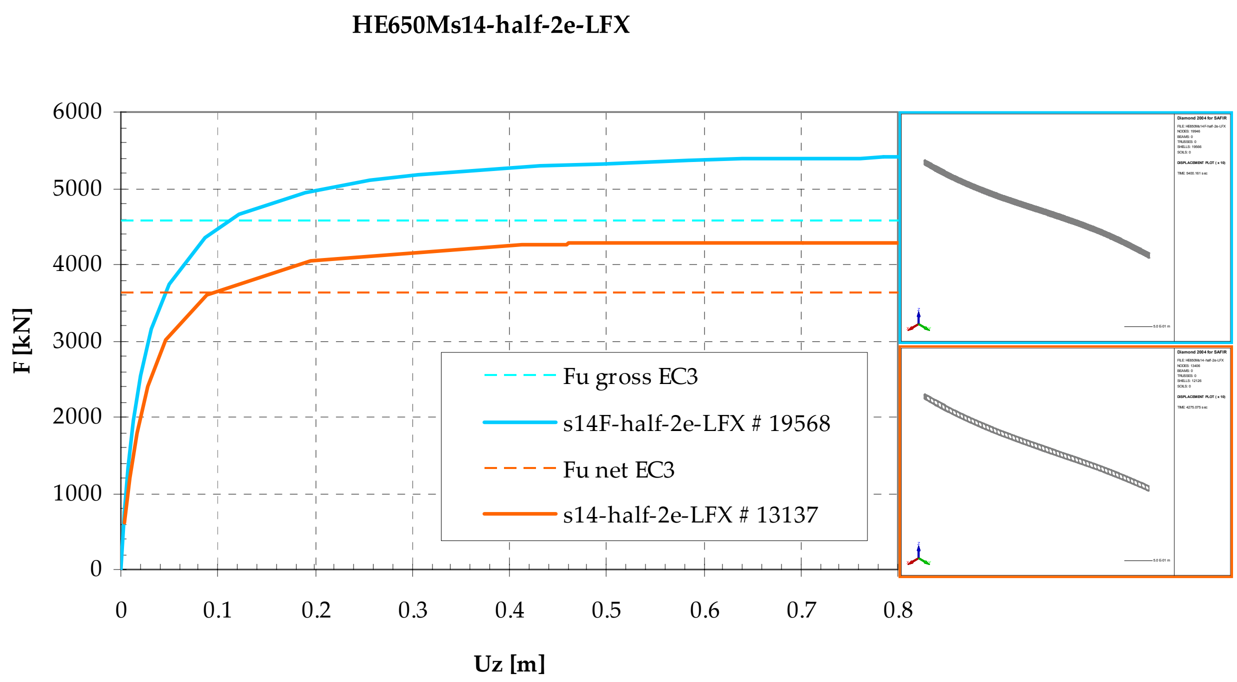

flexural buckling load [kN]	**EC3**	**FEM**	**Δ [%]**
HE650Ms14F-half-2e-LFX	4587.6	5400.2	+17.7
HE650Ms14-half-2e-LFX	3648.4	4275.1	+17.2

C FEM RESULTS OF PARAMETER STUDY INTO WEB-POST BUCKLING

C.1 Introduction

This Annex presents the results of the numerical analysis of web-post buckling of cellular members, also subjected to a axial compressive force.
For each base section, two web-post widths were analysed. The FEM results are presented here separately for the ACB and the LWO model. These results have been discussed in Chapter 8.

The calculations according to both theoretical models have been done using a number of Excel-spreadsheets. These are illustrated hereafter briefly. Extensive use has been made of macros in order to automate searching for the ultimate load.

C.1.1 Arcelor model for web-post buckling

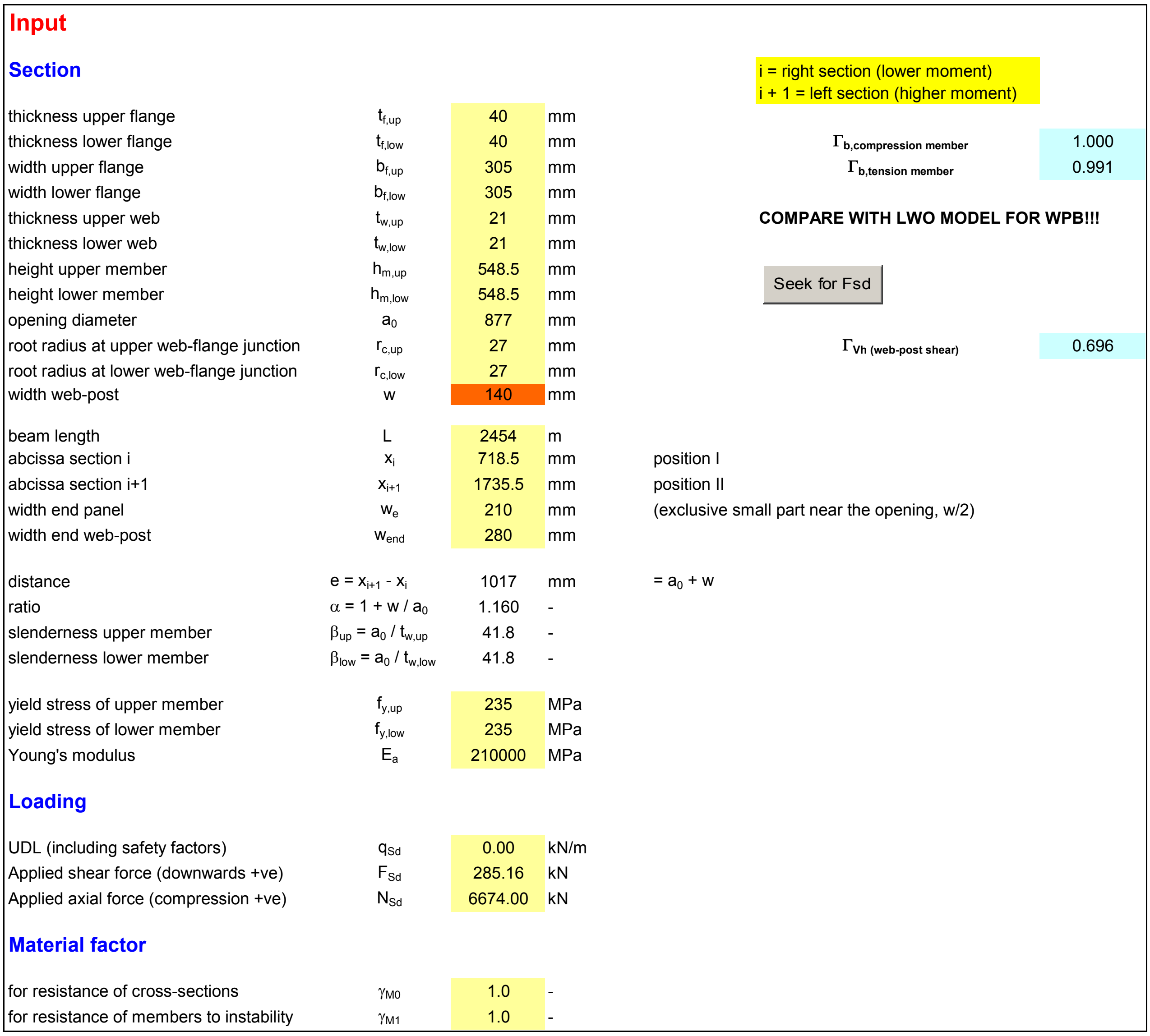

Input

Section

i = right section (lower moment)
i + 1 = left section (higher moment)

thickness upper flange	$t_{f,up}$	40	mm
thickness lower flange	$t_{f,low}$	40	mm
width upper flange	$b_{f,up}$	305	mm
width lower flange	$b_{f,low}$	305	mm
thickness upper web	$t_{w,up}$	21	mm
thickness lower web	$t_{w,low}$	21	mm
height upper member	$h_{m,up}$	548.5	mm
height lower member	$h_{m,low}$	548.5	mm
opening diameter	a_0	877	mm
root radius at upper web-flange junction	$r_{c,up}$	27	mm
root radius at lower web-flange junction	$r_{c,low}$	27	mm
width web-post	w	140	mm

$\Gamma_{b,compression\ member}$ 1.000
$\Gamma_{b,tension\ member}$ 0.991

COMPARE WITH LWO MODEL FOR WPB!!!

Seek for Fsd

$\Gamma_{Vh\ (web\text{-}post\ shear)}$ 0.696

beam length	L	2454	m	
abcissa section i	x_i	718.5	mm	position I
abcissa section i+1	x_{i+1}	1735.5	mm	position II
width end panel	w_e	210	mm	(exclusive small part near the opening, w/2)
width end web-post	w_{end}	280	mm	

distance	$e = x_{i+1} - x_i$	1017	mm	$= a_0 + w$
ratio	$\alpha = 1 + w / a_0$	1.160	-	
slenderness upper member	$\beta_{up} = a_0 / t_{w,up}$	41.8	-	
slenderness lower member	$\beta_{low} = a_0 / t_{w,low}$	41.8	-	

yield stress of upper member	$f_{y,up}$	235	MPa
yield stress of lower member	$f_{y,low}$	235	MPa
Young's modulus	E_a	210000	MPa

Loading

UDL (including safety factors)	q_{Sd}	0.00	kN/m
Applied shear force (downwards +ve)	F_{Sd}	285.16	kN
Applied axial force (compression +ve)	N_{Sd}	6674.00	kN

Material factor

for resistance of cross-sections	γ_{M0}	1.0	-
for resistance of members to instability	γ_{M1}	1.0	-

Worksheet "Input" – Geometrical data and loading

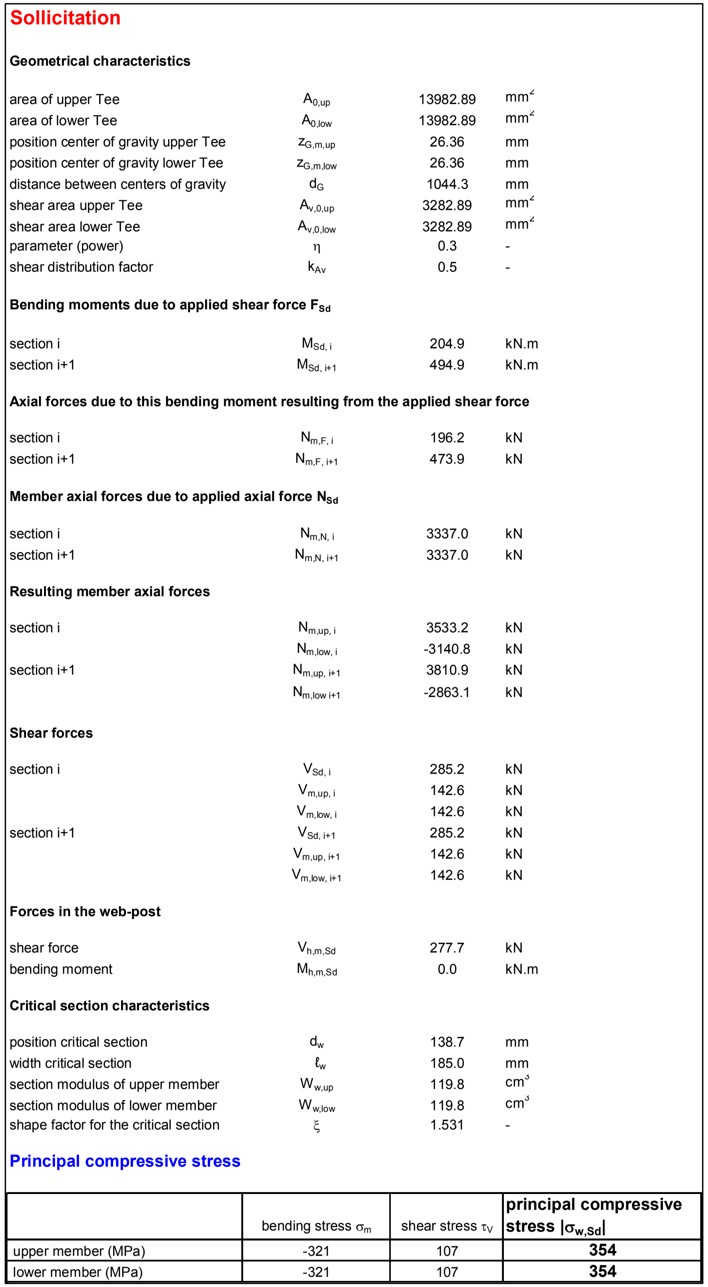

Sollicitation			
Geometrical characteristics			
area of upper Tee	$A_{0,up}$	13982.89	mm²
area of lower Tee	$A_{0,low}$	13982.89	mm²
position center of gravity upper Tee	$z_{G,m,up}$	26.36	mm
position center of gravity lower Tee	$z_{G,m,low}$	26.36	mm
distance between centers of gravity	d_G	1044.3	mm
shear area upper Tee	$A_{v,0,up}$	3282.89	mm²
shear area lower Tee	$A_{v,0,low}$	3282.89	mm²
parameter (power)	η	0.3	-
shear distribution factor	k_{Av}	0.5	-
Bending moments due to applied shear force F_{Sd}			
section i	$M_{Sd,\,i}$	204.9	kN.m
section i+1	$M_{Sd,\,i+1}$	494.9	kN.m
Axial forces due to this bending moment resulting from the applied shear force			
section i	$N_{m,F,\,i}$	196.2	kN
section i+1	$N_{m,F,\,i+1}$	473.9	kN
Member axial forces due to applied axial force N_{Sd}			
section i	$N_{m,N,\,i}$	3337.0	kN
section i+1	$N_{m,N,\,i+1}$	3337.0	kN
Resulting member axial forces			
section i	$N_{m,up,\,i}$	3533.2	kN
	$N_{m,low,\,i}$	-3140.8	kN
section i+1	$N_{m,up,\,i+1}$	3810.9	kN
	$N_{m,low\,i+1}$	-2863.1	kN
Shear forces			
section i	$V_{Sd,\,i}$	285.2	kN
	$V_{m,up,\,i}$	142.6	kN
	$V_{m,low,\,i}$	142.6	kN
section i+1	$V_{Sd,\,i+1}$	285.2	kN
	$V_{m,up,\,i+1}$	142.6	kN
	$V_{m,low,\,i+1}$	142.6	kN
Forces in the web-post			
shear force	$V_{h,m,Sd}$	277.7	kN
bending moment	$M_{h,m,Sd}$	0.0	kN.m
Critical section characteristics			
position critical section	d_w	138.7	mm
width critical section	ℓ_w	185.0	mm
section modulus of upper member	$W_{w,up}$	119.8	cm³
section modulus of lower member	$W_{w,low}$	119.8	cm³
shape factor for the critical section	ξ	1.531	-

Principal compressive stress

	bending stress σ_m	shear stress τ_V	**principal compressive stress $\lvert\sigma_{w,Sd}\rvert$**
upper member (MPa)	-321	107	**354**
lower member (MPa)	-321	107	**354**

Worksheet “Sollicitation” – Calculation of internal forces and stresses

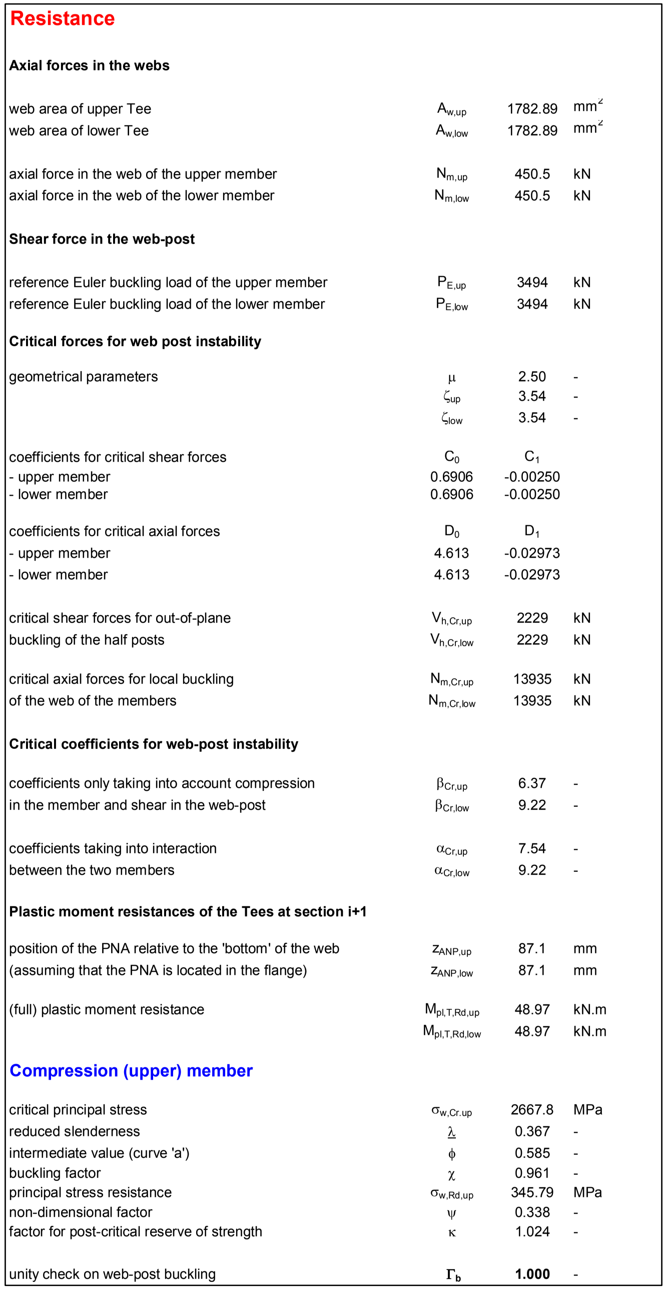

Resistance			
Axial forces in the webs			
web area of upper Tee	$A_{w,up}$	1782.89	mm²
web area of lower Tee	$A_{w,low}$	1782.89	mm²
axial force in the web of the upper member	$N_{m,up}$	450.5	kN
axial force in the web of the lower member	$N_{m,low}$	450.5	kN
Shear force in the web-post			
reference Euler buckling load of the upper member	$P_{E,up}$	3494	kN
reference Euler buckling load of the lower member	$P_{E,low}$	3494	kN
Critical forces for web post instability			
geometrical parameters	μ	2.50	-
	ζ_{up}	3.54	-
	ζ_{low}	3.54	-
coefficients for critical shear forces	C_0	C_1	
- upper member	0.6906	-0.00250	
- lower member	0.6906	-0.00250	
coefficients for critical axial forces	D_0	D_1	
- upper member	4.613	-0.02973	
- lower member	4.613	-0.02973	
critical shear forces for out-of-plane	$V_{h,Cr,up}$	2229	kN
buckling of the half posts	$V_{h,Cr,low}$	2229	kN
critical axial forces for local buckling	$N_{m,Cr,up}$	13935	kN
of the web of the members	$N_{m,Cr,low}$	13935	kN
Critical coefficients for web-post instability			
coefficients only taking into account compression	$\beta_{Cr,up}$	6.37	-
in the member and shear in the web-post	$\beta_{Cr,low}$	9.22	-
coefficients taking into interaction	$\alpha_{Cr,up}$	7.54	-
between the two members	$\alpha_{Cr,low}$	9.22	-
Plastic moment resistances of the Tees at section i+1			
position of the PNA relative to the 'bottom' of the web	$z_{ANP,up}$	87.1	mm
(assuming that the PNA is located in the flange)	$z_{ANP,low}$	87.1	mm
(full) plastic moment resistance	$M_{pl,T,Rd,up}$	48.97	kN.m
	$M_{pl,T,Rd,low}$	48.97	kN.m
Compression (upper) member			
critical principal stress	$\sigma_{w,Cr,up}$	2667.8	MPa
reduced slenderness	$\underline{\lambda}$	0.367	-
intermediate value (curve 'a')	ϕ	0.585	-
buckling factor	χ	0.961	-
principal stress resistance	$\sigma_{w,Rd,up}$	345.79	MPa
non-dimensional factor	ψ	0.338	-
factor for post-critical reserve of strength	κ	1.024	-
unity check on web-post buckling	Γ_b	**1.000**	-

Worksheet “Resistance” – Verification against web-post buckling

C.1.2 Arcelor model for Vierendeel bending

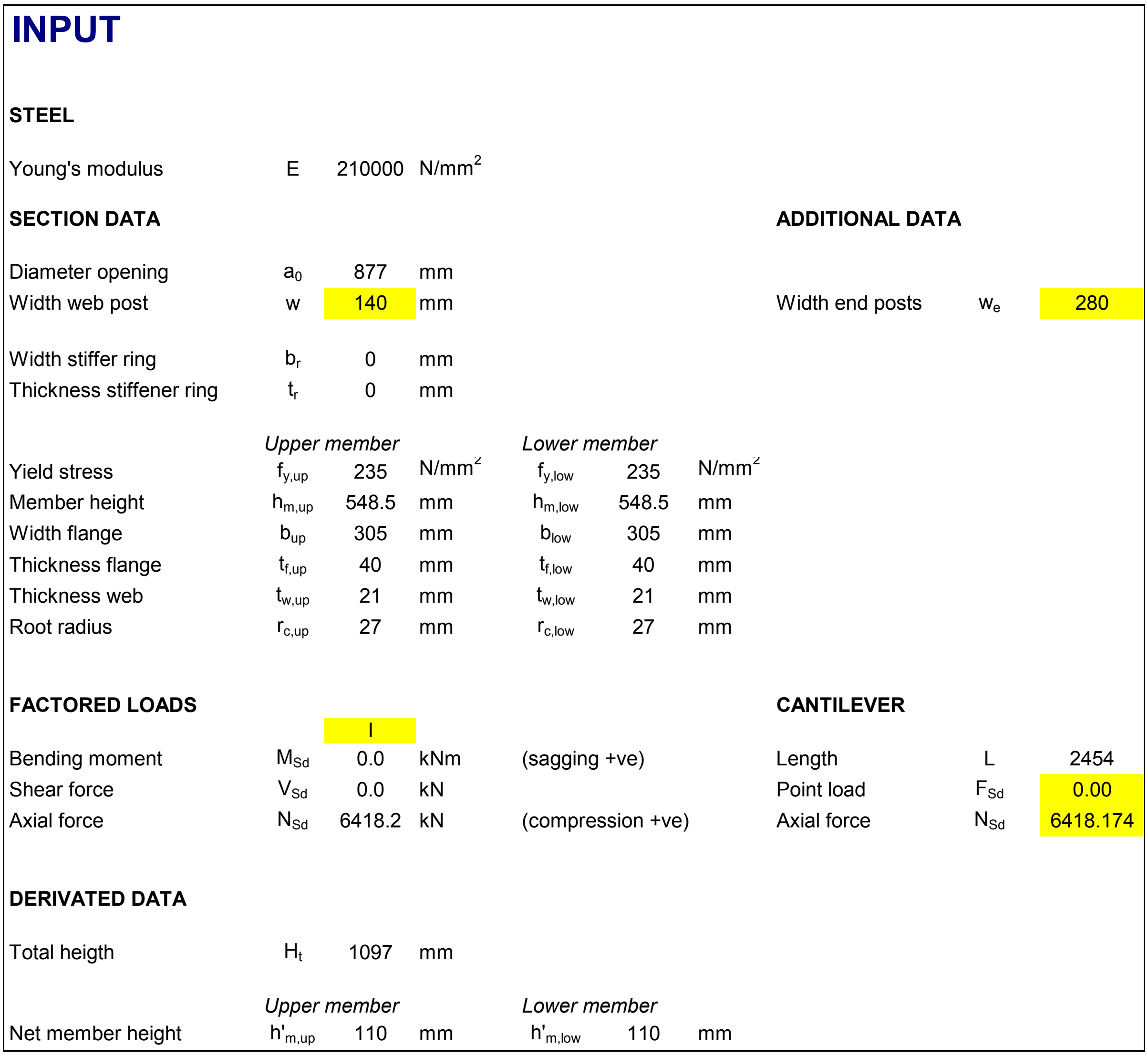

INPUT

STEEL

Young's modulus	E	210000	N/mm^2

SECTION DATA

Diameter opening	a_0	877	mm
Width web post	w	140	mm
Width stiffer ring	b_r	0	mm
Thickness stiffener ring	t_r	0	mm

ADDITIONAL DATA

Width end posts	w_e	280

	Upper member			*Lower member*		
Yield stress	$f_{y,up}$	235	N/mm^2	$f_{y,low}$	235	N/mm^2
Member height	$h_{m,up}$	548.5	mm	$h_{m,low}$	548.5	mm
Width flange	b_{up}	305	mm	b_{low}	305	mm
Thickness flange	$t_{f,up}$	40	mm	$t_{f,low}$	40	mm
Thickness web	$t_{w,up}$	21	mm	$t_{w,low}$	21	mm
Root radius	$r_{c,up}$	27	mm	$r_{c,low}$	27	mm

FACTORED LOADS

		I		
Bending moment	M_{Sd}	0.0	kNm	(sagging +ve)
Shear force	V_{Sd}	0.0	kN	
Axial force	N_{Sd}	6418.2	kN	(compression +ve)

CANTILEVER

Length	L	2454
Point load	F_{Sd}	0.00
Axial force	N_{Sd}	6418.174

DERIVATED DATA

Total heigth	H_t	1097	mm

	Upper member			*Lower member*		
Net member height	$h'_{m,up}$	110	mm	$h'_{m,low}$	110	mm

Worksheet "Input" – Geometrical data and loading

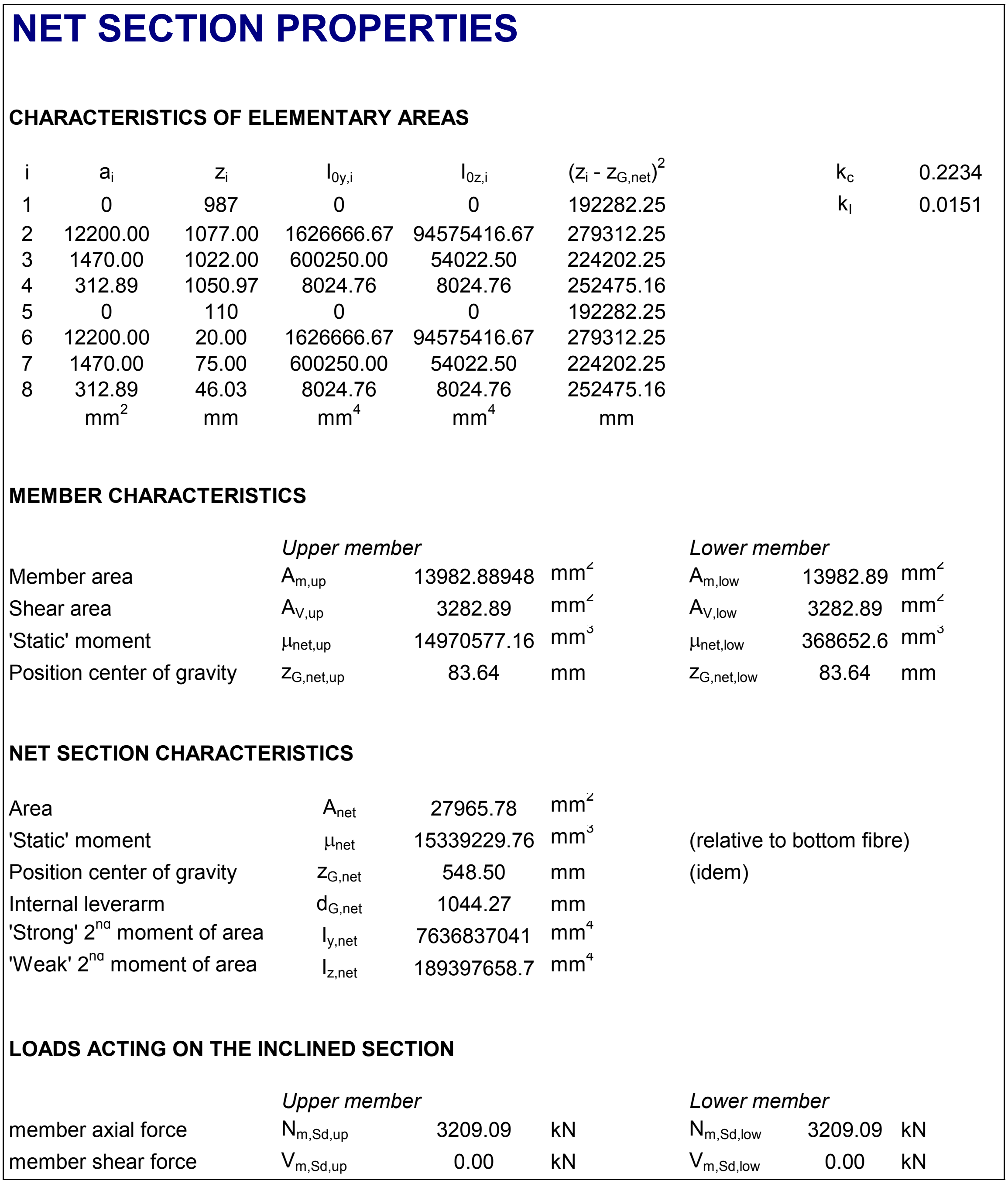

NET SECTION PROPERTIES

CHARACTERISTICS OF ELEMENTARY AREAS

i	a_i	z_i	$I_{0y,i}$	$I_{0z,i}$	$(z_i - z_{G,net})^2$
1	0	987	0	0	192282.25
2	12200.00	1077.00	1626666.67	94575416.67	279312.25
3	1470.00	1022.00	600250.00	54022.50	224202.25
4	312.89	1050.97	8024.76	8024.76	252475.16
5	0	110	0	0	192282.25
6	12200.00	20.00	1626666.67	94575416.67	279312.25
7	1470.00	75.00	600250.00	54022.50	224202.25
8	312.89	46.03	8024.76	8024.76	252475.16
	mm^2	mm	mm^4	mm^4	mm

k_c	0.2234
k_l	0.0151

MEMBER CHARACTERISTICS

	Upper member			*Lower member*		
Member area	$A_{m,up}$	13982.88948	mm^2	$A_{m,low}$	13982.89	mm^2
Shear area	$A_{V,up}$	3282.89	mm^2	$A_{V,low}$	3282.89	mm^2
'Static' moment	$\mu_{net,up}$	14970577.16	mm^3	$\mu_{net,low}$	368652.6	mm^3
Position center of gravity	$z_{G,net,up}$	83.64	mm	$z_{G,net,low}$	83.64	mm

NET SECTION CHARACTERISTICS

Area	A_{net}	27965.78	mm^2	
'Static' moment	μ_{net}	15339229.76	mm^3	(relative to bottom fibre)
Position center of gravity	$z_{G,net}$	548.50	mm	(idem)
Internal leverarm	$d_{G,net}$	1044.27	mm	
'Strong' 2nd moment of area	$I_{y,net}$	7636837041	mm^4	
'Weak' 2nd moment of area	$I_{z,net}$	189397658.7	mm^4	

LOADS ACTING ON THE INCLINED SECTION

	Upper member			*Lower member*		
member axial force	$N_{m,Sd,up}$	3209.09	kN	$N_{m,Sd,low}$	3209.09	kN
member shear force	$V_{m,Sd,up}$	0.00	kN	$V_{m,Sd,low}$	0.00	kN

Worksheet “Net section” – Geometrical properties of the net section

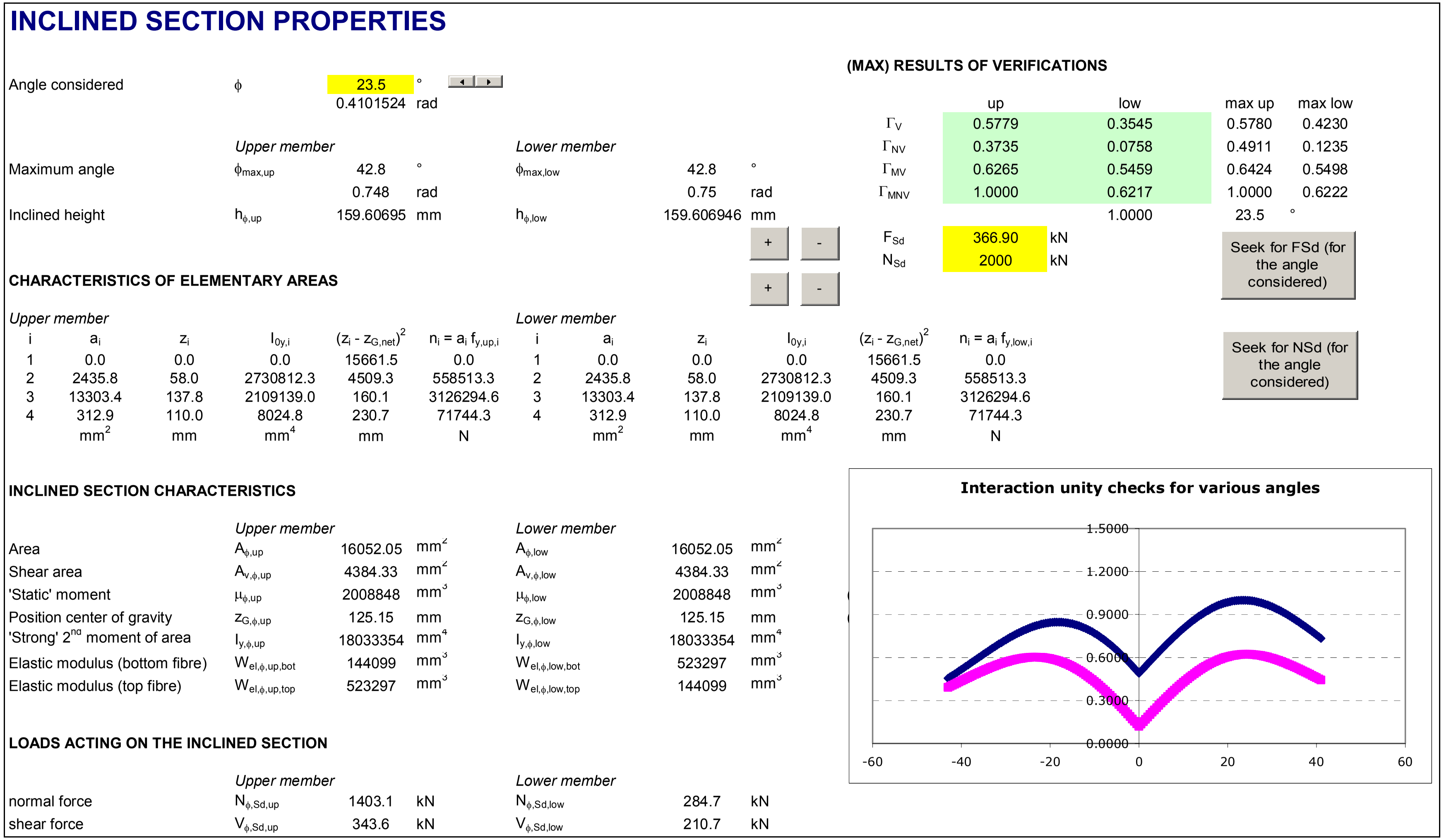

INCLINED SECTION PROPERTIES

Angle considered	ϕ	23.5	°				
		0.4101524	rad				
	Upper member			*Lower member*			
Maximum angle	$\phi_{max,up}$	42.8	°	$\phi_{max,low}$	42.8	°	
		0.748	rad		0.75	rad	
Inclined height	$h_{\phi,up}$	159.60695	mm	$h_{\phi,low}$	159.606946	mm	

(MAX) RESULTS OF VERIFICATIONS

	up	low	max up	max low
Γ_V	0.5779	0.3545	0.5780	0.4230
Γ_{NV}	0.3735	0.0758	0.4911	0.1235
Γ_{MV}	0.6265	0.5459	0.6424	0.5498
Γ_{MNV}	1.0000	0.6217	1.0000	0.6222
		1.0000	23.5	°

F_{Sd} 366.90 kN

N_{Sd} 2000 kN

Seek for FSd (for the angle considered)

Seek for NSd (for the angle considered)

CHARACTERISTICS OF ELEMENTARY AREAS

Upper member

i	a_i	z_i	$I_{0y,i}$	$(z_i - z_{G,net})^2$	$n_i = a_i\, f_{y,up,i}$
1	0.0	0.0	0.0	15661.5	0.0
2	2435.8	58.0	2730812.3	4509.3	558513.3
3	13303.4	137.8	2109139.0	160.1	3126294.6
4	312.9	110.0	8024.8	230.7	71744.3
	mm^2	mm	mm^4	mm	N

Lower member

i	a_i	z_i	$I_{0y,i}$	$(z_i - z_{G,net})^2$	$n_i = a_i\, f_{y,low,i}$
1	0.0	0.0	0.0	15661.5	0.0
2	2435.8	58.0	2730812.3	4509.3	558513.3
3	13303.4	137.8	2109139.0	160.1	3126294.6
4	312.9	110.0	8024.8	230.7	71744.3
	mm^2	mm	mm^4	mm	N

INCLINED SECTION CHARACTERISTICS

	Upper member			*Lower member*		
Area	$A_{\phi,up}$	16052.05	mm^2	$A_{\phi,low}$	16052.05	mm^2
Shear area	$A_{v,\phi,up}$	4384.33	mm^2	$A_{v,\phi,low}$	4384.33	mm^2
'Static' moment	$\mu_{\phi,up}$	2008848	mm^3	$\mu_{\phi,low}$	2008848	mm^3
Position center of gravity	$z_{G,\phi,up}$	125.15	mm	$z_{G,\phi,low}$	125.15	mm
'Strong' 2nd moment of area	$I_{y,\phi,up}$	18033354	mm^4	$I_{y,\phi,low}$	18033354	mm^4
Elastic modulus (bottom fibre)	$W_{el,\phi,up,bot}$	144099	mm^3	$W_{el,\phi,low,bot}$	523297	mm^3
Elastic modulus (top fibre)	$W_{el,\phi,up,top}$	523297	mm^3	$W_{el,\phi,low,top}$	144099	mm^3

LOADS ACTING ON THE INCLINED SECTION

	Upper member			*Lower member*		
normal force	$N_{\phi,Sd,up}$	1403.1	kN	$N_{\phi,Sd,low}$	284.7	kN
shear force	$V_{\phi,Sd,up}$	343.6	kN	$V_{\phi,Sd,low}$	210.7	kN

Worksheet "Inclined section" – Verification against Vierendeel bending

C.1.3 LWO model for both web-post buckling and Vierendeel bending

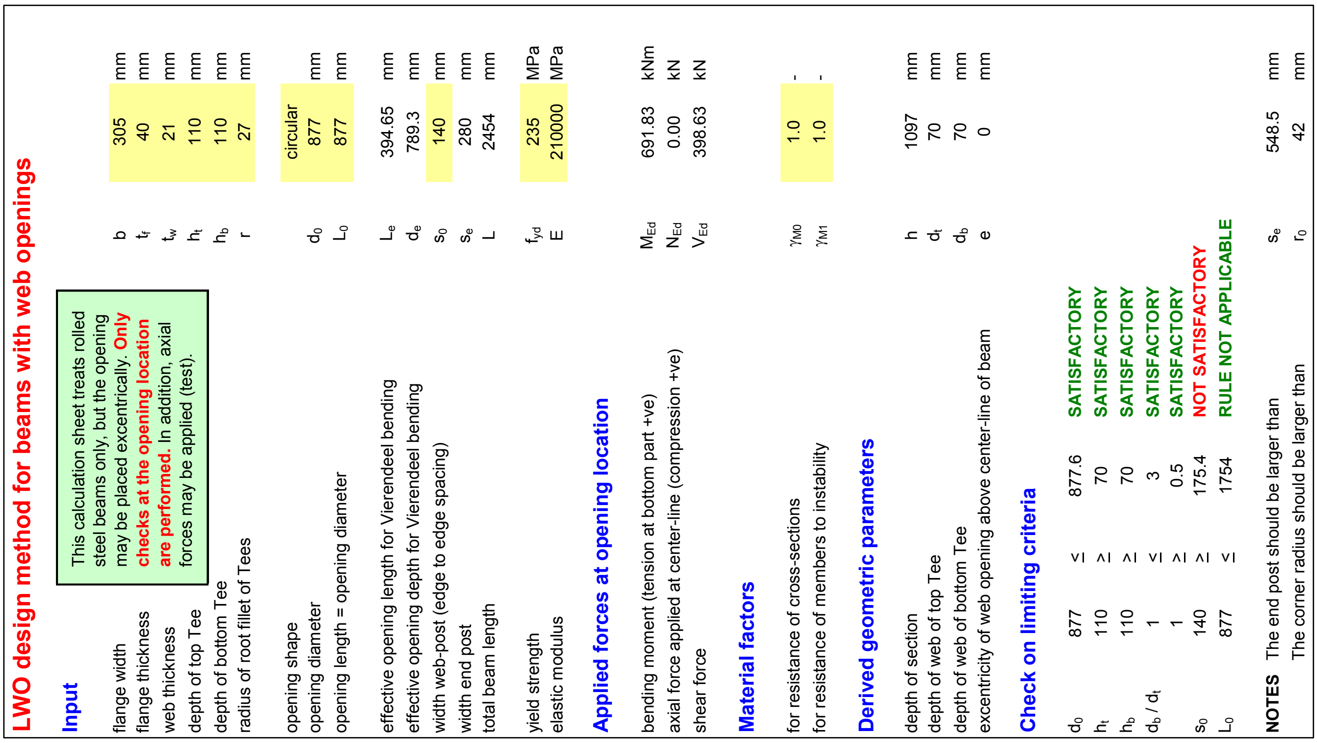

LWO design method for beams with web openings

Input

This calculation sheet treats rolled steel beams only, but the opening may be placed excentrically. **Only checks at the opening location are performed.** In addition, axial forces may be applied (test).

flange width	b	305	mm
flange thickness	t_f	40	mm
web thickness	t_w	21	mm
depth of top Tee	h_t	110	mm
depth of bottom Tee	h_b	110	mm
radius of root fillet of Tees	r	27	mm
opening shape		circular	
opening diameter	d_0	877	mm
opening length = opening diameter	L_0	877	mm
effective opening length for Vierendeel bending	L_e	394.65	mm
effective opening depth for Vierendeel bending	d_e	789.3	mm
width web-post (edge to edge spacing)	s_0	140	mm
width end post	s_e	280	mm
total beam length	L	2454	mm
yield strength	f_{yd}	235	MPa
elastic modulus	E	210000	MPa

Applied forces at opening location

bending moment (tension at bottom part +ve)	M_{Ed}	691.83	kNm
axial force applied at center-line (compression +ve)	N_{Ed}	0.00	kN
shear force	V_{Ed}	398.63	kN

Material factors

for resistance of cross-sections	γ_{M0}	1.0	-
for resistance of members to instability	γ_{M1}	1.0	-

Derived geometric parameters

depth of section	h	1097	mm
depth of web of top Tee	d_t	70	mm
depth of web of bottom Tee	d_b	70	mm
excentricity of web opening above center-line of beam	e	0	mm

Check on limiting criteria

d_0	877	≤	877.6	SATISFACTORY
h_t	110	≥	70	SATISFACTORY
h_b	110	≥	70	SATISFACTORY
d_b / d_t	1	≤	3	SATISFACTORY
	1	≥	0.5	SATISFACTORY
s_0	140	≥	175.4	NOT SATISFACTORY
L_0	877	≤	1754	RULE NOT APPLICABLE

NOTES	The end post should be larger than	s_e	548.5	mm
	The corner radius should be larger than	r_0	42	mm

Worksheet “Input” (Part 1) - Geometrical data and loading

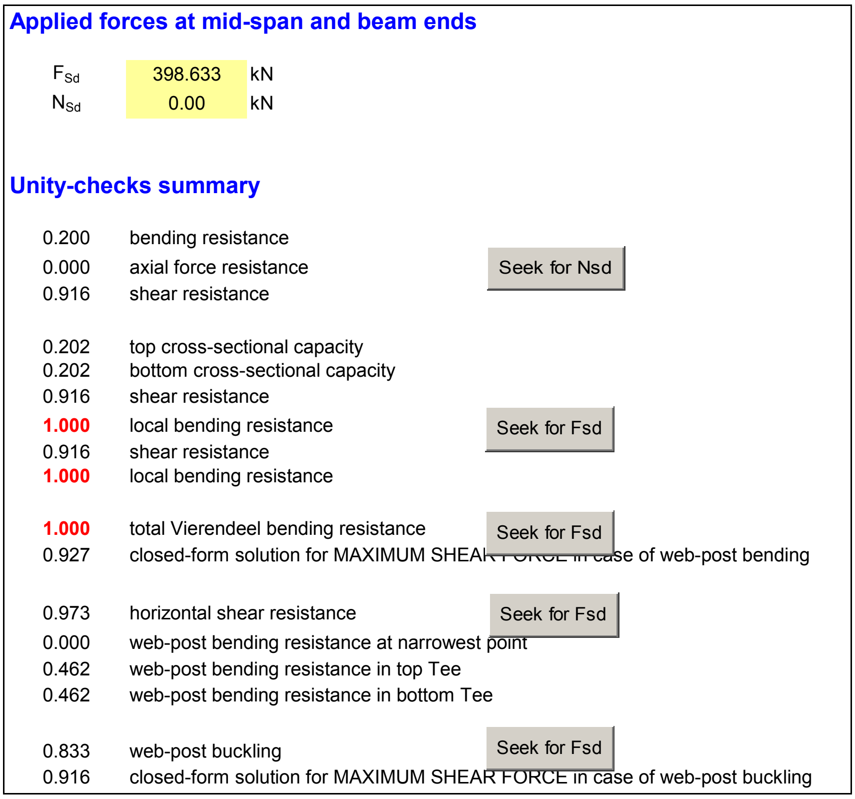

Applied forces at mid-span and beam ends

F_{Sd}	398.633	kN
N_{Sd}	0.00	kN

Unity-checks summary

0.200	bending resistance
0.000	axial force resistance
0.916	shear resistance
0.202	top cross-sectional capacity
0.202	bottom cross-sectional capacity
0.916	shear resistance
1.000	local bending resistance
0.916	shear resistance
1.000	local bending resistance
1.000	total Vierendeel bending resistance
0.927	closed-form solution for MAXIMUM SHEAR FORCE in case of web-post bending
0.973	horizontal shear resistance
0.000	web-post bending resistance at narrowest point
0.462	web-post bending resistance in top Tee
0.462	web-post bending resistance in bottom Tee
0.833	web-post buckling
0.916	closed-form solution for MAXIMUM SHEAR FORCE in case of web-post buckling

Worksheet “Input” (Part 2) – Loads and overview of verification results

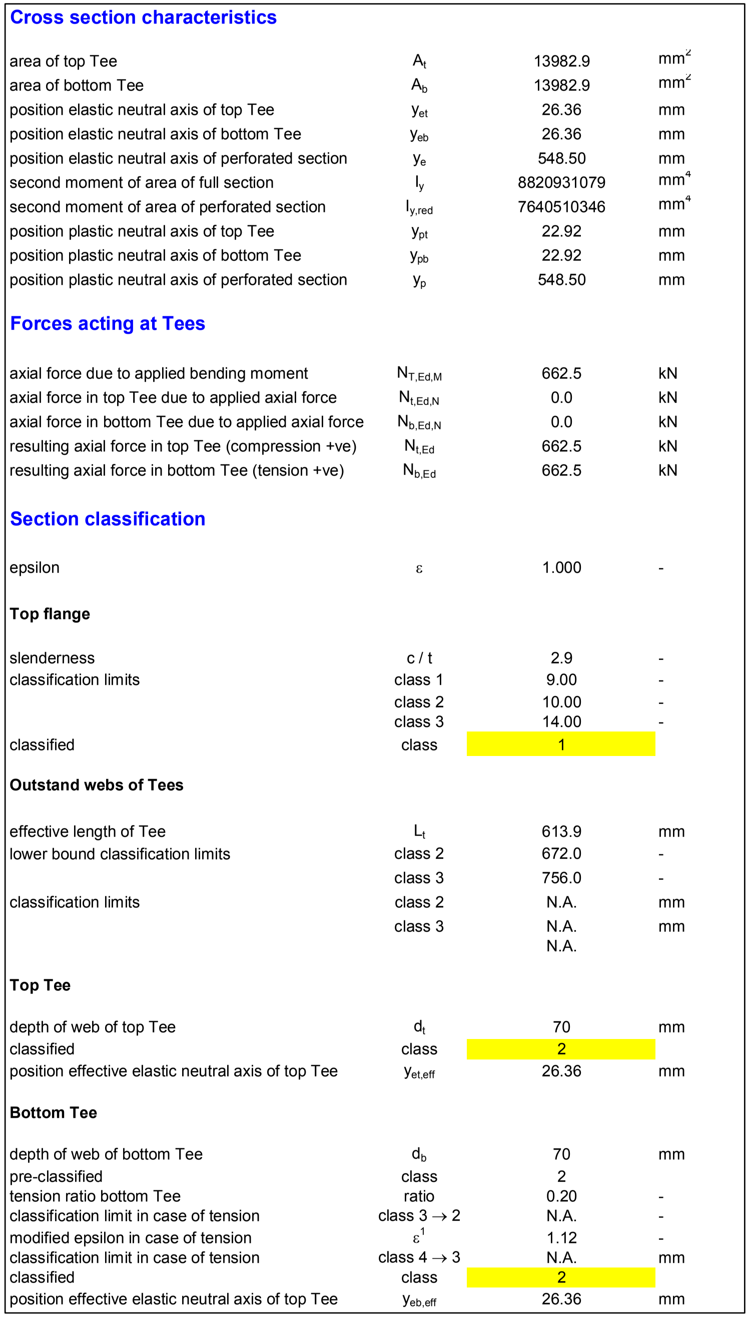

Cross section characteristics

area of top Tee	A_t	13982.9	mm²
area of bottom Tee	A_b	13982.9	mm²
position elastic neutral axis of top Tee	y_{et}	26.36	mm
position elastic neutral axis of bottom Tee	y_{eb}	26.36	mm
position elastic neutral axis of perforated section	y_e	548.50	mm
second moment of area of full section	I_y	8820931079	mm⁴
second moment of area of perforated section	$I_{y,red}$	7640510346	mm⁴
position plastic neutral axis of top Tee	y_{pt}	22.92	mm
position plastic neutral axis of bottom Tee	y_{pb}	22.92	mm
position plastic neutral axis of perforated section	y_p	548.50	mm

Forces acting at Tees

axial force due to applied bending moment	$N_{T,Ed,M}$	662.5	kN
axial force in top Tee due to applied axial force	$N_{t,Ed,N}$	0.0	kN
axial force in bottom Tee due to applied axial force	$N_{b,Ed,N}$	0.0	kN
resulting axial force in top Tee (compression +ve)	$N_{t,Ed}$	662.5	kN
resulting axial force in bottom Tee (tension +ve)	$N_{b,Ed}$	662.5	kN

Section classification

epsilon	ε	1.000	-

Top flange

slenderness	c / t	2.9	-
classification limits	class 1	9.00	-
	class 2	10.00	-
	class 3	14.00	-
classified	class	1	

Outstand webs of Tees

effective length of Tee	L_t	613.9	mm
lower bound classification limits	class 2	672.0	-
	class 3	756.0	-
classification limits	class 2	N.A.	mm
	class 3	N.A.	mm
		N.A.	

Top Tee

depth of web of top Tee	d_t	70	mm
classified	class	2	
position effective elastic neutral axis of top Tee	$y_{et,eff}$	26.36	mm

Bottom Tee

depth of web of bottom Tee	d_b	70	mm
pre-classified	class	2	
tension ratio bottom Tee	ratio	0.20	-
classification limit in case of tension	class 3 → 2	N.A.	-
modified epsilon in case of tension	ε^1	1.12	-
classification limit in case of tension	class 4 → 3	N.A.	mm
classified	class	2	
position effective elastic neutral axis of top Tee	$y_{eb,eff}$	26.36	mm

Worksheet "Calculation" (Part 1) – Geometrical properties and section classification

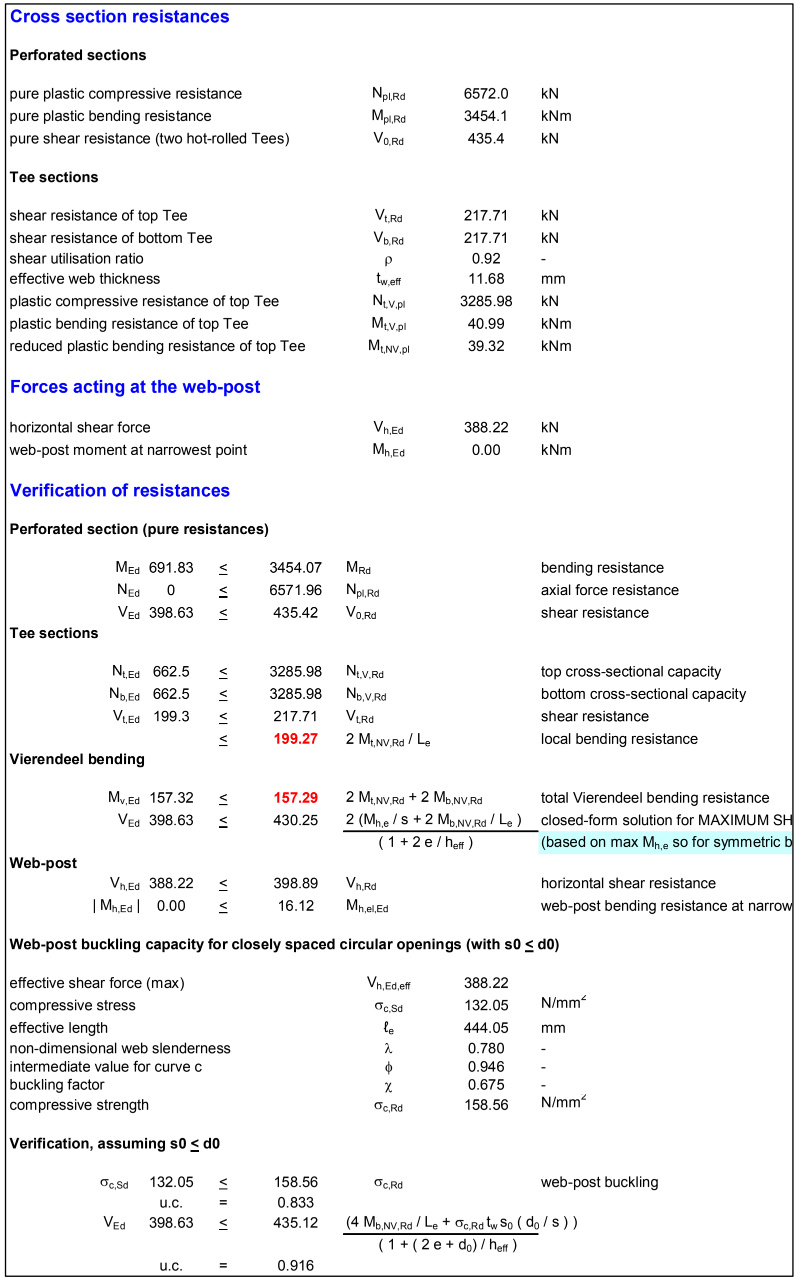

Cross section resistances

Perforated sections

pure plastic compressive resistance	$N_{pl,Rd}$	6572.0	kN
pure plastic bending resistance	$M_{pl,Rd}$	3454.1	kNm
pure shear resistance (two hot-rolled Tees)	$V_{0,Rd}$	435.4	kN

Tee sections

shear resistance of top Tee	$V_{t,Rd}$	217.71	kN
shear resistance of bottom Tee	$V_{b,Rd}$	217.71	kN
shear utilisation ratio	ρ	0.92	-
effective web thickness	$t_{w,eff}$	11.68	mm
plastic compressive resistance of top Tee	$N_{t,V,pl}$	3285.98	kN
plastic bending resistance of top Tee	$M_{t,V,pl}$	40.99	kNm
reduced plastic bending resistance of top Tee	$M_{t,NV,pl}$	39.32	kNm

Forces acting at the web-post

horizontal shear force	$V_{h,Ed}$	388.22	kN
web-post moment at narrowest point	$M_{h,Ed}$	0.00	kNm

Verification of resistances

Perforated section (pure resistances)

M_{Ed}	691.83	≤	3454.07	M_{Rd}	bending resistance
N_{Ed}	0	≤	6571.96	$N_{pl,Rd}$	axial force resistance
V_{Ed}	398.63	≤	435.42	$V_{0,Rd}$	shear resistance

Tee sections

$N_{t,Ed}$	662.5	≤	3285.98	$N_{t,V,Rd}$	top cross-sectional capacity
$N_{b,Ed}$	662.5	≤	3285.98	$N_{b,V,Rd}$	bottom cross-sectional capacity
$V_{t,Ed}$	199.3	≤	217.71	$V_{t,Rd}$	shear resistance
		≤	199.27	$2\ M_{t,NV,Rd} / L_e$	local bending resistance

Vierendeel bending

$M_{v,Ed}$	157.32	≤	157.29	$2\ M_{t,NV,Rd} + 2\ M_{b,NV,Rd}$	total Vierendeel bending resistance
V_{Ed}	398.63	≤	430.25	$\dfrac{2\ (M_{h,e} / s + 2\ M_{b,NV,Rd} / L_e)}{(1 + 2\ e / h_{eff})}$	closed-form solution for MAXIMUM SH (based on max $M_{h,e}$ so for symmetric b

Web-post

$V_{h,Ed}$	388.22	≤	398.89	$V_{h,Rd}$	horizontal shear resistance
$\lvert M_{h,Ed} \rvert$	0.00	≤	16.12	$M_{h,el,Ed}$	web-post bending resistance at narrow

Web-post buckling capacity for closely spaced circular openings (with s0 ≤ d0)

effective shear force (max)	$V_{h,Ed,eff}$	388.22	
compressive stress	$\sigma_{c,Sd}$	132.05	N/mm²
effective length	ℓ_e	444.05	mm
non-dimensional web slenderness	λ	0.780	-
intermediate value for curve c	ϕ	0.946	-
buckling factor	χ	0.675	-
compressive strength	$\sigma_{c,Rd}$	158.56	N/mm²

Verification, assuming s0 ≤ d0

$\sigma_{c,Sd}$	132.05	≤	158.56	$\sigma_{c,Rd}$	web-post buckling
	u.c.	=	0.833		
V_{Ed}	398.63	≤	435.12	$\dfrac{(4\ M_{b,NV,Rd} / L_e + \sigma_{c,Rd}\ t_w\ s_0\ (d_0 / s))}{(1 + (2\ e + d_0) / h_{eff})}$	
	u.c.	=	0.916		

Worksheet "Calculation" (Part 2) – Cross-sectional resistance and verifications

C.2 Base profile IPE140

C.2.1 Web-post width s_0 = 50 mm

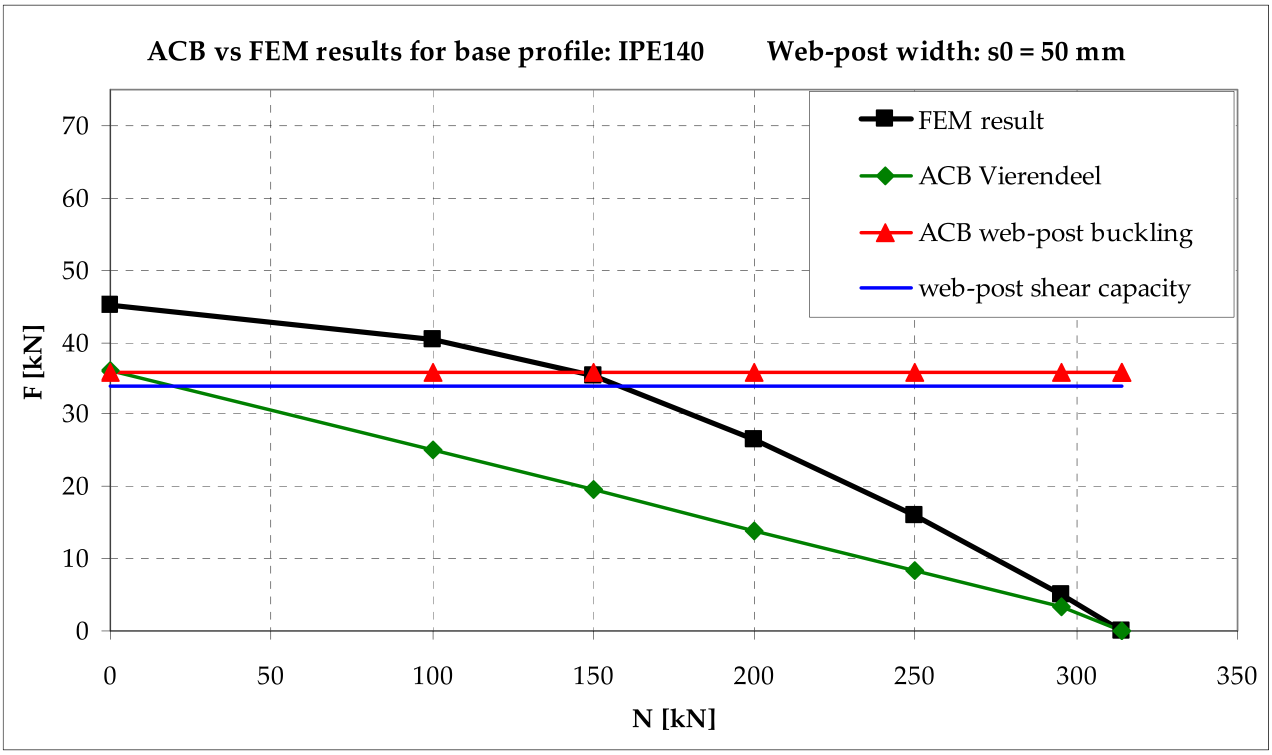

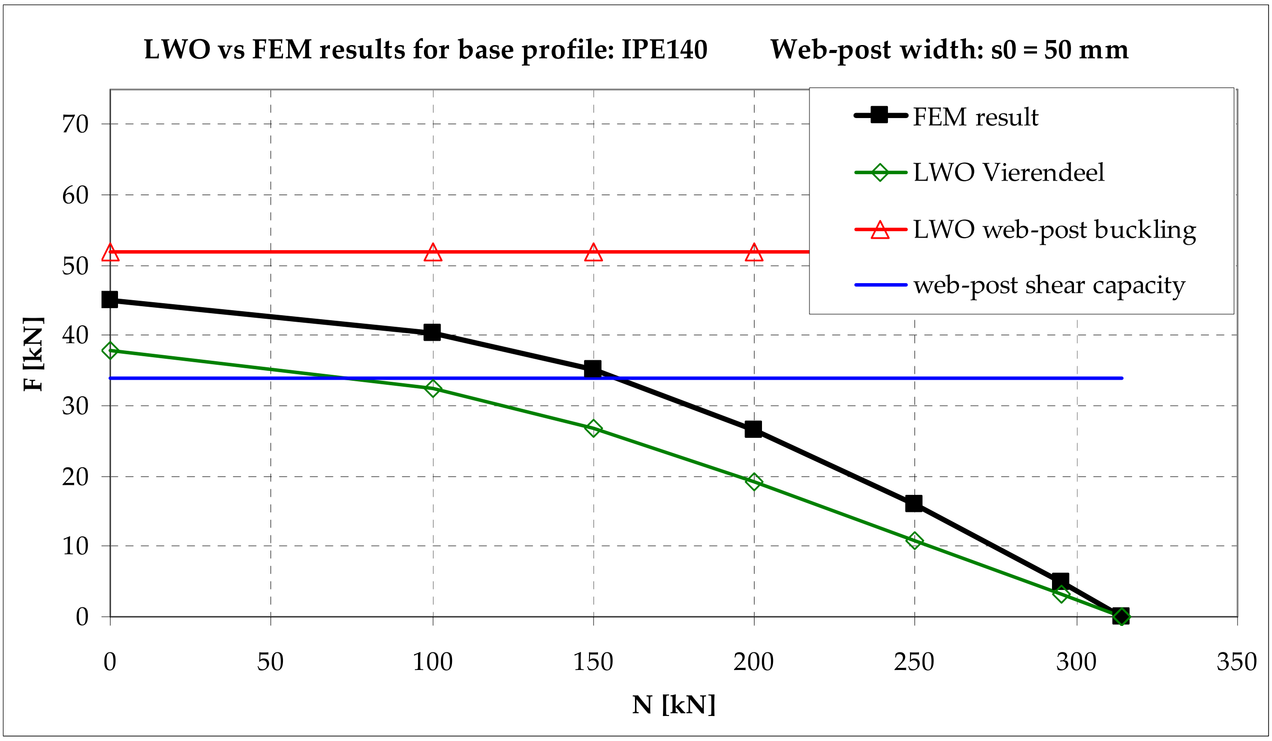

C.2.2 Web-post width s_0 = 100 mm

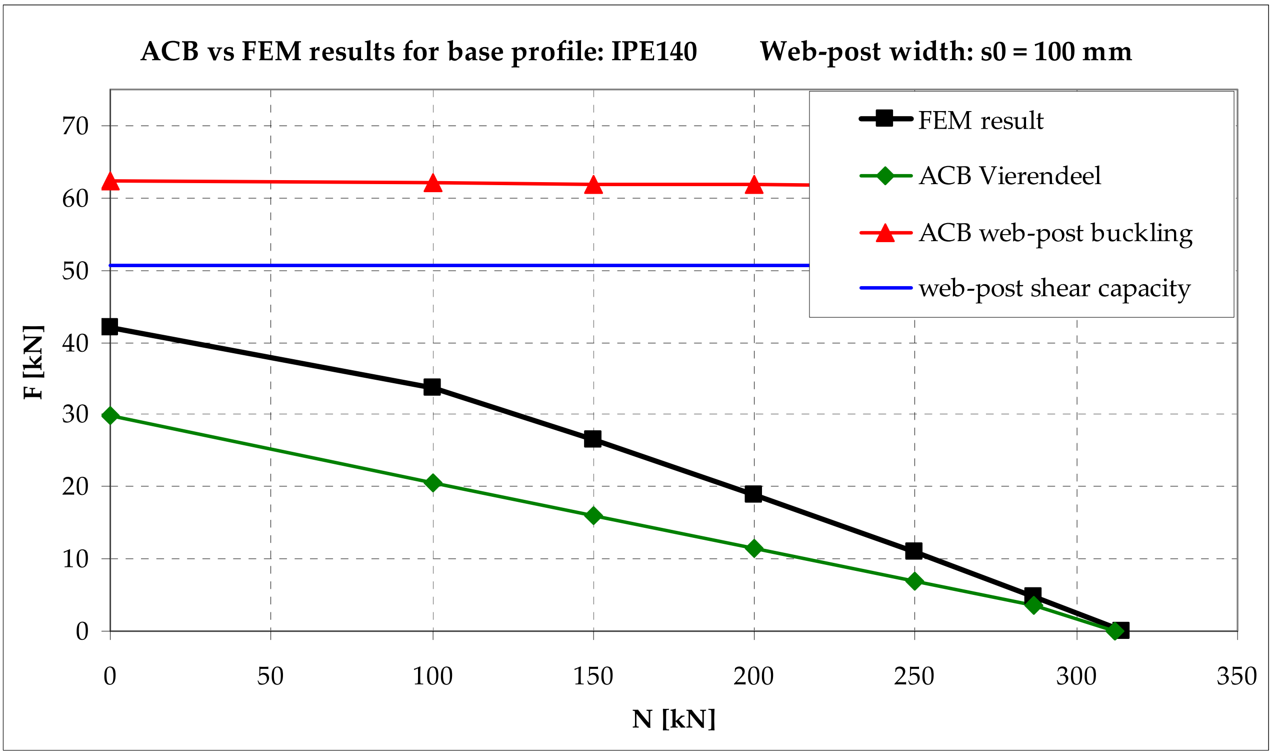

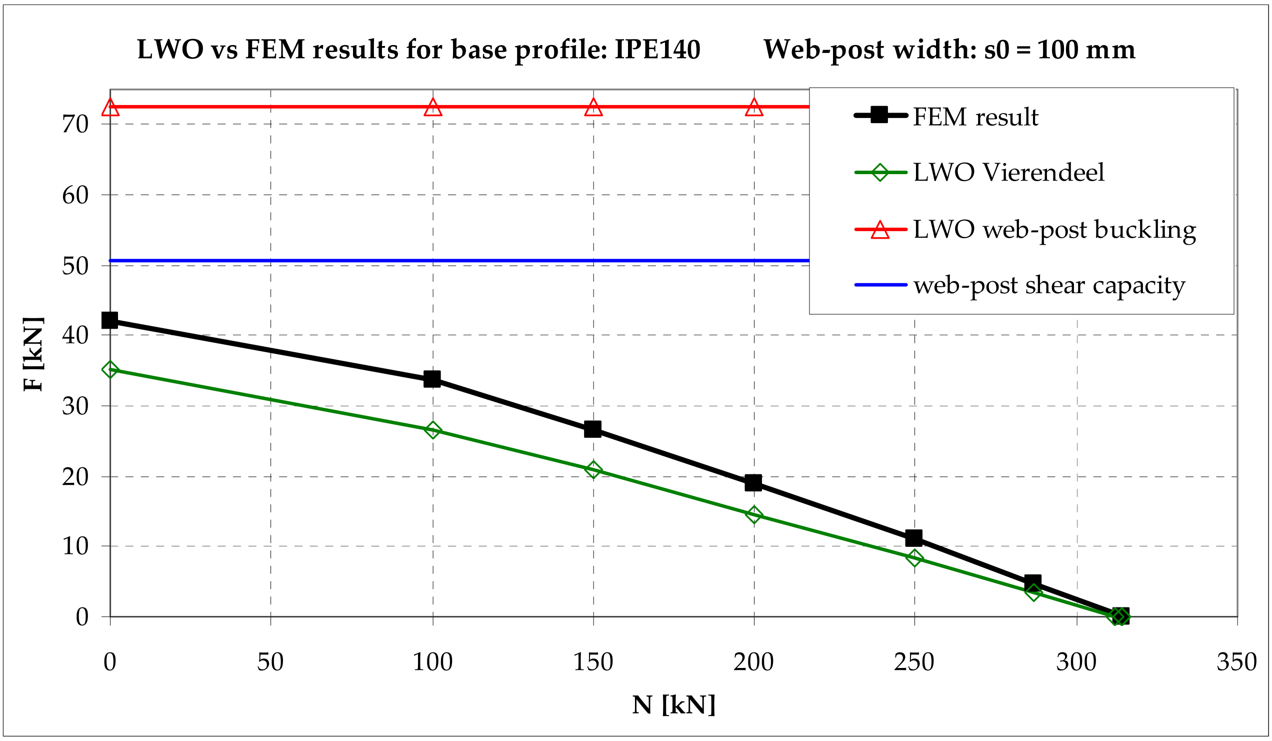

C.3 *Base profile IPE330*

C.3.1 Web-post width s_0 = 50 mm

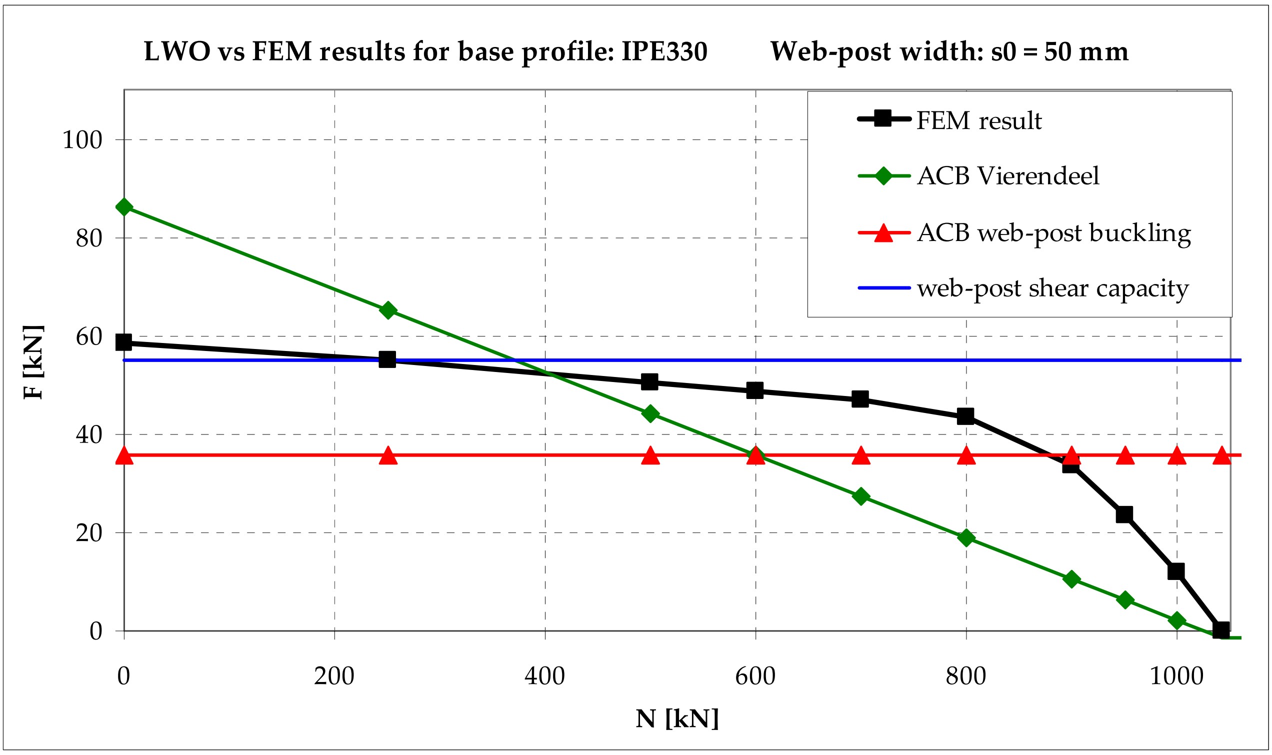

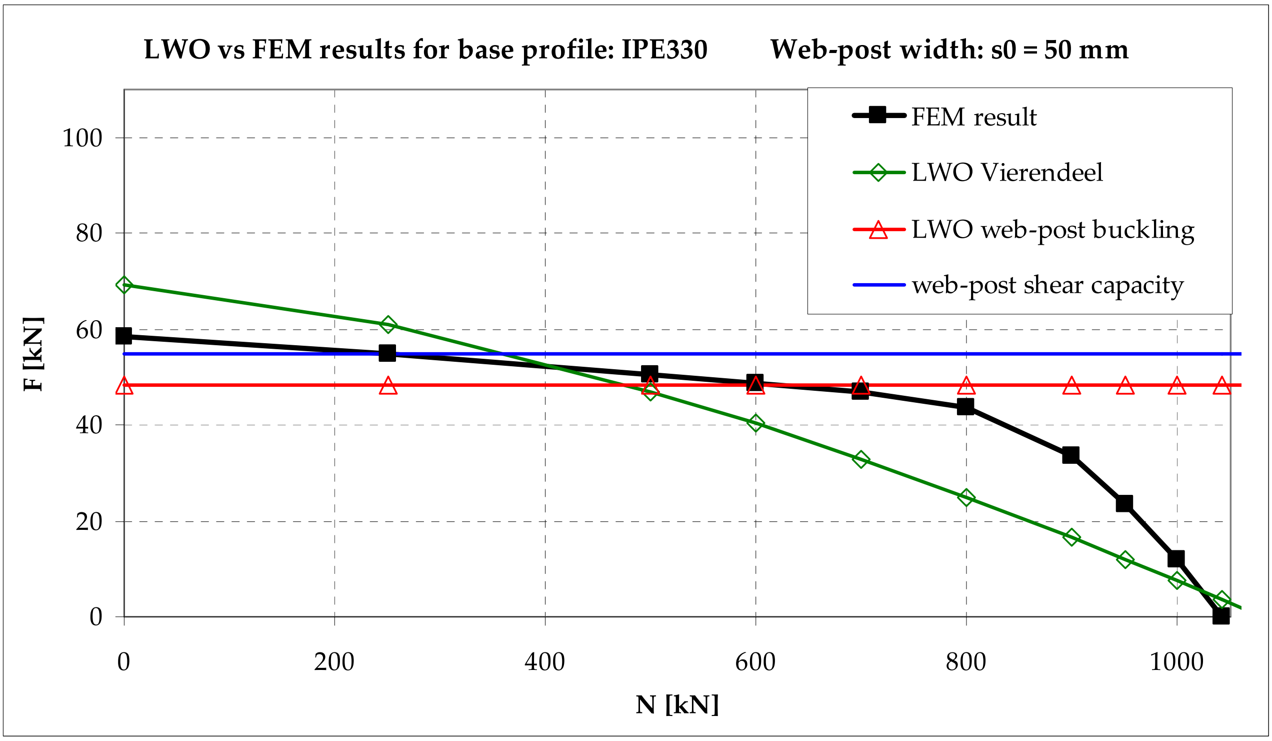

C.3.2 Web-post width s_0 = 100 mm

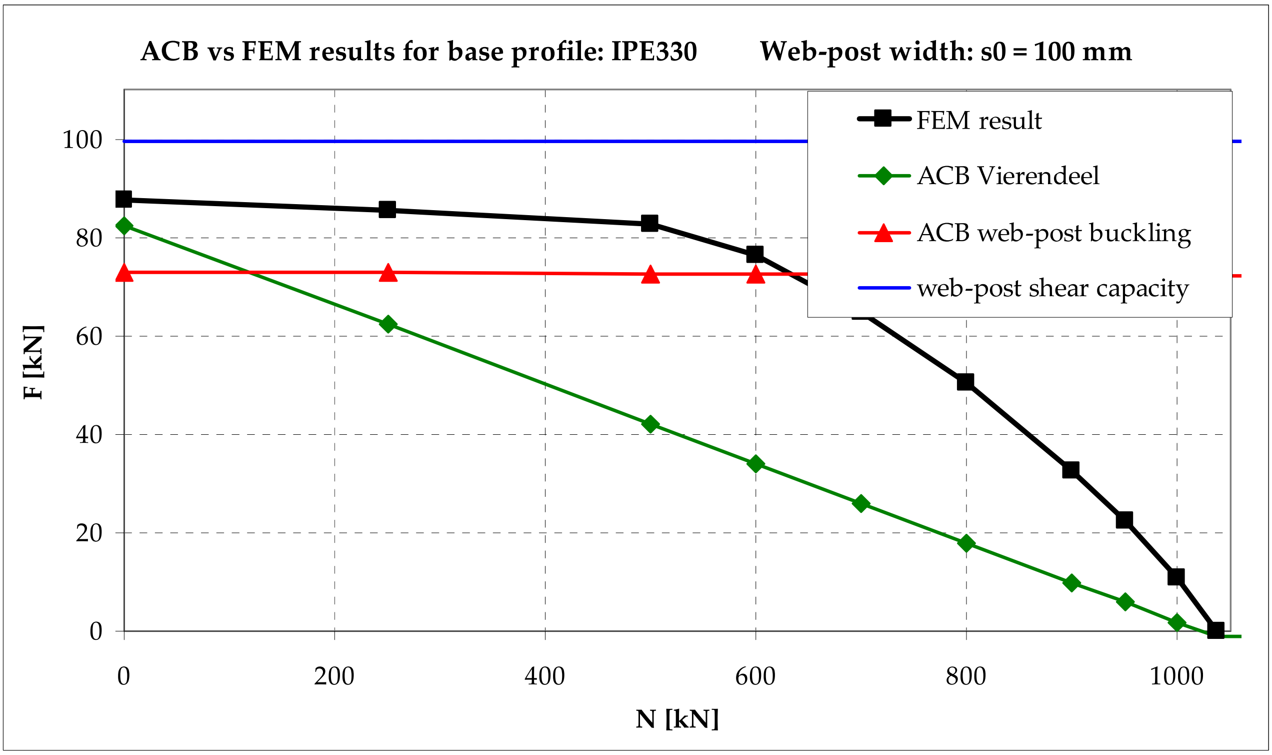

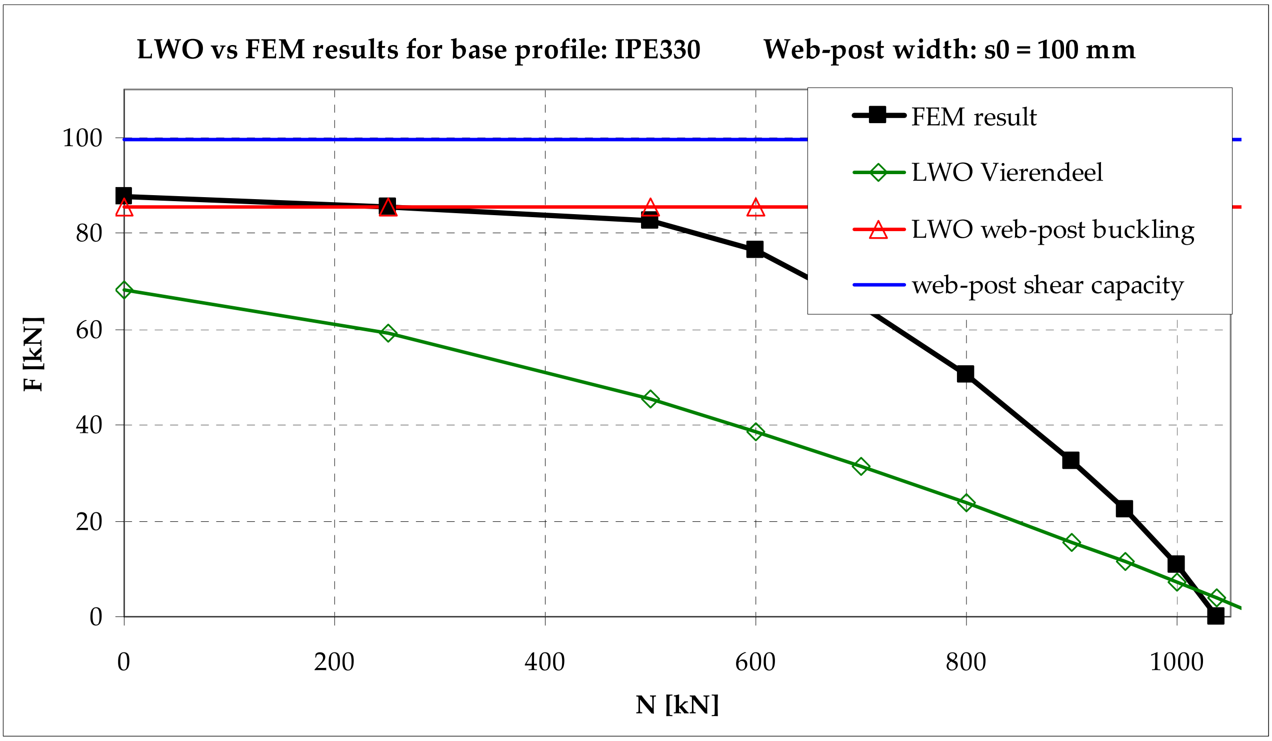

C.4 Base profile IPE600

C.4.1 Web-post width s_0 = 62 mm

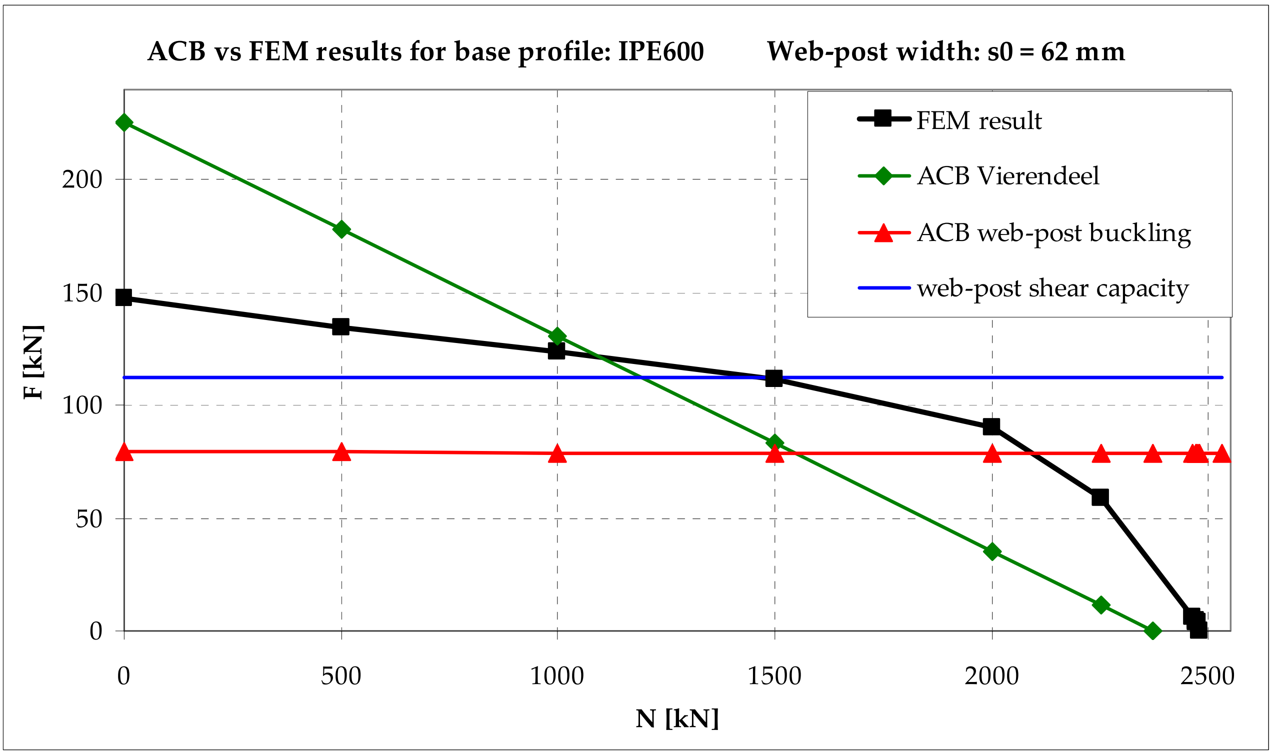

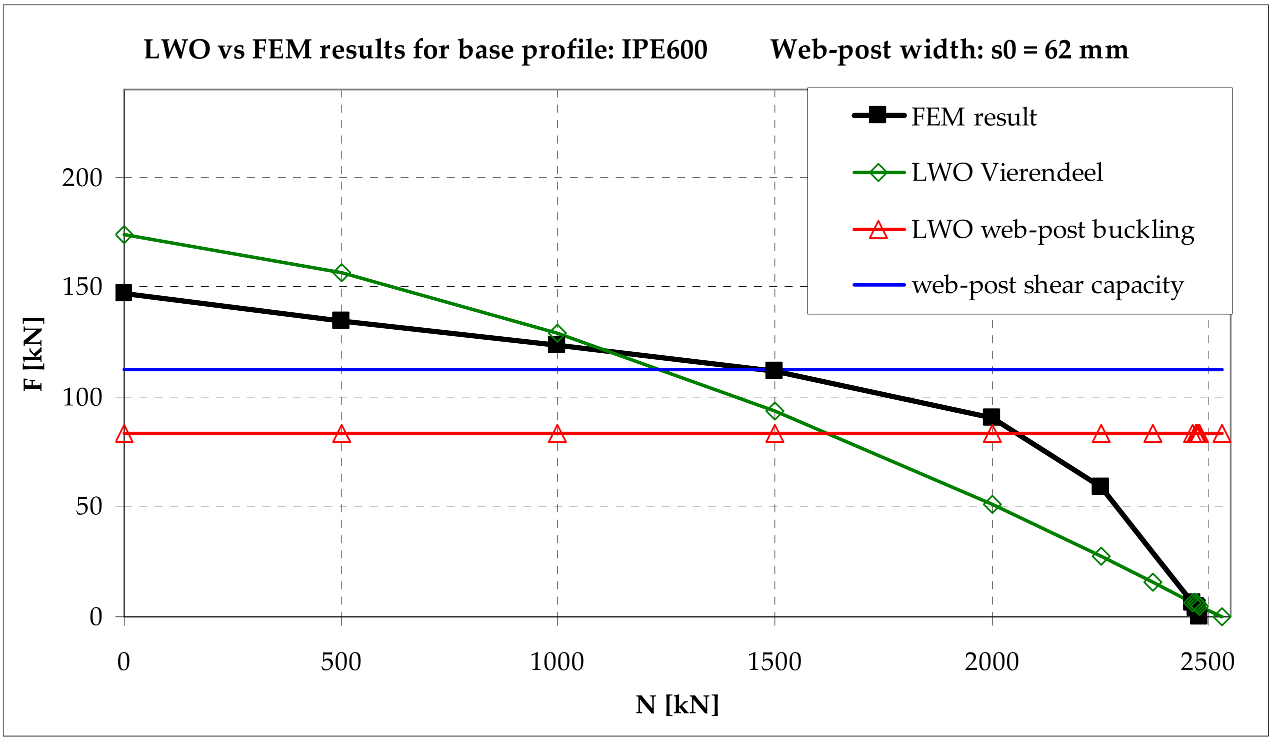

C.4.2 Web-post width s_0 = 124 mm

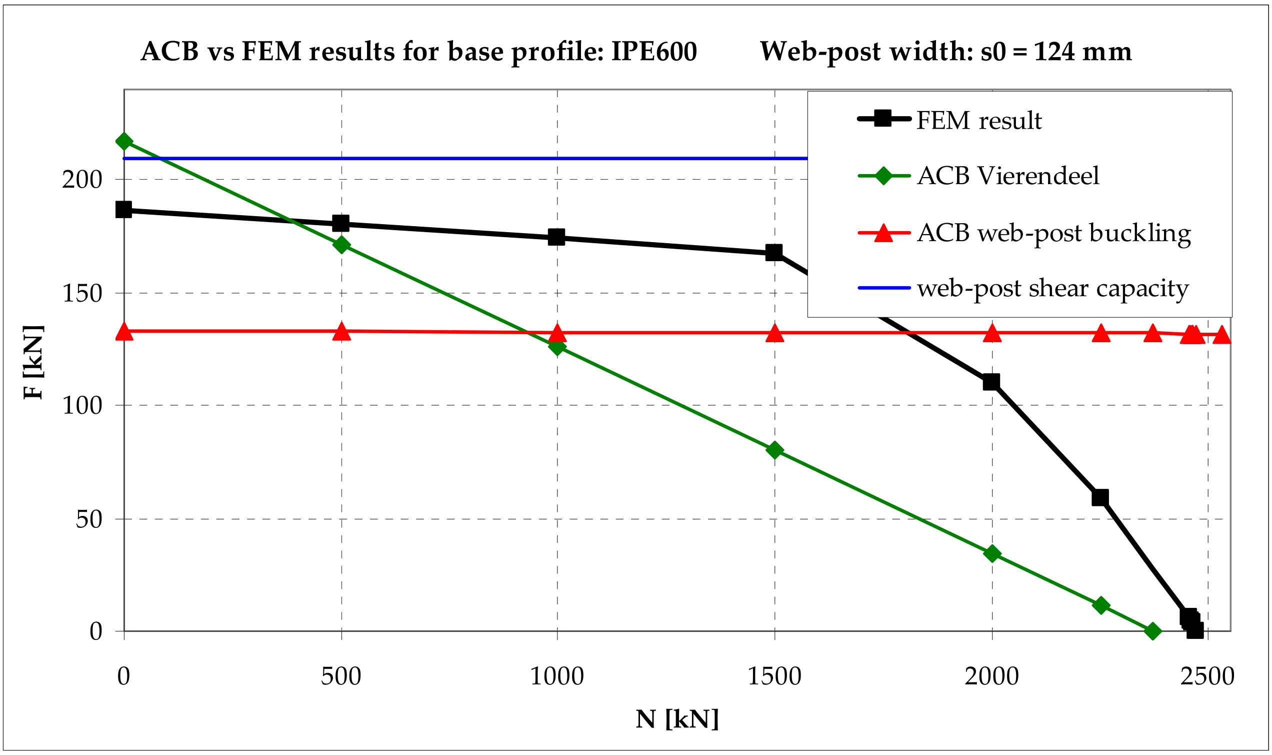

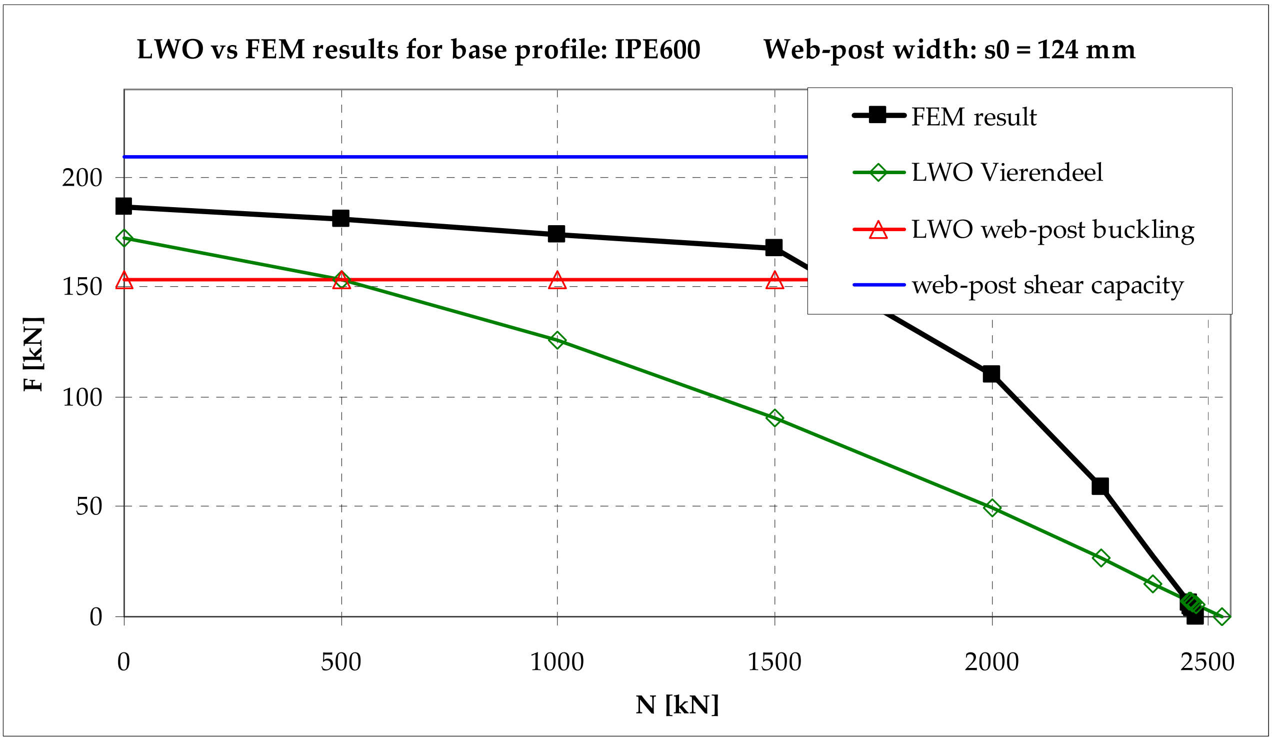

C.5 Base profile HE200A

C.5.1 Web-post width s_0 = 50 mm

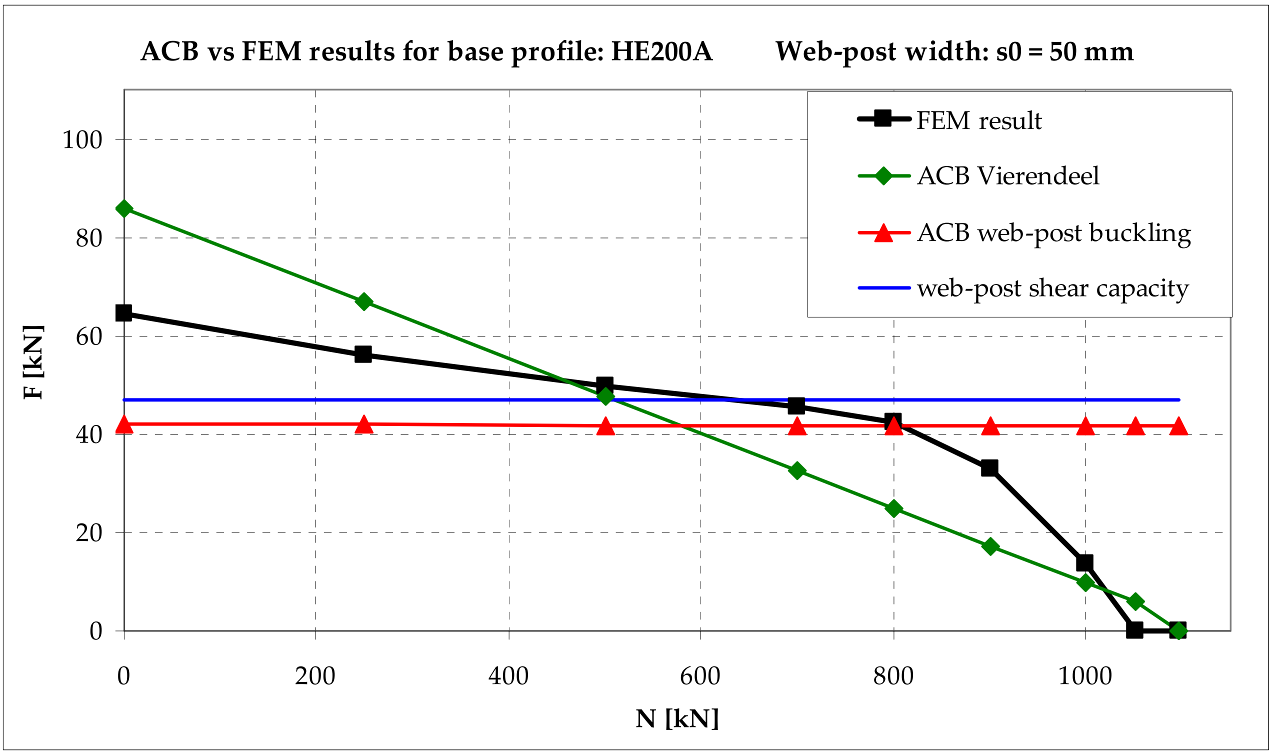

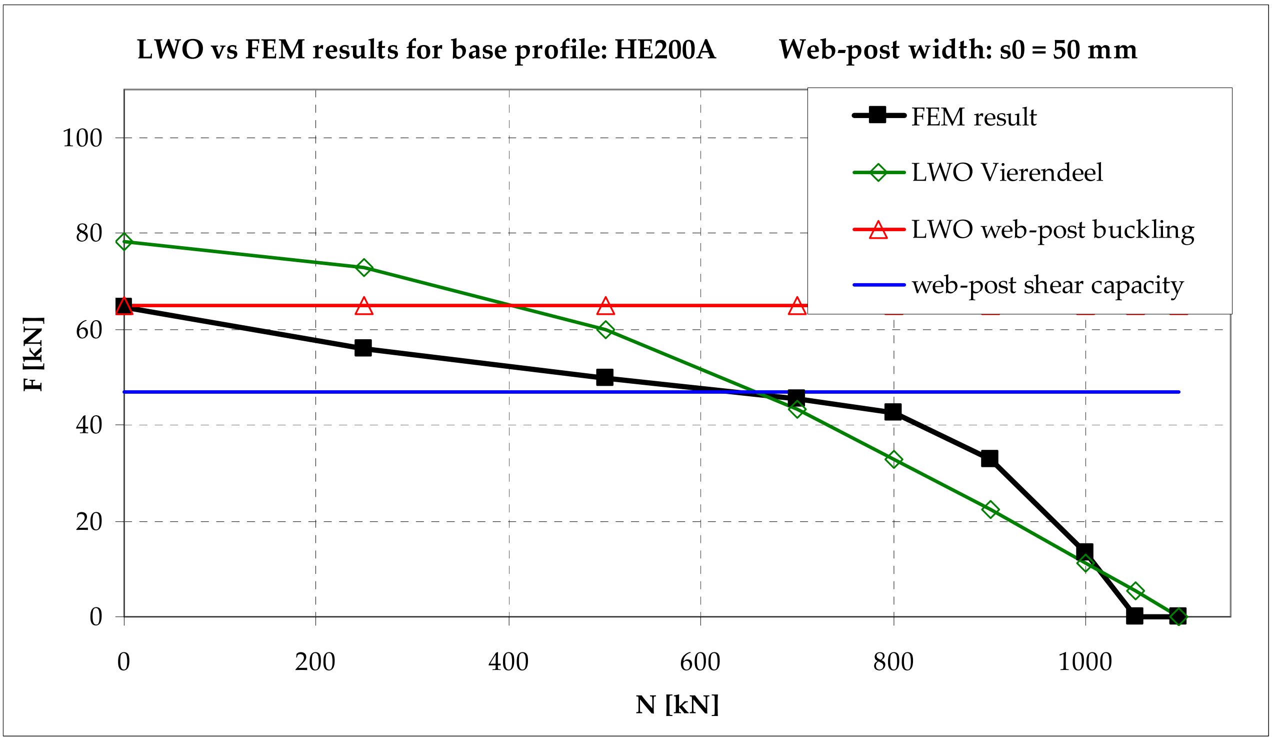

C.5.2 Web-post width s_0 = 100 mm

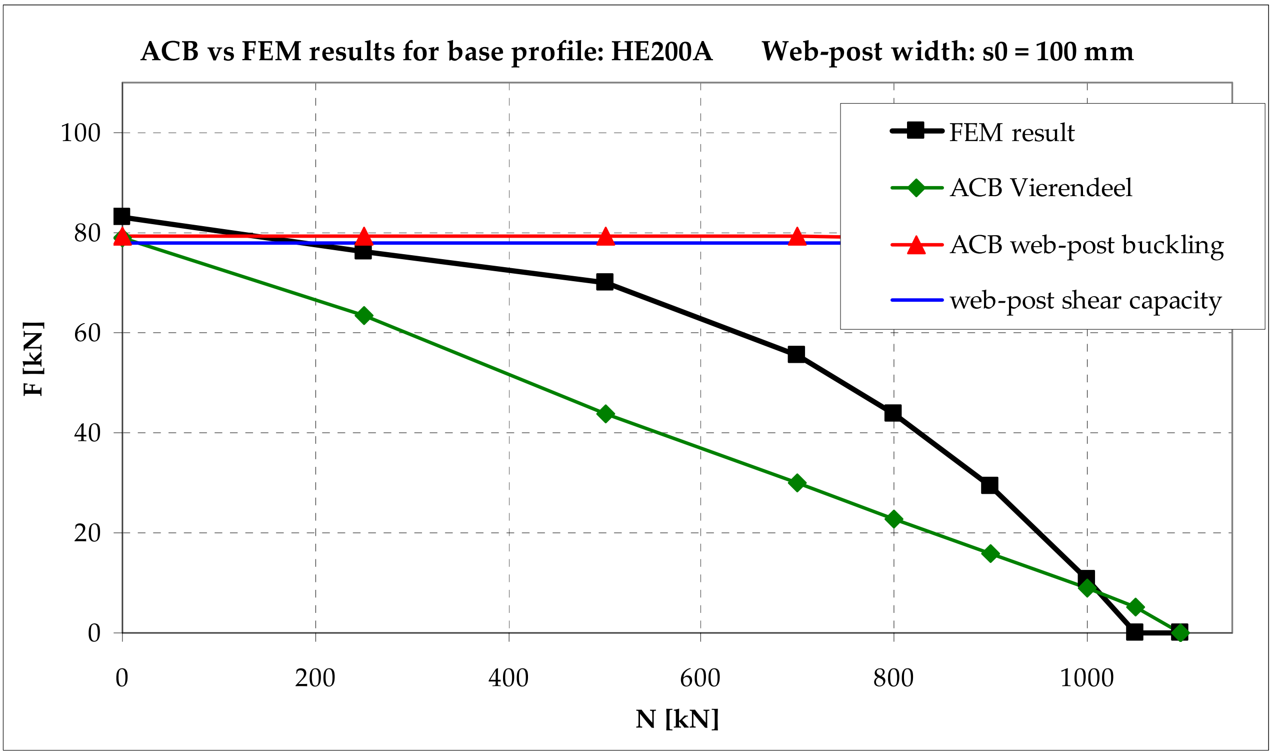

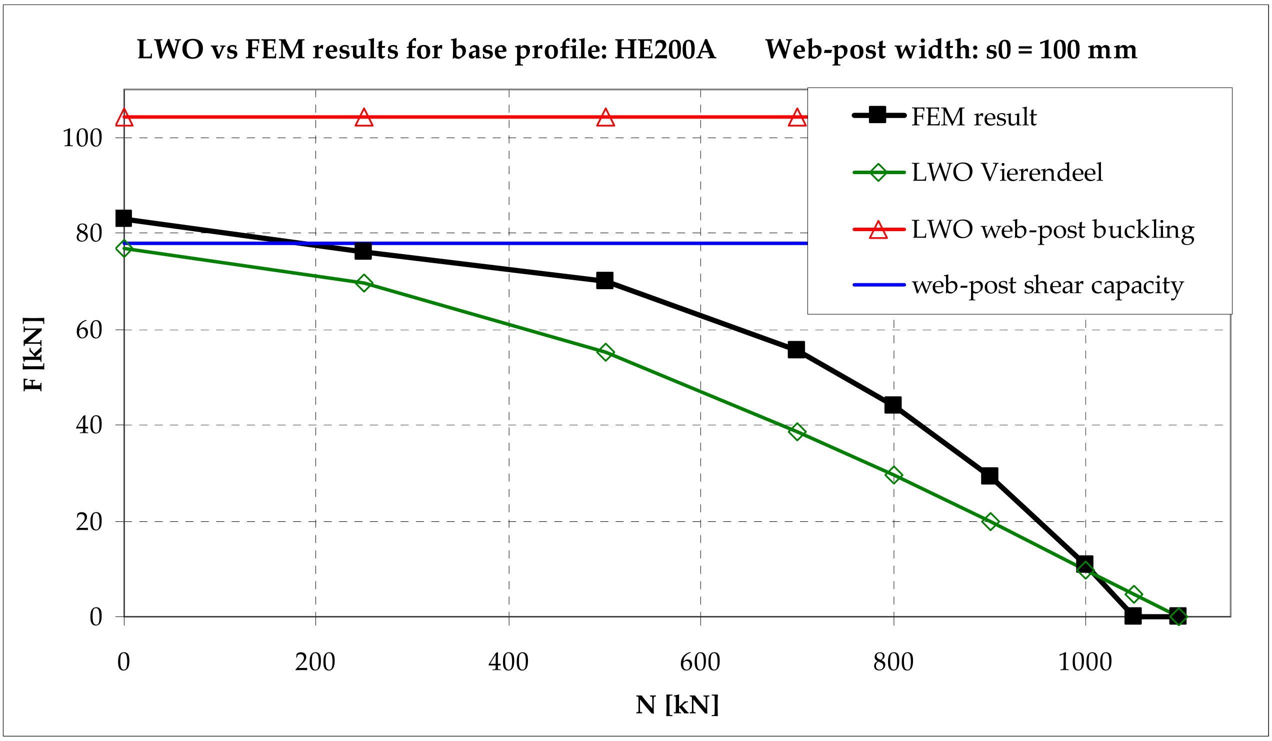

C.6 Base profile HE650M

C.6.1 Web-post width s_0 = 70 mm

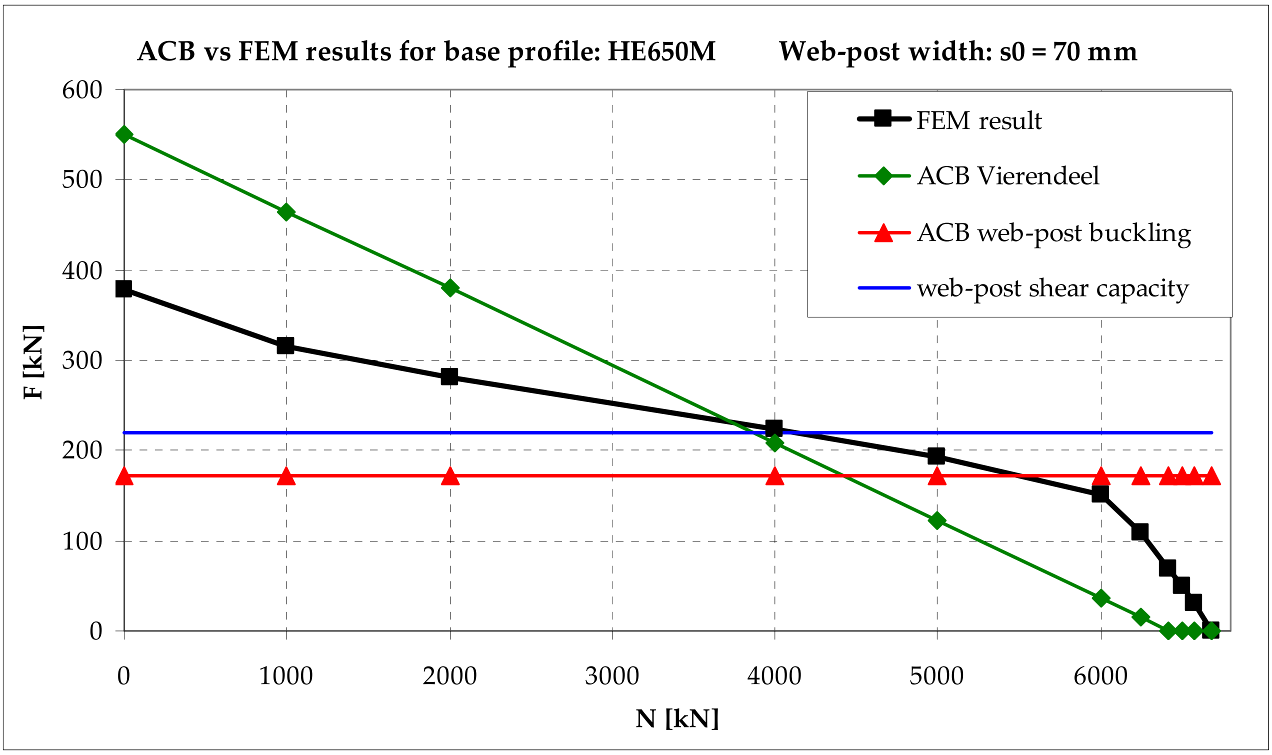

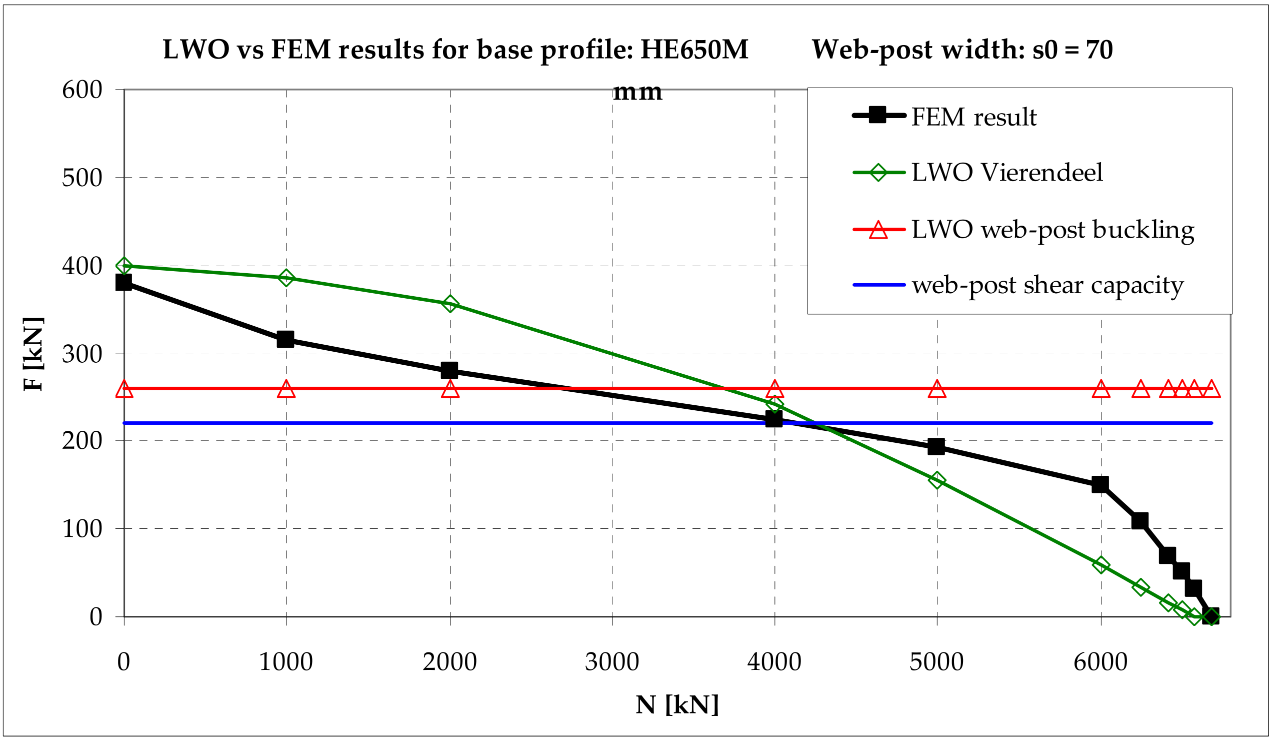

C.6.2 Web-post width s_0 = 140 mm

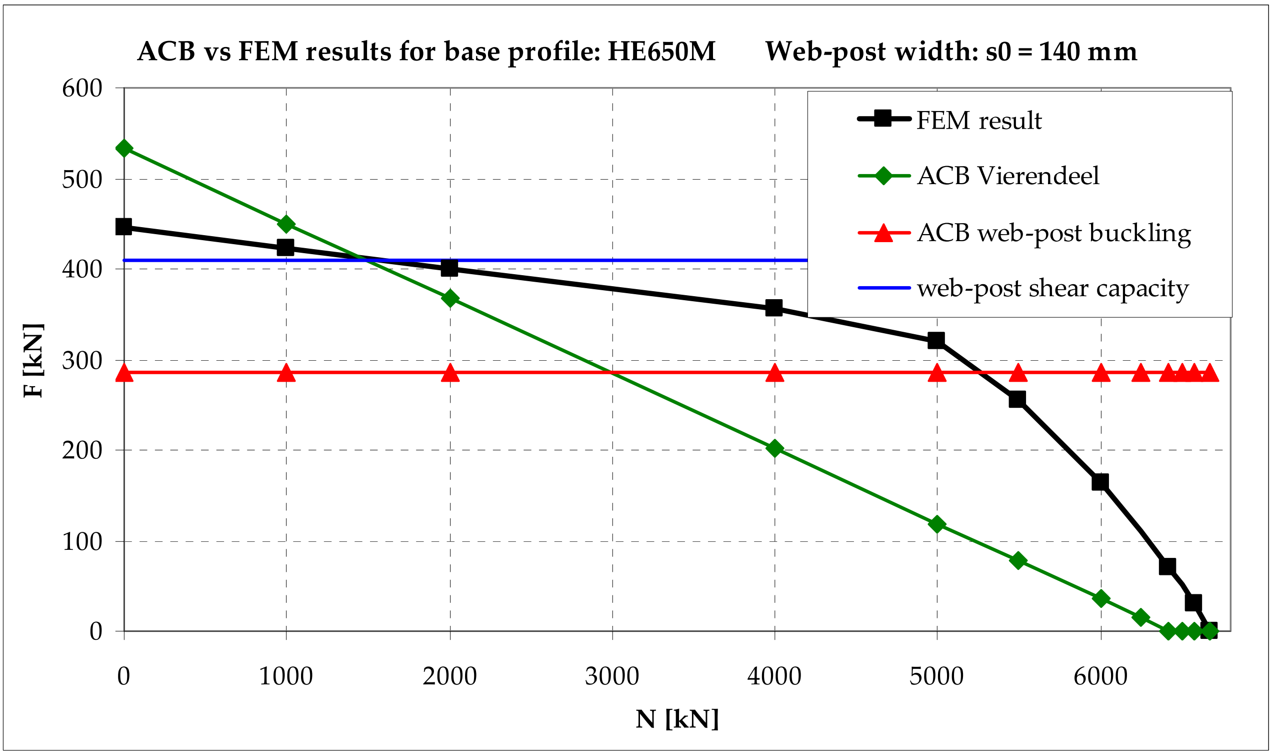

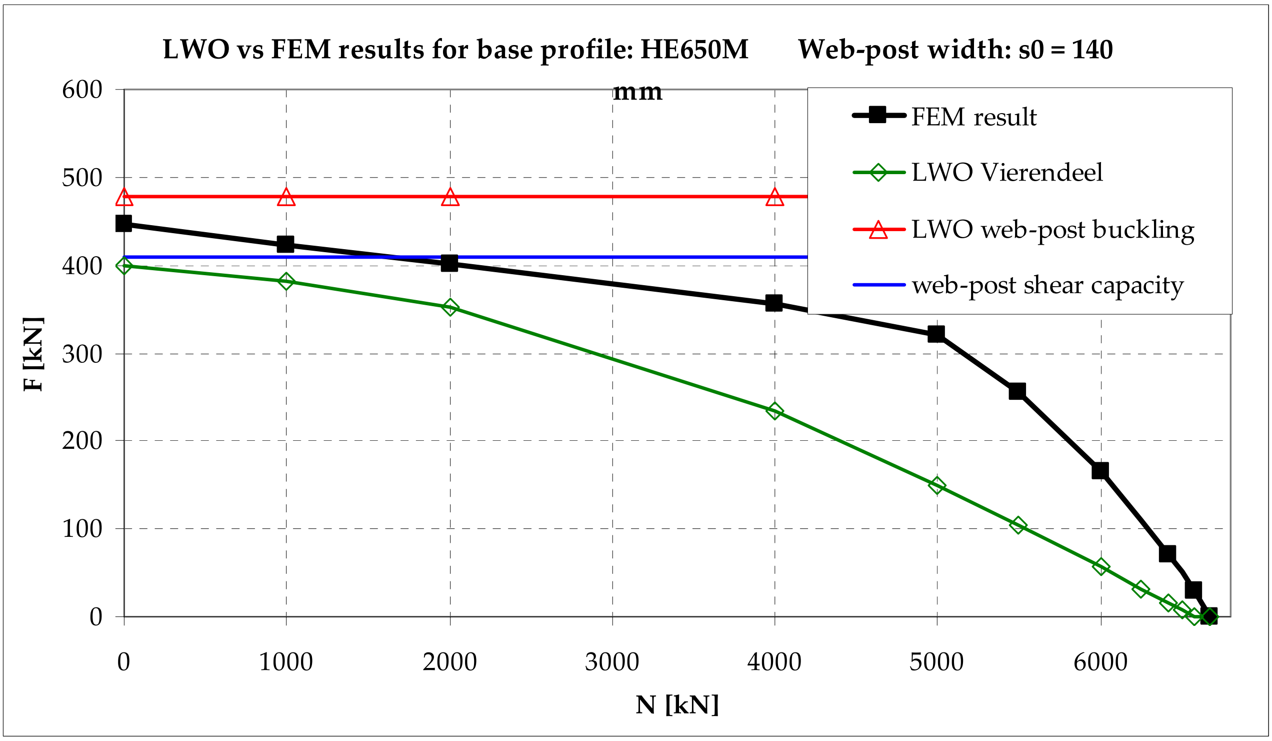

D LIST OF CONTENTS DATA-DVD

All analysis data have been put together on the data-DVD that accompanies this report. Below is an overview of its contents.

Documentation

ECSC-reports	: LTB / LWO / LWO+ / Euro-Build in Steel
Manufacturers	: Arcelor(Mittal) / CMC / Fabsec / MacSteel / Westok
PhD and MSc Theses	: several studies on castellated & cellular beams
Hong-Kong Steel Design Code	: Code of Practise for the Structual Use of Steel 2005
Access-Steel	: design aids for the application of EN1993-1-1
CTICM	: Centre Industriel de la Construction Métallique
SCI	: Steel Construction Institute

FEM calculations

Parameter studies	: Global buckling / Web-post buckling
Case study	: Frame 1 / Frame 2 + info-file on numbering scheme
Other	: development of utility TEM file creator + examples

FEM results

Parameter studies	: Global buckling / Web-post buckling + graphs and pictures + overview of results
Case study	: graphs and pictures

Images

figures and pictures on failure modes, application area, FEM modelling, etc.

Reports

Plan of Action + Final report

Software

Finite element software SAFIR, including pre- and post-processors, documentation and examples + ACB software

TechPapers

scientific papers on structural behaviour of castellated beams, (non-)composite cellular beams, beams with web single web openings, Fire Safety Engineering, the General and Overall method, Instability of frames and members, etc.

Work documents

Excel tool + documents and spreadsheets on different aspects of cellular beams and columns

E ARCELOR PROFIL LUXEMBOURG

Arcelor was created in 2002 by the fusion of the French company Usinor, the Luxembourg ARBED en the firm Spanish Aceralia. Following the merger with the Indian company Mittal Steel in 2006 the world's largest steel producer was formed, Arcelor Mittal, with 330,000 employees in more than 60 countries.

In Europe it covers the industrial, marketing and sales activities for beams, channels and heavy merchant bars with Arcelor Commercial Sections, a Product Unit of the Long Carbon Steel Europe Business Unit. The majority of Arcelor Commercial Sections' products and solutions are used in the construction industry, the mechanical and the transportation sectors.

The Research Centre of Arcelor Profil Luxembourg aims at developing new and innovative products and solutions to meet the specific needs of the markets. In cooperation with the Marketing and Technical Assistance teams special softwares for the Arcelor products are produced. Numerous areas are investigated, with special attendance for fire safety engineering, composite construction, earthquake resistance, etc. Its reports are distributed in conjunction with European technical and promotional organisations. Hereby close relations are maintained with various universities and technical centres.

F IBT INGENIEURS IN BOUWTECHNIEK

Since 1968 IBT Ingenieurs in Bouwtechniek is an independent firm of consulting engineers servicing architects, building contractors and individual clients. IBT is located in both Veenendaal and Papendrecht, The Netherlands.

IBT provides its clients with:

- structural designs including technical drawings in steel, concrete and timber;
- advices for renovation;
- calculations of EPN , ventilation and daylight;
- fire safety engineering calculations.

The team of IBT consist of over 20 employees, which are continuously developing their skills by means of additional courses and their daily work experiences.

The main areas of activity are:

- residential, commercial and industrial building;
- houses, apartment buildings and shopping complexes;
- industrial facilities;
- schools and churches.

Furthermore IBT is involved in developing pre-stressing configurations for a manufacturer of precast concrete structural elements.

G ADDRESSES

Delft University of Technology
Faculty of Civil Engineering and Geosciences
Stevinweg 1
2628 CN Delft
The Netherlands

Prof. Ir. F.S.K. Bijlaard (Chairman)
f.s.k.bijlaard@tudelft.nl
Tel. +31 15 278 45 81

Dr. A. Romeijn (Daily guide)
a.romeijn@tudelft.nl
Tel. +31 15 278 37 05

Ir. R. Abspoel
r.abspoel@tudelft.nl
Tel. +31 15 278 53 58

Dr. Ir. P.C.J. Hoogenboom
p.c.j.hoogenboom@tudelft.nl
Tel. +31 15 278 80 81

J.G. Verweij (Student)
gert_janverweij@hotmail.com
Tel. +316 1276 4759

ArcelorMittal R&D
66, rue de Luxembourg
L-4009 Esch-sur-Alzette
Luxembourg
www.arcelormittal.com/sections

Dr. O. Vassart (Research Manager)
olivier.vassart@arcelormittal.com
Tel. +352 5313 2175

IBT Ingenieurs in Bouwtechniek
Citadel 8a
3905 NK Veenendaal
The Netherlands
www.bouwtechniek.nl

Ir. A. van 't Land
a.vantland@bouwtechniek.nl